Измерение спин-зависимых азимутальных асимметрий в процессах полуинклюзивного глубоко-неупругого рассеяния и Дрелла-Яна

BAKUR PARSAMYAN

CERN, JINR,
University of Turin and INFN

Семинар в связи с выборами на должность СНС

4-ое Апреля 2018
ЛЯП-ОИЯИ, Дубна, РФ

The beginning - scattering experiments in early XXth century

Nucleon spin *puzzle*

- 1964 Quark model   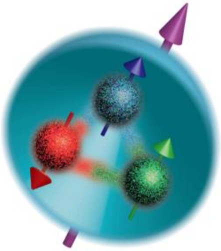
- 1969 Parton model
- 1973 asymptotic freedom and QCD
- 1978 intrinsic transverse motion of quarks and azimuthal asymmetries
- 1988 EMC measurement spin *puzzle*
- 1988 Factorization of Hard Processes in QCD
- 90's spin dependent azimuthal asymmetries and TMDs
- Late 90's – present – future: spin dependent azimuthal asymmetry measurements

Nucleon spin *puzzle*

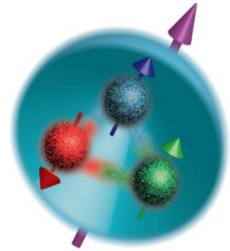

- 1964 Quark model 
- 1969 Parton model 
- 1973 asymptotic freedom and QCD 

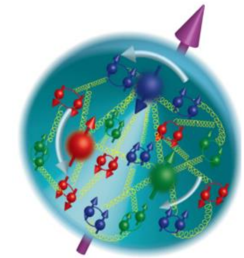

- 1978 intrinsic transverse motion of quarks and azimuthal asymmetries
- 1988 EMC measurement spin *puzzle*
- 1988 Factorization of Hard Processes in QCD
- 90's spin dependent azimuthal asymmetries and TMDs
- Late 90's – present – future: spin dependent azimuthal asymmetry measurements

Nucleon spin *puzzle*

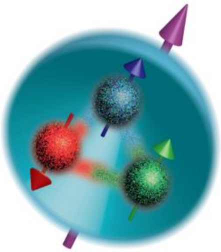

- 1964 Quark model  
- 1969 Parton model 

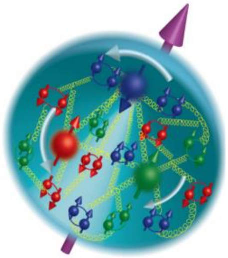

- 1973 asymptotic freedom and QCD    
- 1978 intrinsic transverse motion of quarks and azimuthal asymmetries 
- 1988 EMC measurement spin *puzzle*
- 1988 Factorization of Hard Processes in QCD
- 90's spin dependent azimuthal asymmetries and TMDs
- Late 90's – present – future: spin dependent azimuthal asymmetry measurements

Nucleon spin *puzzle*

- 1964 Quark model 

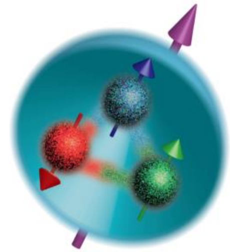

- 1969 Parton model 
- 1973 asymptotic freedom and QCD 

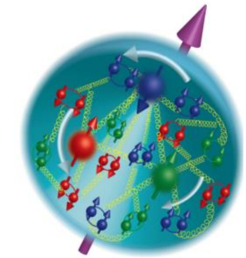

- 1978 intrinsic transverse motion of quarks and azimuthal asymmetries 

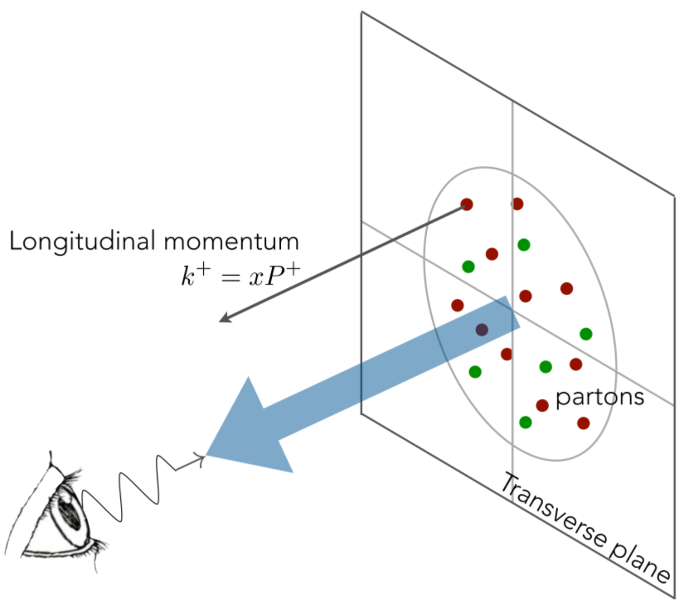

; in QCD

netries and TMDs

endent azimuthal asymmetry measurements

Nucleon spin *puzzle*

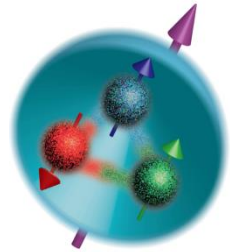

- 1964 Quark model 
- 1969 Parton model 
- 1973 asymptotic freedom and QCD 

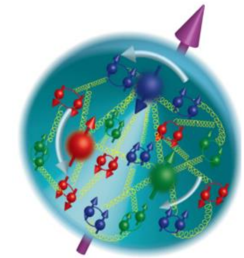

- 1978 intrinsic transverse motion of quarks and azimuthal asymmetries 

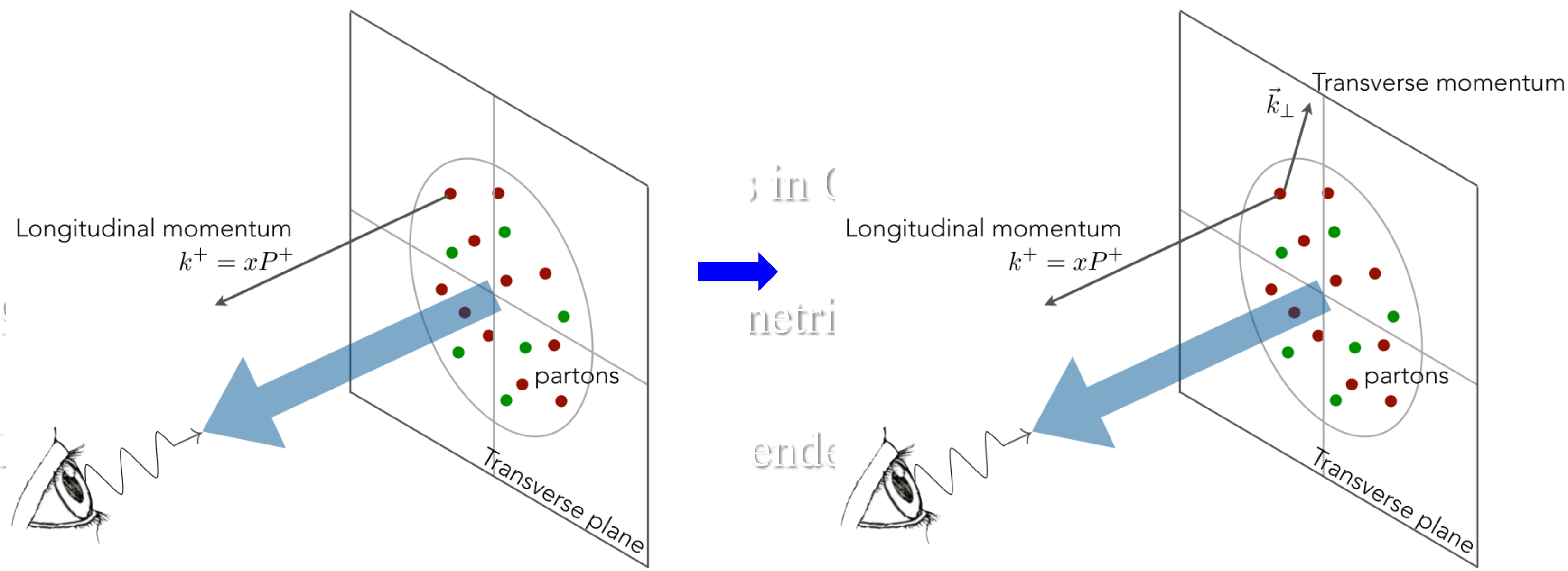

Cahn effect

$$\frac{d\sigma}{dxdydzdP_{hT}^2 d\varphi_h d\psi} = \left[\frac{\alpha}{xyQ^2}\frac{y^2}{2(1-\varepsilon)}\left(1+\frac{\gamma^2}{2x}\right)\right]\times\left(F_{UU,T}+\varepsilon F_{UU,L}\right)\times$$

$$1+\cos\phi_h\times\sqrt{2\varepsilon(1+\varepsilon)}A_{UU}^{\cos\phi_h}+\cos(2\phi_h)\times\varepsilon A_{UU}^{\cos(2\phi_h)}+\ldots$$

Cahn effect

***R. N. Cahn*, PLB 78 (1978)**

The point that there are azimuthal dependences which arise from the transverse momenta of the partons was clearly stated in this papers:

T.P. Cheng and A. Zee, Phys. Rev. D6 (1972) 885;
F. Ravndal, Phys. Lett. 43B (1973) 301.
R.L. Kingsley, Phys. Rev. D10 (1974) 1580;
A.M. Kotsinyan, Teor. Mat. Fiz. 24 (1975) 206;
Engl. transl. **Theor. Math. Phys. 24** (1976) 776.

A. Kotzinian On behalf of:
T.P. Cheng, A. Zee, F. Ravndal, R.L. Kingsley and himself

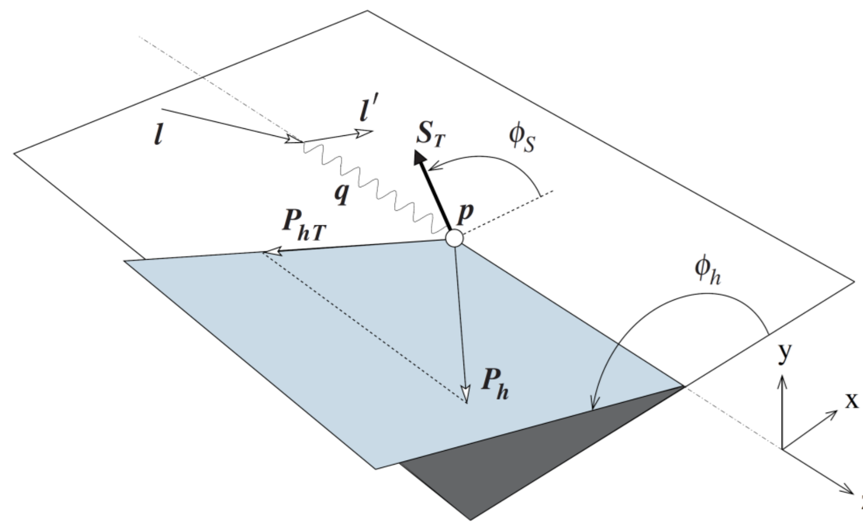

Cahn effect

$$\frac{d\sigma}{dxdydzdP_{hT}^2 d\varphi_h d\psi} = \left[\frac{\alpha}{xyQ^2}\frac{y^2}{2(1-\varepsilon)}\left(1+\frac{\gamma^2}{2x}\right)\right]\times\left(F_{UU,T}+\varepsilon F_{UU,L}\right)\times$$

$$1+\cos\phi_h\times\underbrace{\sqrt{2\varepsilon(1+\varepsilon)}A_{UU}^{\cos\phi_h}}+\cos(2\phi_h)\times\varepsilon A_{UU}^{\cos(2\phi_h)}+\ldots$$

Cahn effect

***R. N. Cahn*, PLB 78 (1978)**

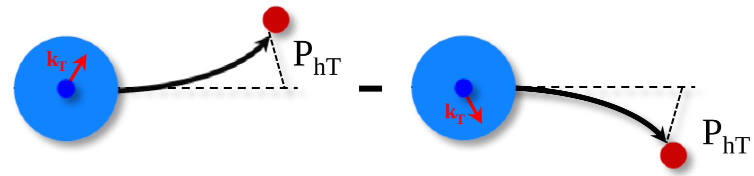

Kinematic effect: non-zero k_T induces an azimuthal modulation

$$\hat{s} \simeq xs\left[1-2\sqrt{1-y}\,\frac{k_T}{Q}\cdot\cos\varphi_q\right]$$

$$\hat{u} \simeq -xs(1-y)\left[1-\frac{2k_T}{Q\sqrt{1-y}}\cdot\cos\varphi_q\right]$$

$$\hat{t} = -Q^2 = -xys, \quad where \quad s=(l+P)^2$$

$$d\sigma^{lp\to l'hX} \propto d\sigma^{lq\to lq} \propto \frac{\hat{s}^2+\hat{u}^2}{\hat{t}^2}$$

$$k_T \to \cos\varphi_q \to \cos\varphi_h$$

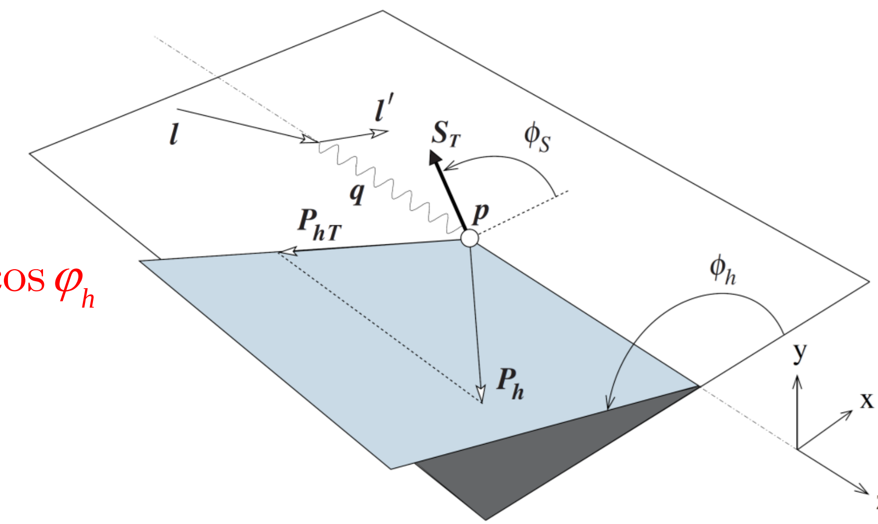

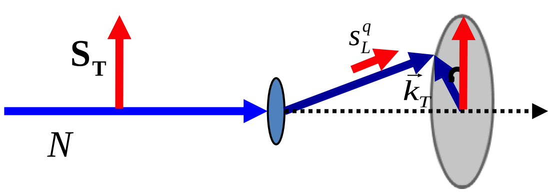

Cahn effect

$$\frac{d\sigma}{dxdydzdP_{hT}^2 d\varphi_h d\psi} = \left[\frac{\alpha}{xyQ^2}\frac{y^2}{2(1-\varepsilon)}\left(1+\frac{\gamma^2}{2x}\right)\right]\times\left(F_{UU,T}+\varepsilon F_{UU,L}\right)\times$$

$$1+\cos\phi_h\times\sqrt{2\varepsilon(1+\varepsilon)}A_{UU}^{\cos\phi_h}+\cos(2\phi_h)\times\varepsilon A_{UU}^{\cos(2\phi_h)}+\ldots$$

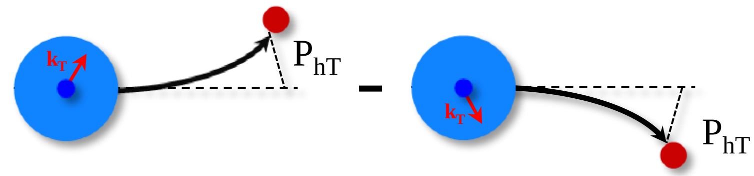

Cahn effect

***R. N. Cahn*, PLB 78 (1978)**

Kinematic effect: non-zero k_T induces an azimuthal modulation

$$\hat{s} \simeq xs\left[1-2\sqrt{1-y}\,\frac{k_T}{Q}\cdot\cos\varphi_q\right]+O\left(\frac{k_T^2}{Q^2}\right)$$

$$\hat{u} \simeq -xs(1-y)\left[1-\frac{2k_T}{Q\sqrt{1-y}}\cdot\cos\varphi_q\right]+O\left(\frac{k_T^2}{Q^2}\right)$$

$$\hat{t} = -Q^2 = -xys, \quad where \quad s=(l+P)^2$$

$$d\sigma^{lp\to l'hX} \propto d\sigma^{lq\to lq} \propto \frac{\hat{s}^2+\hat{u}^2}{\hat{t}^2}$$

$$k_T \to \cos\varphi_q \to \cos\varphi_h$$

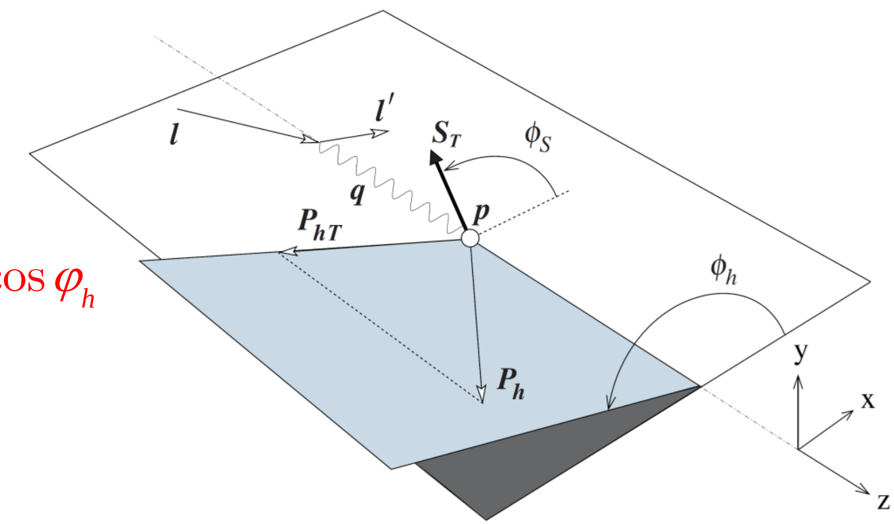

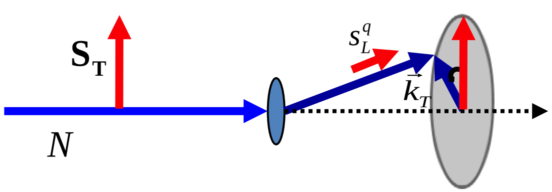

Nucleon spin *puzzle*

- 1964 Quark model 

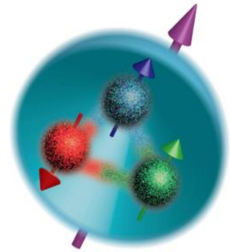

- 1969 Parton model 
- 1973 asymptotic freedom and QCD 

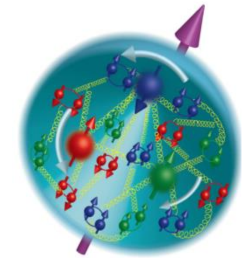

- 1978 intrinsic transverse motion of quarks and azimuthal asymmetries 

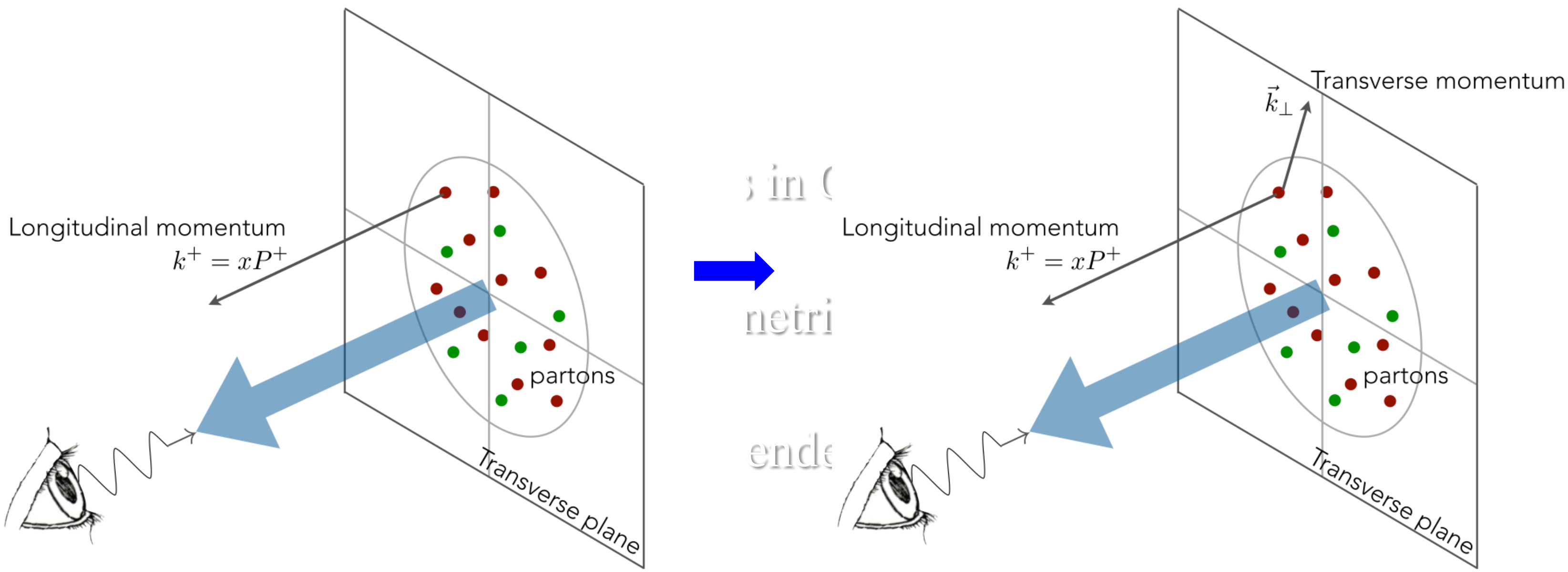

Nucleon spin *puzzle*

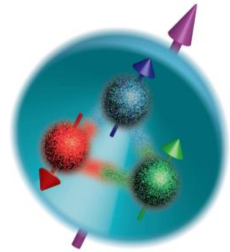

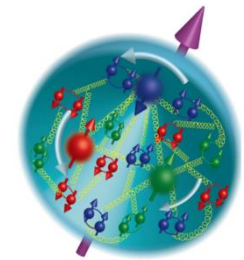

- 1964 Quark model 
- 1969 Parton model 
- 1973 asymptotic freedom and QCD 
- 1978 intrinsic transverse motion of quarks and azimuthal asymmetries 
- 1988 EMC measurement spin *puzzle* 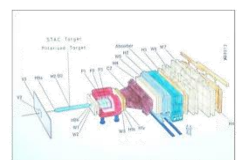

the spin sum rule

$$\frac{1}{2} = \frac{1}{2}\Delta\Sigma$$

- 1988 Factorization of Hard Processes in QCD

$$\Delta q = q^+ - q^-$$

$$\text{Proton: } \Delta u = \tfrac{4}{3} \quad \Delta d = -\tfrac{1}{3} \quad \Delta s = 0 \quad (\text{in } \hbar)$$

$$\Delta\Sigma = \Delta u + \Delta d + \Delta s = 1$$

- 90's spin dependent azimuthal asymmetries and TMDs
- Late 90's – present – future: spin dependent azimuthal asymmetry measurements

Nucleon spin *puzzle*

- 1964 Quark model  

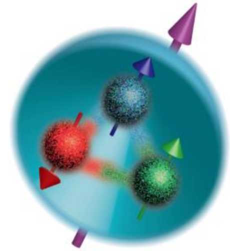

- 1969 Parton model 
- 1973 asymptotic freedom and QCD    

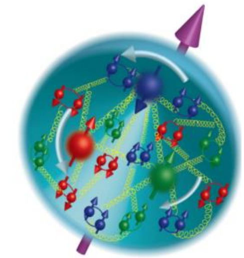

- 1978 intrinsic transverse motion of quarks and azimuthal asymmetries 
- 1988 EMC measurement spin *puzzle* 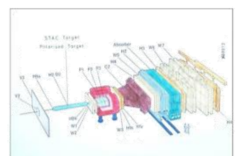

the spin sum rule

$$\frac{1}{2} = \frac{1}{2}\Delta\Sigma + \Delta G + L_q + L_g$$

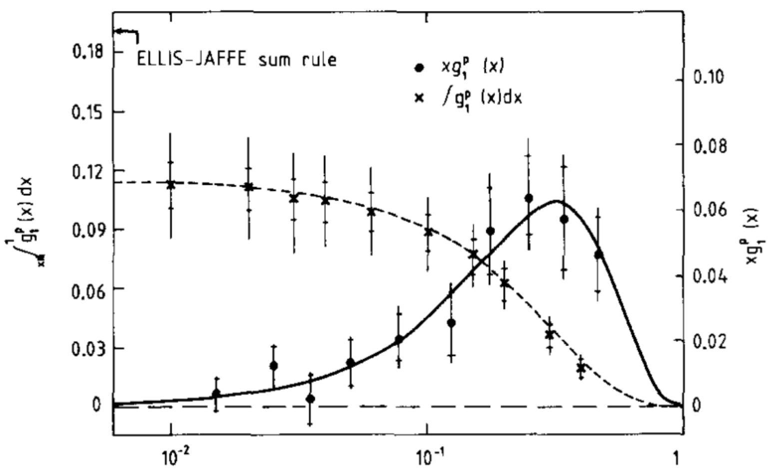

$\Delta q = q^+ - q^-$

Proton: $\Delta u = \frac{4}{3}$ $\Delta d = -\frac{1}{3}$ $\Delta s = 0$ (in $\hbar$)

$\Delta\Sigma = \Delta u + \Delta d + \Delta s = 1$

EMC 1988: $\Delta\Sigma \approx 0.12$ – spin crisis

Now: $\Delta\Sigma \approx 0.30$

ΔG – *small* (~0.1) *positive*

Orbital momentum – ?

Nucleon spin *puzzle*

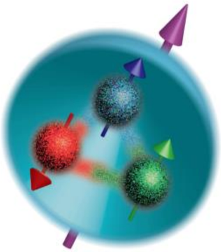

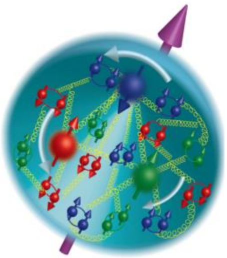

- 1964 Quark model  
- 1969 Parton model 
- 1973 asymptotic freedom and QCD    
- 1978 intrinsic transverse motion of quarks and azimuthal asymmetries 
- 1988 EMC measurement spin *puzzle* 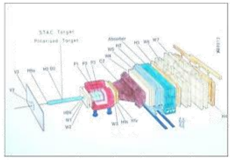

the spin sum rule

$$\frac{1}{2} = \frac{1}{2}\Delta\Sigma + \Delta G + L_q + L_g$$

- 1988 Factorization of Hard Processes in QCD     
- 90's spin dependent azimuthal asymmetries and TMDs
- Late 90's – present – future: spin dependent azimuthal asymmetry measurements

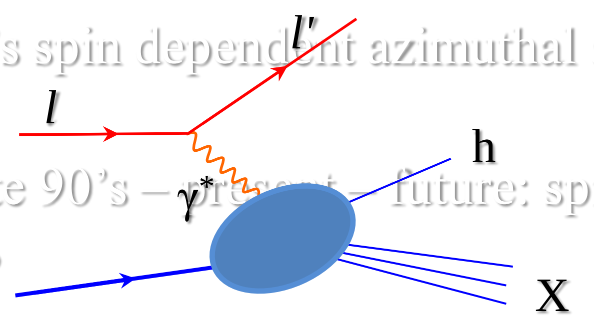

Nucleon spin *puzzle*

- 1964 Quark model

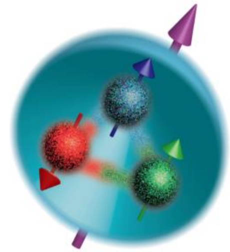

- 1969 Parton model

- 1973 asymptotic freedom and QCD

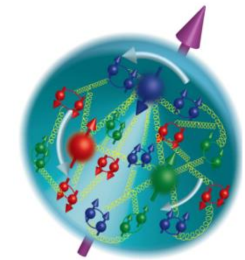

- 1978 intrinsic transverse motion of quarks and azimuthal asymmetries

- 1988 EMC measurement spin *puzzle*

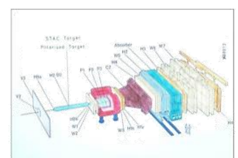

the spin sum rule

$$\frac{1}{2} = \frac{1}{2}\Delta\Sigma + \Delta G + L_q + L_g$$

- 1988 Factorization of Hard Processes in QCD

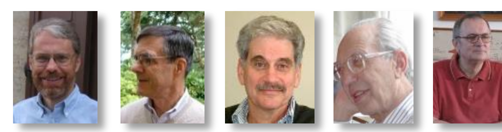

- 90's spin dependent azimuthal asymmetries and TMDs
- Late 90's – present – future: spin dependent azimuthal asymmetry measurements

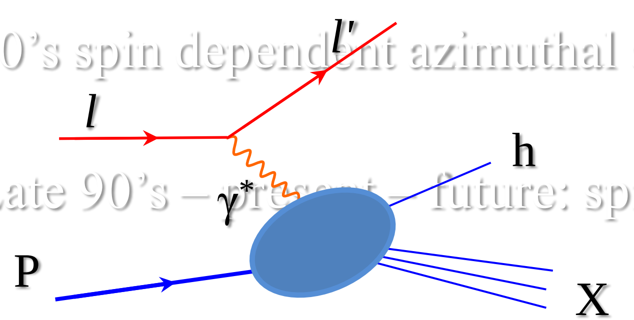

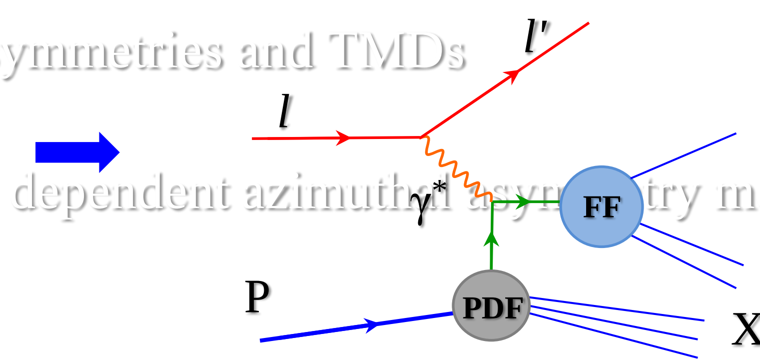

Experiments in last 35 years: part I

EMC CERN (μ-p, μ-d) @ 280 GeV

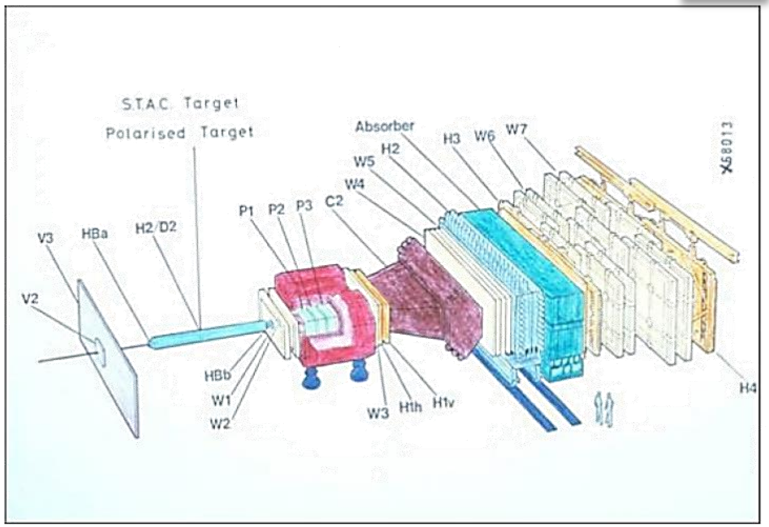

Fermilab E665 (μ-p, μ-d) @ 490 GeV

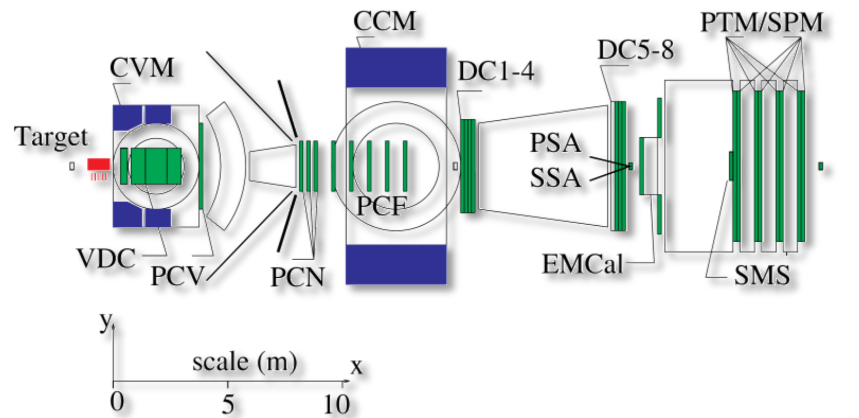

SLAC (e-p, e-d) @ 19.5 GeV

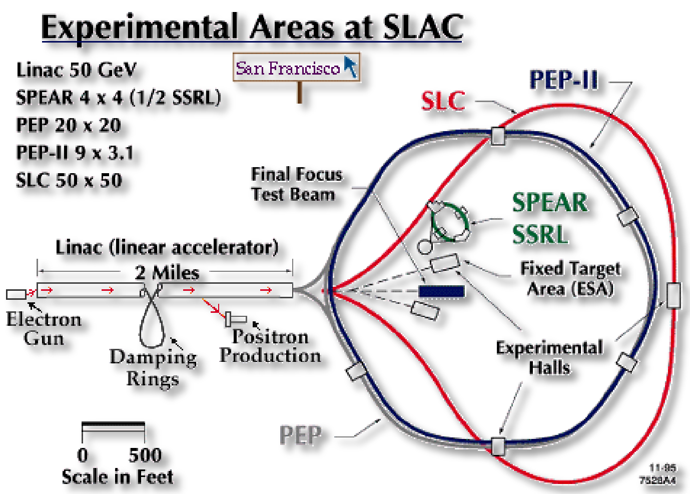

and e-p collider HERA, DESY

e-27.5 GeV: p-920 GeV, p-820 GeV

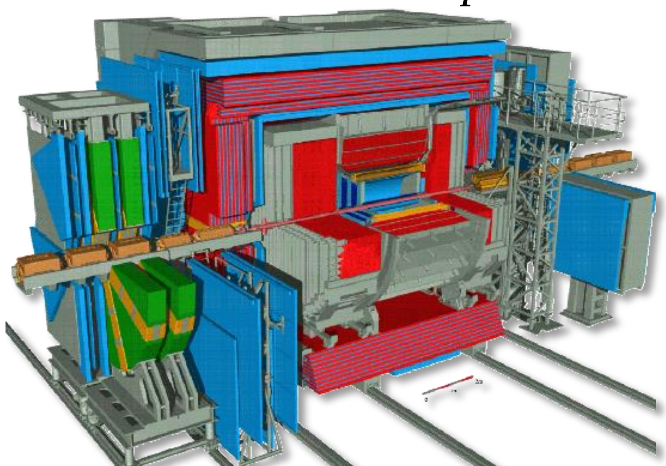

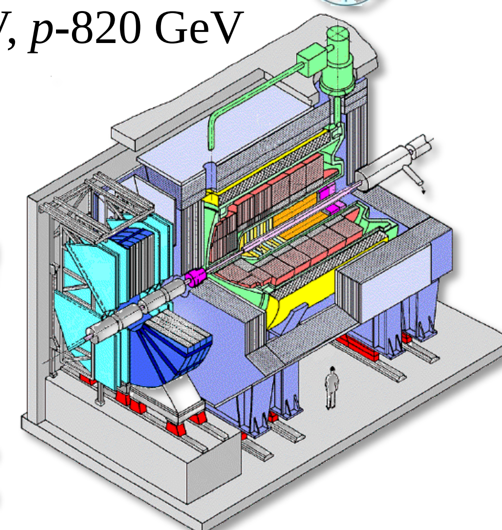

Jefferson Lab experimental halls

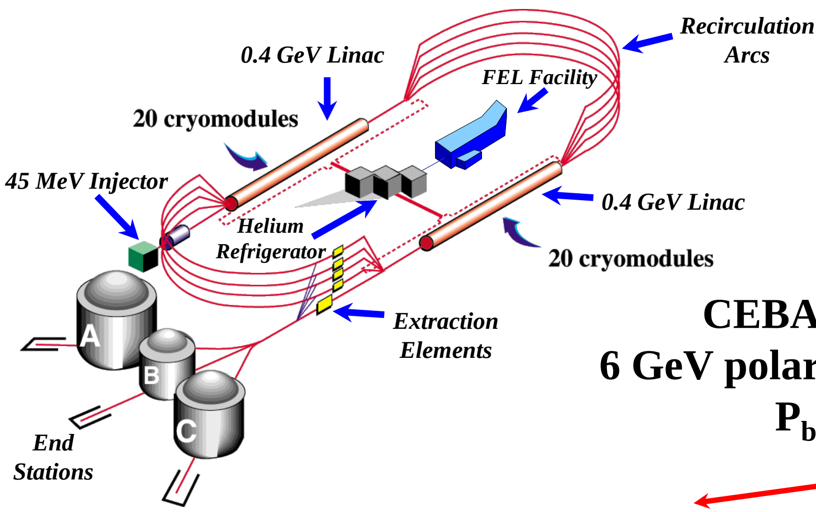

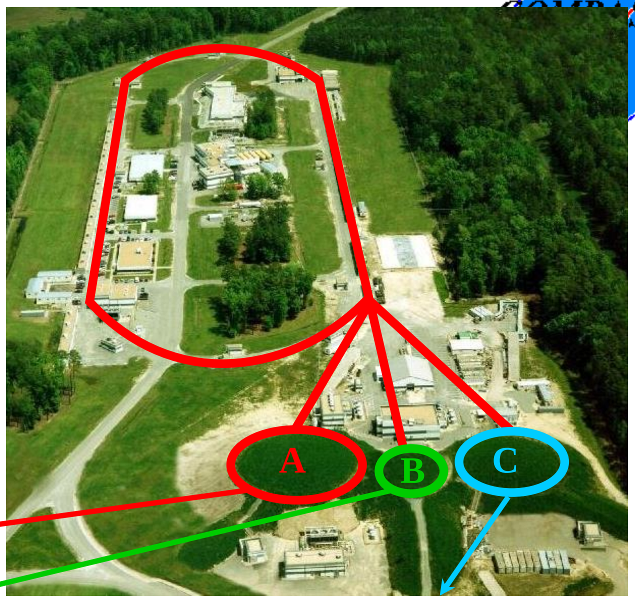

CEBAF accelerator
6 GeV polarized electron beam
$P_{beam} \approx 85\%$

Hall A: two HRS'

$^3\overrightarrow{He}$ gas target (40 cm)

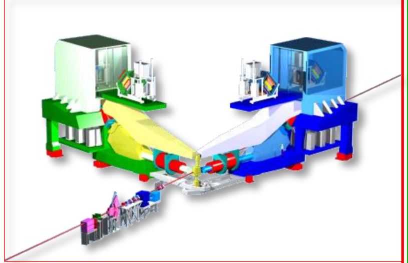

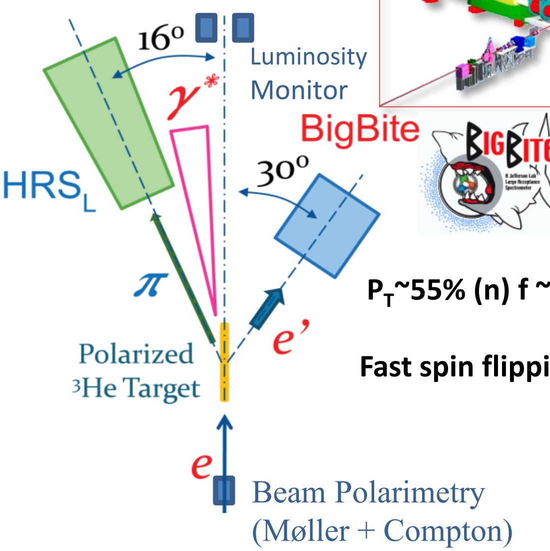

P_T~55% (n) f ~ 0.1-0.3

Fast spin flipping (30 Hz)

Hall B: CLAS

$N\vec{H}_3$ and $N\vec{D}_3$ HD-Ice targets

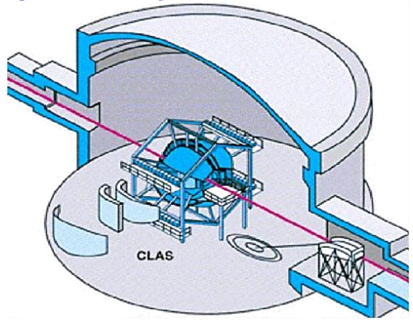

Polarizations
Beam: ~80%
NH_3 proton 80%
ND_3 ~30%
HD-Ice
(H-75%,D-25%)
f ~ 0.15

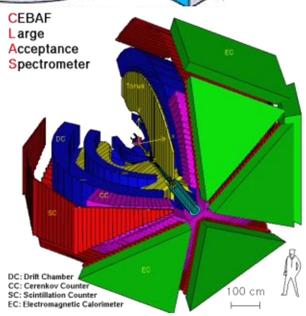

Hall C: HMS+SOS

$N\vec{H}_3$ and $N\vec{D}_3$ LiD targets

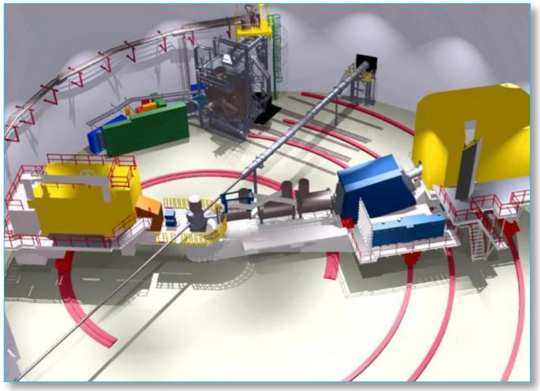

Polarizations
NH3: ~70-90% f ~ 0.15
ND3: ~30-50%
LiD: ~30 %

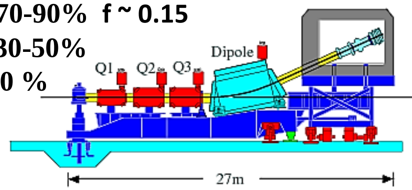

Experiments in last 35 years: first results

(SLAC) Phys. Rev. Lett. 31, 786 (1973)
(EMC) Phys. Lett. B 130 (1983) 118,
(EMC) Z. Phys. C34 (1987) 277
(EMC) Z. Phys. C52, 361 (1991).
(E665) Phys. Rev. D48 (1993) 5057
(ZEUS) Eur. Phys. J. C11, 251 (1999)
(ZEUS) Phys. Lett. B 481, 199 (2000)
(H1) Phys. Lett. B654, 148 (2007)

EMC, E665, H1 and ZEUS

High beam energy, broad kinematic range
No hadron type and charge distinction
(averaged over any possible flavor dependence)
EMC, ZEUS – only hydrogen target
E665 – combined hydrogen and deuterium targets
Not enough statistics to look at differential x-sections in more than two kinematic variables

SLAC, JLab hall C

Relatively low beam energy, restricted kinematic range
x-sections measured only at a few kinematic points

CLAS Collaboration (JLab hall B)

Relatively low beam energy
access to 4D multi-differential x-section

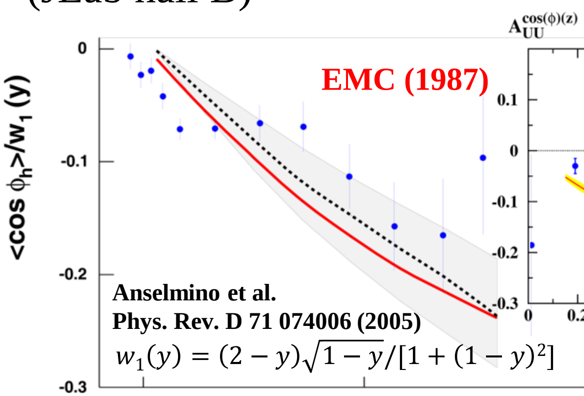

P. Schweitzer et al.
Phys. Rev. D 81, 094019

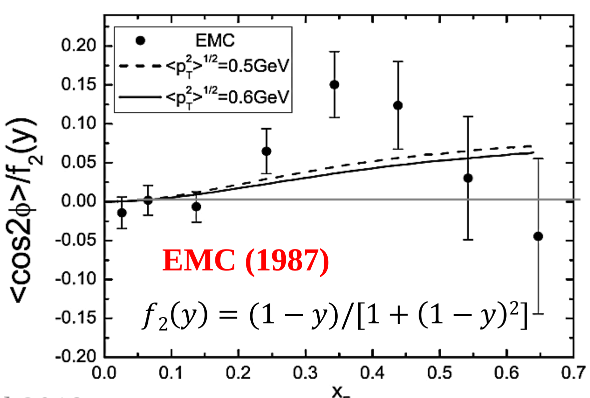

Experiments in last 35 years: first results

(SLAC) Phys. Rev. Lett. 31, 786 (1973)
(EMC) Phys. Lett. B 130 (1983) 118,
(EMC) Z. Phys. C34 (1987) 277
(EMC) Z. Phys. C52, 361 (1991).
(E665) Phys. Rev. D48 (1993) 5057
(ZEUS) Eur. Phys. J. C11, 251 (1999)
(ZEUS) Phys. Lett. B 481, 199 (2000)
(H1) Phys. Lett. B654, 148 (2007)

EMC, E665, H1 and ZEUS	High beam energy, broad kinematic range No hadron type and charge distinction (averaged over any possible flavor dependence) EMC, ZEUS – only hydrogen target E665 – combined hydrogen and deuterium targets Not enough statistics to look at differential x-sections in more than two kinematic variables
SLAC, JLab hall C	Relatively low beam energy, restricted kinematic range x-sections measured only at a few kinematic points
CLAS Collaboration (JLab hall B)	Relatively low beam energy access to 4D multi-differential x-section

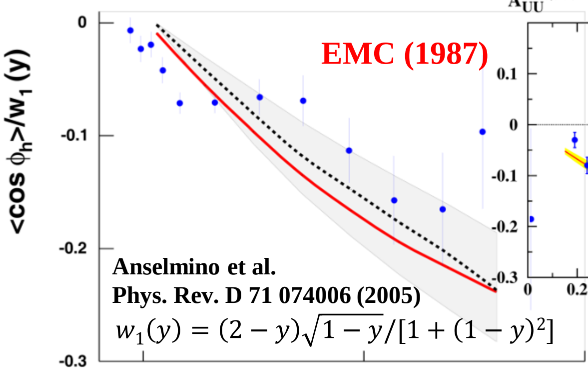

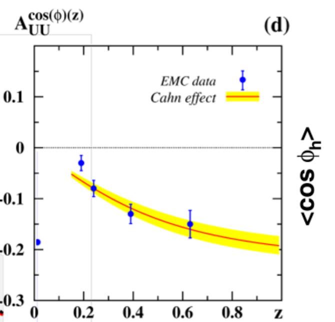

P. Schweitzer et al.
Phys. Rev. D 81, 094019

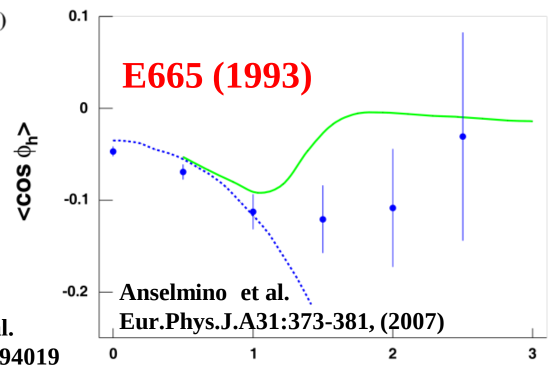

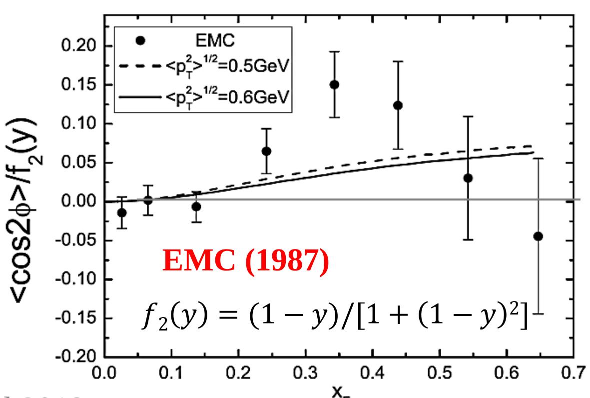

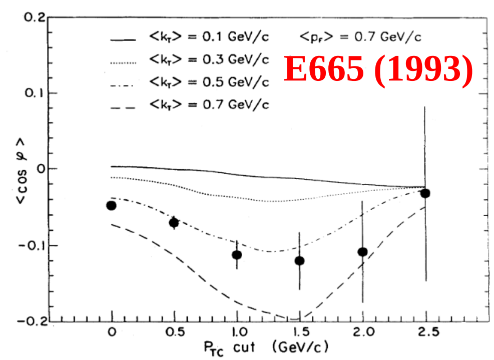

J. Chay, S. D. Ellis, and J. W. Stirling,
Phys. Rev. D 45, 46 (1992), Phys. Lett. B 269, 175 (1991).

Experiments in last 35 years: first results

(SLAC) Phys. Rev. Lett. 31, 786 (1973)
(EMC) Phys. Lett. B 130 (1983) 118,
(EMC) Z. Phys. C34 (1987) 277
(EMC) Z. Phys. C52, 361 (1991).
(E665) Phys. Rev. D48 (1993) 5057
(ZEUS) Eur. Phys. J. C11, 251 (1999)
(ZEUS) Phys. Lett. B 481, 199 (2000)
(H1) Phys. Lett. B654, 148 (2007)

EMC, E665, H1 and ZEUS	High beam energy, broad kinematic range No hadron type and charge distinction (averaged over any possible flavor dependence) EMC, ZEUS – only hydrogen target E665 – combined hydrogen and deuterium targets Not enough statistics to look at differential x-sections in more than two kinematic variables
SLAC, JLab hall C	Relatively low beam energy, restricted kinematic range x-sections measured only at a few kinematic points
CLAS Collaboration (JLab hall B)	Relatively low beam energy access to 4D multi-differential x-section

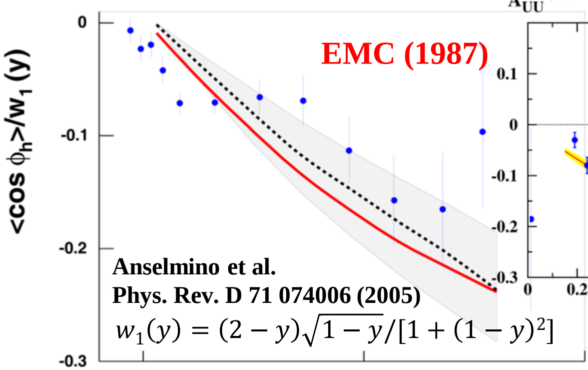

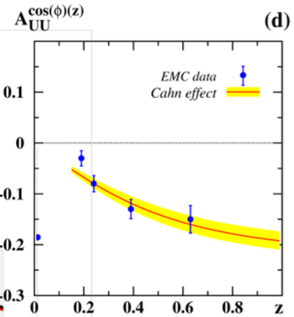

P. Schweitzer et al.
Phys. Rev. D 81, 094019

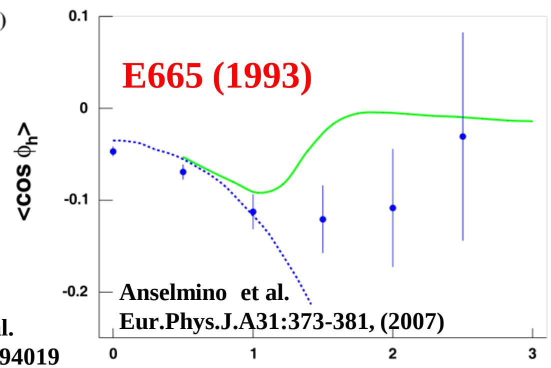

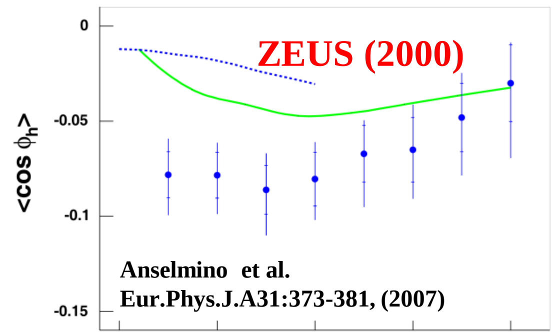

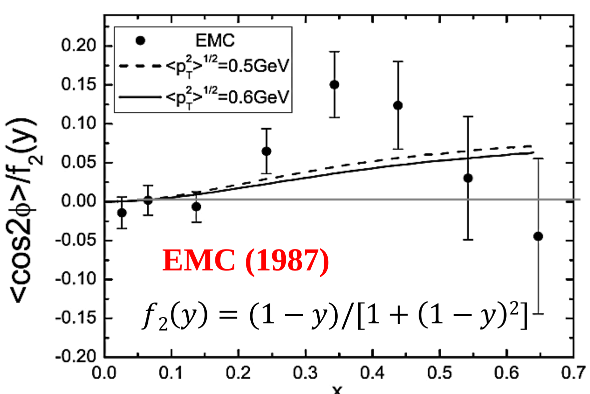

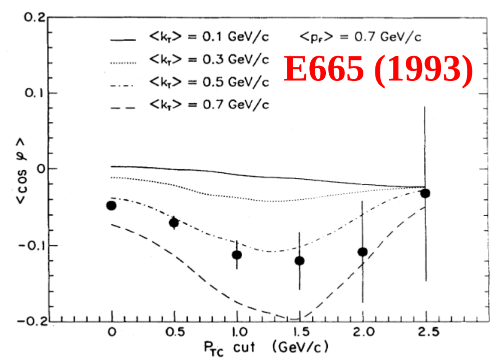

J. Chay, S. D. Ellis, and J. W. Stirling,
Phys. Rev. D 45, 46 (1992), Phys. Lett. B 269, 175 (1991).

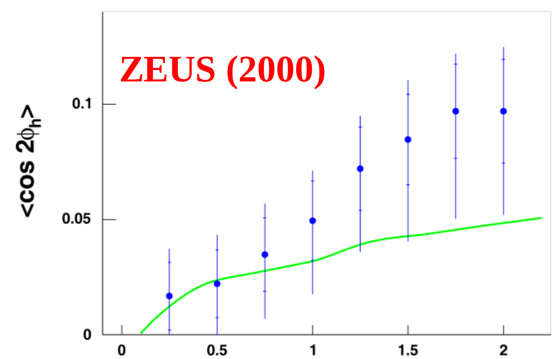

Anselmino et al.
Eur.Phys.J.A31:373-381, (2007)

P_T^{cut} (GeV/c)

CLAS (JLab hall B) results

M. Osipenko et al. (CLAS Collaboration)
Phys.Rev.D80:032004,2009

Positive pions

$1.4 < Q^2 < 7$ (GeV/c)^2
$0.15 < x < 1$
$0.07 < z < 1$
$0.005 < P_{hT}^2 < 1.5$ (GeV/c)^2
Beam energy 5.75 GeV

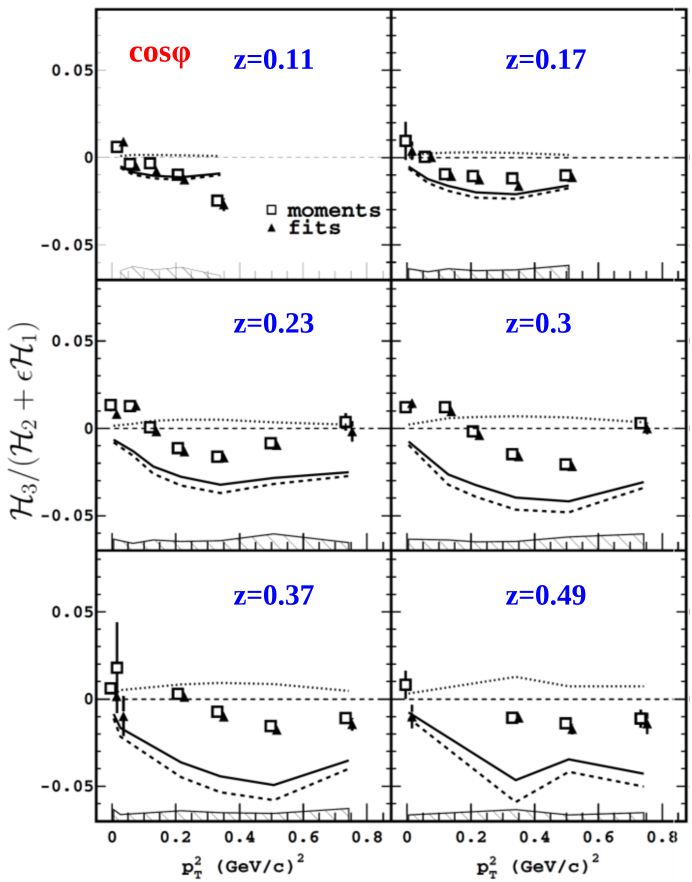

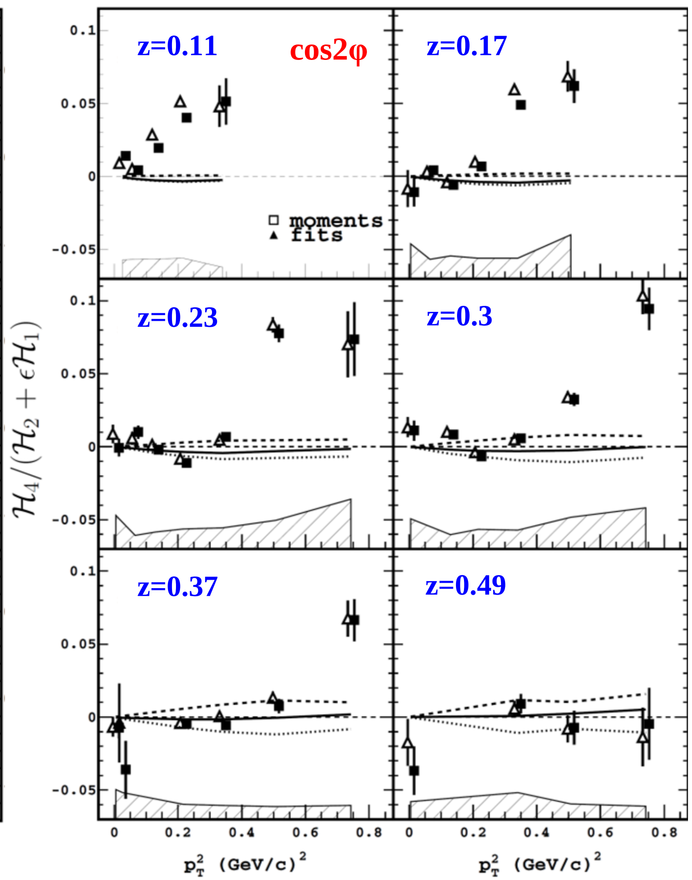

cosφ amplitude (nonzero)
is in strong disagreement with the theoretical predictions

cos2φ amplitude
is compatible with zero except low z region where it is positive

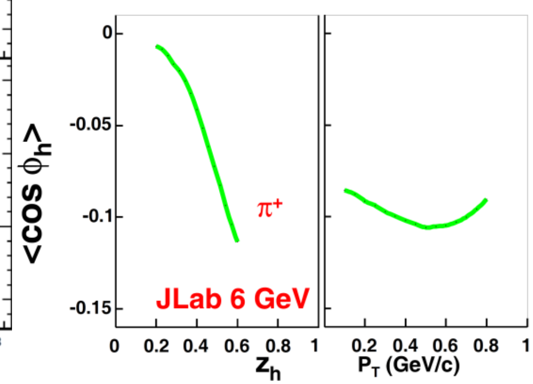

Curves for Cahn contribution only
Anselmino et al. Eur. Phys. J. A 31, 373-381 (2007)

Theoretical predictions: Cahn effect + Berger effect
***R. N. Cahn*, Phys. Rev. D40,** 3107 (1989).
***M. Anselmino et al.*, Phys. Rev. D71,** 074006 (2005).
***A. Brandenburg, V. V. Khoze, and D. Mueller*, Phys. Lett. B347,** 413 (1995).

Nucleon spin *puzzle*

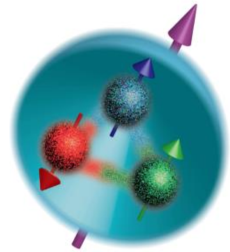

- 1964 Quark model

- 1969 Parton model

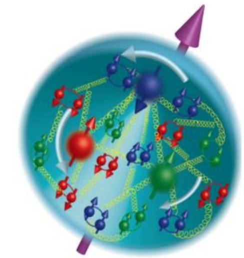

- 1973 asymptotic freedom and QCD

- 1978 intrinsic transverse motion of quarks and azimuthal asymmetries

- 1988 EMC measurement spin *puzzle*

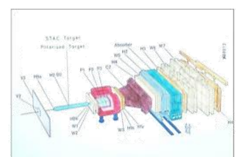

the spin sum rule

$$\frac{1}{2} = \frac{1}{2}\Delta\Sigma + \Delta G + L_q + L_g$$

- 1988 Factorization of Hard Processes in QCD

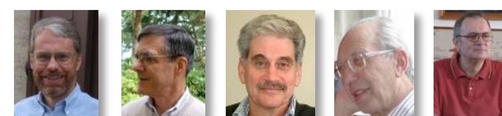

- 90's spin dependent azimuthal asymmetries and TMDs

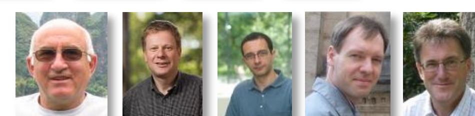

- Late 90's – present – future: spin dependent azimuthal asymmetry measurements

Nucleon spin *puzzle*

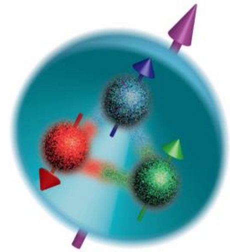

- 1964 Quark model 
- 1969 Parton model 
- 1973 asymptotic freedom and QCD 

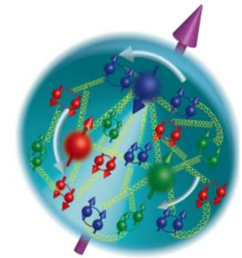

- 1978 intrinsic transverse motion of quarks and azimuthal asymmetries 
- 1988 EMC measurement spin *puzzle* 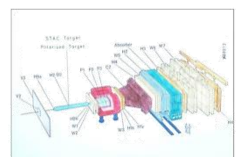

the spin sum rule

$$\frac{1}{2} = \frac{1}{2}\Delta\Sigma + \Delta G + L_q + L_g$$

- 1988 Factorization of Hard Processes in QCD 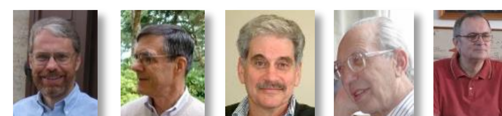
- 90's spin dependent azimuthal asymmetries and TMDs 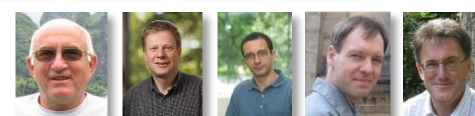
- Late 90's – present – future: spin dependent azimuthal asymmetry measurements

hermes COMPASS Jefferson Lab STAR PHENIX SeaQuest E906 AFTER panda NICA

SIDIS x-section

A.Kotzinian, Nucl. Phys. B441, 234 (1995).
Bacchetta, Diehl, Goeke, Metz, Mulders and Schlegel JHEP 0702:093 (2007).

All measured by COMPASS

$$\frac{d\sigma}{dx\,dy\,dz\,dp_T^2\,d\phi_h\,d\phi_S} = \left[\frac{\alpha}{xyQ^2}\frac{y^2}{2(1-\varepsilon)}\left(1+\frac{\gamma^2}{2x}\right)\right]\left(F_{UU,T}+\varepsilon F_{UU,L}\right)$$

$$\times\left\{\begin{array}{l}
1+\sqrt{2\varepsilon(1+\varepsilon)}A_{UU}^{\cos\phi_h}\cos\phi_h+\varepsilon A_{UU}^{\cos 2\phi_h}\cos 2\phi_h \\
+\ \lambda\sqrt{2\varepsilon(1-\varepsilon)}A_{LU}^{\sin\phi_h}\sin\phi_h \\
+\ S_L\left[\sqrt{2\varepsilon(1+\varepsilon)}A_{UL}^{\sin\phi_h}\sin\phi_h+\varepsilon A_{UL}^{\sin 2\phi_h}\sin 2\phi_h\right] \\
+\ S_L\lambda\left[\sqrt{1-\varepsilon^2}A_{LL}+\sqrt{2\varepsilon(1-\varepsilon)}A_{LL}^{\cos\phi_h}\cos\phi_h\right] \\
+\ S_T\left[\begin{array}{l}
A_{UT}^{\sin(\phi_h-\phi_S)}\sin(\phi_h-\phi_S) \\
+\ \varepsilon A_{UT}^{\sin(\phi_h+\phi_S)}\sin(\phi_h+\phi_S) \\
+\ \varepsilon A_{UT}^{\sin(3\phi_h-\phi_S)}\sin(3\phi_h-\phi_S) \\
+\ \sqrt{2\varepsilon(1+\varepsilon)}A_{UT}^{\sin\phi_S}\sin\phi_S \\
+\ \sqrt{2\varepsilon(1+\varepsilon)}A_{UT}^{\sin(2\phi_h-\phi_S)}\sin(2\phi_h-\phi_S)
\end{array}\right] \\
+\ S_T\lambda\left[\begin{array}{l}
\sqrt{(1-\varepsilon^2)}A_{LT}^{\cos(\phi_h-\phi_S)}\cos(\phi_h-\phi_S) \\
+\ \sqrt{2\varepsilon(1-\varepsilon)}A_{LT}^{\cos\phi_S}\cos\phi_S \\
+\ \sqrt{2\varepsilon(1-\varepsilon)}A_{LT}^{\cos(2\phi_h-\phi_S)}\cos(2\phi_h-\phi_S)
\end{array}\right]
\end{array}\right\}$$

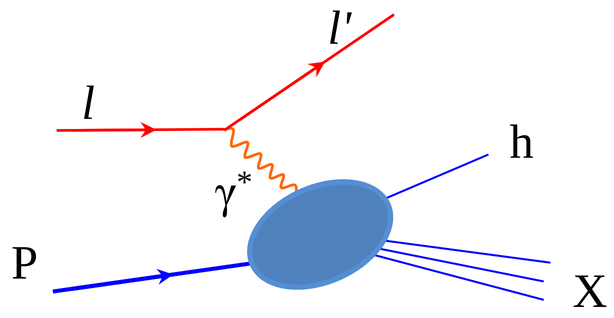

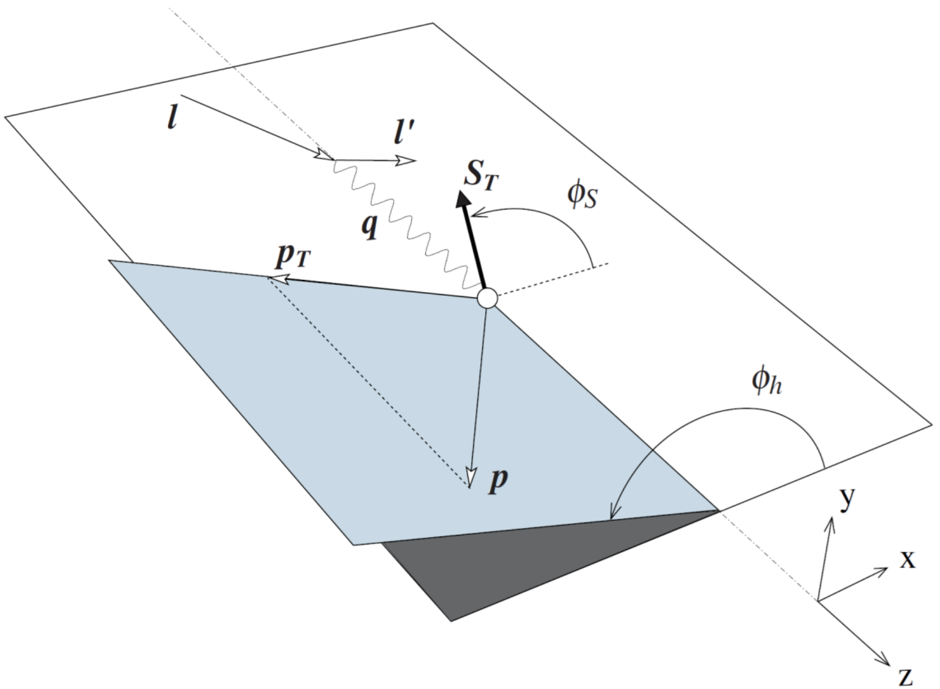

$$A_{U(L),T}^{w(\varphi_h,\varphi_s)}=\frac{F_{U(L),T}^{w(\varphi_h,\varphi_s)}}{F_{UU,T}+\varepsilon F_{UU,L}};\quad \varepsilon=\frac{1-y-\frac{1}{4}\gamma^2y^2}{1-y+\frac{1}{2}y^2+\frac{1}{4}\gamma^2y^2},\quad \gamma=\frac{2Mx}{Q}$$

SIDIS x-section and TMDs at twist-2

All measured by COMPASS

$$\frac{d\sigma}{dxdydzdp_T^2 d\phi_h d\phi_S} = \left[\frac{\alpha}{xyQ^2}\frac{y^2}{2(1-\varepsilon)}\left(1+\frac{\gamma^2}{2x}\right)\right]\left(F_{UU,T}+\varepsilon F_{UU,L}\right)$$

$$\times \left\{ \begin{array}{l} 1+\sqrt{2\varepsilon(1+\varepsilon)}A_{UU}^{\cos\phi_h}\cos\phi_h+\varepsilon A_{UU}^{\cos 2\phi_h}\cos 2\phi_h \\ +\lambda\sqrt{2\varepsilon(1-\varepsilon)}A_{LU}^{\sin\phi_h}\sin\phi_h \\ +S_L\left[\sqrt{2\varepsilon(1+\varepsilon)}A_{UL}^{\sin\phi_h}\sin\phi_h+\varepsilon A_{UL}^{\sin 2\phi_h}\sin 2\phi_h\right] \\ +S_L\lambda\left[\sqrt{1-\varepsilon^2}A_{LL}+\sqrt{2\varepsilon(1-\varepsilon)}A_{LL}^{\cos\phi_h}\cos\phi_h\right] \\ +S_T\left[\begin{array}{l} A_{UT}^{\sin(\phi_h-\phi_S)}\sin(\phi_h-\phi_S) \\ +\varepsilon A_{UT}^{\sin(\phi_h+\phi_S)}\sin(\phi_h+\phi_S) \\ +\varepsilon A_{UT}^{\sin(3\phi_h-\phi_S)}\sin(3\phi_h-\phi_S) \\ +\sqrt{2\varepsilon(1+\varepsilon)}A_{UT}^{\sin\phi_S}\sin\phi_S \\ +\sqrt{2\varepsilon(1+\varepsilon)}A_{UT}^{\sin(2\phi_h-\phi_S)}\sin(2\phi_h-\phi_S) \end{array}\right] \\ +S_T\lambda\left[\begin{array}{l} \sqrt{(1-\varepsilon^2)}A_{LT}^{\cos(\phi_h-\phi_S)}\cos(\phi_h-\phi_S) \\ +\sqrt{2\varepsilon(1-\varepsilon)}A_{LT}^{\cos\phi_S}\cos\phi_S \\ +\sqrt{2\varepsilon(1-\varepsilon)}A_{LT}^{\cos(2\phi_h-\phi_S)}\cos(2\phi_h-\phi_S) \end{array}\right] \end{array} \right\}$$

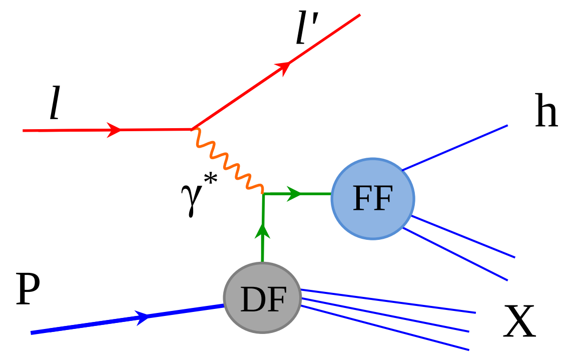

Nucleon \ Quark	U	L	T
U	$f_1^q(x,\boldsymbol{k}_T^2)$ **number density**		$h_1^{\perp q}(x,\boldsymbol{k}_T^2)$ **Boer-Mulders**
L		$g_1^q(x,\boldsymbol{k}_T^2)$ **helicity**	$h_{1L}^{\perp q}(x,\boldsymbol{k}_T^2)$ **worm-gear L**
T	$f_{1T}^{\perp q}(x,\boldsymbol{k}_T^2)$ **Sivers**	$g_{1T}^q(x,\boldsymbol{k}_T^2)$ **Kotzinian-Mulders worm-gear T**	$h_1^q(x,\boldsymbol{k}_T^2)$ **transversity** $h_{1T}^{\perp q}(x,\boldsymbol{k}_T^2)$ **pretzelosity**

+ two FFs: $D_{1q}^h(z,P_\perp^2)$ and $H_{1q}^{\perp h}(z,P_\perp^2)$

SIDIS x-section and TMDs at twist-2

All measured by COMPASS

$$\frac{d\sigma}{dx\,dy\,dz\,dp_T^2\,d\phi_h\,d\phi_S} = \left[\frac{\alpha}{xyQ^2}\frac{y^2}{2(1-\varepsilon)}\left(1+\frac{\gamma^2}{2x}\right)\right]\left(F_{UU,T}+\varepsilon F_{UU,L}\right)$$

$$\times \left\{ \begin{array}{l} 1+\sqrt{2\varepsilon(1+\varepsilon)}A_{UU}^{\cos\phi_h}\cos\phi_h+\varepsilon A_{UU}^{\cos 2\phi_h}\cos 2\phi_h \\ +\lambda\sqrt{2\varepsilon(1-\varepsilon)}A_{LU}^{\sin\phi_h}\sin\phi_h \\ +S_L\left[\sqrt{2\varepsilon(1+\varepsilon)}A_{UL}^{\sin\phi_h}\sin\phi_h+\varepsilon A_{UL}^{\sin 2\phi_h}\sin 2\phi_h\right] \\ +S_L\lambda\left[\sqrt{1-\varepsilon^2}A_{LL}+\sqrt{2\varepsilon(1-\varepsilon)}A_{LL}^{\cos\phi_h}\cos\phi_h\right] \\ +S_T\left[\begin{array}{l} A_{UT}^{\sin(\phi_h-\phi_S)}\sin(\phi_h-\phi_S) \\ +\varepsilon A_{UT}^{\sin(\phi_h+\phi_S)}\sin(\phi_h+\phi_S) \\ +\varepsilon A_{UT}^{\sin(3\phi_h-\phi_S)}\sin(3\phi_h-\phi_S) \\ +\sqrt{2\varepsilon(1+\varepsilon)}A_{UT}^{\sin\phi_S}\sin\phi_S \\ +\sqrt{2\varepsilon(1+\varepsilon)}A_{UT}^{\sin(2\phi_h-\phi_S)}\sin(2\phi_h-\phi_S) \end{array}\right] \\ +S_T\lambda\left[\begin{array}{l} \sqrt{(1-\varepsilon^2)}A_{LT}^{\cos(\phi_h-\phi_S)}\cos(\phi_h-\phi_S) \\ +\sqrt{2\varepsilon(1-\varepsilon)}A_{LT}^{\cos\phi_S}\cos\phi_S \\ +\sqrt{2\varepsilon(1-\varepsilon)}A_{LT}^{\cos(2\phi_h-\phi_S)}\cos(2\phi_h-\phi_S) \end{array}\right] \end{array} \right\}$$

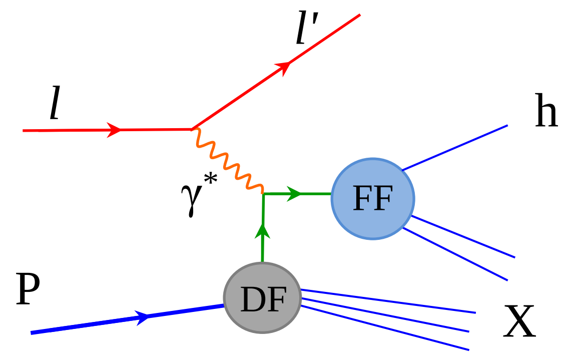

Nucleon \ Quark	U	L	T
U	number density		Boer-Mulders
L		helicity	worm-gear L
T	Sivers	Kotzinian-Mulders worm-gear T	transversity pretzelosity

spin of the nucleon — spin of the quark — k_T

SIDIS x-section and TMDs at twist-2

All measured by COMPASS

$$\frac{d\sigma}{dx\,dy\,dz\,dp_T^2\,d\phi_h\,d\phi_S} = \left[\frac{\alpha}{xyQ^2}\frac{y^2}{2(1-\varepsilon)}\left(1+\frac{\gamma^2}{2x}\right)\right]\left(F_{UU,T}+\varepsilon F_{UU,L}\right)$$

$$\times\left\{\begin{array}{l}
1+\sqrt{2\varepsilon(1+\varepsilon)}A_{UU}^{\cos\phi_h}\cos\phi_h+\varepsilon A_{UU}^{\cos 2\phi_h}\cos 2\phi_h \\
+\lambda\sqrt{2\varepsilon(1-\varepsilon)}A_{LU}^{\sin\phi_h}\sin\phi_h \\
+S_L\left[\sqrt{2\varepsilon(1+\varepsilon)}A_{UL}^{\sin\phi_h}\sin\phi_h+\varepsilon A_{UL}^{\sin 2\phi_h}\sin 2\phi_h\right] \\
+S_L\lambda\left[\sqrt{1-\varepsilon^2}A_{LL}+\sqrt{2\varepsilon(1-\varepsilon)}A_{LL}^{\cos\phi_h}\cos\phi_h\right] \\
+S_T\left[\begin{array}{l}
A_{UT}^{\sin(\phi_h-\phi_S)}\sin(\phi_h-\phi_S) \\
+\varepsilon A_{UT}^{\sin(\phi_h+\phi_S)}\sin(\phi_h+\phi_S) \\
+\varepsilon A_{UT}^{\sin(3\phi_h-\phi_S)}\sin(3\phi_h-\phi_S) \\
+\sqrt{2\varepsilon(1+\varepsilon)}A_{UT}^{\sin\phi_S}\sin\phi_S \\
+\sqrt{2\varepsilon(1+\varepsilon)}A_{UT}^{\sin(2\phi_h-\phi_S)}\sin(2\phi_h-\phi_S)
\end{array}\right] \\
+S_T\lambda\left[\begin{array}{l}
\sqrt{(1-\varepsilon^2)}A_{LT}^{\cos(\phi_h-\phi_S)}\cos(\phi_h-\phi_S) \\
+\sqrt{2\varepsilon(1-\varepsilon)}A_{LT}^{\cos\phi_S}\cos\phi_S \\
+\sqrt{2\varepsilon(1-\varepsilon)}A_{LT}^{\cos(2\phi_h-\phi_S)}\cos(2\phi_h-\phi_S)
\end{array}\right]
\end{array}\right\}$$

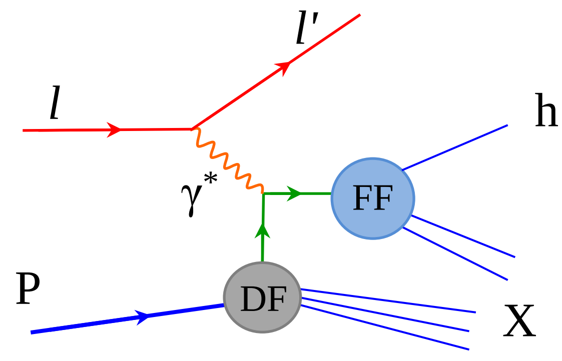

$$A_{UT}^{\sin(\phi_h-\phi_s)} \propto f_{1T}^{\perp q}\otimes D_{1q}^{h}$$

$$A_{UT}^{\sin(\phi_h+\phi_s)} \propto h_1^{q}\otimes H_{1q}^{\perp h}$$

$$A_{UT}^{\sin(3\phi_h-\phi_s)} \propto h_{1T}^{\perp q}\otimes H_{1q}^{\perp h}$$

$$A_{UT}^{\sin(\phi_s)} \overset{WW}{\propto} Q^{-1}\left(h_1^{q}\otimes H_{1q}^{\perp h}+f_{1T}^{\perp q}\otimes D_{1q}^{h}+\ldots\right)$$

$$A_{UT}^{\sin(2\phi_h-\phi_s)} \overset{WW}{\propto} Q^{-1}\left(h_{1T}^{\perp q}\otimes H_{1q}^{\perp h}+f_{1T}^{\perp q}\otimes D_{1q}^{h}+\ldots\right)$$

$$A_{LT}^{\cos(\phi_h-\phi_s)} \propto g_{1T}^{q}\otimes D_{1q}^{h}$$

$$A_{LT}^{\cos(\phi_s)} \overset{WW}{\propto} Q^{-1}\left(g_{1T}^{q}\otimes D_{1q}^{h}+\ldots\right)$$

$$A_{LT}^{\cos(2\phi_h-\phi_s)} \overset{WW}{\propto} Q^{-1}\left(g_{1T}^{q}\otimes D_{1q}^{h}+\ldots\right)$$

Twist-2

Twist-3

Boer-Mulders effect

$$\frac{d\sigma}{dxdydzdP_{hT}^2 d\varphi_h d\psi} = \left[\frac{\alpha}{xyQ^2}\frac{y^2}{2(1-\varepsilon)}\left(1+\frac{\gamma^2}{2x}\right)\right] \times \left(F_{UU,T} + \varepsilon F_{UU,L}\right) \times$$

$$1 + \cos\varphi_h \times \sqrt{2\varepsilon(1+\varepsilon)} A_{UU}^{\cos\varphi_h} + \underbrace{\cos(2\varphi_h) \times \varepsilon A_{UU}^{\cos(2\varphi_h)}} + \ldots$$


Boer-Mulders effect

***D. Boer and P. J. Mulders*, PRD 57 (1998)**

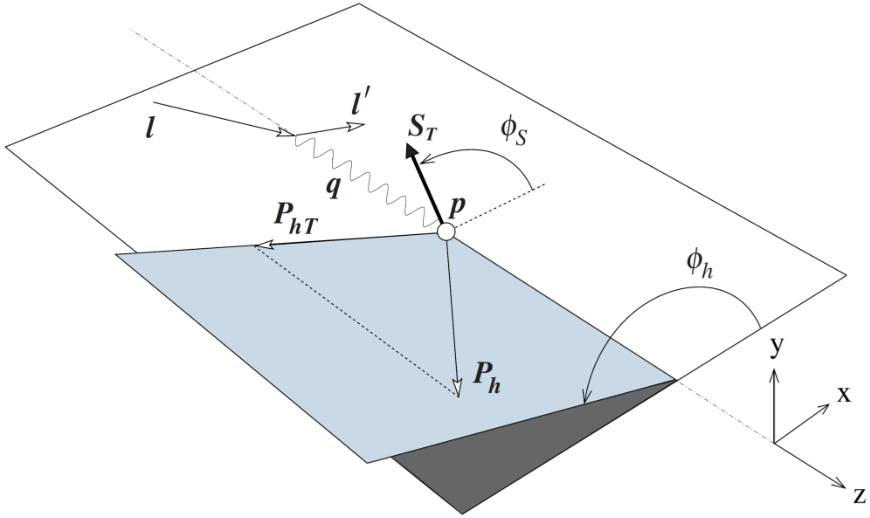

Boer-Mulders effect

Bacchetta, Diehl, Goeke, Metz, Mulders and Schlegel JHEP 0702:093 (2007).

$$\frac{d\sigma}{dxdydzdP_{hT}^2 d\varphi_h d\psi} = \left[\frac{\alpha}{xyQ^2}\frac{y^2}{2(1-\varepsilon)}\left(1+\frac{\gamma^2}{2x}\right)\right]\times\left(F_{UU,T}+\varepsilon F_{UU,L}\right)\times$$

$$1+\cos\varphi_h \times \sqrt{2\varepsilon(1+\varepsilon)}A_{UU}^{\cos\varphi_h} + \cos(2\varphi_h)\times\varepsilon A_{UU}^{\cos(2\varphi_h)} + \ldots$$

Boer-Mulders-Collins effect

***D. Boer and P. J. Mulders*, PRD 57 (1998)**

Boer-Mulders PDF   Collins FF

$$F_{UU}^{\cos 2\phi_h} = C\left\{-\frac{2\left(\hat{\boldsymbol{h}}\cdot\boldsymbol{p}_T\right)\left(\hat{\boldsymbol{h}}\cdot\boldsymbol{k}_T\right)-\boldsymbol{p}_T\cdot\boldsymbol{k}_T}{MM_h}h_1^{\perp q}H_{1q}^{\perp h}\right\}$$

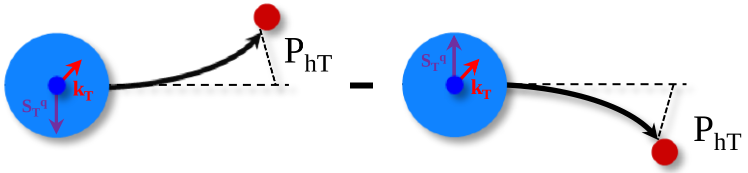

Arises due to the correlations between quark transverse spin and intrinsic transverse momentum

Is a leading order effect

Boer-Mulders effect

Bacchetta, Diehl, Goeke, Metz, Mulders and Schlegel JHEP 0702:093 (2007).

$$\frac{d\sigma}{dxdydzdP_{hT}^2 d\varphi_h d\psi} = \left[\frac{\alpha}{xyQ^2}\frac{y^2}{2(1-\varepsilon)}\left(1+\frac{\gamma^2}{2x}\right)\right]\times\left(F_{UU,T}+\varepsilon F_{UU,L}\right)\times$$

$$1+\cos\varphi_h\times\sqrt{2\varepsilon(1+\varepsilon)}A_{UU}^{\cos\varphi_h}+\cos(2\varphi_h)\times\varepsilon A_{UU}^{\cos(2\varphi_h)}+\ldots$$

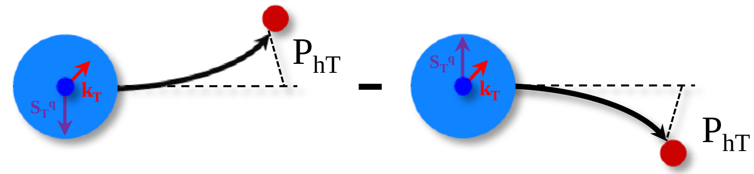

Arises due to the correlations between quark transverse spin and intrinsic transverse momentum

Boer-Mulders-Collins effect

***D. Boer and P. J. Mulders*, PRD 57 (1998)**

Boer-Mulders PDF Collins FF

Cahn effect

$$F_{UU}^{\cos 2\phi_h} = C\left\{-\frac{2(\hat{\boldsymbol{h}}\cdot\boldsymbol{p}_T)(\hat{\boldsymbol{h}}\cdot\boldsymbol{k}_T)-\boldsymbol{p}_T\cdot\boldsymbol{k}_T}{MM_h}h_1^{\perp q}H_{1q}^{\perp h}\right\}$$

$$F_{UU}^{\cos 2\phi_h} = C\left\{-\frac{2(\hat{\boldsymbol{h}}\cdot\boldsymbol{p}_T)(\hat{\boldsymbol{h}}\cdot\boldsymbol{k}_T)-\boldsymbol{p}_T\cdot\boldsymbol{k}_T}{MM_h}h_1^{\perp q}H_{1q}^{\perp h}\right\}+\left(\frac{M}{Q}\right)^2 C\left\{-\frac{2(\hat{\boldsymbol{h}}\cdot\boldsymbol{k}_T)^2-k_T^2}{M^2}f_1^q D_{1q}^h+\ldots\right\}$$

Boer-Mulders effect + twist-4 Cahn effect

Boer-Mulders effect

Bacchetta, Diehl, Goeke, Metz, Mulders and Schlegel JHEP 0702:093 (2007).

$$\frac{d\sigma}{dxdydzdP_{hT}^2 d\varphi_h d\psi} = \left[\frac{\alpha}{xyQ^2}\frac{y^2}{2(1-\varepsilon)}\left(1+\frac{\gamma^2}{2x}\right)\right]\times\left(F_{UU,T}+\varepsilon F_{UU,L}\right)\times$$

$$1+\cos\varphi_h\times\sqrt{2\varepsilon(1+\varepsilon)}A_{UU}^{\cos\varphi_h}+\cos(2\varphi_h)\times\varepsilon A_{UU}^{\cos(2\varphi_h)}+\ldots$$

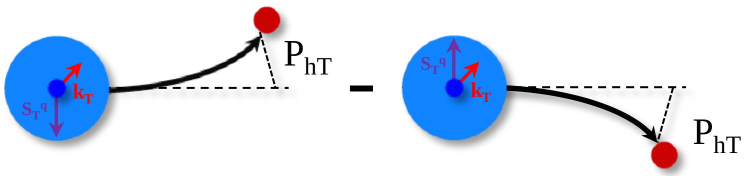

Arises due to the correlations between quark transverse spin and intrinsic transverse momentum

Boer-Mulders-Collins effect

***D. Boer and P. J. Mulders*, PRD 57 (1998)**

Boer-Mulders PDF Collins FF

Cahn effect

$$F_{UU}^{\cos 2\phi_h} = C\left\{-\frac{2(\hat{h}\cdot p_T)(\hat{h}\cdot k_T)-p_T\cdot k_T}{MM_h}h_1^{\perp q}H_{1q}^{\perp h}\right\}$$

$$F_{UU}^{\cos 2\phi_h} = C\left\{-\frac{2(\hat{h}\cdot p_T)(\hat{h}\cdot k_T)-p_T\cdot k_T}{MM_h}h_1^{\perp q}H_{1q}^{\perp h}\right\}+\left(\frac{M}{Q}\right)^2 C\left\{-\frac{2(\hat{h}\cdot k_T)^2-k_T^2}{M^2}f_1^q D_{1q}^h+\ldots\right\}$$

Boer-Mulders effect + twist-4 Cahn effect

can be accessed also through DY

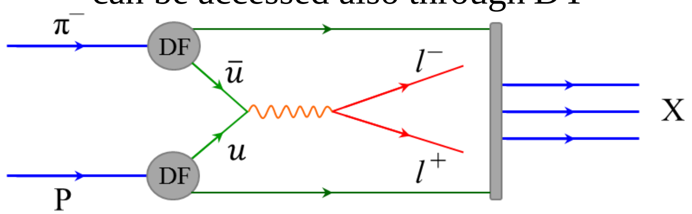

SIDIS hermes COMPASS …

e^+e^- BELLE BABAR

COMPASS bridge

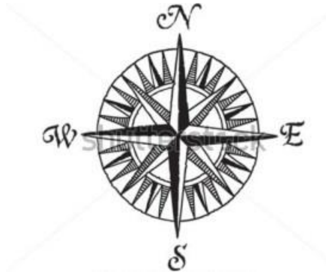

SIDIS and single-polarized DY x-sections

SIDIS

$$\frac{d\sigma}{dx\,dy\,dz\,dp_T^2\,d\phi_h\,d\phi_S} = \left[\frac{\alpha}{xyQ^2}\frac{y^2}{2(1-\varepsilon)}\left(1+\frac{\gamma^2}{2x}\right)\right]\left(F_{UU,T}+\varepsilon F_{UU,L}\right)$$

$$\times\left\{\begin{array}{l}
1+\sqrt{2\varepsilon(1+\varepsilon)}A_{UU}^{\cos\phi_h}\cos\phi_h+\varepsilon A_{UU}^{\cos 2\phi_h}\cos 2\phi_h \\
+\ \lambda\sqrt{2\varepsilon(1-\varepsilon)}A_{LU}^{\sin\phi_h}\sin\phi_h \\
+\ S_L\left[\sqrt{2\varepsilon(1+\varepsilon)}A_{UL}^{\sin\phi_h}\sin\phi_h+\varepsilon A_{UL}^{\sin 2\phi_h}\sin 2\phi_h\right] \\
+\ S_L\lambda\left[\sqrt{1-\varepsilon^2}A_{LL}+\sqrt{2\varepsilon(1-\varepsilon)}A_{LL}^{\cos\phi_h}\cos\phi_h\right] \\
+\ S_T\left[\begin{array}{l}
A_{UT}^{\sin(\phi_h-\phi_S)}\sin(\phi_h-\phi_S) \\
+\ \varepsilon A_{UT}^{\sin(\phi_h+\phi_S)}\sin(\phi_h+\phi_S) \\
+\ \varepsilon A_{UT}^{\sin(3\phi_h-\phi_S)}\sin(3\phi_h-\phi_S) \\
+\ \sqrt{2\varepsilon(1+\varepsilon)}A_{UT}^{\sin\phi_S}\sin\phi_S \\
+\ \sqrt{2\varepsilon(1+\varepsilon)}A_{UT}^{\sin(2\phi_h-\phi_S)}\sin(2\phi_h-\phi_S)
\end{array}\right] \\
+\ S_T\lambda\left[\begin{array}{l}
\sqrt{(1-\varepsilon^2)}A_{LT}^{\cos(\phi_h-\phi_S)}\cos(\phi_h-\phi_S) \\
+\ \sqrt{2\varepsilon(1-\varepsilon)}A_{LT}^{\cos\phi_S}\cos\phi_S \\
+\ \sqrt{2\varepsilon(1-\varepsilon)}A_{LT}^{\cos(2\phi_h-\phi_S)}\cos(2\phi_h-\phi_S)
\end{array}\right]
\end{array}\right\}$$

DY

$$\frac{d\sigma}{d\Omega}\propto\left(F_U^1+F_U^2\right)$$

$$\times\left\{\begin{array}{l}
1+A_U^1\cos^2\theta_{CS} \\
+\ \sin 2\theta_{CS}A_U^{\cos\varphi_{CS}}\cos\varphi_{CS}+\sin^2\theta_{CS}A_U^{\cos 2\varphi_{CS}}\cos 2\varphi_{CS} \\
+\ S_L\left[\sin\theta_{CS}A_L^{\sin\varphi_{CS}}\sin\varphi_{CS}+\sin^2\theta_{CS}A_L^{\sin 2\varphi_{CS}}\sin 2\varphi_{CS}\right] \\
+\ S_T\left[\begin{array}{l}
\left(A_T^{\sin\varphi_S}+\cos^2\theta_{CS}\tilde{A}_T^{\sin\varphi_S}\right)\sin\varphi_S \\
+\sin^2\theta_{CS}\left(\begin{array}{l}A_T^{\sin(2\varphi_{CS}-\varphi_S)}\sin(2\varphi_{CS}-\varphi_S) \\ +\ A_T^{\sin(2\varphi_{CS}+\varphi_S)}\sin(2\varphi_{CS}+\varphi_S)\end{array}\right) \\
+\sin 2\theta_{CS}\left(\begin{array}{l}A_T^{\sin(\varphi_{CS}-\varphi_S)}\sin(\varphi_{CS}-\varphi_S) \\ +\ A_T^{\sin(\varphi_{CS}+\varphi_S)}\sin(\varphi_{CS}+\varphi_S)\end{array}\right)
\end{array}\right]
\end{array}\right\}$$

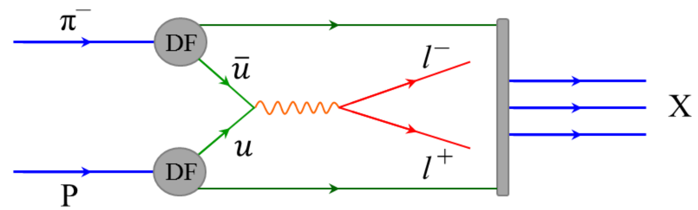

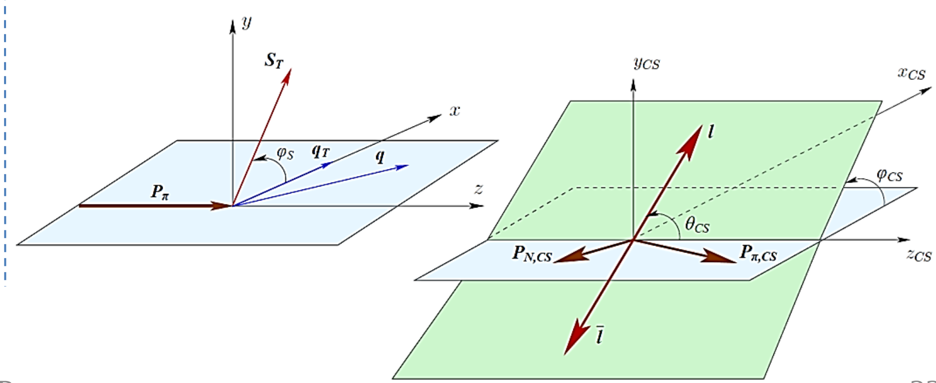

SIDIS and single-polarized DY x-sections at twist-2 (LO)

SIDIS

$$\frac{d\sigma^{LO}}{dxdydzdp_T^2 d\phi_h d\phi_S} \propto \left(F_{UU,T} + \varepsilon F_{UU,L}\right)$$

$$\times \left\{ \begin{aligned} &1 + \boxed{\varepsilon A_{UU}^{\cos 2\phi_h} \cos 2\phi_h} \\ &+ S_L\, \varepsilon A_{UL}^{\sin 2\phi_h} \sin 2\phi_h + S_L \lambda \sqrt{1-\varepsilon^2} A_{LL} \\ &\boxed{+ S_T \left[\begin{aligned} &A_{UT}^{\sin(\phi_h-\phi_S)} \sin(\phi_h - \phi_S) \\ &+ \varepsilon A_{UT}^{\sin(\phi_h+\phi_S)} \sin(\phi_h + \phi_S) \\ &+ \varepsilon A_{UT}^{\sin(3\phi_h-\phi_S)} \sin(3\phi_h - \phi_S) \end{aligned} \right]} \\ &+ S_T \lambda \left[\sqrt{\left(1-\varepsilon^2\right)} A_{LT}^{\cos(\phi_h-\phi_S)} \cos(\phi_h - \phi_S) \right] \end{aligned} \right\}$$

DY

$$\frac{d\sigma^{LO}}{d\Omega} \propto F_U^1 \left(1 + \cos^2\theta_{CS}\right)$$

$$\times \left\{ \begin{aligned} &1 + \boxed{D_{[\sin^2\theta_{CS}]} A_U^{\cos 2\varphi_{CS}} \cos 2\varphi_{CS}} \\ &+ S_L \sin^2\theta_{CS} A_L^{\sin 2\varphi_{CS}} \sin 2\varphi_{CS} \\ &\boxed{+ S_T \left[\begin{aligned} &A_T^{\sin\varphi_S} \sin\varphi_S \\ &+ D_{[\sin^2\theta_{CS}]} \left(\begin{aligned} &A_T^{\sin(2\varphi_{CS}-\varphi_S)} \sin(2\varphi_{CS} - \varphi_S) \\ &+ A_T^{\sin(2\varphi_{CS}+\varphi_S)} \sin(2\varphi_{CS} + \varphi_S) \end{aligned} \right) \end{aligned} \right]} \end{aligned} \right\}$$

where $D_{[\sin^2\theta_{CS}]} = \sin^2\theta_{CS} / \left(1 + \cos^2\theta_{CS}\right)$

COMPASS

SIDIS and single-polarized DY x-sections at twist-2 (LO)

SIDIS

$$\frac{d\sigma^{LO}}{dxdydzdp_T^2 d\phi_h d\phi_S} \propto \left(F_{UU,T} + \varepsilon F_{UU,L}\right) \times \left\{ \begin{array}{l} 1 + \boxed{\varepsilon A_{UU}^{\cos 2\phi_h} \cos 2\phi_h} \\ + S_L\, \varepsilon A_{UL}^{\sin 2\phi_h} \sin 2\phi_h + S_L \lambda \sqrt{1-\varepsilon^2}\, A_{LL} \\ \boxed{+ S_T \left[\begin{array}{l} A_{UT}^{\sin(\phi_h-\phi_S)} \sin(\phi_h-\phi_S) \\ + \varepsilon A_{UT}^{\sin(\phi_h+\phi_S)} \sin(\phi_h+\phi_S) \\ + \varepsilon A_{UT}^{\sin(3\phi_h-\phi_S)} \sin(3\phi_h-\phi_S) \end{array} \right]} \\ + S_T \lambda \left[\sqrt{\left(1-\varepsilon^2\right)} A_{LT}^{\cos(\phi_h-\phi_S)} \cos(\phi_h-\phi_S) \right] \end{array} \right\}$$

DY

$$\frac{d\sigma^{LO}}{d\Omega} \propto F_U^1 \left(1+\cos^2\theta_{CS}\right) \times \left\{ \begin{array}{l} 1 + \boxed{D_{[\sin^2\theta_{CS}]} A_U^{\cos 2\varphi_{CS}} \cos 2\varphi_{CS}} \\ + S_L \sin^2\theta_{CS} A_L^{\sin 2\varphi_{CS}} \sin 2\varphi_{CS} \\ \boxed{+ S_T \left[\begin{array}{l} A_T^{\sin\varphi_S} \sin\varphi_S \\ + D_{[\sin^2\theta_{CS}]} \left(\begin{array}{l} A_T^{\sin(2\varphi_{CS}-\varphi_S)} \sin(2\varphi_{CS}-\varphi_S) \\ + A_T^{\sin(2\varphi_{CS}+\varphi_S)} \sin(2\varphi_{CS}+\varphi_S) \end{array} \right) \end{array} \right]} \end{array} \right\}$$

where $D_{[\sin^2\theta_{CS}]} = \sin^2\theta_{CS} / \left(1+\cos^2\theta_{CS}\right)$

SIDIS		DY
$A_{UU}^{\cos 2\phi_h} \propto h_1^{\perp q} \otimes H_{1q}^{\perp h} + \ldots$	⟷ Boer-Mulders ⟷	$A_U^{\cos 2\varphi_{CS}} \propto h_{1,\pi}^{\perp q} \otimes h_{1,p}^{\perp q}$
$A_{UT}^{\sin(\phi_h-\phi_S)} \propto f_{1T}^{\perp q} \otimes D_{1q}^h$	⟷ Sivers ⟷	$A_T^{\sin\varphi_S} \propto f_{1,\pi}^q \otimes f_{1T,p}^{\perp q}$
$A_{UT}^{\sin(\phi_h+\phi_S)} \propto h_1^q \otimes H_{1q}^{\perp h}$	⟷ Transversity ⟷	$A_T^{\sin(2\varphi_{CS}-\varphi_S)} \propto h_{1,\pi}^{\perp q} \otimes h_{1,p}^q$
$A_{UT}^{\sin(3\phi_h-\phi_S)} \propto h_{1T}^{\perp q} \otimes H_{1q}^{\perp h}$	⟷ Pretzelosity ⟷	$A_T^{\sin(2\varphi_{CS}+\varphi_S)} \propto h_{1,\pi}^{\perp q} \otimes h_{1T,p}^{\perp q}$
$A_{UL}^{\sin 2\phi_h} \propto h_{1L}^{\perp q} \otimes H_{1q}^{\perp h}$	⟷ Worm-gear L ⟷	$A_L^{\sin 2\varphi_{CS}} \propto h_{1,\pi}^{\perp q} \otimes h_{1L,p}^{\perp q}$
$A_{LL} \propto g_{1L}^q \otimes D_{1q}^h,\ A_{LT}^{\cos(\phi_h-\phi_s)} \propto g_{1T}^q \otimes D_{1q}^h$	⟷	Double polarized DY only

COMPASS accesses all 8 twist-2 nucleon TMD PDFs in SIDIS and 5 nucleon+2 pion TMD PDFs in DY

SIDIS and single-polarized DY x-sections at twist-2 (LO)

SIDIS

$$\frac{d\sigma^{LO}}{dxdydzdp_T^2 d\phi_h d\phi_S} \propto \left(F_{UU,T} + \varepsilon F_{UU,L}\right) \times \left\{ \begin{array}{l} 1 + \varepsilon A_{UU}^{\cos 2\phi_h} \cos 2\phi_h \\ + S_L\, \varepsilon A_{UL}^{\sin 2\phi_h} \sin 2\phi_h + S_L \lambda \sqrt{1-\varepsilon^2} A_{LL} \\ + S_T \left[\begin{array}{l} A_{UT}^{\sin(\phi_h - \phi_S)} \sin(\phi_h - \phi_S) \\ + \varepsilon A_{UT}^{\sin(\phi_h + \phi_S)} \sin(\phi_h + \phi_S) \\ + \varepsilon A_{UT}^{\sin(3\phi_h - \phi_S)} \sin(3\phi_h - \phi_S) \end{array} \right] \\ + S_T \lambda \left[\sqrt{\left(1-\varepsilon^2\right)} A_{LT}^{\cos(\phi_h - \phi_S)} \cos(\phi_h - \phi_S) \right] \end{array} \right\}$$

DY

$$\frac{d\sigma^{LO}}{d\Omega} \propto F_U^1 \left(1 + \cos^2\theta_{CS}\right) \times \left\{ \begin{array}{l} 1 + D_{[\sin^2\theta_{CS}]} A_U^{\cos 2\varphi_{CS}} \cos 2\varphi_{CS} \\ + S_L \sin^2\theta_{CS} A_L^{\sin 2\varphi_{CS}} \sin 2\varphi_{CS} \\ + S_T \left[\begin{array}{l} A_T^{\sin\varphi_S} \sin\varphi_S \\ + D_{[\sin^2\theta_{CS}]} \left(\begin{array}{l} A_T^{\sin(2\varphi_{CS} - \varphi_S)} \sin(2\varphi_{CS} - \varphi_S) \\ + A_T^{\sin(2\varphi_{CS} + \varphi_S)} \sin(2\varphi_{CS} + \varphi_S) \end{array} \right) \end{array} \right] \end{array} \right\}$$

where $D_{[\sin^2\theta_{CS}]} = \sin^2\theta_{CS} / \left(1 + \cos^2\theta_{CS}\right)$

SIDIS		DY
$A_{UU}^{\cos 2\phi_h} \propto h_1^{\perp q} \otimes H_{1q}^{\perp h} + \ldots$	← Boer-Mulders →	$A_U^{\cos 2\varphi_{CS}} \propto h_{1,\pi}^{\perp q} \otimes h_{1,p}^{\perp q}$
$A_{UT}^{\sin(\phi_h - \phi_S)} \propto f_{1T}^{\perp q} \otimes D_{1q}^{h}$	← Sivers →	$A_T^{\sin\varphi_S} \propto f_{1,\pi}^{q} \otimes f_{1T,p}^{\perp q}$
$A_{UT}^{\sin(\phi_h + \phi_S)} \propto h_1^{q} \otimes H_{1q}^{\perp h}$	← Transversity →	$A_T^{\sin(2\varphi_{CS} - \varphi_S)} \propto h_{1,\pi}^{\perp q} \otimes h_{1,p}^{q}$
$A_{UT}^{\sin(3\phi_h - \phi_S)} \propto h_{1T}^{\perp q} \otimes H_{1q}^{\perp h}$	← Pretzelosity →	$A_T^{\sin(2\varphi_{CS} + \varphi_S)} \propto h_{1,\pi}^{\perp q} \otimes h_{1T,p}^{\perp q}$

within QCD TMD-framework:

$h_1^{\perp q}$ & $f_{1T}^{\perp q}$ TMD PDFs are expected to be "conditionally" universal (SIDIS ↔ DY: sign change)

h_1^{q} & $h_{1T}^{\perp q}$ TMD PDFs are expected to be "genuinely" universal (SIDIS ↔ DY: no sign change)

SIDIS and single-polarized DY x-sections at twist-2 (LO)

SIDIS

$$\frac{d\sigma^{LO}}{dxdydzdp_T^2 d\phi_h d\phi_S} \propto \left(F_{UU,T}+\varepsilon F_{UU,L}\right) \times \left\{ \begin{array}{l} 1+\varepsilon A_{UU}^{\cos 2\phi_h}\cos 2\phi_h \\ +\ S_L\, \varepsilon A_{UL}^{\sin 2\phi_h}\sin 2\phi_h + S_L\lambda\sqrt{1-\varepsilon^2}\,A_{LL} \\ +\ S_T \left[\begin{array}{l} A_{UT}^{\sin(\phi_h-\phi_S)}\sin(\phi_h-\phi_S) \\ +\ \varepsilon A_{UT}^{\sin(\phi_h+\phi_S)}\sin(\phi_h+\phi_S) \\ +\ \varepsilon A_{UT}^{\sin(3\phi_h-\phi_S)}\sin(3\phi_h-\phi_S) \end{array} \right] \\ +\ S_T\lambda\left[\sqrt{\left(1-\varepsilon^2\right)}A_{LT}^{\cos(\phi_h-\phi_S)}\cos(\phi_h-\phi_S)\right] \end{array} \right\}$$

DY

$$\frac{d\sigma^{LO}}{d\Omega} \propto F_U^1\left(1+\cos^2\theta_{CS}\right) \times \left\{ \begin{array}{l} 1+D_{\left[\sin^2\theta_{CS}\right]}A_U^{\cos 2\varphi_{CS}}\cos 2\varphi_{CS} \\ +\ S_L\sin^2\theta_{CS}A_L^{\sin 2\varphi_{CS}}\sin 2\varphi_{CS} \\ +\ S_T \left[\begin{array}{l} A_T^{\sin\varphi_S}\sin\varphi_S \\ +D_{\left[\sin^2\theta_{CS}\right]}\left(\begin{array}{l} A_T^{\sin(2\varphi_{CS}-\varphi_S)}\sin(2\varphi_{CS}-\varphi_S) \\ +\ A_T^{\sin(2\varphi_{CS}+\varphi_S)}\sin(2\varphi_{CS}+\varphi_S) \end{array} \right) \end{array} \right] \end{array} \right\}$$

where $D_{\left[\sin^2\theta_{CS}\right]} = \sin^2\theta_{CS}/\left(1+\cos^2\theta_{CS}\right)$

SIDIS		DY
$A_{UU}^{\cos 2\phi_h} \propto h_1^{\perp q}\otimes H_{1q}^{\perp h} + \ldots$	Boer-Mulders	$A_U^{\cos 2\varphi_{CS}} \propto h_{1,\pi}^{\perp q}\otimes h_{1,p}^{\perp q}$
$A_{UT}^{\sin(\phi_h-\phi_S)} \propto f_{1T}^{\perp q}\otimes D_{1q}^h$	Sivers	$A_T^{\sin\varphi_S} \propto f_{1,\pi}^q\otimes f_{1T,p}^{\perp q}$
$A_{UT}^{\sin(\phi_h+\phi_S)} \propto h_1^q\otimes H_{1q}^{\perp h}$	Transversity	$A_T^{\sin(2\varphi_{CS}-\varphi_S)} \propto h_{1,\pi}^{\perp q}\otimes h_{1,p}^q$
$A_{UT}^{\sin(3\phi_h-\phi_S)} \propto h_{1T}^{\perp q}\otimes H_{1q}^{\perp h}$	Pretzelosity	$A_T^{\sin(2\varphi_{CS}+\varphi_S)} \propto h_{1,\pi}^{\perp q}\otimes h_{1T,p}^{\perp q}$

Complementary information from different channels:

- SIDIS-DY bridging of nucleon TMD PDFs
- Multiple access to Collins FF $H_{1q}^{\perp h}$ and pion Boer-Mulders PDF $h_{1,\pi}^{\perp q}$

Nucleon TMD PDFs accessed in SIDIS and DY

SIDIS		Single polarized DY (LO)
$A_{UU}^{\cos\phi_h} \propto Q^{-1}\left(f_1^q \otimes D_{1q}^h - h_1^{\perp q} \otimes H_{1q}^{\perp h} + \ldots\right)$	Boer-Mulders	$A_U^{\cos 2\varphi_{CS}} \propto h_{1,\pi}^{\perp q} \otimes h_{1,p}^{\perp q}$
$A_{UU}^{\cos 2\phi_h} \propto h_1^{\perp q} \otimes H_{1q}^{\perp h} + Q^{-1}\left(f_1^q \otimes D_{1q}^h + \ldots\right)$	Boer-Mulders	
$A_{UT}^{\sin(\phi_h - \phi_s)} \propto f_{1T}^{\perp q} \otimes D_{1q}^h$	Sivers	$A_T^{\sin\varphi_S} \propto f_{1,\pi}^q \otimes f_{1T,p}^{\perp q}$
$A_{UT}^{\sin(\phi_h + \phi_s)} \propto h_1^q \otimes H_{1q}^{\perp h}$	Transversity	$A_T^{\sin(2\varphi_{CS} - \varphi_S)} \propto h_{1,\pi}^{\perp q} \otimes h_{1,p}^q$
$A_{UT}^{\sin(3\phi_h - \phi_s)} \propto h_{1T}^{\perp q} \otimes H_{1q}^{\perp h}$	Pretzelosity	$A_T^{\sin(2\varphi_{CS} + \varphi_S)} \propto h_{1,\pi}^{\perp q} \otimes h_{1T,p}^{\perp q}$

$$A_{LT}^{\cos(\phi_h - \phi_s)} \propto g_{1T}^q \otimes D_{1q}^h$$

$$A_{UT}^{\sin(\phi_s)} \propto Q^{-1}\left(h_1^q \otimes H_{1q}^{\perp h} + f_{1T}^{\perp q} \otimes D_{1q}^h + \ldots\right)$$

$$A_{UT}^{\sin(2\phi_h - \phi_s)} \propto Q^{-1}\left(h_{1T}^{\perp q} \otimes H_{1q}^{\perp h} + f_{1T}^{\perp q} \otimes D_{1q}^h + \ldots\right)$$

$$A_{LT}^{\cos(\phi_s)} \propto Q^{-1}\left(g_{1T}^q \otimes D_{1q}^h + \ldots\right)$$

$$A_{LT}^{\cos(2\phi_h - \phi_s)} \propto Q^{-1}\left(g_{1T}^q \otimes D_{1q}^h + \ldots\right)$$

Quark → / Nucleon ↓	U	L	T
U	$f_1^q(x, \boldsymbol{k}_T^2)$ number density		$h_1^{\perp q}(x, \boldsymbol{k}_T^2)$ Boer-Mulders
L		$g_1^q(x, \boldsymbol{k}_T^2)$ helicity	$h_{1L}^{\perp q}(x, \boldsymbol{k}_T^2)$ worm-gear L
T	$f_{1T}^{\perp q}(x, \boldsymbol{k}_T^2)$ Sivers	$g_{1T}^q(x, \boldsymbol{k}_T^2)$ Kotzinian-Mulders worm-gear T	$h_1^q(x, \boldsymbol{k}_T^2)$ transversity $h_{1T}^{\perp q}(x, \boldsymbol{k}_T^2)$ pretzelosity

Nucleon TMD PDFs accessed in SIDIS and DY

COMPASS

SIDIS

$$A_{UU}^{\cos\phi_h} \propto Q^{-1}\left(f_1^q \otimes D_{1q}^h - h_1^{\perp q}\otimes H_{1q}^{\perp h} + \ldots\right)$$

$$A_{UU}^{\cos 2\phi_h} \propto h_1^{\perp q}\otimes H_{1q}^{\perp h} + Q^{-1}\left(f_1^q\otimes D_{1q}^h+\ldots\right)$$

$$A_{UT}^{\sin(\phi_h-\phi_s)} \propto f_{1T}^{\perp q}\otimes D_{1q}^h$$

$$A_{UT}^{\sin(\phi_h+\phi_s)} \propto h_1^q\otimes H_{1q}^{\perp h}$$

$$A_{UT}^{\sin(3\phi_h-\phi_s)} \propto h_{1T}^{\perp q}\otimes H_{1q}^{\perp h}$$

$$A_{LT}^{\cos(\phi_h-\phi_s)} \propto g_{1T}^q\otimes D_{1q}^h$$

$$A_{UT}^{\sin(\phi_s)} \propto Q^{-1}\left(h_1^q\otimes H_{1q}^{\perp h} + f_{1T}^{\perp q}\otimes D_{1q}^h + \ldots\right)$$

$$A_{UT}^{\sin(2\phi_h-\phi_s)} \propto Q^{-1}\left(h_{1T}^{\perp q}\otimes H_{1q}^{\perp h} + f_{1T}^{\perp q}\otimes D_{1q}^h+\ldots\right)$$

$$A_{LT}^{\cos(\phi_s)} \propto Q^{-1}\left(g_{1T}^q\otimes D_{1q}^h+\ldots\right)$$

$$A_{LT}^{\cos(2\phi_h-\phi_s)} \propto Q^{-1}\left(g_{1T}^q\otimes D_{1q}^h+\ldots\right)$$

Single polarized DY (LO)

$$A_U^{\cos 2\varphi_{CS}} \propto h_{1,\pi}^{\perp q}\otimes h_{1,p}^{\perp q}$$

$$A_T^{\sin\varphi_S} \propto f_{1,\pi}^{q}\otimes f_{1T,p}^{\perp q}$$

$$A_T^{\sin(2\varphi_{CS}-\varphi_S)} \propto h_{1,\pi}^{\perp q}\otimes h_{1,p}^{q}$$

$$A_T^{\sin(2\varphi_{CS}+\varphi_S)} \propto h_{1,\pi}^{\perp q}\otimes h_{1T,p}^{\perp q}$$

Boer-Mulders

Boer-Mulders

Sivers

Transversity

Pretzelosity

All the answers are encoded in the data...
In few years many new asymmetries measured by different experiments in different reactions, at different energies and kinematical ranges will wait for a "global analysis"…

- Who can do that?

COMPASS collaboration

Common Muon and Proton Apparatus for Structure and Spectroscopy

24 institutions from 13 countries
nearly 250 physicists

- **CERN SPS north area**
- **Fixed target experiment**
- **Approved in 1997 (20 years)**
- **Taking data since 2002**

Wide physics program

COMPASS-I

- **Data taking 2002-2011**
- **Muon and hadron beams**
- **Nucleon spin structure**
- **Spectroscopy**

COMPASS-II

- **Data taking 2012-2018 (2021?)**
- **Primakoff**
- **DVCS (GPD+SIDIS)**
- **Polarized Drell-Yan**
- **Transverse deuteron SIDIS**

Many "beyond 2021" ideas

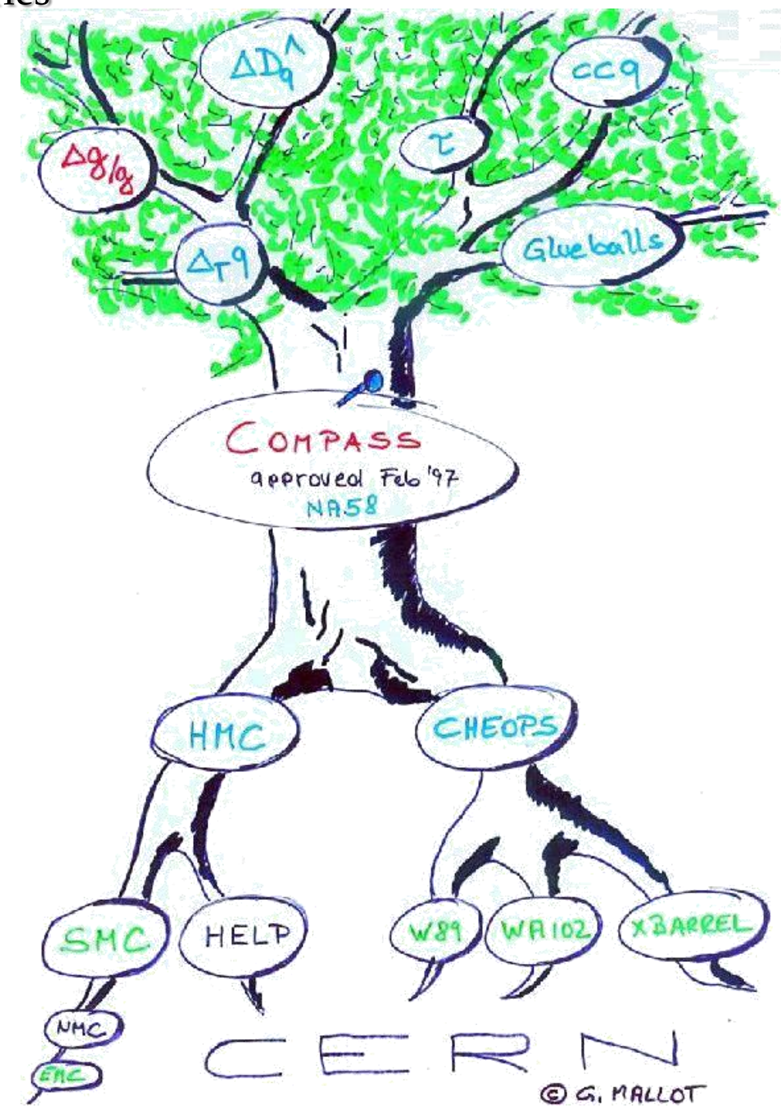

COMPASS web page: http://wwwcompass.cern.ch

COMPASS collaboration

Common Muon and Proton Apparatus for Structure and Spectroscopy

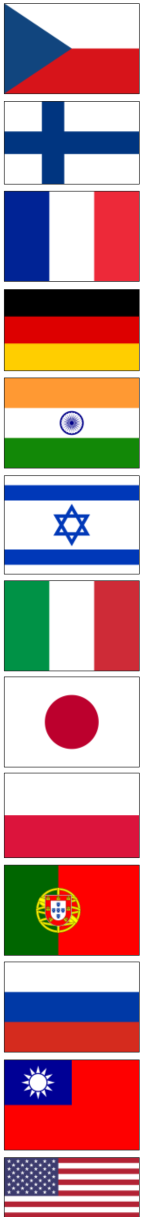

24 institutions from 13 countries
nearly 250 physicists
Over 60 papers, over 100 PhD theses, over 100 Master/Bachelor theses

- **CERN SPS north area**
- **Fixed target experiment**
- **Approved in 1997 (20 years)**
- **Taking data since 2002**

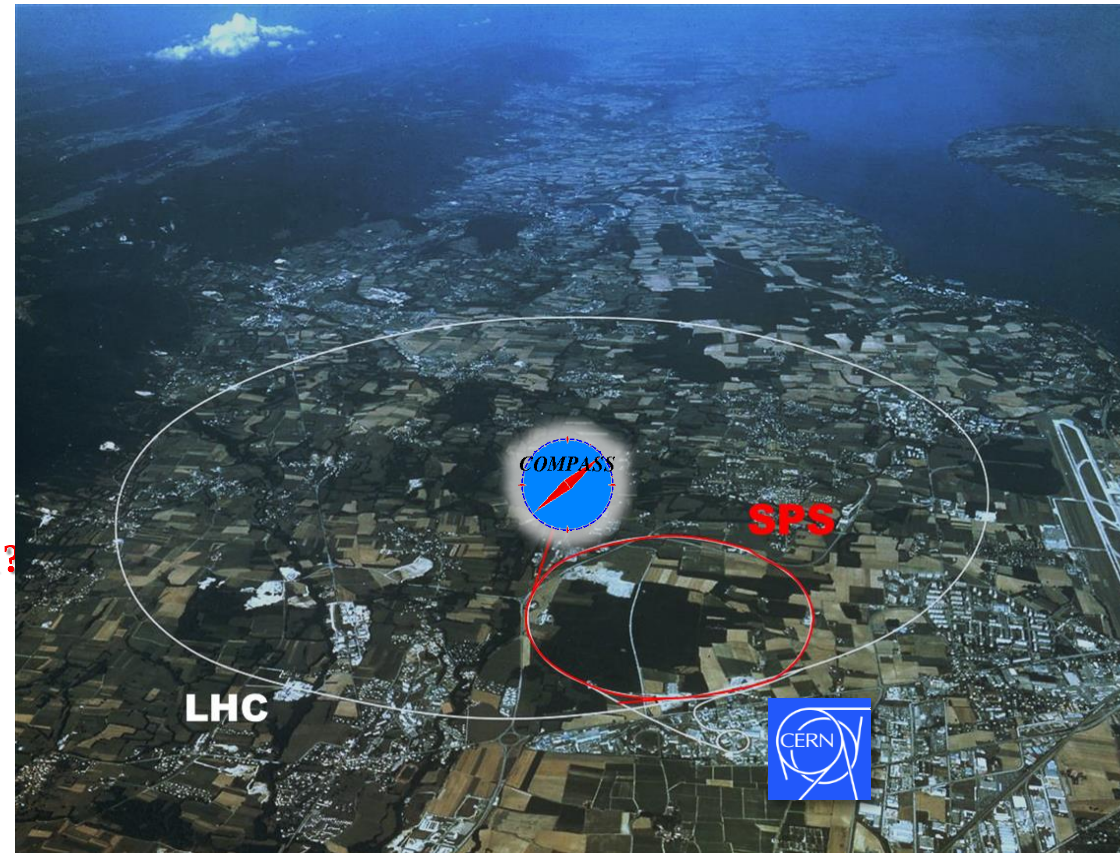

Wide physics program

COMPASS-I
- **Data taking 2002-2011**
- **Muon and hadron beams**
- **Nucleon spin structure**
- **Spectroscopy**

COMPASS-II
- **Data taking 2012-2018 (2021?**
- **Primakoff**
- **DVCS (GPD+SIDIS)**
- **Polarized Drell-Yan**
- **Transverse deuteron SIDIS**

Many “beyond 2021” ideas

COMPASS web page: http://wwwcompass.cern.ch

COMPASS experimental setup: Phase I (muon program)

Two-stage spectrometer
- Large Angle Spectrometer (SM1 magnet)
- Small Angle Spectrometer (SM2 magnet)

- High energy beam
- Large angular acceptance
- Broad kinematical range
- Momentum, tracking and calorimetric measurements, PID

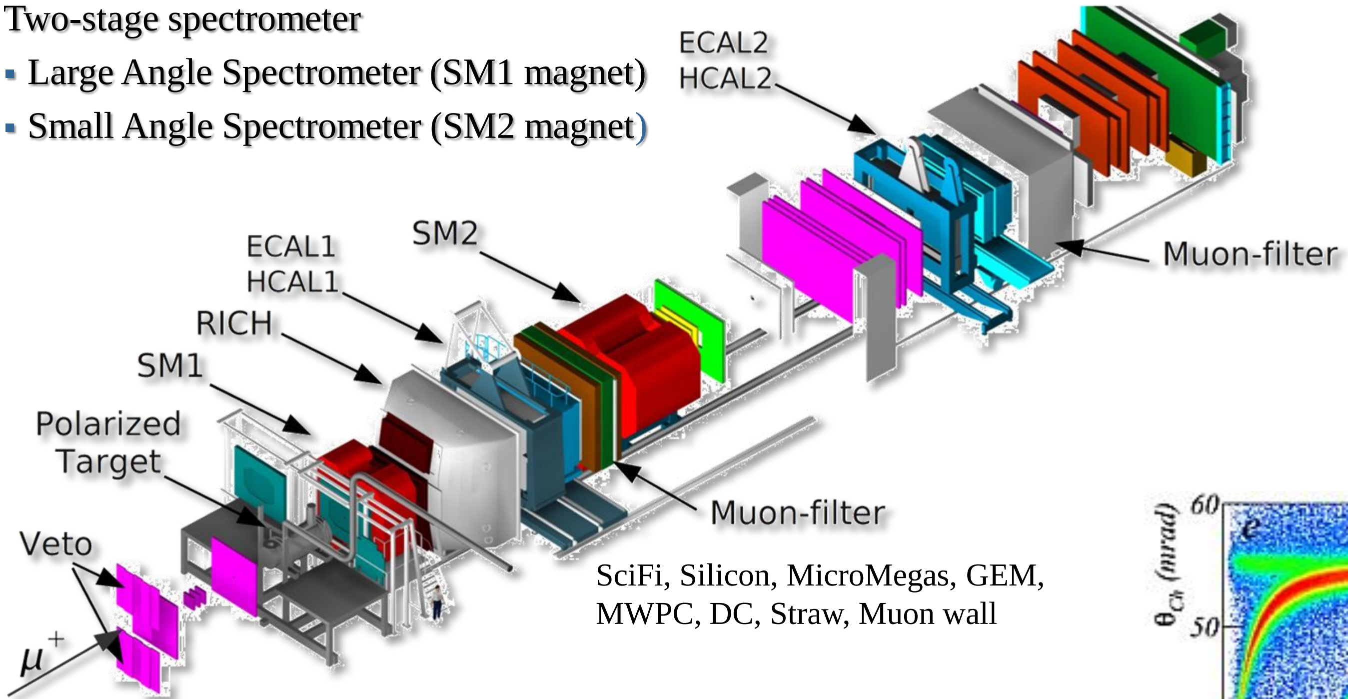

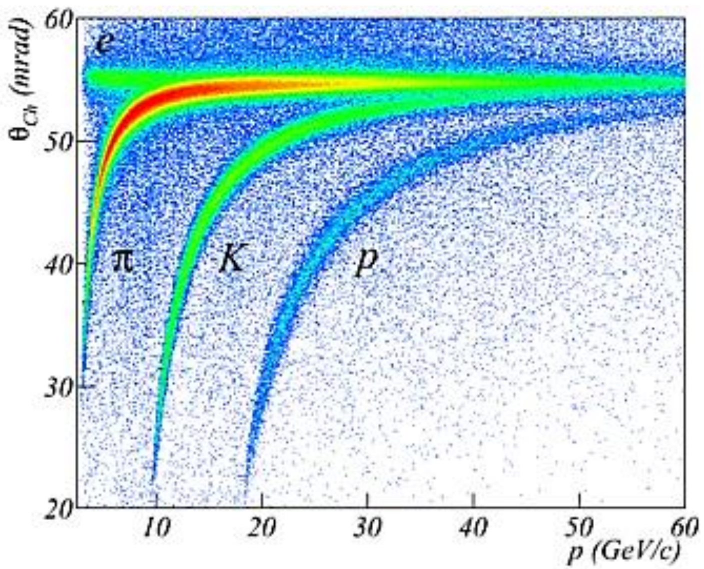

Data-taking years: 2002-2011

Longitudinally polarized (80%) μ^+ beam:
Energy: 160/200 GeV/c, Intensity: $2 \cdot 10^8$ μ^+/spill (4.8s).

Target: Solid state *(^6LiD or NH_3)*

- ^{6}LiD 2-cell configuration. Polarization (L & T) ~ 50%, f ~ 0.38
- NH_3 3-cell configuration. Polarization (L & T) ~ 80%, f ~ 0.14

See talks by: A. Bressan, J. Matoušek, A. Moretti

COMPASS experimental setup: Phase I (muon program)

Two-stage spectrometer

- Large Angle Spectrometer (SM1 magnet)
- Small Angle Spectrometer (SM2 magnet)

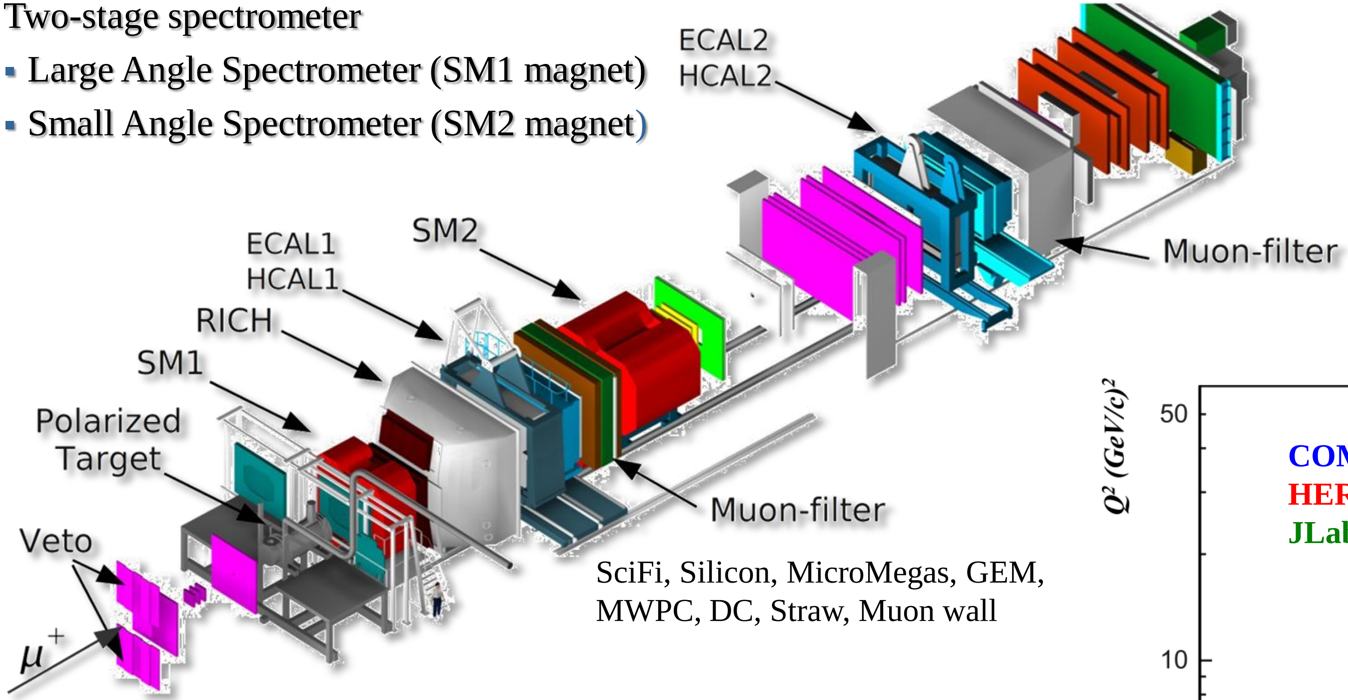

- High energy beam
- Large angular acceptance
- Broad kinematical range
- Momentum, tracking and calorimetric measurements, PID

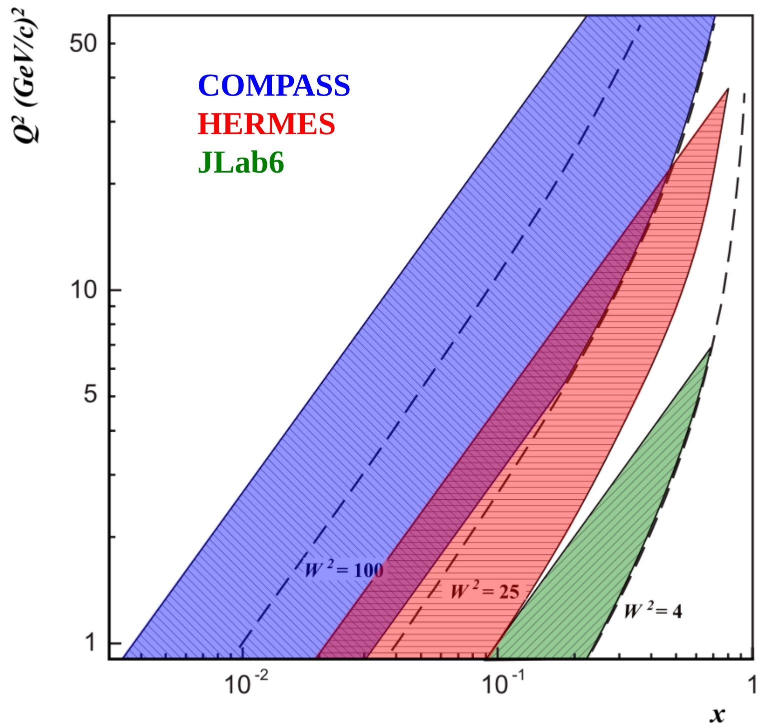

Data-taking years: 2002-2011

Longitudinally polarized (80%) μ^+ beam:

Energy: 160/200 GeV/c, Intensity: $2 \cdot 10^8$ μ^+/spill (4.8s).

Target: Solid state *(^{6}LiD or NH_3)*

- ^{6}LiD 2-cell configuration. Polarization (L & T) ~ 50%, f ~ 0.38
- NH_3 3-cell configuration. Polarization (L & T) ~ 80%, f ~ 0.14

COMPASS experimental setup: Phase II (DY program)

Two-stage spectrometer
- Large Angle Spectrometer (SM1 magnet)
- Small Angle Spectrometer (SM2 magnet)

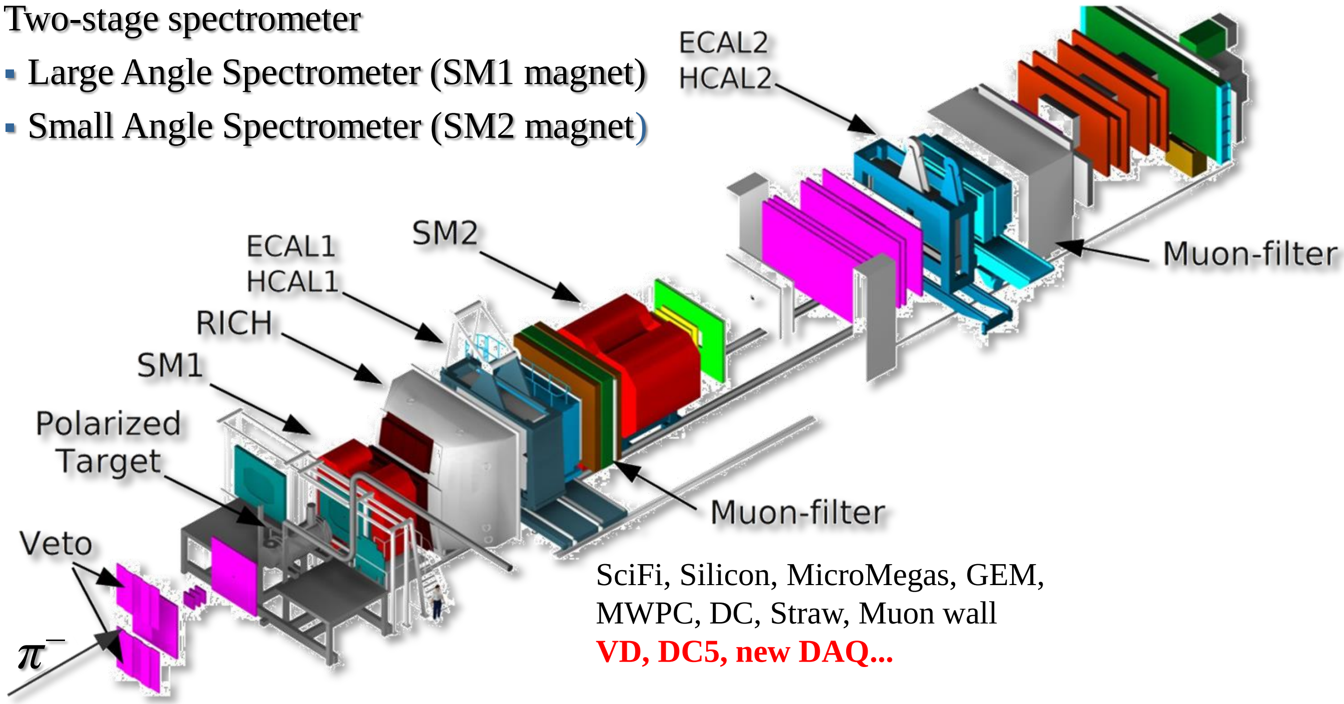

- High energy beam
- Large angular acceptance
- Broad kinematical range
- Momentum, tracking and calorimetric measurements, PID

SciFi, Silicon, MicroMegas, GEM, MWPC, DC, Straw, Muon wall
VD, DC5, new DAQ...

Data-taking years: 2014 (test) 2015 and 2018

High energy π^- beam:
Energy: 190 GeV/c, Intensity: 10^8 π/s

Target: Solid state

- NH_3 2-cell configuration. Polarization T ~ 73%, f ~ 0.18
- Data is collected simultaneously with both target spin orientations
  Periodic polarization reversal to minimize systematic effects

COMPASS experimental setup: Phase II (DY program)

Two-stage spectrometer
- Large Angle Spectrometer (SM1 magnet)
- Small Angle Spectrometer (SM2 magnet)

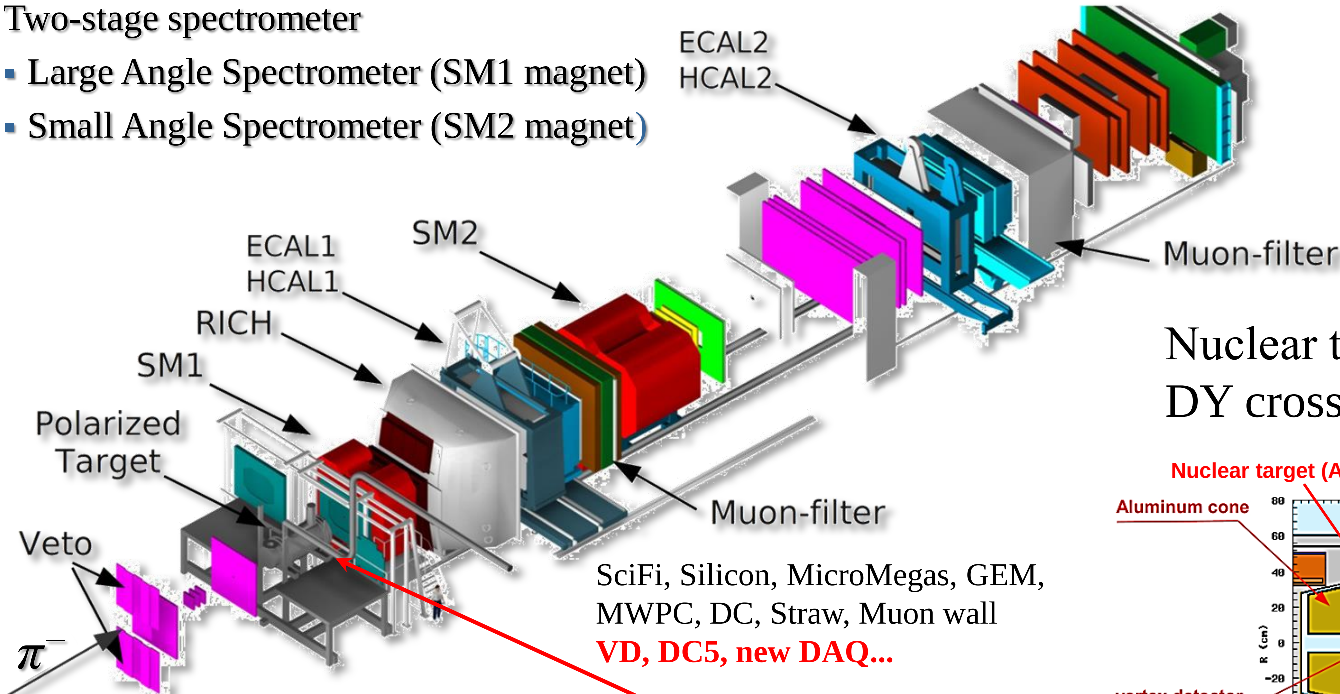

- High energy beam
- Large angular acceptance
- Broad kinematical range
- Momentum, tracking and calorimetric measurements, PID

Nuclear targets → unpolarized DY, DY cross-sections, EMC effect

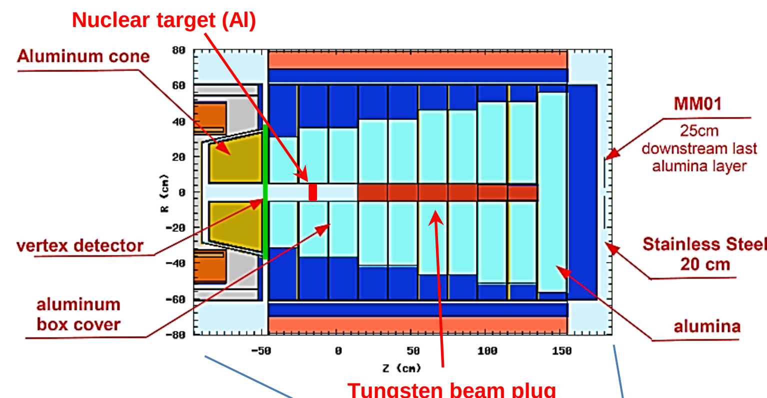

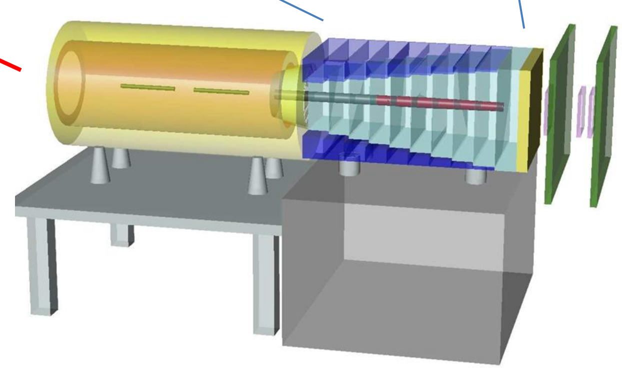

Data-taking years: 2014 (test) 2015 and 2018

High energy π^- beam:

Energy: 190 GeV/c, Intensity: 10^8 π/s

Target: Solid state

- NH_3 2-cell configuration. Polarization T ~ 73%, f ~ 0.18
- Data is collected simultaneously with both target spin orientations
  Periodic polarization reversal to minimize systematic effects

COMPASS experimental setup: Phase II (DY program)

Two-stage spectrometer
- Large Angle Spectrometer (SM1 magnet)
- Small Angle Spectrometer (SM2 magnet)

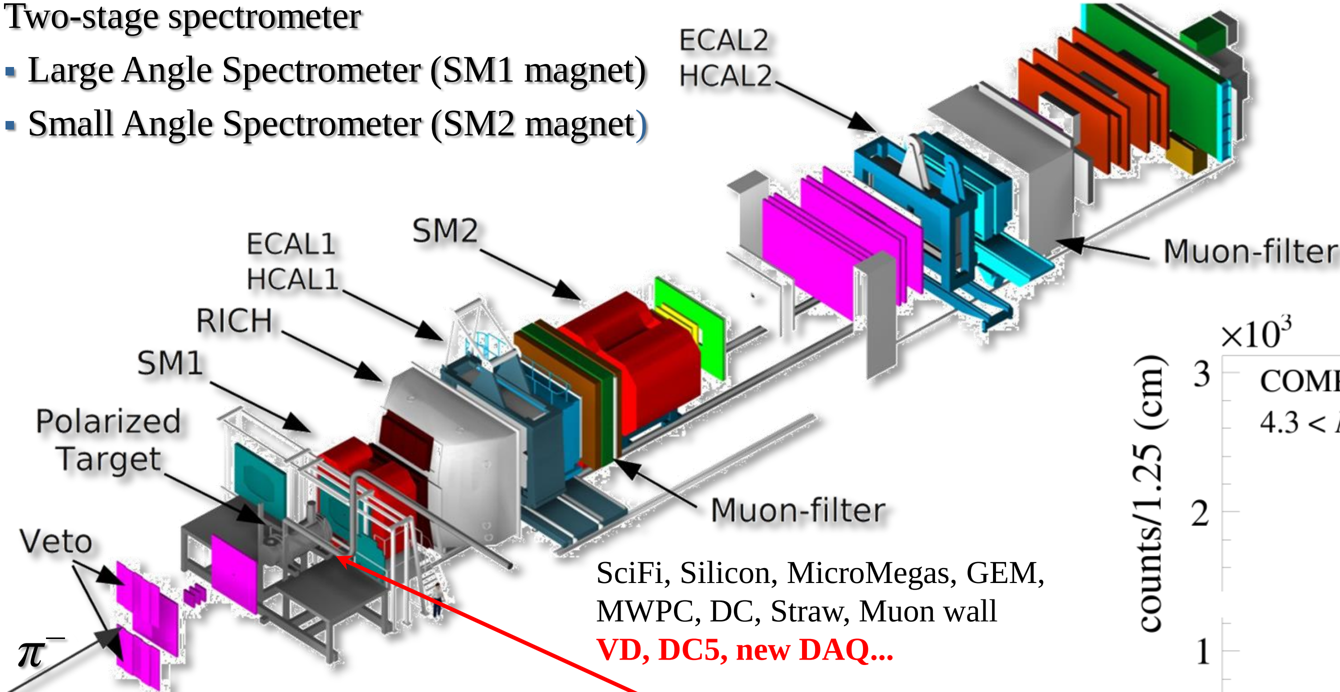

- High energy beam
- Large angular acceptance
- Broad kinematical range
- Momentum, tracking and calorimetric measurements, PID

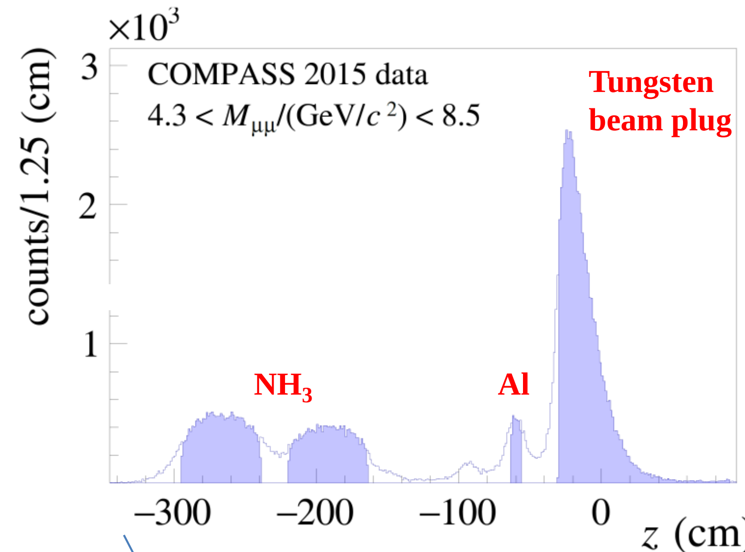

Data-taking years: 2014 (test) 2015 and 2018

High energy π^- beam:

Energy: 190 GeV/c, Intensity: 10^8 π/s

Target: Solid state

- NH_3 2-cell configuration. Polarization T ~ 73%, f ~ 0.18
- Data is collected simultaneously with both target spin orientations
  Periodic polarization reversal to minimize systematic effects

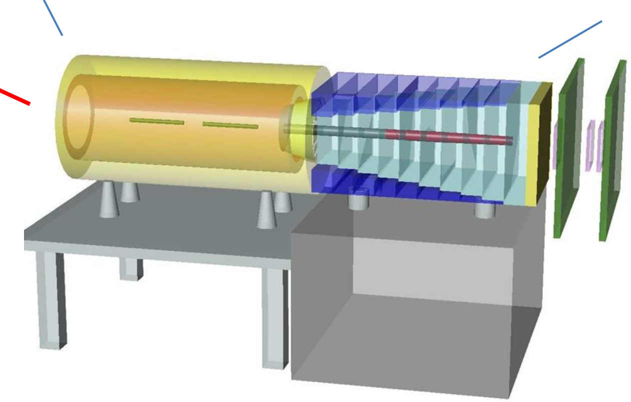

COMPASS experimental setup: Phase II (DY program)

Two-stage spectrometer
- Large Angle Spectrometer (SM1 magnet)
- Small Angle Spectrometer (SM2 magnet)

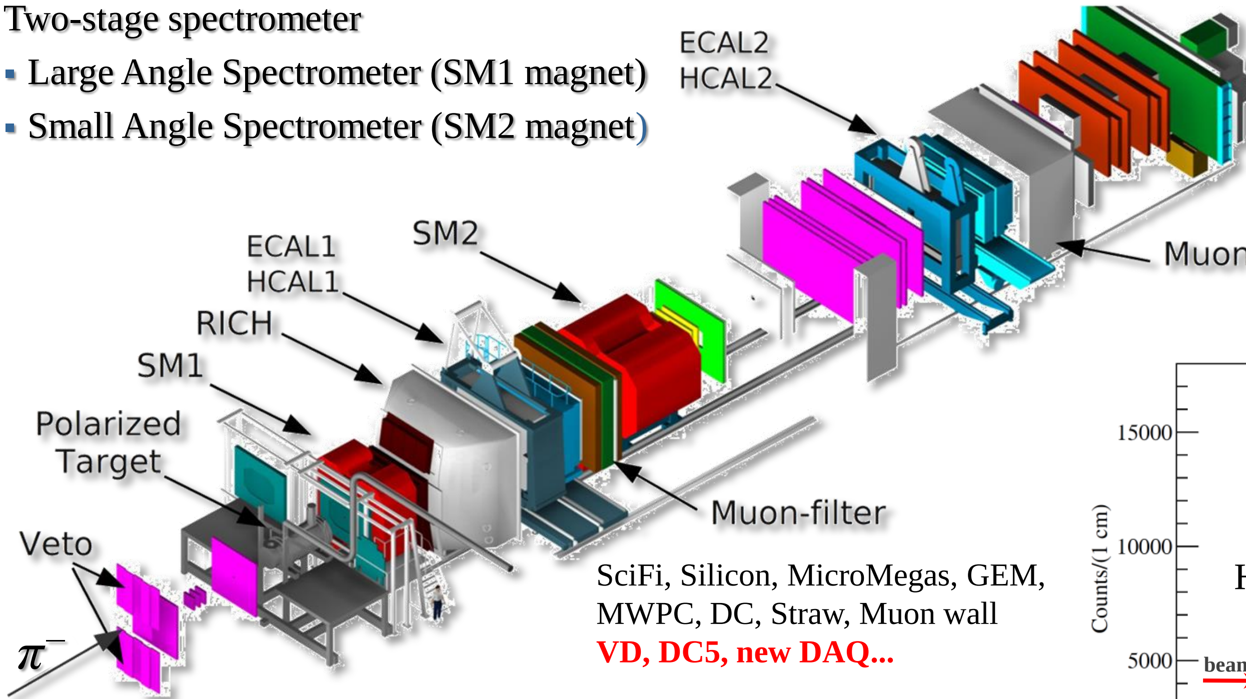

SciFi, Silicon, MicroMegas, GEM, MWPC, DC, Straw, Muon wall
VD, DC5, new DAQ...

- High energy beam
- Large angular acceptance
- Broad kinematical range
- Momentum, tracking and calorimetric measurements, PID

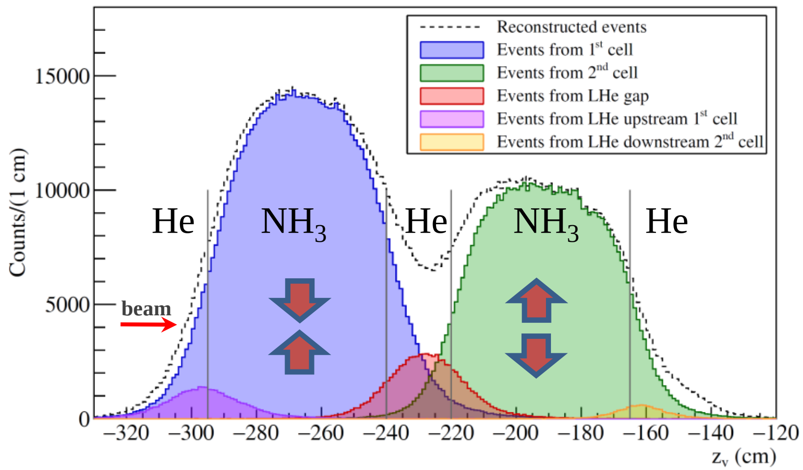

Data-taking years: 2014 (test) 2015 and 2018

High energy π^- beam:
Energy: 190 GeV/c, Intensity: 10^8 π/s

Target: Solid state

- NH_3 2-cell configuration. Polarization T ~ 73%, f ~ 0.18
- Data is collected simultaneously with both target spin orientations
  Periodic polarization reversal to minimize systematic effects

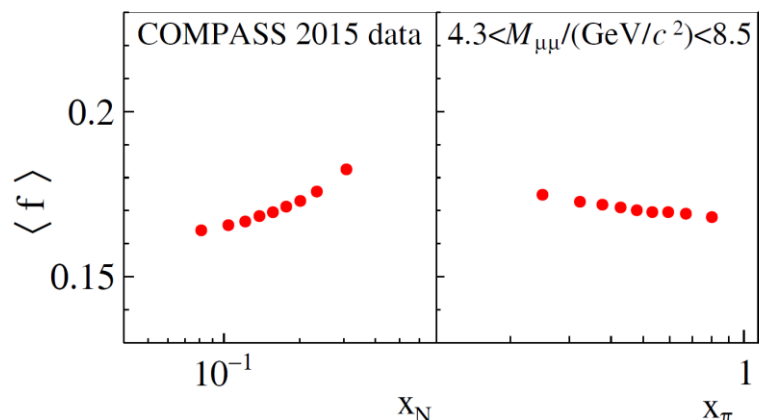

COMPASS experimental setup: Phase II (DY program)

Two-stage spectrometer

- Large Angle Spectrometer (SM1 magnet)
- Small Angle Spectrometer (SM2 magnet)

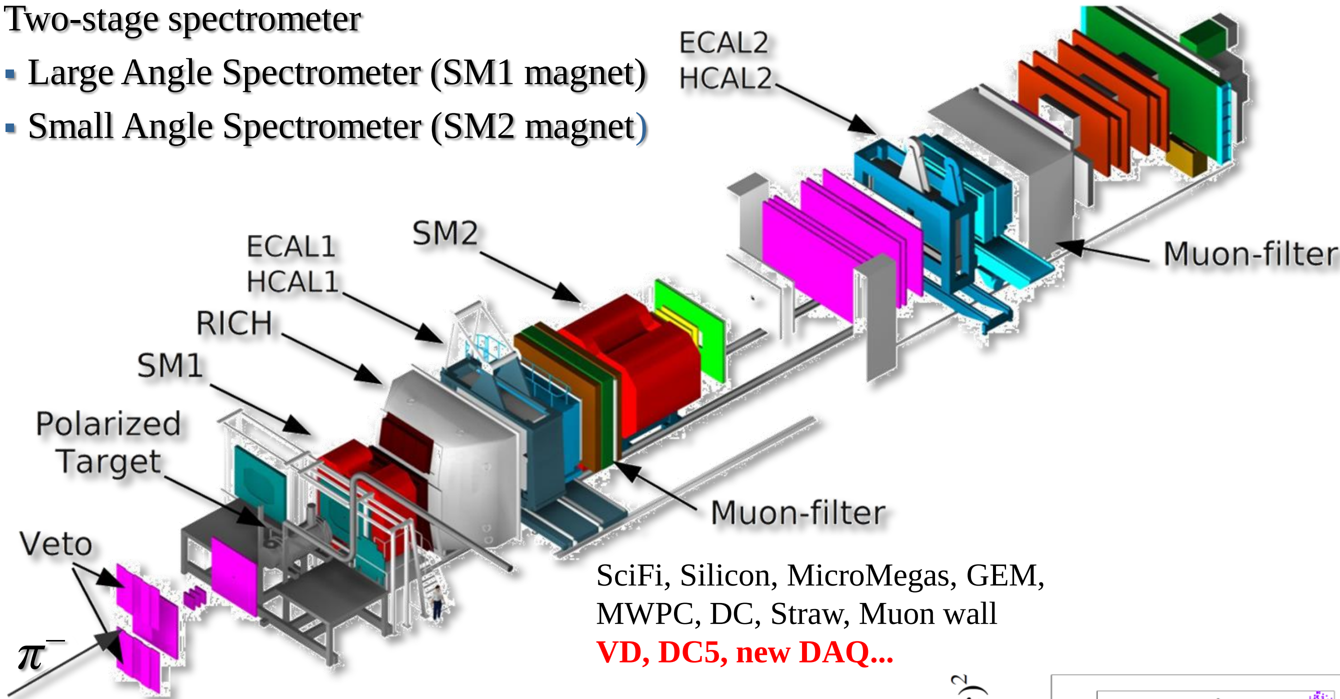

- High energy beam
- Large angular acceptance
- Broad kinematical range
- Momentum, tracking and calorimetric measurements, PID

SciFi, Silicon, MicroMegas, GEM, MWPC, DC, Straw, Muon wall

VD, DC5, new DAQ...

Data-taking years: 2014 (test) 2015 and 2018

High energy π^- beam:

Energy: 190 GeV/c, Intensity: 10^8 π/s

Target: Solid state

- NH_3 2-cell configuration. Polarization T ~ 73%, f ~ 0.18
- Data is collected simultaneously with both target spin orientations
  Periodic polarization reversal to minimize systematic effects

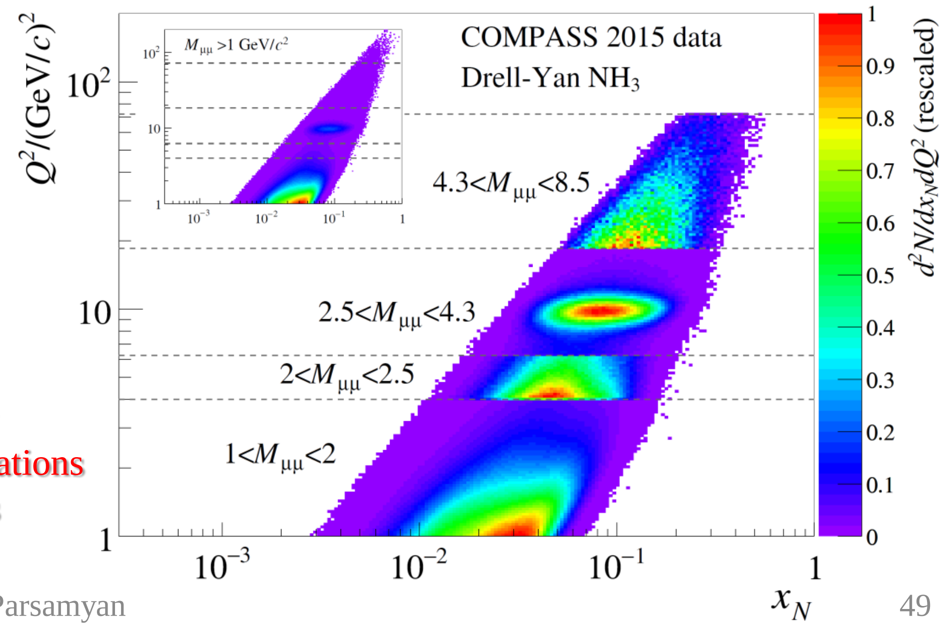

COMPASS DY mass ranges

- 1.0 < M /(GeV/c²) < 2.0 "Low mass"
  - Large background contamination, combinatorial, Open-charm (B) $D\bar{D}$, $B\bar{B}$, π, K decays
- 2.0 < M /(GeV/c²) < 2.5 "Intermediate mass"
  - High DY-cross section
  - Still low DY-signal/background ratio
- 2.5 < M /(GeV/c²) < 4.3 "Charmonia mass"
  - Strong J/ψ-signal → study of J/ψ physics
  - Good signal/background
- 4.3 < M /(GeV/c²) < 8.5 "High mass"
  - Low DY cross-section
  - Beyond charmonium region, background < 3%
  - Valence region → largest asymmetries

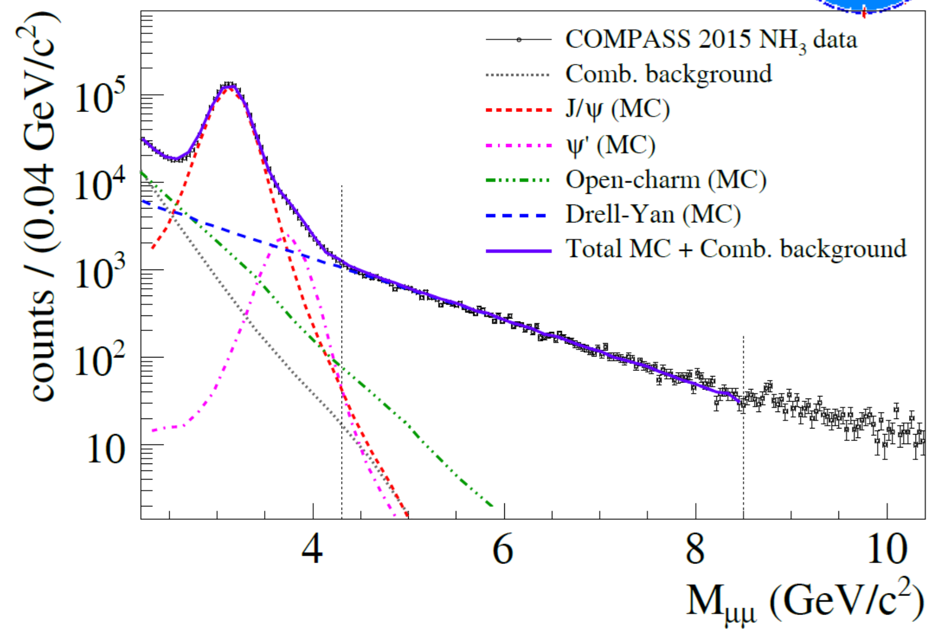

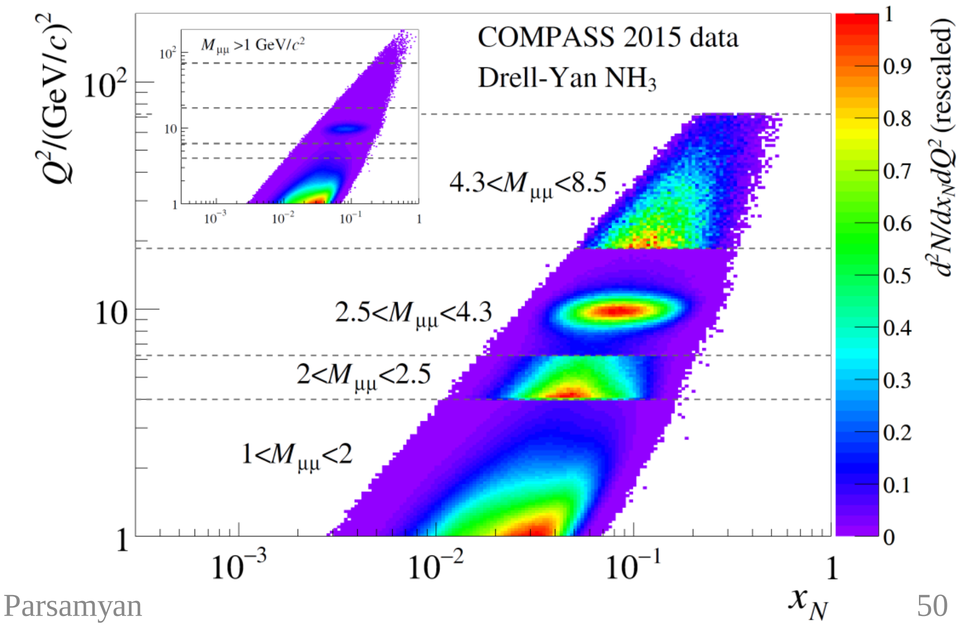

COMPASS DY: high mass range

- $1.0 < M/(GeV/c^2) < 2.0$ "Low mass"
  - Large background contamination, combinatorial, Open-charm (B) $D\bar{D}$, $B\bar{B}$, π, K decays
- $2.0 < M/(GeV/c^2) < 2.5$ "Intermediate mass"
  - High DY-cross section
  - Still low DY-signal/background ratio
- $2.5 < M/(GeV/c^2) < 4.3$ "Charmonia mass"
  - Strong J/ψ-signal → study of J/ψ physics
  - Good signal/background
- $4.3 < M/(GeV/c^2) < 8.5$ "High mass"
  - Low DY cross-section
  - Beyond charmonium region, background < 3%
  - Valence region → largest asymmetries

Final sample: 35 000 dimuons in HM

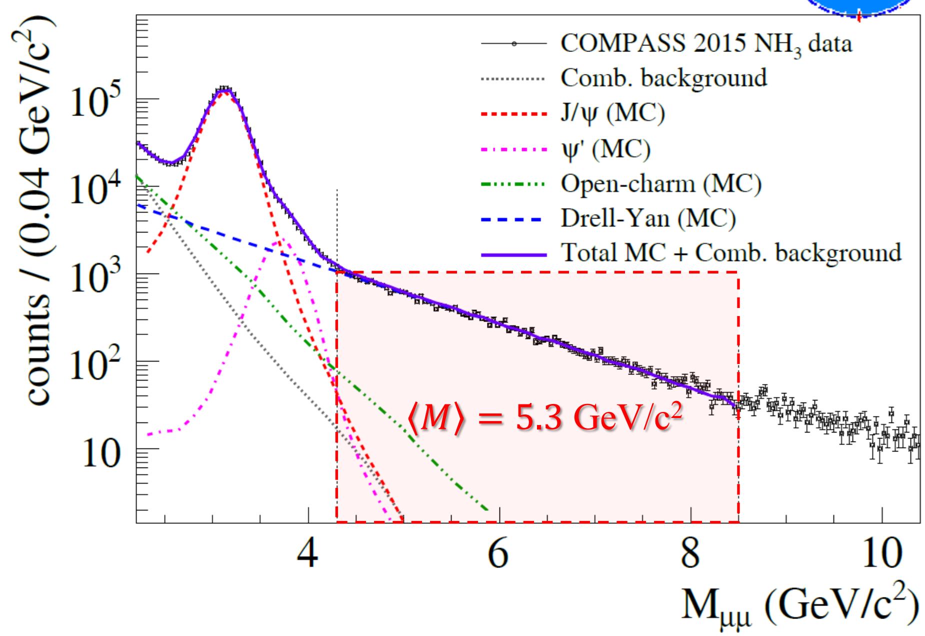

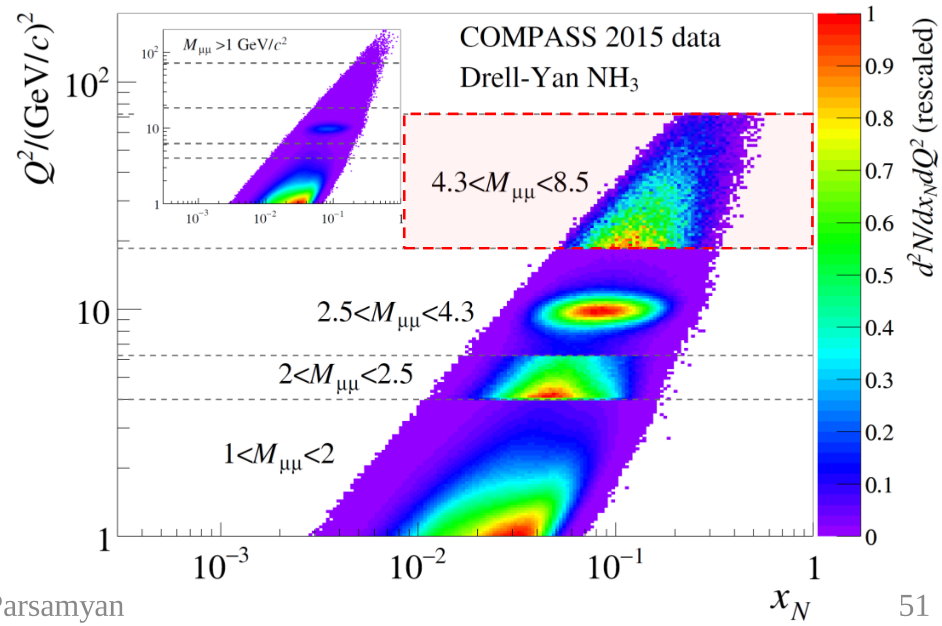

COMPASS DY: high mass range

- $1.0 < M/(\text{GeV}/c^2) < 2.0$ “Low mass”
  - Large background contamination, combinatorial, Open-charm (B) $D\bar{D}$, $B\bar{B}$, π, K decays
- $2.0 < M/(\text{GeV}/c^2) < 2.5$ “Intermediate mass”
  - High DY-cross section
  - Still low DY-signal/background ratio
- $2.5 < M/(\text{GeV}/c^2) < 4.3$ “Charmonia mass”
  - Strong J/ψ-signal → study of J/ψ physics
  - Good signal/background
- $4.3 < M/(\text{GeV}/c^2) < 8.5$ “High mass”
  - Low DY cross-section
  - Beyond charmonium region, background < 3%
  - Valence region → largest asymmetries

Final sample: 35 000 dimuons in HM

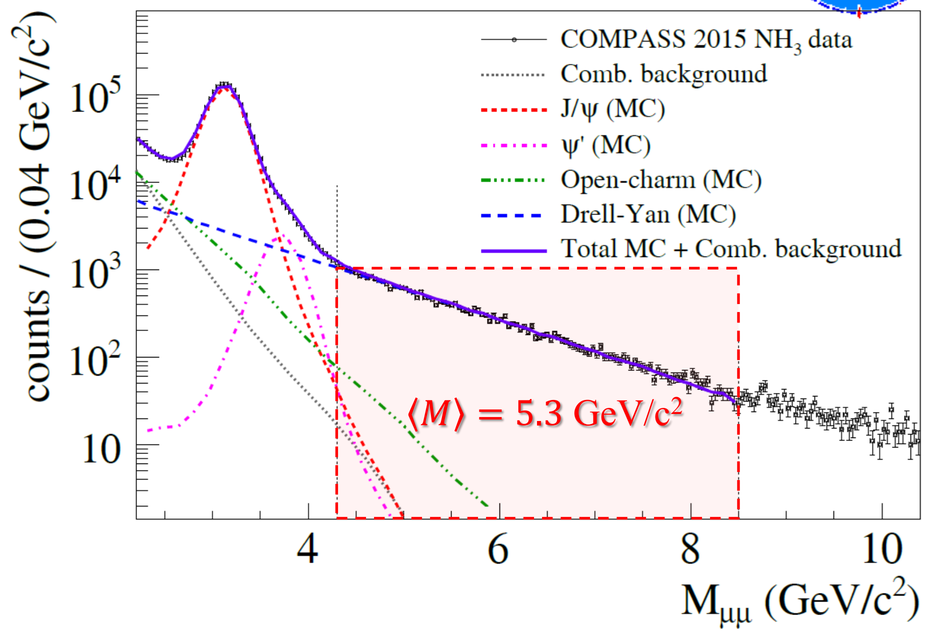

HM events are in the valence quark range

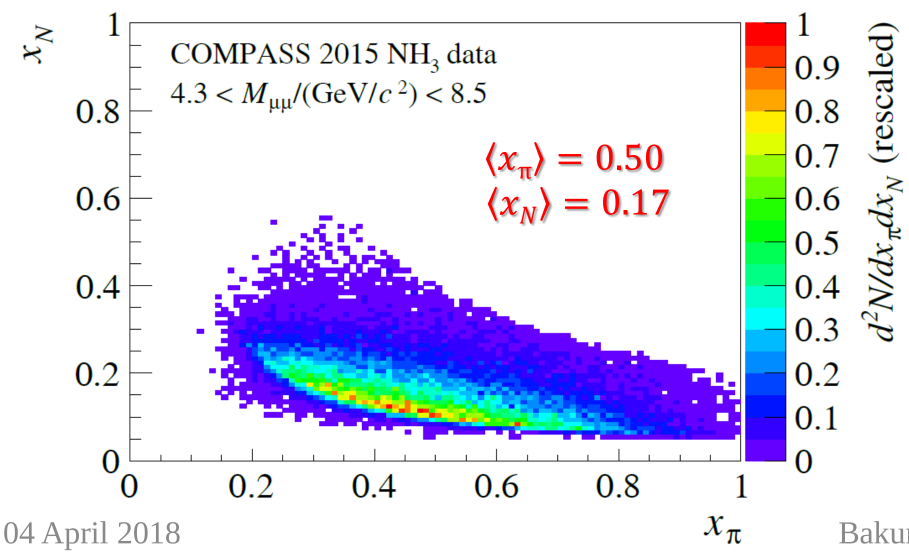

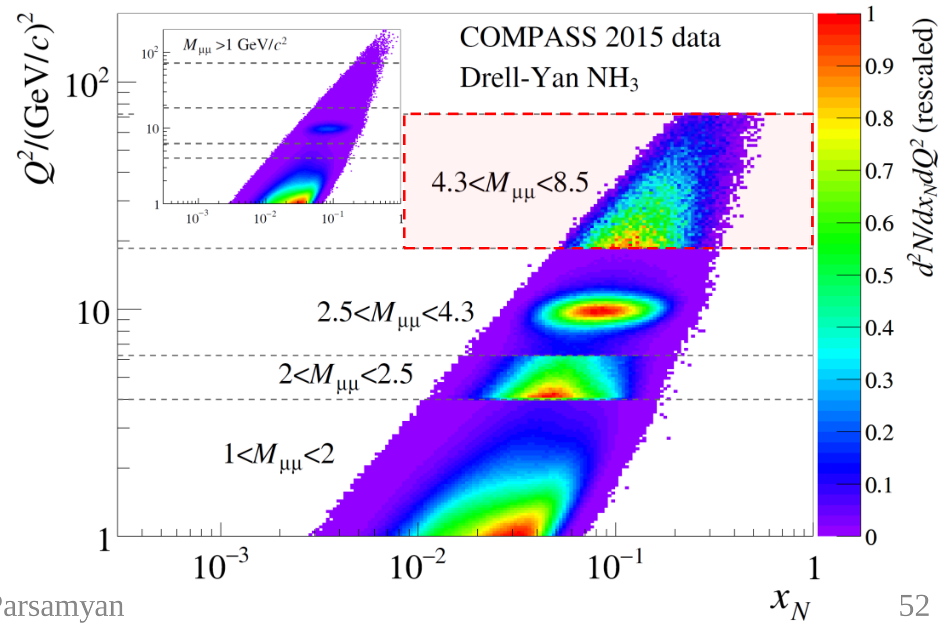

COMPASS DY: high mass range

- 1.0 < M /(GeV/c²) < 2.0 "Low mass"
  - Large background contamination, combinatorial, Open-charm (B) $D\bar{D}$, $B\bar{B}$, π, K decays
- 2.0 < M /(GeV/c²) < 2.5 "Intermediate mass"
  - High DY-cross section
  - Still low DY-signal/background ratio
- 2.5 < M /(GeV/c²) < 4.3 "Charmonia mass"
  - Strong J/ψ-signal → study of J/ψ physics
  - Good signal/background
- 4.3 < M /(GeV/c²) < 8.5 "High mass"
  - Low DY cross-section
  - Beyond charmonium region, background < 3%
  - Valence region → largest asymmetries

Final sample: 35 000 dimuons in HM

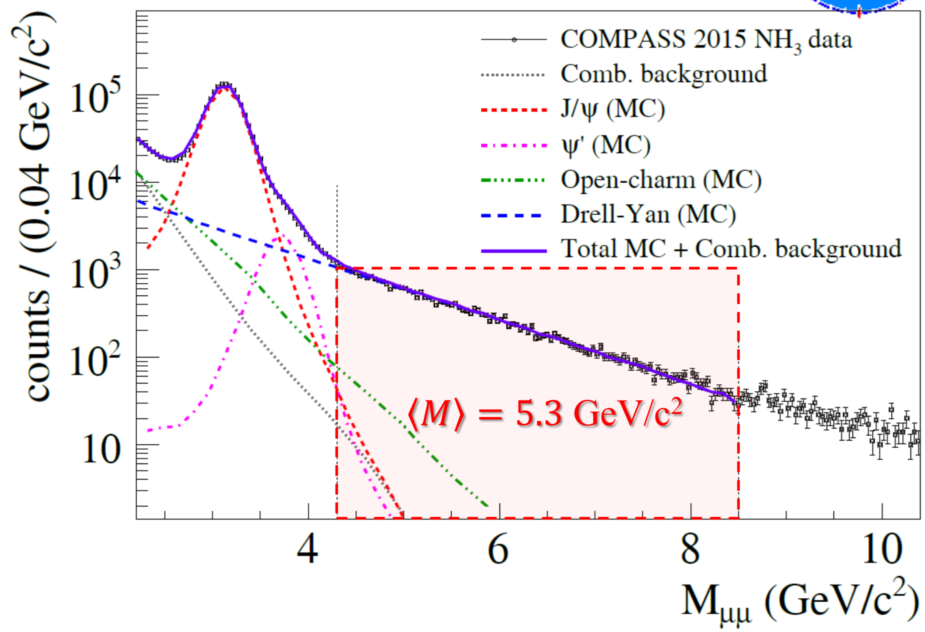

Dimuon transverse momentum q_T > 0.4 GeV/c

$\langle x_F \rangle = 0.33,\ \langle q_T \rangle = 1.2$ GeV/c

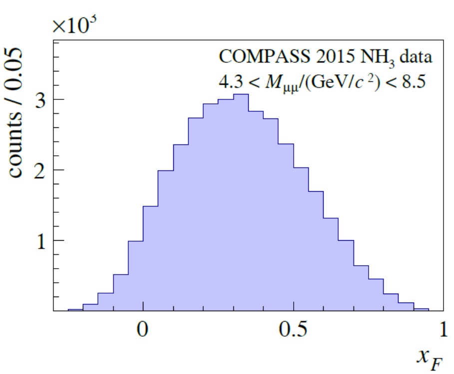

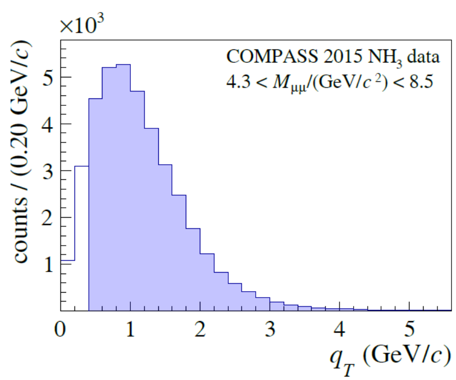

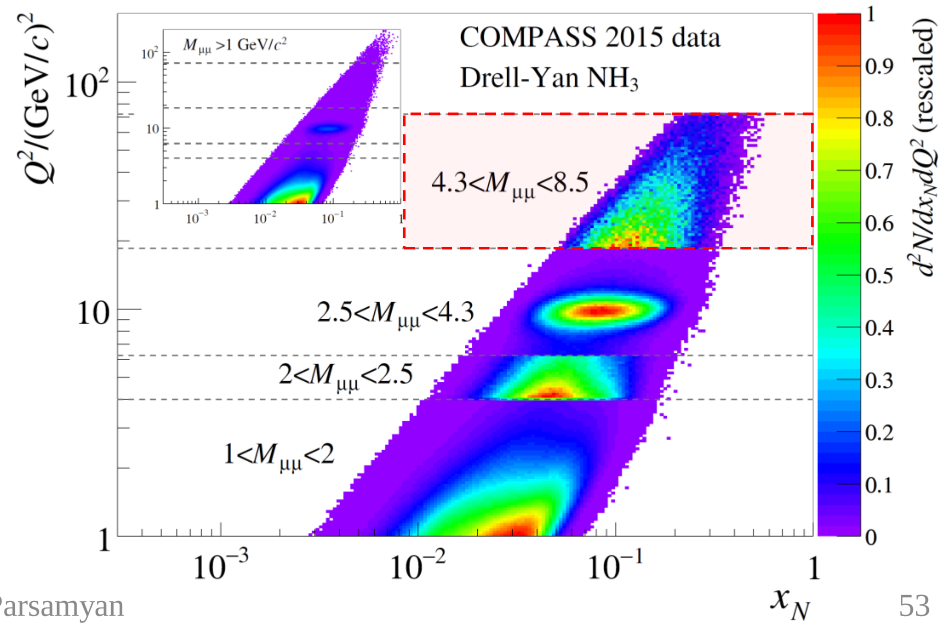

COMPASS DY: Charmonia mass range

ongoing analysis

- $1.0 < M/(\text{GeV}/c^2) < 2.0$ "Low mass"
  - Large background contamination, combinatorial, Open-charm (B) $D\bar{D}$, $B\bar{B}$, π, K decays
- $2.0 < M/(\text{GeV}/c^2) < 2.5$ "Intermediate mass"
  - High DY-cross section
  - Still low DY-signal/background ratio
- $2.5 < M/(\text{GeV}/c^2) < 4.3$ "Charmonia mass"
  - Strong J/ψ-signal → study of J/ψ physics
  - Good signal/background
- $4.3 < M/(\text{GeV}/c^2) < 8.5$ "High mass"
  - Low DY cross-section
  - Beyond charmonium region, background < 3%
  - Valence region → largest asymmetries

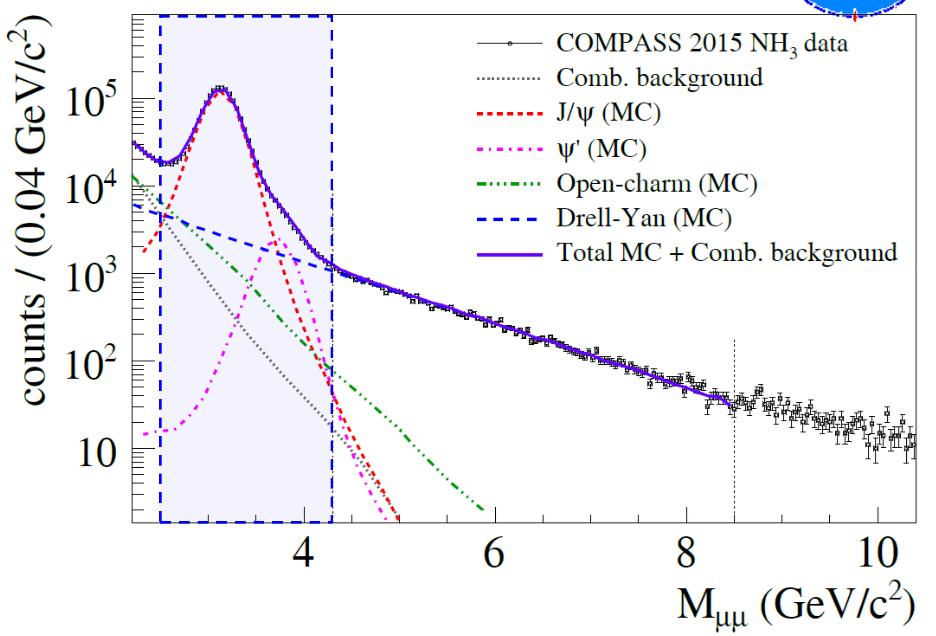

$\langle x_\pi \rangle = 0.31, \langle x_N \rangle = 0.09, \langle x_F \rangle = 0.22, \langle q_T \rangle = 1.1$ GeV/c

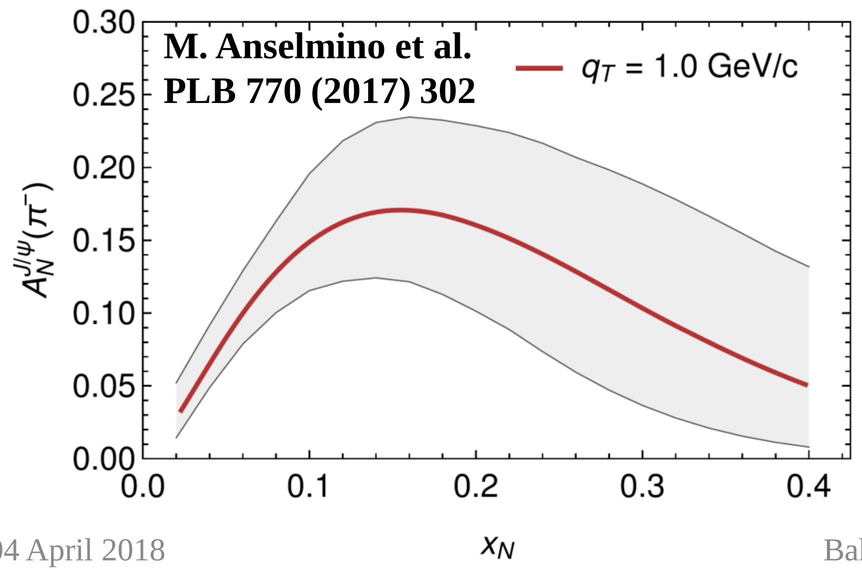

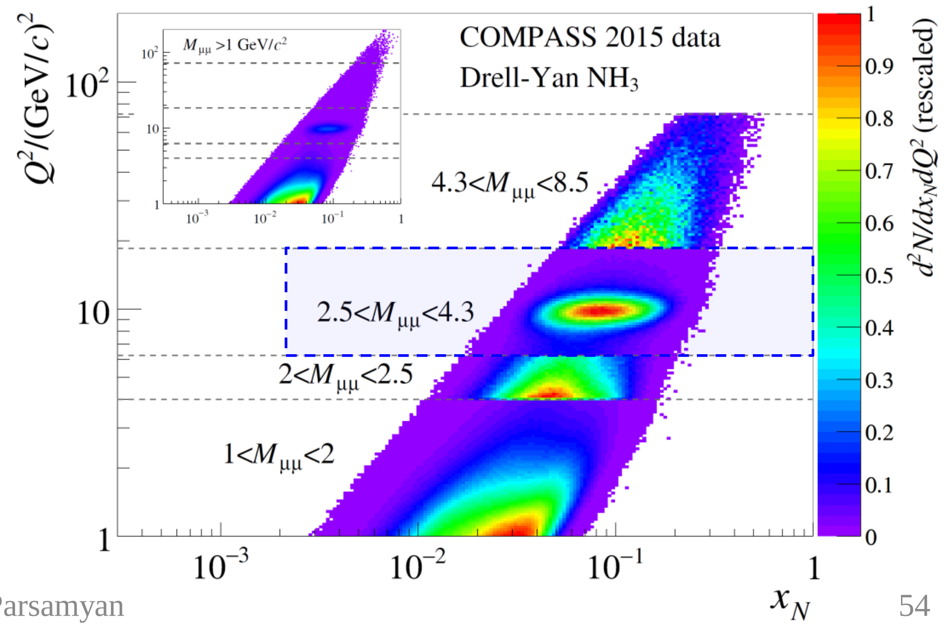

SIDIS and single-polarized DY x-sections at twist-2 (LO)

SIDIS

$$\frac{d\sigma^{LO}}{dxdydzdp_T^2 d\phi_h d\phi_S} \propto \left(F_{UU,T} + \varepsilon F_{UU,L}\right)$$

$$\times \left\{ \begin{array}{l} 1 + \boxed{\varepsilon A_{UU}^{\cos 2\phi_h} \cos 2\phi_h} \\ + S_L\, \varepsilon A_{UL}^{\sin 2\phi_h} \sin 2\phi_h + S_L \lambda \sqrt{1-\varepsilon^2} A_{LL} \\ \boxed{+ S_T \left[\begin{array}{l} A_{UT}^{\sin(\phi_h-\phi_S)} \sin(\phi_h-\phi_S) \\ + \varepsilon A_{UT}^{\sin(\phi_h+\phi_S)} \sin(\phi_h+\phi_S) \\ + \varepsilon A_{UT}^{\sin(3\phi_h-\phi_S)} \sin(3\phi_h-\phi_S) \end{array} \right]} \\ + S_T \lambda \left[\sqrt{\left(1-\varepsilon^2\right)} A_{LT}^{\cos(\phi_h-\phi_S)} \cos(\phi_h-\phi_S) \right] \end{array} \right\}$$

DY

$$\frac{d\sigma^{LO}}{d\Omega} \propto F_U^1 \left(1+\cos^2\theta_{CS}\right)$$

$$\times \left\{ \begin{array}{l} 1 + \boxed{D_{[\sin^2\theta_{CS}]} A_U^{\cos 2\varphi_{CS}} \cos 2\varphi_{CS}} \\ + S_L \sin^2\theta_{CS} A_L^{\sin 2\varphi_{CS}} \sin 2\varphi_{CS} \\ \boxed{+ S_T \left[\begin{array}{l} A_T^{\sin\varphi_S} \sin\varphi_S \\ + D_{[\sin^2\theta_{CS}]} \left(\begin{array}{l} A_T^{\sin(2\varphi_{CS}-\varphi_S)} \sin(2\varphi_{CS}-\varphi_S) \\ + A_T^{\sin(2\varphi_{CS}+\varphi_S)} \sin(2\varphi_{CS}+\varphi_S) \end{array} \right) \end{array} \right]} \end{array} \right\}$$

where $D_{[\sin^2\theta_{CS}]} = \sin^2\theta_{CS} / \left(1+\cos^2\theta_{CS}\right)$

SIDIS-DY bridge

Comparable x:Q² coverage – minimization of possible Q²-evolution effects

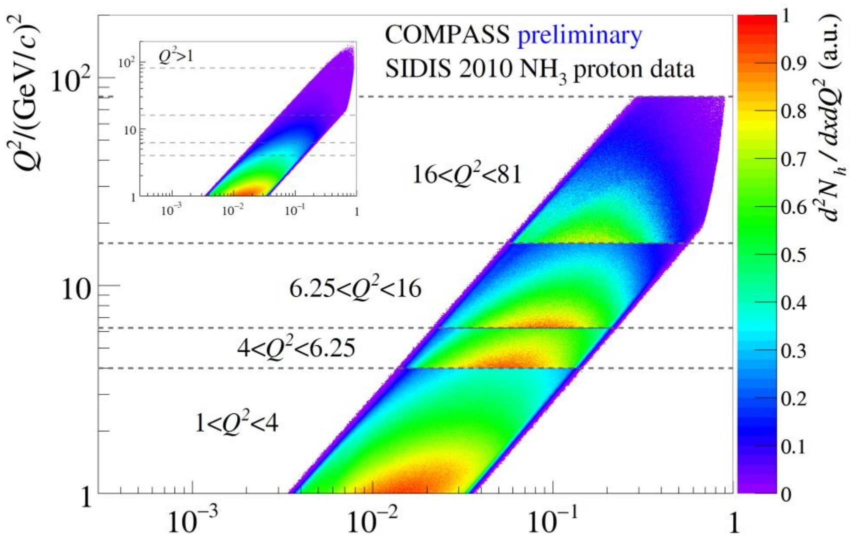

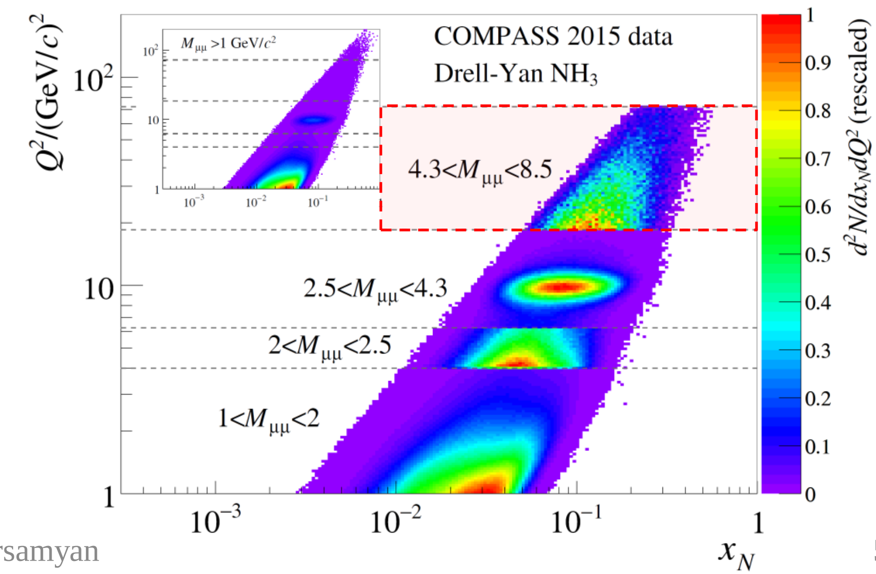

- Selected COMPASS-HERMES SIDIS results

Experiments in last 35 years: part II

HERA MEasurement of Spin

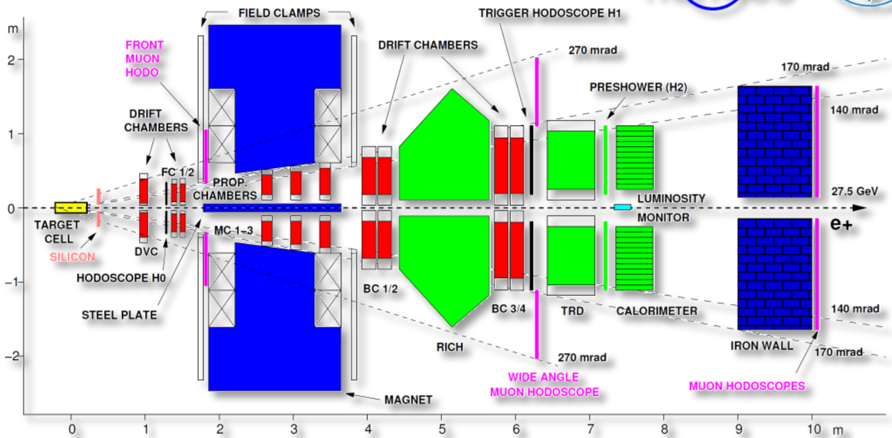

Location: DESY, HERA

Beam: *e^+/e^-, polarized (both helicity states)(<60%), 27.5 GeV*

Target: *Gaseous target (H/D)*

- H/D Polarization (L & T) ~ 70-85%, f ~ 1
- Direct access to hydrogen or deuterium

Fast spin reversal (<1s)

- Same acceptance for different polarization states
- single cell configuration
- Hydrogen - measurements only with transverse polarization
- Deuterium - both transverse and longitudinal polarization measurements

COmmon Muon Proton Apparatus for Structure and Spectroscopy

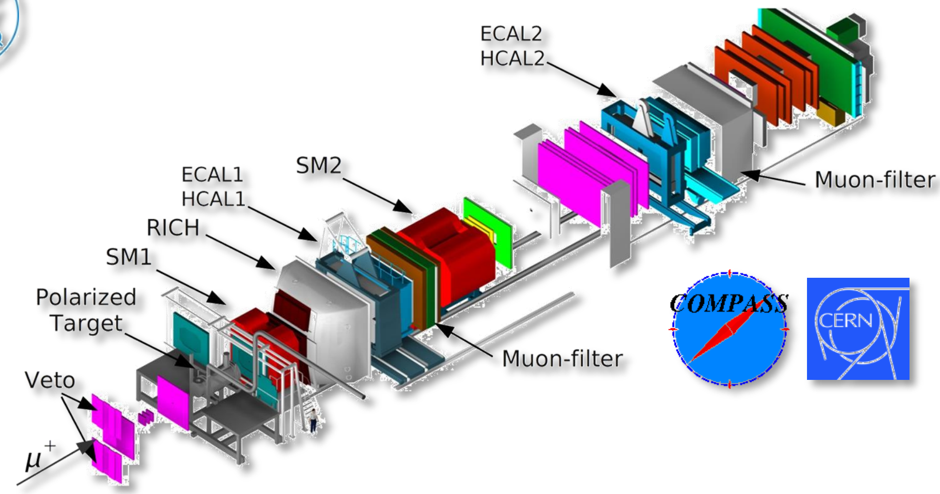

Location: CERN SPS North Area. (2-stage spectrometer LAS-SAS)

Beam: *μ^+, longitudinally polarized (~80%), 160 GeV*

Target: *Solid state target (^6LiD or NH_3)*

- ^6LiD Polarization (L & T) ~ 50%, f ~ 0.38
- NH_3 Polarization (L & T) ~ 80%, f ~ 0.14

2-cell target configuration for ^6LiD and 3-cell for NH_3

Neighboring cells are polarized in opposite directions

- Data is collected simultaneously for the two target spin orientations
- Spin reversal after each ~4-5 days
- Such a construction allows to reduce systematic effects due to the acceptance

Experiments in last 35 years: part II

HERA MEasurement of Spin

COmmon Muon Proton Apparatus for Structure and Spectroscopy

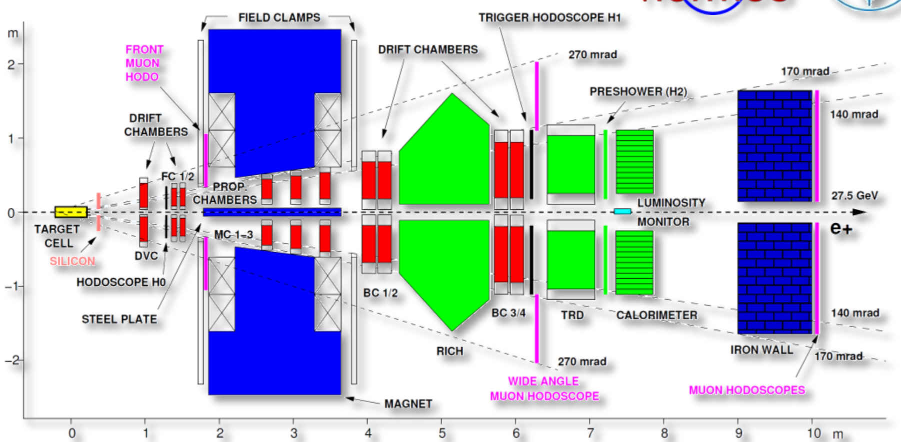

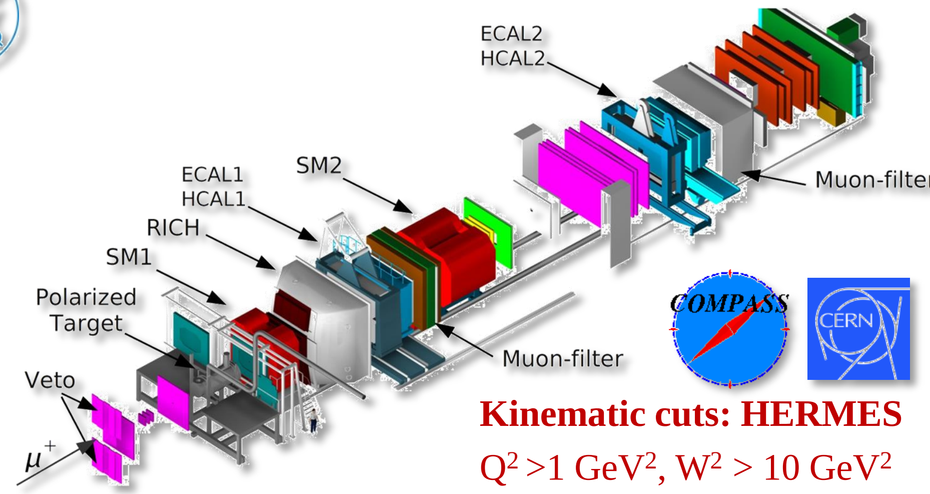

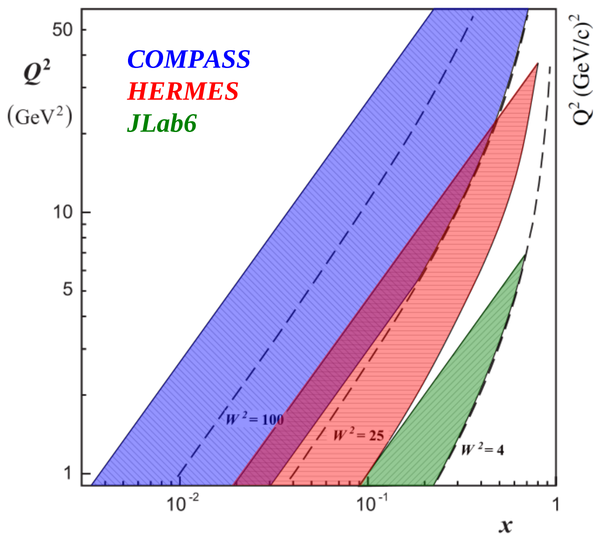

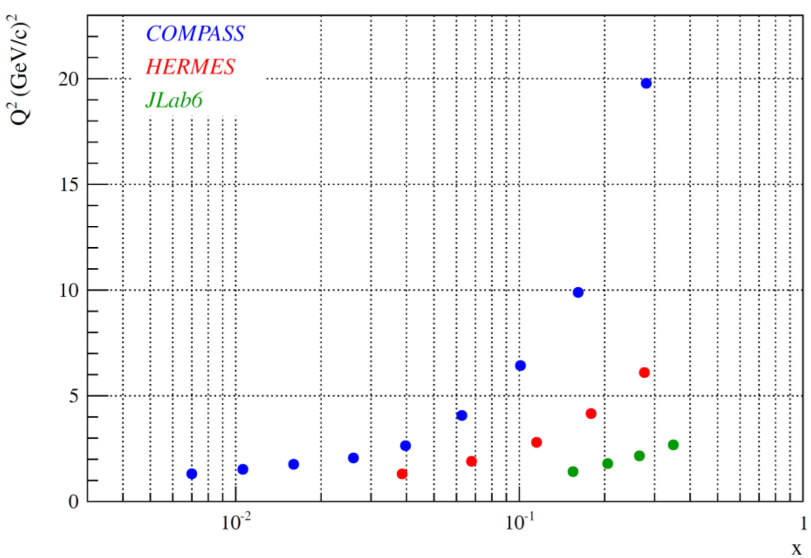

Kinematic cuts: HERMES

$Q^2 > 1$ GeV^2, $W^2 > 10$ GeV^2

$0.023 < x < 0.6$, $0.2 < y < 0.85$

$z > 0.2$ and $x_F > 0.2$

Pions 1 GeV $< P_h < 15$ GeV

Kaons 2 GeV $< P_h < 15$ GeV

Kinematic cuts: COMPASS

$Q^2 > 1$ GeV^2, $W^2 > 25$ GeV

$\theta_\gamma^{lab} < 0.06$

$0.003 < x < 0.13$, $0.2 < y < 0.9$

$0.2 < z < 0.85$

$0.1 < P_{hT} < 1$ GeV/c

Kinematic cuts: JLab

$Q^2 > 1$ GeV^2, $W^2 > 4$ GeV^2

$0.14 < x < 0.48$, $0.4 < y < 0.7$

$0.4 < z < 0.7$

$A_{UU}^{\cos\varphi}$ and $A_{UU}^{\cos2\varphi}$ amplitudes h^+/h^-

Different kinematic regions!

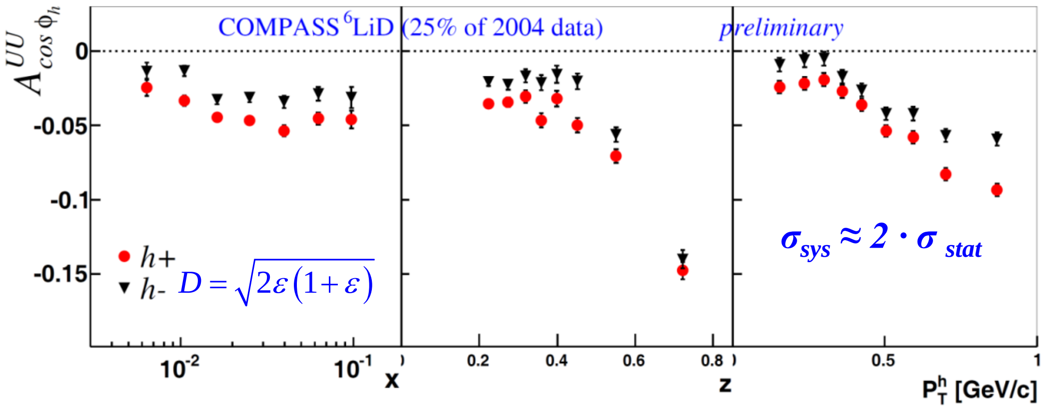

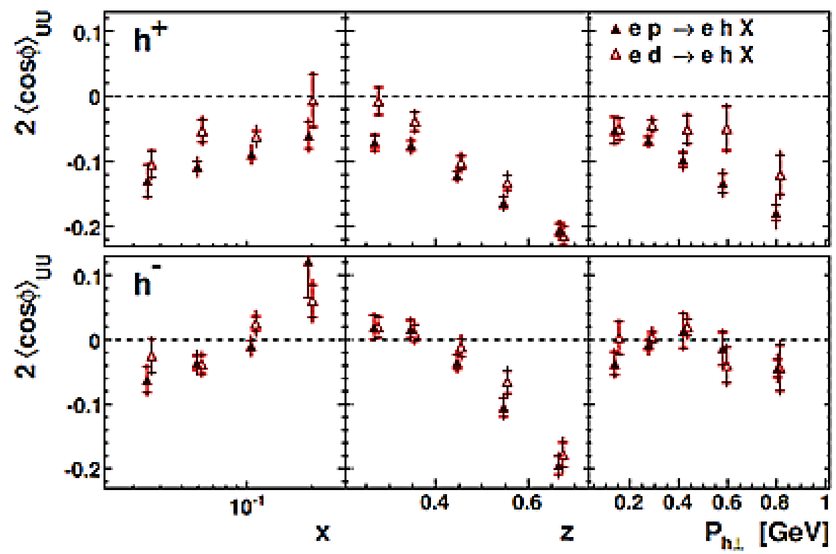

- ➢ Similar trends for h^+/h^-

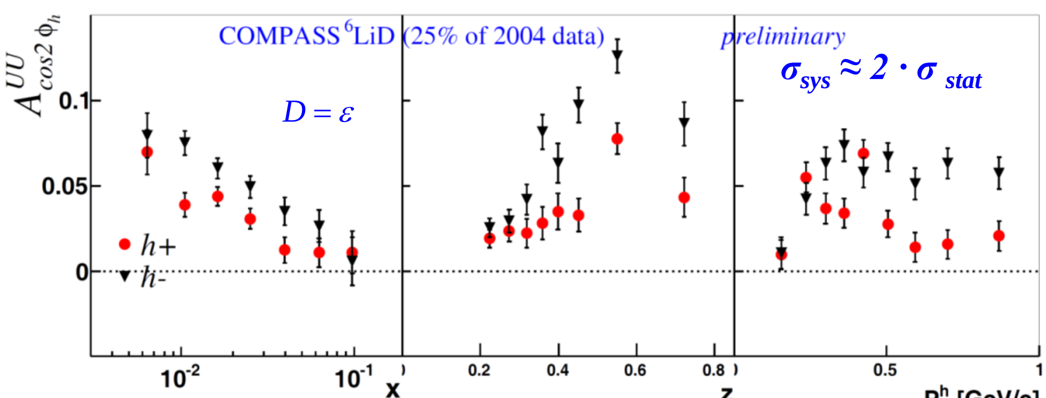

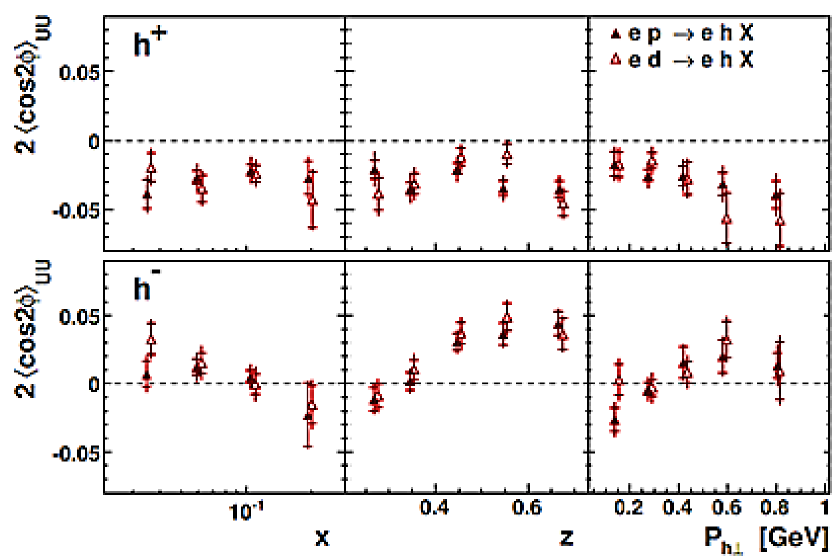

- ➢ Similar trends for h^+/h^-
- ➢ No sign change for h^+/h^- at COMPASS

The $A_{UU}^{\cos\phi_h}$ and $A_{UU}^{\cos 2\phi_h}$ asymmetries (Cahn+BM)

$$\frac{d\sigma}{dxdydzdp_T^2 d\phi_h d\phi_S} \propto \left(F_{UU,T} + \varepsilon F_{UU,L}\right)$$

$$\times \left\{ \begin{array}{l} 1 + \sqrt{2\varepsilon(1+\varepsilon)} A_{UU}^{\cos\phi_h} \cos\phi_h + \varepsilon A_{UU}^{\cos 2\phi_h} \cos 2\phi_h \\ + \lambda \sqrt{2\varepsilon(1-\varepsilon)} A_{LU}^{\sin\phi_h} \sin\phi_h \end{array} \right\}$$

- Complicated mixture Cahn+BM
- Large effects both for h^+ and h^-
- Multi-D results available HERMES P/D COMPASS D and currently also P (DVCS)
- Global Cahn+BM fit attempts see f.i. PRD91,074019 (2015)

COMPASS **NPB 886 (2014) 1046**

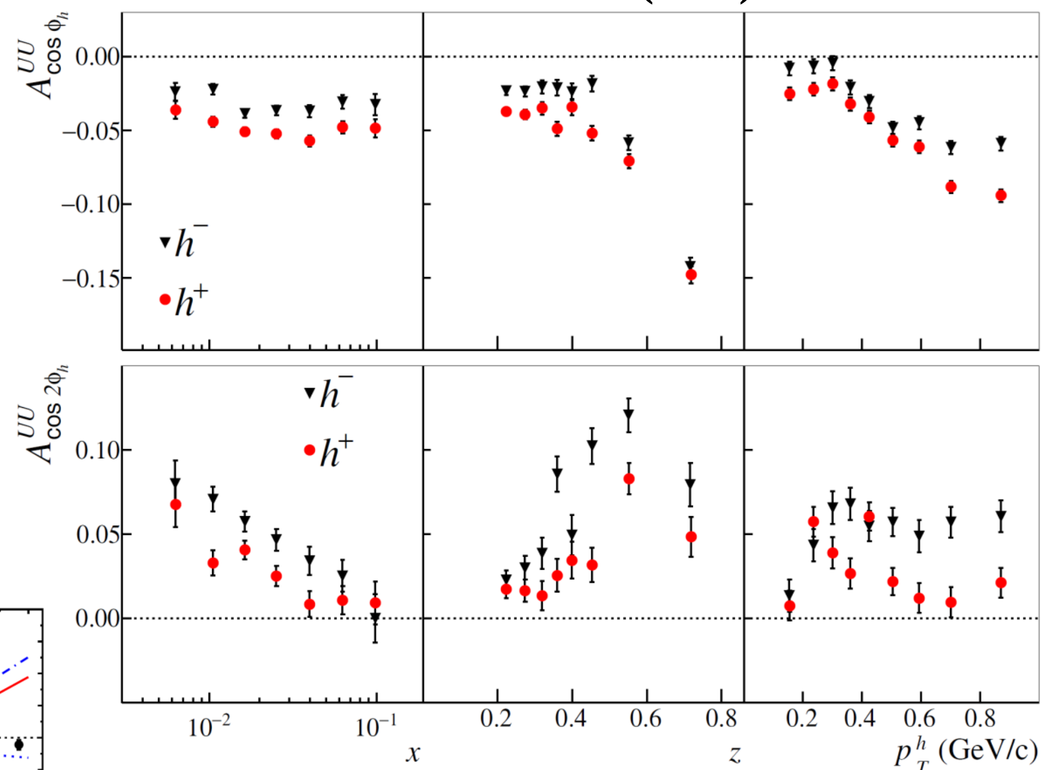

$$A_{UU}^{\cos\phi_h} \propto \frac{2M}{Q}\left\{ -f_1^q \otimes D_{1q}^h - h_1^{\perp q} \otimes H_{1q}^{\perp h} \right\}$$

$$A_{UU}^{\cos 2\phi_h} \propto -h_1^{\perp q} \otimes H_{1q}^{\perp h} + \left(\frac{M}{Q}\right)^2 f_1^q \otimes D_{1q}^h + \ldots.$$

V. Barone, S. Melis, A. Prokudin, **PRD 81,** 114026 (2010)

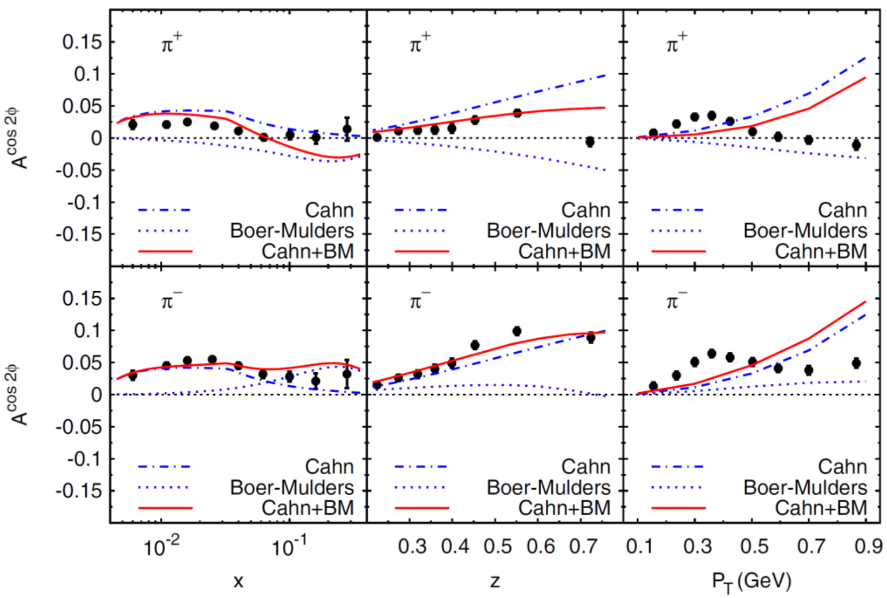

SIDIS: target longitudinal spin dependent asymmetries

$$\frac{d\sigma}{dxdydzdp_T^2 d\phi_h d\phi_S} \propto \left(F_{UU,T} + \varepsilon F_{UU,L}\right)\left\{ 1 + \ldots \right.$$

$$+ S_L \left[\sqrt{2\varepsilon(1+\varepsilon)} A_{UL}^{\sin\phi_h} \sin\phi_h + \varepsilon A_{UL}^{\sin 2\phi_h} \sin 2\phi_h \right]$$

$$\left. + S_L \lambda \left[\sqrt{1-\varepsilon^2} A_{LL} + \sqrt{2\varepsilon(1-\varepsilon)} A_{LL}^{\cos\phi_h} \cos\phi_h \right] \right\}$$

$$F_{UL}^{\sin\phi_h} = \frac{2M}{Q}\mathcal{C}\left\{ -\frac{\hat{\boldsymbol{h}}\cdot \boldsymbol{p}_T}{M_h}\left(x h_L^q H_{1q}^{\perp h} + \frac{M_h}{M} g_{1L}^q \frac{\tilde{G}_q^{\perp h}}{z} \right) + \frac{\hat{\boldsymbol{h}}\cdot \boldsymbol{k}_T}{M}\left(x f_L^{\perp q} D_{1q}^h - \frac{M_h}{M} h_{1L}^{\perp q} \frac{\tilde{H}_q^h}{z} \right) \right\}$$

$$F_{UL}^{\sin 2\phi_h} = \mathcal{C}\left\{ -\frac{2\left(\hat{\boldsymbol{h}}\cdot \boldsymbol{p}_T\right)\left(\hat{\boldsymbol{h}}\cdot \boldsymbol{k}_T\right) - \boldsymbol{p}_T\cdot \boldsymbol{k}_T}{M M_h} h_{1L}^{\perp q} H_{1q}^{\perp h} \right\}$$

$$F_{LL}^{1} = \mathcal{C}\left\{ g_{1L}^q D_{1q}^h \right\}$$

$$F_{LL}^{\cos\phi_h} = \frac{2M}{Q}\mathcal{C}\left\{ -\frac{\hat{\boldsymbol{h}}\cdot \boldsymbol{p}_T}{M_h}\left(x e_L^q H_{1q}^{\perp h} + \frac{M_h}{M} g_{1L}^q \frac{\tilde{D}_q^{\perp h}}{z} \right) + \frac{\hat{\boldsymbol{h}}\cdot \boldsymbol{k}_T}{M}\left(x g_L^{\perp q} D_{1q}^h - \frac{M_h}{M} h_{1L}^{\perp q} \frac{\tilde{E}_q^h}{z} \right) \right\}$$

SIDIS: target longitudinal spin dependent asymmetries

$$\frac{d\sigma}{dxdydzdp_T^2 d\phi_h d\phi_S} \propto \left(F_{UU,T} + \varepsilon F_{UU,L}\right)\left\{ 1+\ldots \right.$$

$$+ S_L \left[\sqrt{2\varepsilon\left(1+\varepsilon\right)} A_{UL}^{\sin\phi_h} \sin\phi_h + \varepsilon A_{UL}^{\sin 2\phi_h} \sin 2\phi_h \right]$$

$$\left. + S_L\lambda \left[\sqrt{1-\varepsilon^2} A_{LL} + \sqrt{2\varepsilon\left(1-\varepsilon\right)} A_{LL}^{\cos\phi_h} \cos\phi_h \right] \right\}$$

$$F_{UL}^{\sin\phi_h} = \frac{2M}{Q}\mathcal{C}\left\{ -\frac{\hat{\boldsymbol{h}}\cdot\boldsymbol{p_T}}{M_h}\left(x h_L^q H_{1q}^{\perp h} + \frac{M_h}{M} g_{1L}^q \frac{\tilde{G}_q^{\perp h}}{z} \right) + \frac{\hat{\boldsymbol{h}}\cdot\boldsymbol{k_T}}{M}\left(x f_L^{\perp q} D_{1q}^h - \frac{M_h}{M} h_{1L}^{\perp q} \frac{\tilde{H}_q^h}{z} \right) \right\}$$

$$F_{UL}^{\sin 2\phi_h} = \mathcal{C}\left\{ -\frac{2\left(\hat{\boldsymbol{h}}\cdot\boldsymbol{p_T}\right)\left(\hat{\boldsymbol{h}}\cdot\boldsymbol{k_T}\right) - \boldsymbol{p_T}\cdot\boldsymbol{k_T}}{MM_h} h_{1L}^{\perp q} H_{1q}^{\perp h} \right\}$$

$$F_{LL}^{1} = \mathcal{C}\left\{ g_{1L}^q D_{1q}^h \right\}$$

$$F_{LL}^{\cos\phi_h} = \frac{2M}{Q}\mathcal{C}\left\{ -\frac{\hat{\boldsymbol{h}}\cdot\boldsymbol{p_T}}{M_h}\left(x e_L^q H_{1q}^{\perp h} + \frac{M_h}{M} g_{1L}^q \frac{\tilde{D}_q^{\perp h}}{z} \right) + \frac{\hat{\boldsymbol{h}}\cdot\boldsymbol{k_T}}{M}\left(x g_L^{\perp q} D_{1q}^h - \frac{M_h}{M} h_{1L}^{\perp q} \frac{\tilde{E}_q^h}{z} \right) \right\}$$

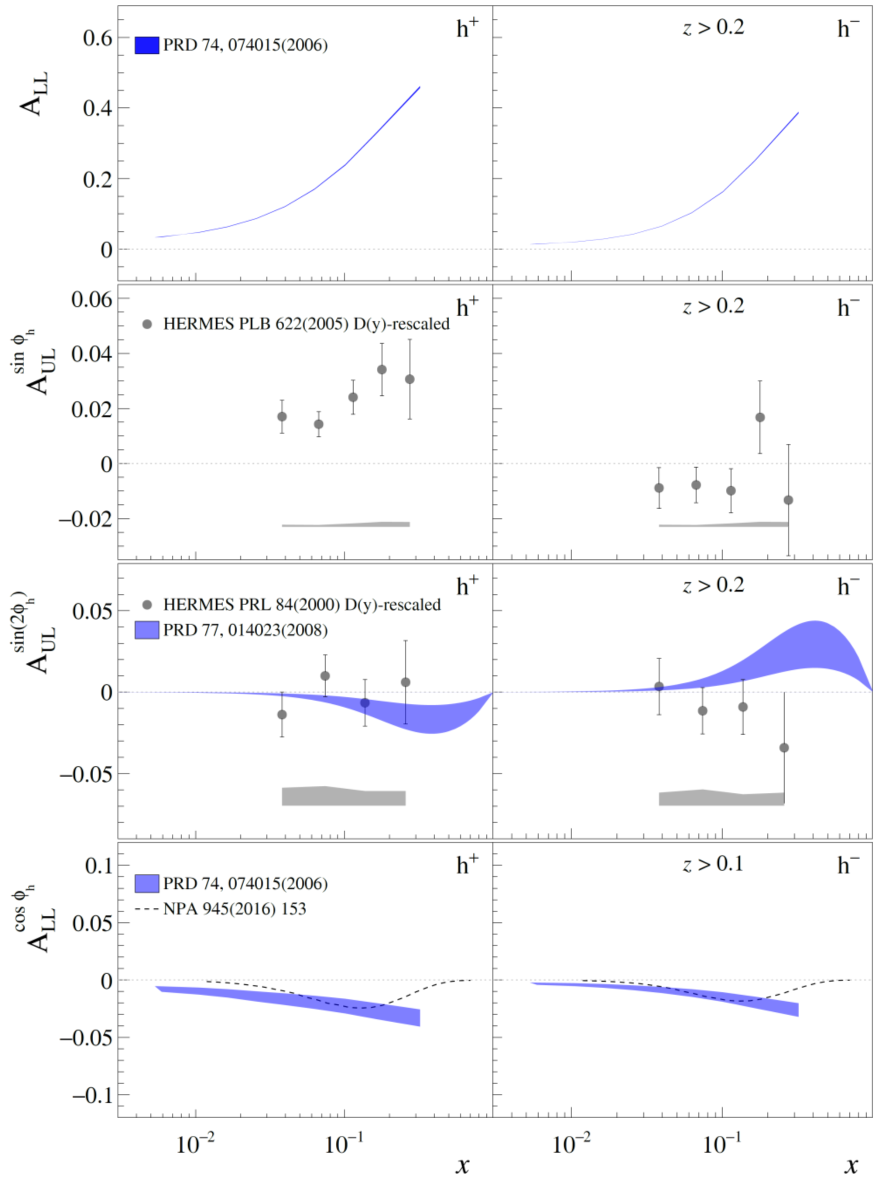

SIDIS: target longitudinal spin dependent asymmetries

$$\frac{d\sigma}{dxdydzdp_T^2d\phi_h d\phi_S} \propto \left(F_{UU,T}+\varepsilon F_{UU,L}\right)\Big\{ 1+\ldots + S_L\left[\sqrt{2\varepsilon(1+\varepsilon)}A_{UL}^{\sin\phi_h}\sin\phi_h + \varepsilon A_{UL}^{\sin 2\phi_h}\sin 2\phi_h\right] + S_L\lambda\left[\sqrt{1-\varepsilon^2}A_{LL} + \sqrt{2\varepsilon(1-\varepsilon)}A_{LL}^{\cos\phi_h}\cos\phi_h\right]\Big\}$$

COMPASS collected large amount of L-SIDIS data

Unprecedented precision!

$A_{UL}^{\sin\phi_h}$
- Q-suppression, Various different “twist” ingredients
- Sizable TSA-mixing
- **Significant h⁺ asymmetry, clear *z*-dependence,**
- **h⁻ compatible with zero**

$A_{UL}^{\sin 2\phi_h}$
- Only “twist-2” ingredients
- Additional p_T-suppression
- **Compatible with zero, in agreement with models**
- **Collins-like behavior?**

$A_{LL}^{\cos\phi_h}$
- Q-suppression, Various different “twist” ingredients
- **Compatible with zero, in agreement with models**

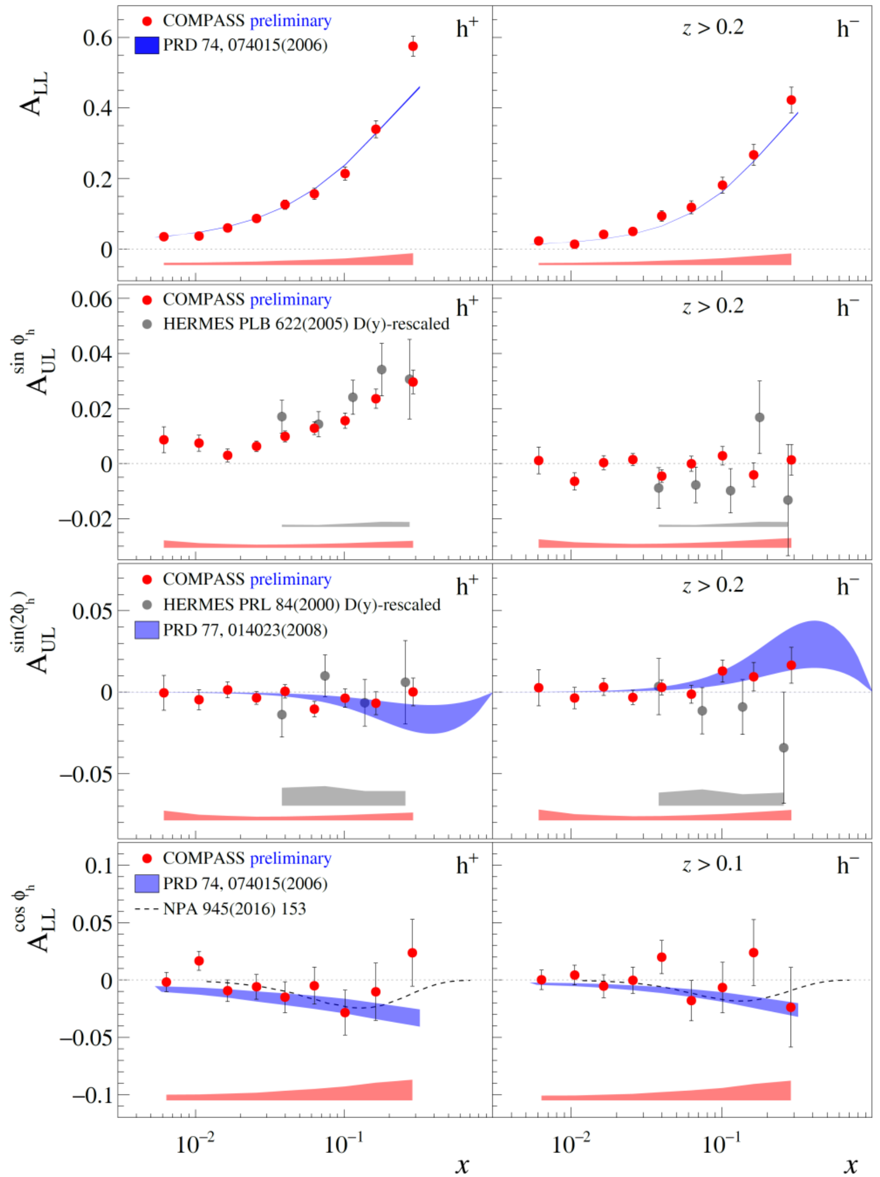

SIDIS: target longitudinal spin dependent asymmetries

$$\frac{d\sigma}{dxdydzdp_T^2d\phi_h d\phi_S} \propto \left(F_{UU,T} + \varepsilon F_{UU,L}\right)\left\{ 1 + \ldots \right.$$
$$+ S_L \left[\sqrt{2\varepsilon(1+\varepsilon)} A_{UL}^{\sin\phi_h} \sin\phi_h + \varepsilon A_{UL}^{\sin 2\phi_h} \sin 2\phi_h \right]$$
$$\left. + S_L \lambda \left[\sqrt{1-\varepsilon^2} A_{LL} + \sqrt{2\varepsilon(1-\varepsilon)} A_{LL}^{\cos\phi_h} \cos\phi_h \right] \right\}$$

COMPASS collected large amount of L-SIDIS data

Unprecedented precision!

$A_{UL}^{\sin\phi_h}$

- Q-suppression, Various different "twist" ingredients
- Sizable TSA-mixing
- **Significant h⁺ asymmetry, clear *z*-dependence,**
- **h⁻ compatible with zero**

$A_{UL}^{\sin 2\phi_h}$

- Only "twist-2" ingredients
- Additional p_T-suppression
- **Compatible with zero, in agreement with models**
- **Collins-like behavior?**

$A_{LL}^{\cos\phi_h}$

- Q-suppression, Various different "twist" ingredients
- **Compatible with zero, in agreement with models**

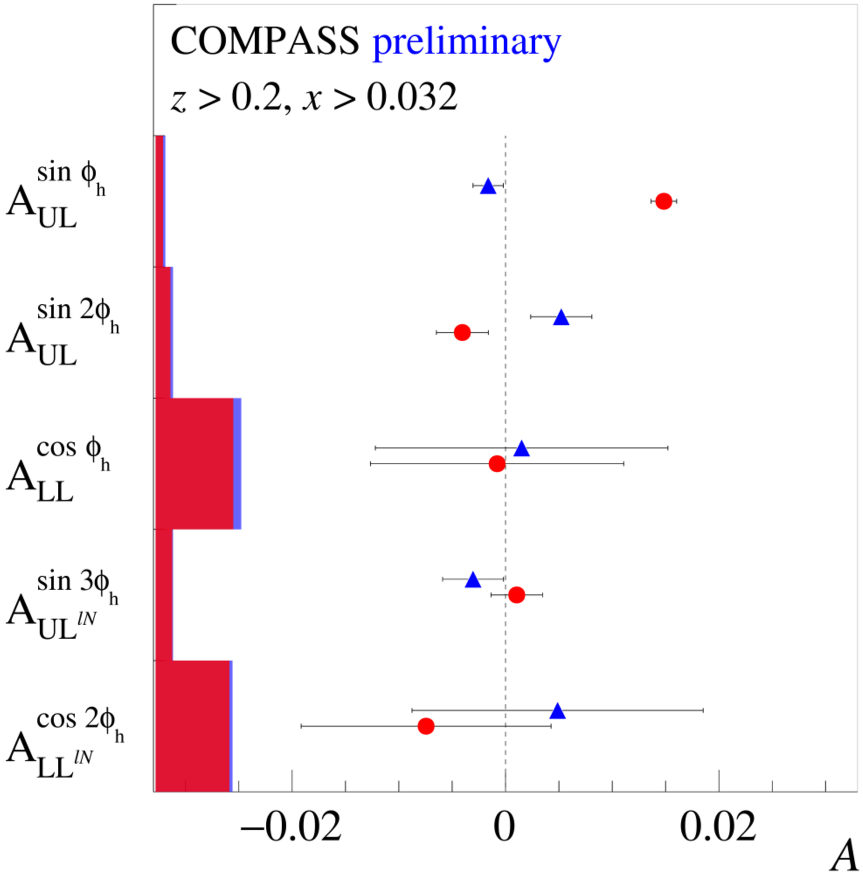

SIDIS: target transverse spin dependent asymmetries

$$\frac{d\sigma}{dxdydzdp_T^2 d\phi_h d\phi_S} \propto \left(F_{UU,T} + \varepsilon F_{UU,L}\right)\left\{ 1 + \ldots \right.$$

$$+ \ S_T \left[\begin{array}{l} + \ \varepsilon A_{UT}^{\sin(3\phi_h - \phi_S)} \sin(3\phi_h - \phi_S) \\ + \ \sqrt{2\varepsilon(1+\varepsilon)} A_{UT}^{\sin\phi_S} \sin\phi_S \\ + \ \ldots \end{array} \right]$$

$$\left. + \ S_T \lambda \left[\begin{array}{l} \sqrt{(1-\varepsilon^2)} A_{LT}^{\cos(\phi_h - \phi_S)} \cos(\phi_h - \phi_S) \\ + \ \ldots \end{array} \right] \right\}$$

SIDIS: target transverse spin dependent asymmetries

$$\frac{d\sigma}{dxdydzdp_T^2 d\phi_h d\phi_S} \propto \left(F_{UU,T} + \varepsilon F_{UU,L}\right)\Bigg\{ 1 + \ldots$$
$$+ S_T \left[+ \varepsilon A_{UT}^{\sin(3\phi_h - \phi_S)} \sin(3\phi_h - \phi_S) + \sqrt{2\varepsilon(1+\varepsilon)} A_{UT}^{\sin\phi_S} \sin\phi_S + \ldots \right]$$
$$+ S_T \lambda \left[\sqrt{(1-\varepsilon^2)} A_{LT}^{\cos(\phi_h - \phi_S)} \cos(\phi_h - \phi_S) + \ldots \right] \Bigg\}$$

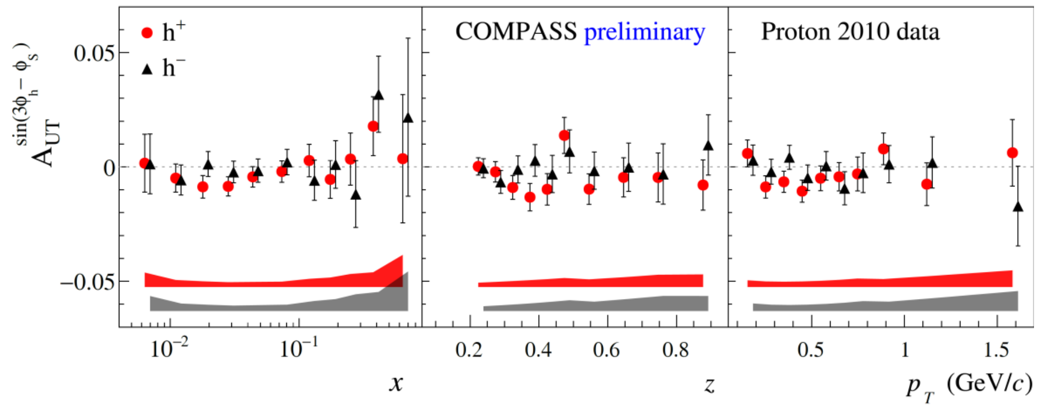

$$F_{UT}^{\sin(3\phi_h - \phi_S)} = C\left[\frac{2(\hat{h}\cdot k_T)(k_T \cdot p_T) + k_T^2(\hat{h}\cdot p_T) - 4(\hat{h}\cdot k_T)^2(\hat{h}\cdot p_T)}{2M^2 M_h} h_{1T}^{\perp q} H_{1q}^{\perp h} \right]$$

COMPASS results

$A_{UT}^{\sin(3\phi_h - \phi_S)}$

- Only “twist-2” ingredients, p_T^2-suppression
- **Small, compatible with zero asymmetry**

B. Pasquini, S. Boffi, A.V. Efremov, P. Schweitzer arXiv:0912.1761 [hep-ph]

C. Lefky, A. Prokudin **PRD91 (2015) 034010**

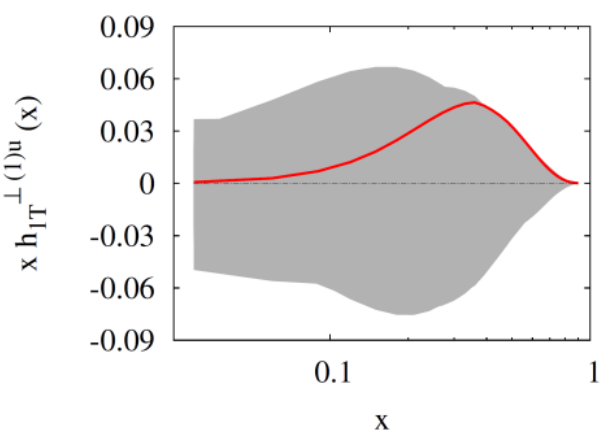

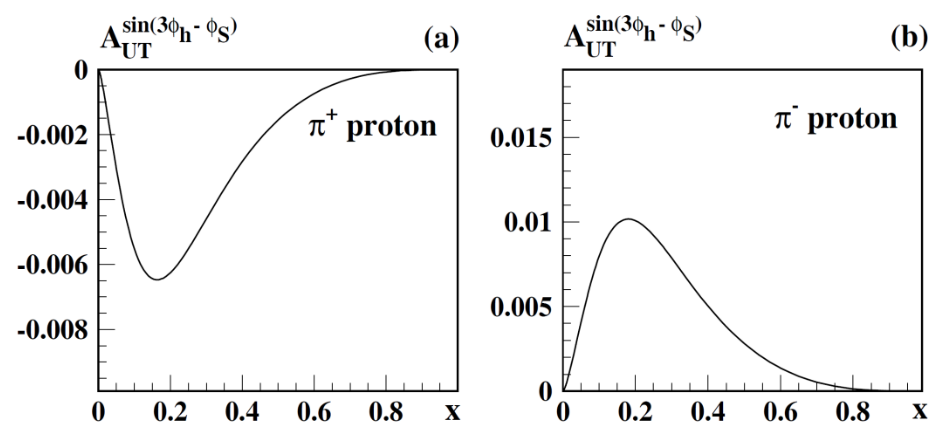

SIDIS: target transverse spin dependent asymmetries

$$\frac{d\sigma}{dxdydzdp_T^2 d\phi_h d\phi_S} \propto \left(F_{UU,T}+\varepsilon F_{UU,L}\right)\left\{ 1+\ldots \right.$$

$$+\ S_T \left[\begin{array}{l} +\ \varepsilon A_{UT}^{\sin(3\phi_h-\phi_S)} \sin(3\phi_h-\phi_S) \\ +\ \sqrt{2\varepsilon(1+\varepsilon)} A_{UT}^{\sin\phi_S} \sin\phi_S \\ +\ \ldots \end{array} \right]$$

$$\left. +\ S_T\lambda \left[\begin{array}{l} \sqrt{(1-\varepsilon^2)} A_{LT}^{\cos(\phi_h-\phi_S)} \cos(\phi_h-\phi_S) \\ +\ \ldots \end{array} \right] \right\}$$

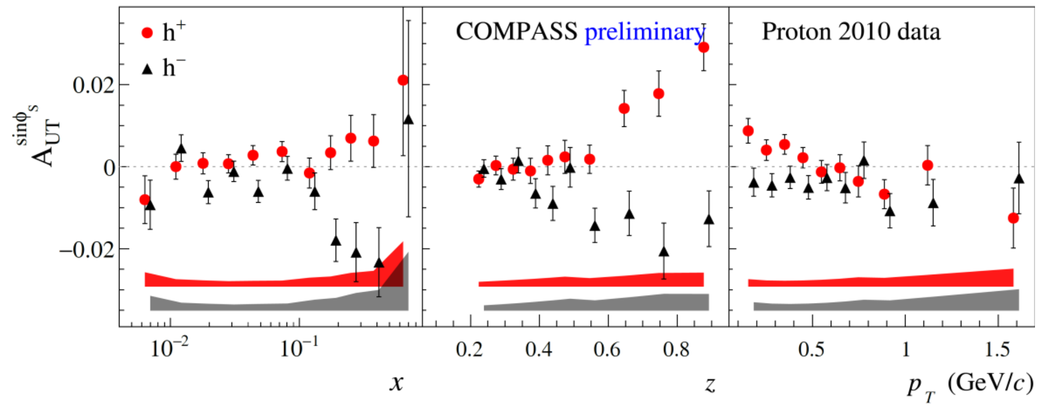

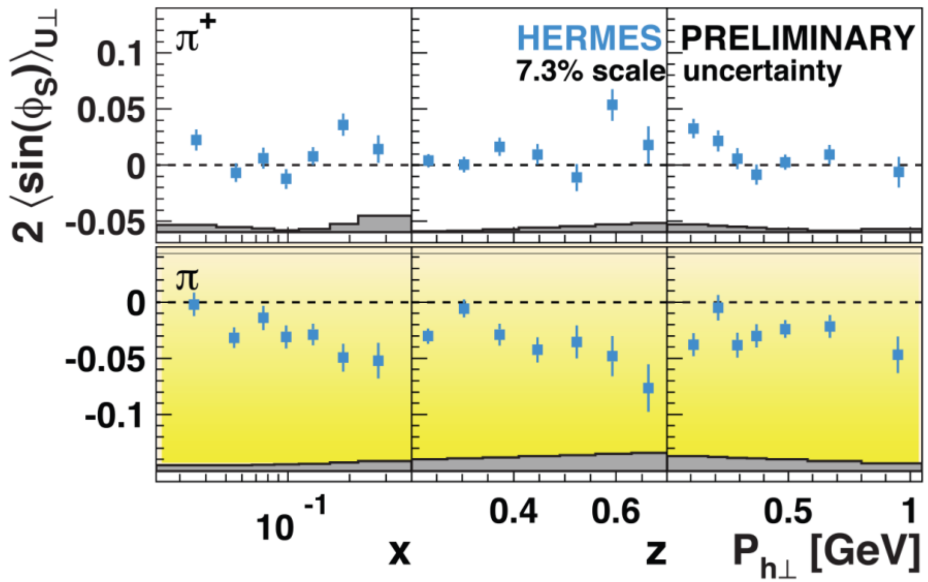

COMPASS results

$A_{UT}^{\sin\phi_S}$

- Q-suppression
- Various different "twist" ingredients
- **Small asymmetry, non-zero signal for h⁻?**

$$F_{UT}^{\sin\phi_S} = \frac{2M}{Q} C \left\{ \left(x f_T^q D_{1q}^h - \frac{M_h}{M} h_1^q \frac{\tilde{H}_q^h}{z} \right) - \frac{\boldsymbol{p}_T \cdot \boldsymbol{k}_T}{2MM_h} \left[\left(x h_T^q H_{1q}^{\perp h} + \frac{M_h}{M} g_{1T}^q \frac{\tilde{G}_q^{\perp h}}{z} \right) - \left(x h_T^{\perp q} H_{1q}^{\perp h} - \frac{M_h}{M} f_{1T}^{\perp q} \frac{\tilde{D}_q^{\perp h}}{z} \right) \right] \right\}$$

SIDIS: target transverse spin dependent asymmetries

$$\frac{d\sigma}{dx\,dy\,dz\,dp_T^2\,d\phi_h\,d\phi_S} \propto \left(F_{UU,T}+\varepsilon F_{UU,L}\right)\left\{ 1+\ldots \right.$$

$$+\ S_T \left[\begin{array}{l} +\ \varepsilon A_{UT}^{\sin(3\phi_h-\phi_S)} \sin(3\phi_h-\phi_S) \\ +\ \sqrt{2\varepsilon(1+\varepsilon)}\,A_{UT}^{\sin\phi_S} \sin\phi_S \\ +\ \ldots \end{array} \right]$$

$$\left. +\ S_T\lambda \left[\begin{array}{l} \sqrt{(1-\varepsilon^2)}\,A_{LT}^{\cos(\phi_h-\phi_S)} \cos(\phi_h-\phi_S) \\ +\ \ldots \end{array} \right] \right\}$$

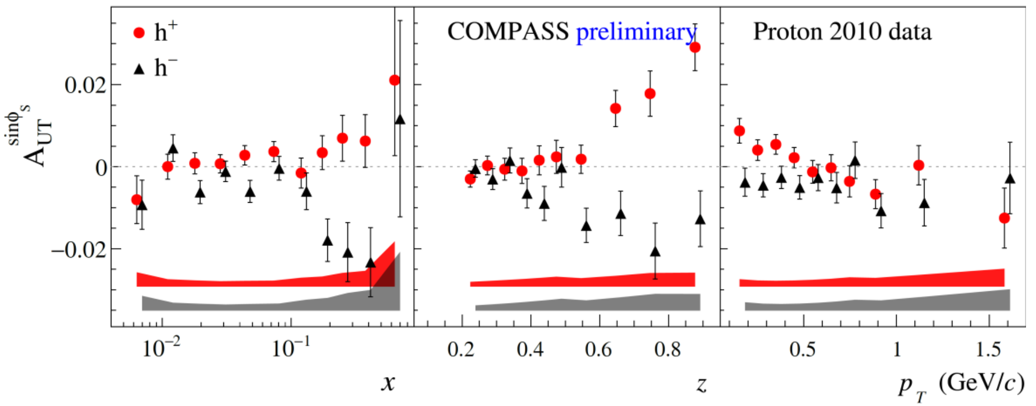

COMPASS results

$A_{UT}^{\sin\phi_S}$

- Q-suppression
- Various different "twist" ingredients
- **Small asymmetry, non-zero signal for h⁻ ?**

W. Mao, Z. Lu and B.Q. Ma **Phys.Rev. D 90 (2014) 014048**

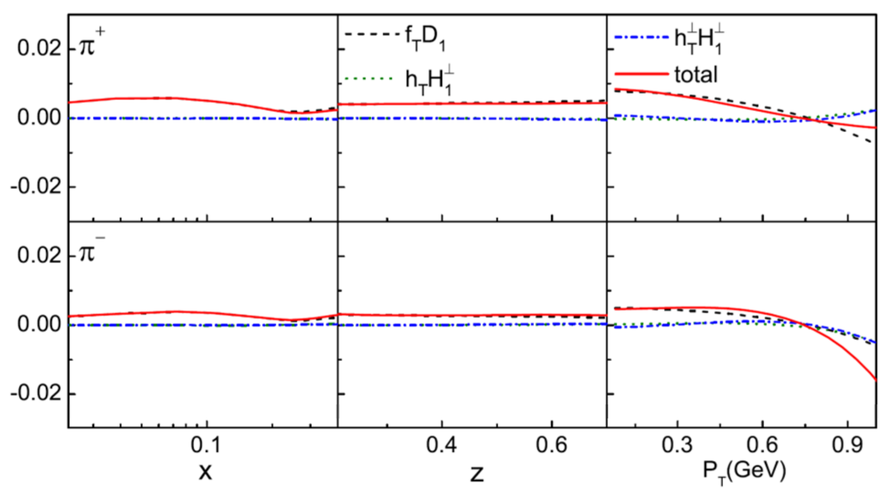

$$F_{UT}^{\sin\phi_S} = \frac{2M}{Q} C \left\{ \left(x f_T^q D_{1q}^h - \frac{M_h}{M} h_1^q \frac{\tilde{H}_q^h}{z} \right) - \frac{\boldsymbol{p}_T \cdot \boldsymbol{k}_T}{2MM_h} \left[\left(x h_T^q H_{1q}^{\perp h} + \frac{M_h}{M} g_{1T}^q \frac{\tilde{G}_q^{\perp h}}{z} \right) - \left(x h_T^{\perp q} H_{1q}^{\perp h} - \frac{M_h}{M} f_{1T}^{\perp q} \frac{\tilde{D}_q^{\perp h}}{z} \right) \right] \right\}$$

SIDIS: target transverse spin dependent asymmetries

$$\frac{d\sigma}{dxdydzdp_T^2 d\phi_h d\phi_S} \propto \left(F_{UU,T} + \varepsilon F_{UU,L}\right)\left\{ 1 + \ldots \right.$$

$$+ S_T \left[+ \varepsilon A_{UT}^{\sin(3\phi_h-\phi_S)} \sin(3\phi_h - \phi_S) + \sqrt{2\varepsilon(1+\varepsilon)} A_{UT}^{\sin\phi_S} \sin\phi_S + \ldots \right]$$

$$\left. + S_T\lambda \left[\sqrt{(1-\varepsilon^2)} A_{LT}^{\cos(\phi_h-\phi_S)} \cos(\phi_h - \phi_S) + \ldots \right] \right\}$$

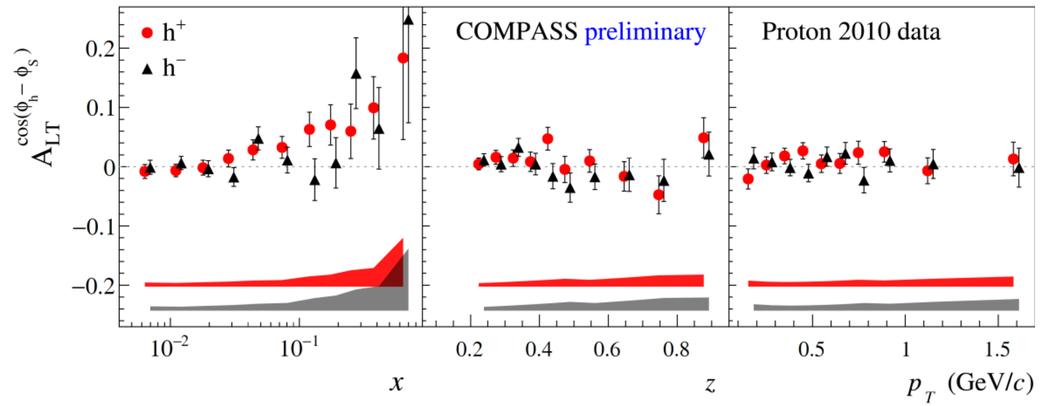

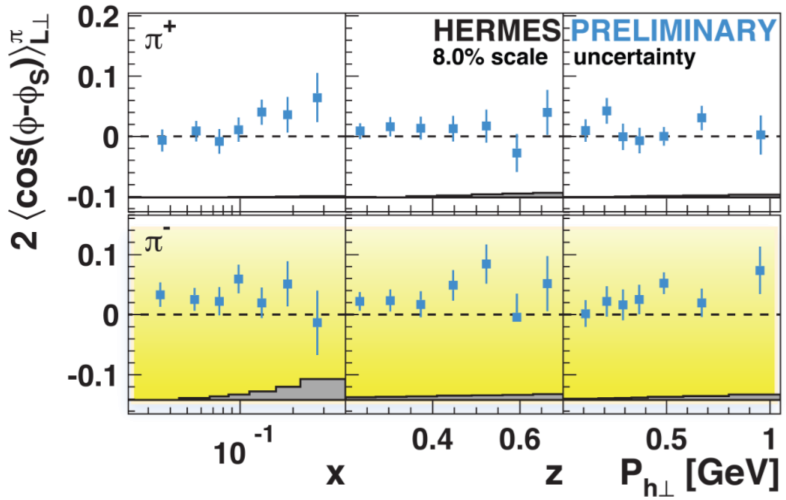

COMPASS results

$A_{LT}^{\cos(\phi_h-\phi_S)}$

- Only "twist-2" ingredients
- **Sizable non-zero effect for h+ !**

$$F_{LT}^{\cos(\phi_h-\phi_S)} = C\left[\frac{\hat{\boldsymbol{h}}\cdot\boldsymbol{k}_T}{M} g_{1T}^q D_{1q}^h\right]$$

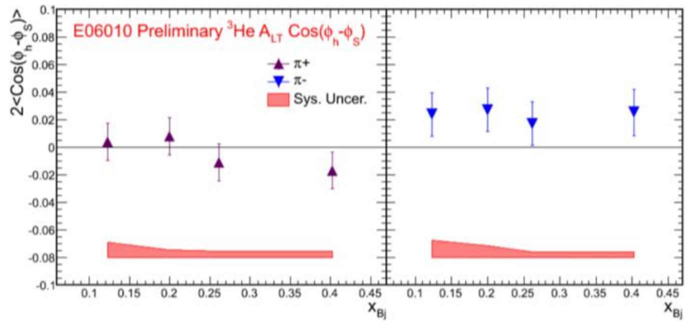

SIDIS: target transverse spin dependent asymmetries

$$\frac{d\sigma}{dxdydzdp_T^2 d\phi_h d\phi_S} \propto \left(F_{UU,T} + \varepsilon F_{UU,L}\right)\left\{ 1 + \ldots \right.$$

$$+ S_T \left[\begin{array}{l} + \varepsilon A_{UT}^{\sin(3\phi_h - \phi_S)} \sin(3\phi_h - \phi_S) \\ + \sqrt{2\varepsilon(1+\varepsilon)} A_{UT}^{\sin\phi_S} \sin\phi_S \\ + \ldots \end{array} \right]$$

$$\left. + S_T \lambda \left[\begin{array}{l} \sqrt{(1-\varepsilon^2)} A_{LT}^{\cos(\phi_h - \phi_S)} \cos(\phi_h - \phi_S) \\ + \ldots \end{array} \right] \right\}$$

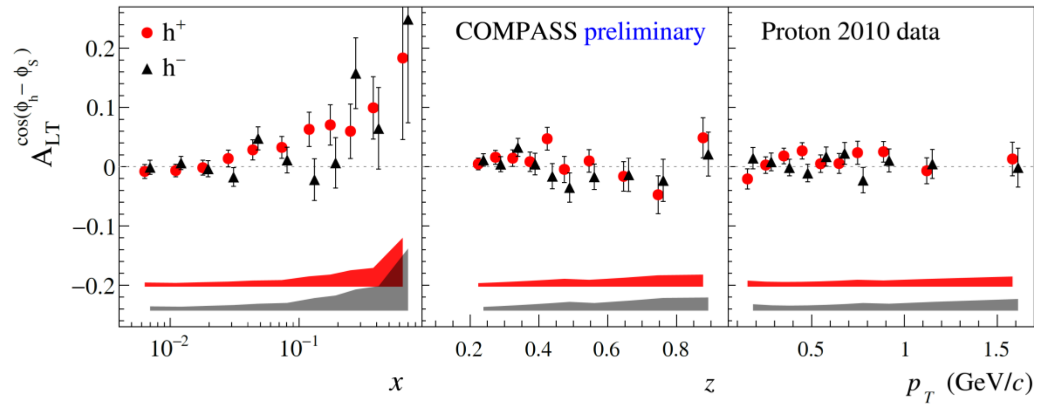

COMPASS results

$A_{LT}^{\cos(\phi_h - \phi_S)}$

- Only "twist-2" ingredients
- **Sizable non-zero effect for h⁺ !**

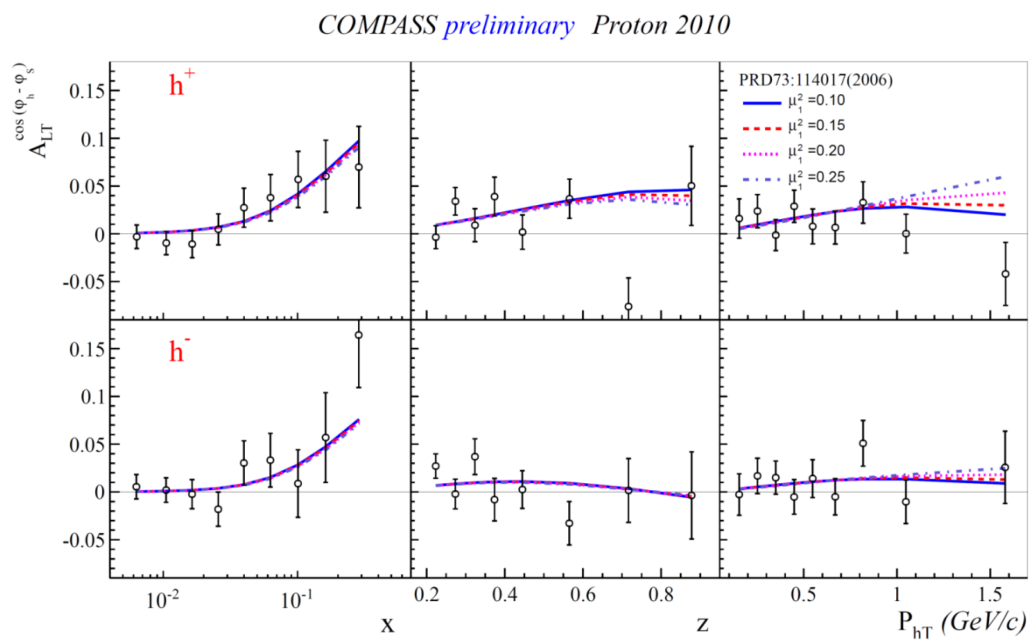

$$F_{LT}^{\cos(\phi_h - \phi_S)} = C\left[\frac{\hat{\boldsymbol{h}} \cdot \boldsymbol{k}_T}{M} g_{1T}^q D_{1q}^h\right]$$

$A_{LT}^{\cos(\phi_h-\phi_S)}$: x, z, p_T and W dependences in 5 Q^2-ranges

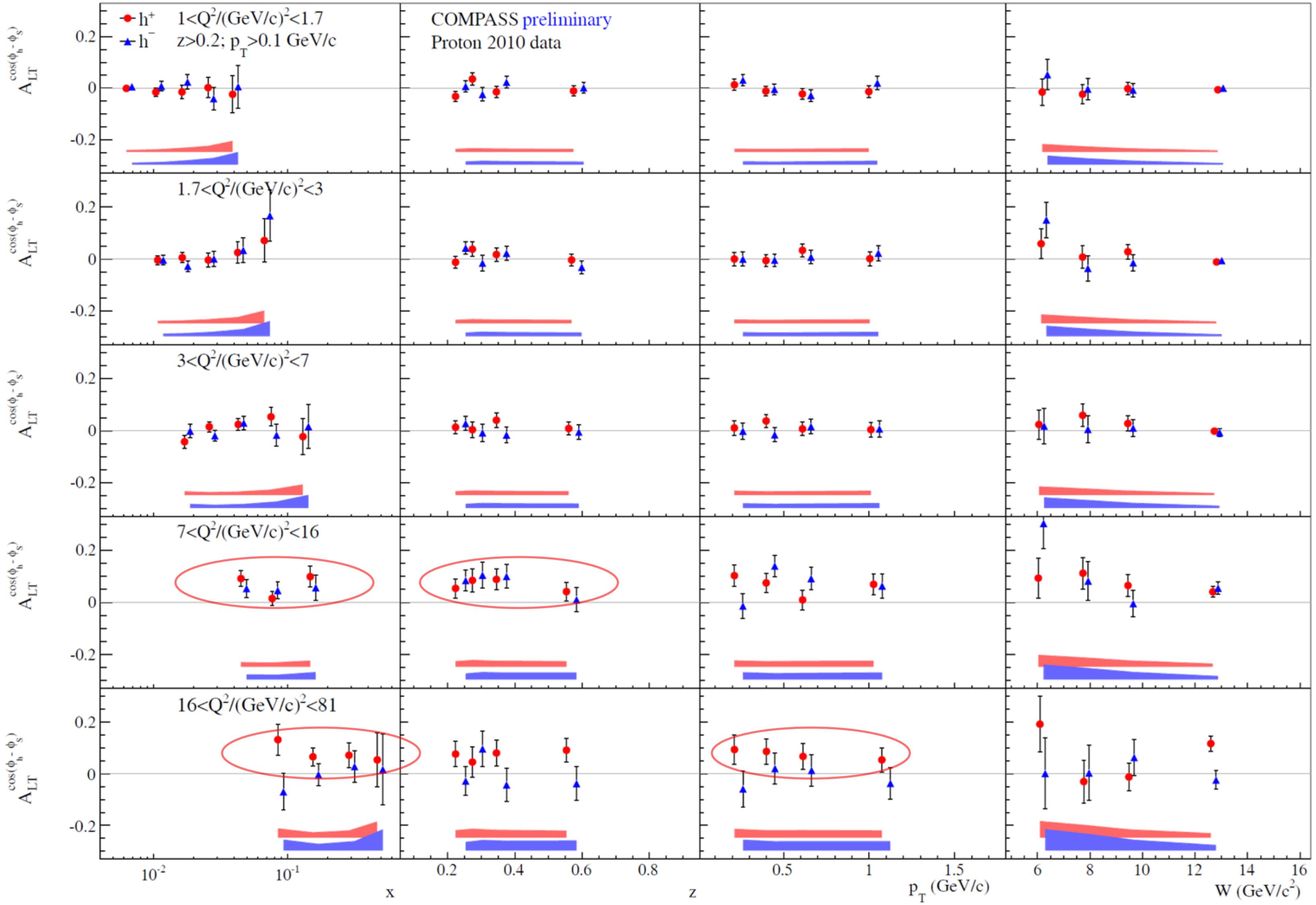

2D

- **Positive amplitude for h^+ at large x (>0.032) and Q^2 (>3)**
- **Signal for negative hadrons is not evident.**

$A_{LT}^{\cos(\phi_h-\phi_S)}$: 5 Q^2 ranges. Predictions - PRD 73, 114017(2006)

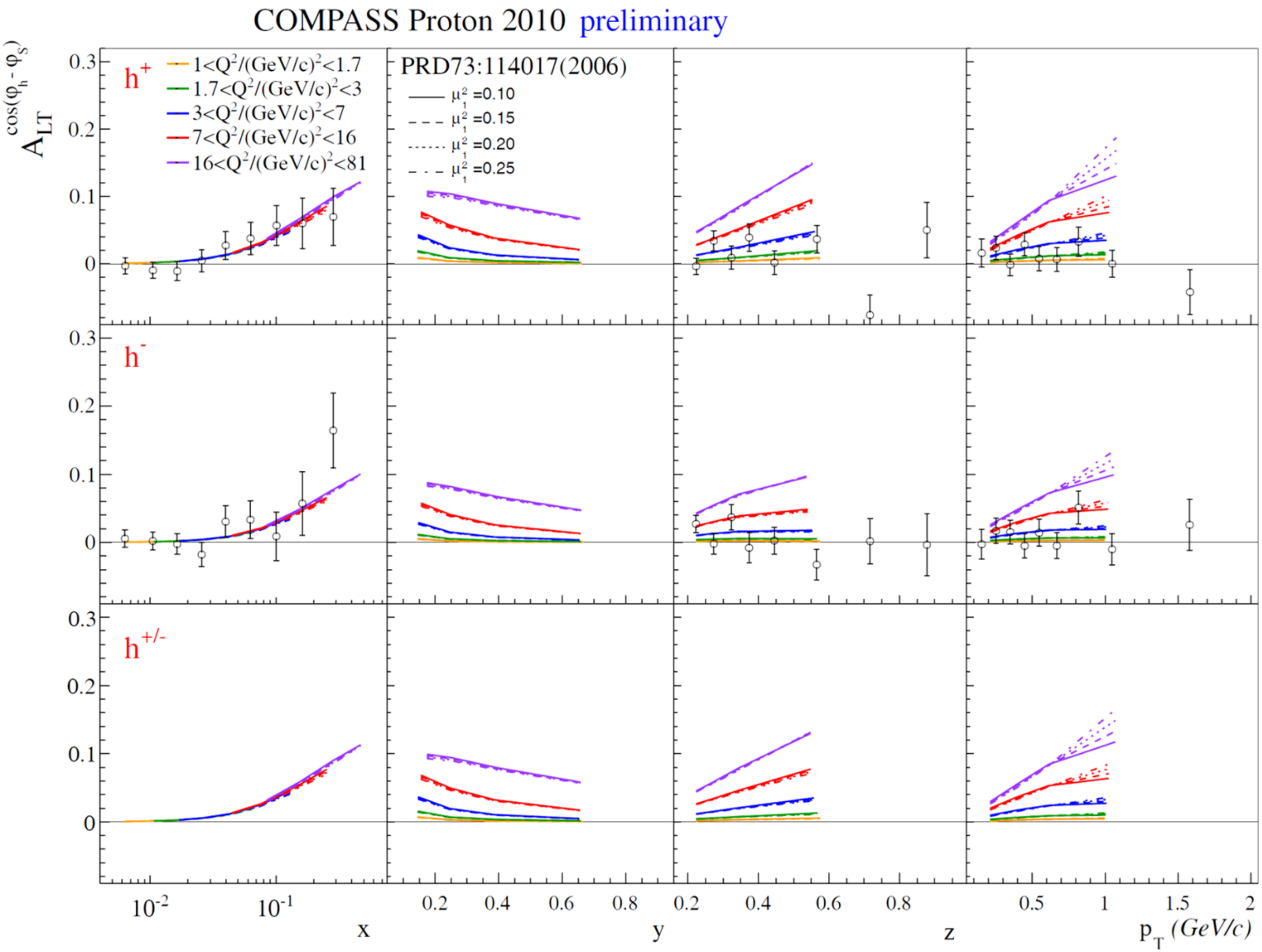

Asymmetry is evaluated in COMPASS specific mean kinematic points extracted from the data.
The predictions show a good level of agreement with the experimentally extracted asymmetry

SIDIS TSAs (Collins)

$$\frac{d\sigma}{dxdydzdp_T^2 d\phi_h d\phi_S} \propto \left(F_{UU,T} + \varepsilon F_{UU,L}\right)\left\{1 + \ldots + S_T \, \varepsilon A_{UT}^{\sin(\phi_h+\phi_S)} \sin(\phi_h+\phi_S) + \ldots\right\}$$

$$F_{UT}^{\sin(\phi_h+\phi_S)} = C\left[-\frac{\hat{\boldsymbol{h}}\cdot \boldsymbol{p_T}}{M_h} h_1^q H_{1q}^{\perp h}\right]$$

- Measured on P/D in SIDIS and in dihadron SIDIS

COMPASS PLB 744 (2015) 250

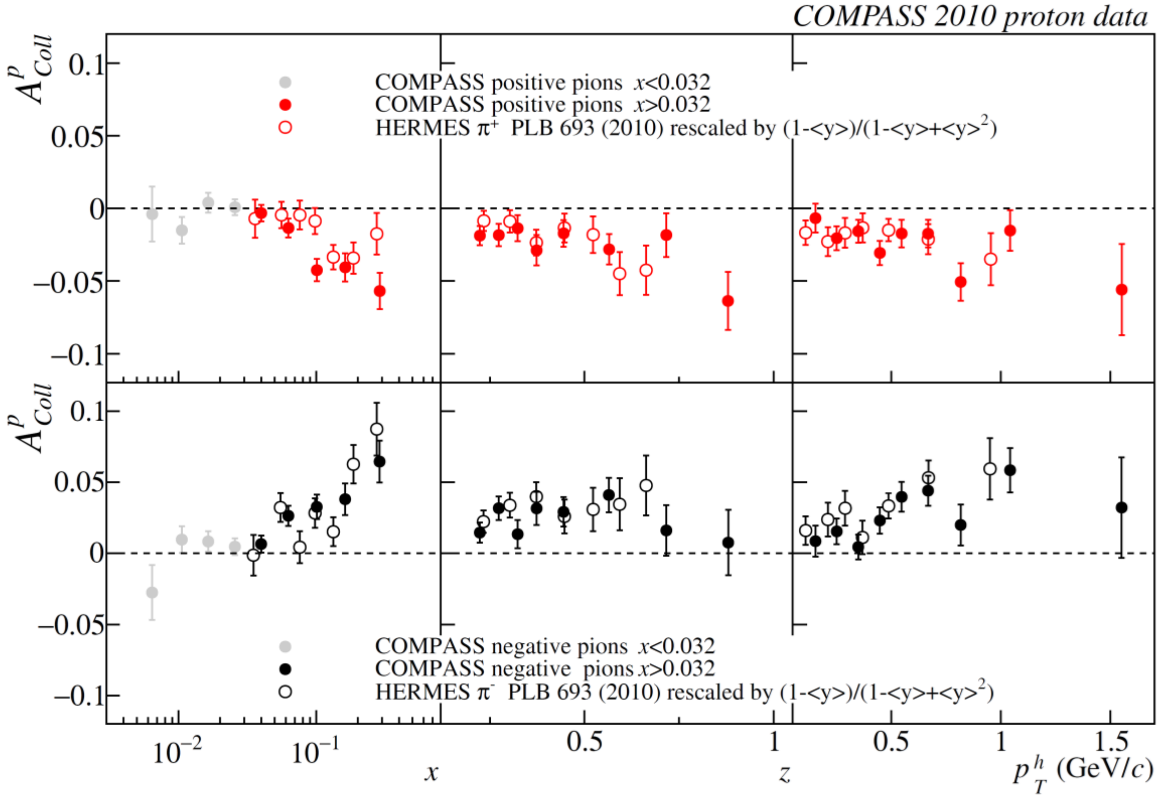

SIDIS TSAs (Collins)

$$\frac{d\sigma}{dxdydzdp_T^2 d\phi_h d\phi_S} \propto \left(F_{UU,T} + \varepsilon F_{UU,L}\right)\left\{1 + \ldots + S_T\, \varepsilon A_{UT}^{\sin(\phi_h+\phi_S)} \sin(\phi_h+\phi_S) + \ldots\right\}$$

$$F_{UT}^{\sin(\phi_h+\phi_S)} = C\left[-\frac{\hat{\boldsymbol{h}}\cdot \boldsymbol{p_T}}{M_h} h_1^q H_{1q}^{\perp h}\right]$$

- Measured on P/D in SIDIS and in dihadron SIDIS
- Compatible results COMPASS/HERMES (Q^2 is different by a factor of ~2-3)
- **No Q^2-evolution? Intriguing result!**

COMPASS PLB 744 (2015) 250

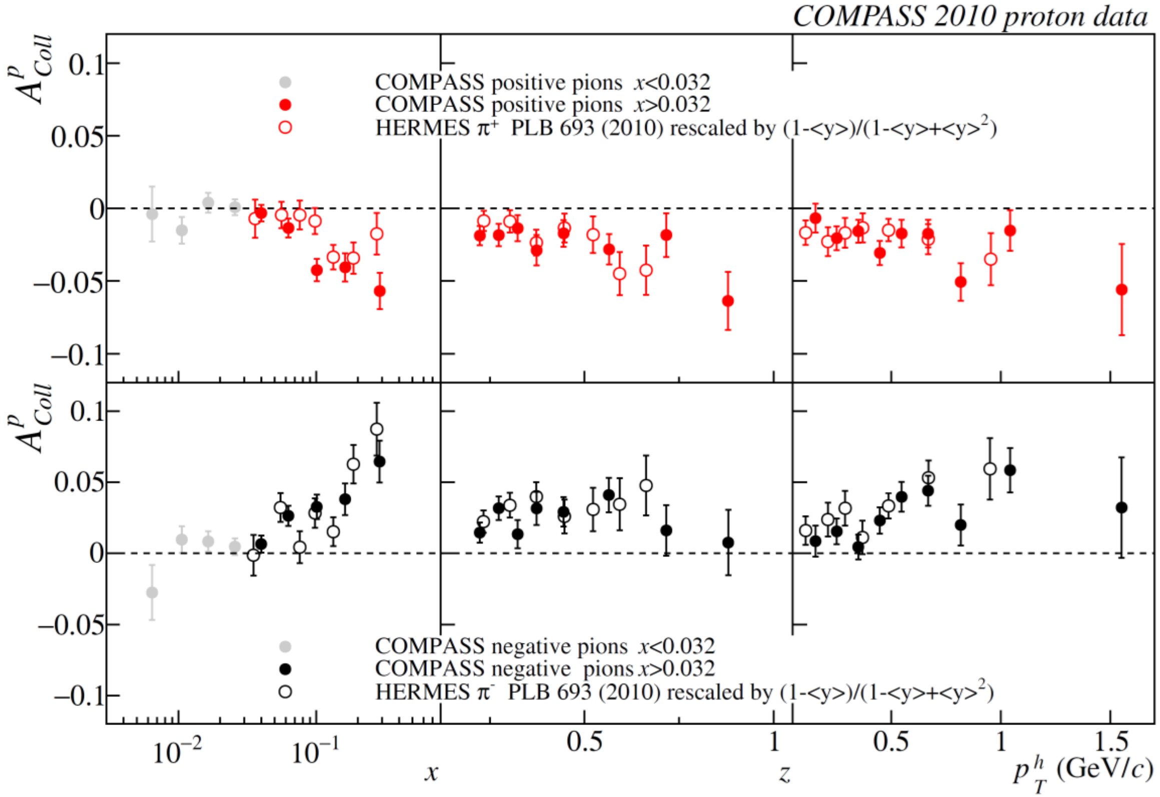

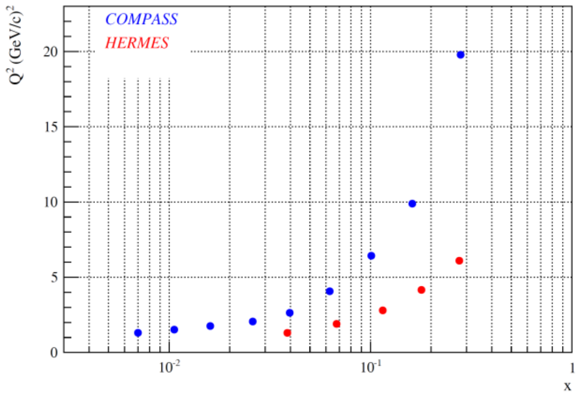

SIDIS TSAs (Collins)

$$\frac{d\sigma}{dxdydzdp_T^2 d\phi_h d\phi_S} \propto \left(F_{UU,T} + \varepsilon F_{UU,L}\right)\left\{1 + \ldots + S_T\, \varepsilon A_{UT}^{\sin(\phi_h+\phi_S)} \sin(\phi_h + \phi_S) + \ldots\right\}$$

$$F_{UT}^{\sin(\phi_h+\phi_S)} = C\left[-\frac{\hat{\boldsymbol{h}}\cdot \boldsymbol{p_T}}{M_h} h_1^q H_{1q}^{\perp h}\right]$$

- Measured on P/D in SIDIS and in dihadron SIDIS
- Compatible results COMPASS/HERMES (Q^2 is different by a factor of ~2-3)
- **No Q^2-evolution? Intriguing result!**
- Extensive phenomenological studies and various global fits by different groups

Global fit HERMES-COMPASS-BELLE data
Anselmino et al. **Phys.Rev. D92 (2015) 114023**

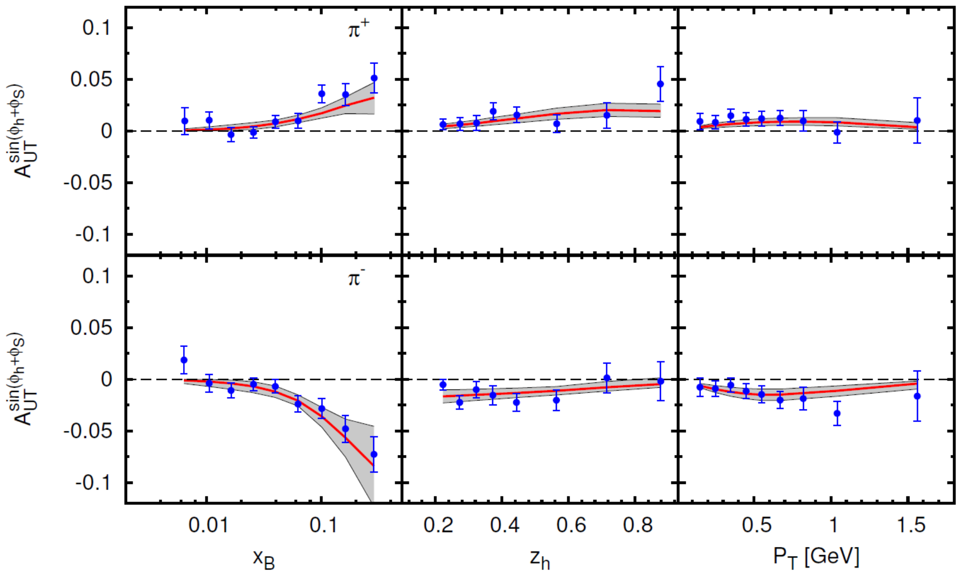

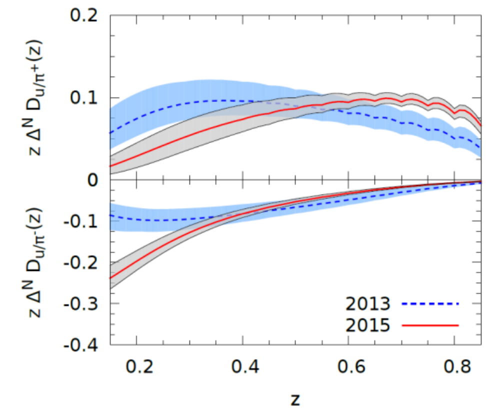

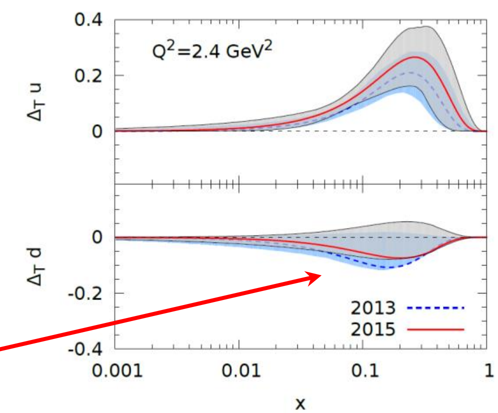

COMPASS-II (2021)

- Deuteron measurement to be repeated
- Will be crucial to constrain the transversity TMD PDF for the d-quark

SIDIS TSAs (Collins)

$$\frac{d\sigma}{dxdydzdp_T^2 d\phi_h d\phi_S} \propto \left(F_{UU,T} + \varepsilon F_{UU,L}\right)\left\{1 + \ldots + S_T\, \varepsilon A_{UT}^{\sin(\phi_h+\phi_S)} \sin(\phi_h+\phi_S) + \ldots\right\}$$

$$F_{UT}^{\sin(\phi_h+\phi_S)} = C\left[-\frac{\hat{\boldsymbol{h}}\cdot \boldsymbol{p_T}}{M_h} h_1^q H_{1q}^{\perp h}\right]$$

- Measured on P/D in SIDIS and in dihadron SIDIS
- Compatible results COMPASS/HERMES (Q^2 is different by a factor of ~2-3)
- **No Q^2-evolution? Intriguing result!**
- Extensive phenomenological studies and various global fits by different groups

Addendum to the COMPASS-II Proposal
Projected uncertainties for transversity PDF

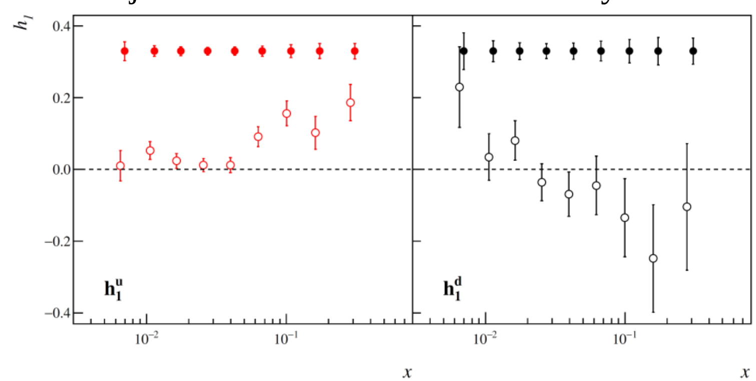

Addendum to the COMPASS-II Proposal
Projected uncertainties for Collins asymmetry

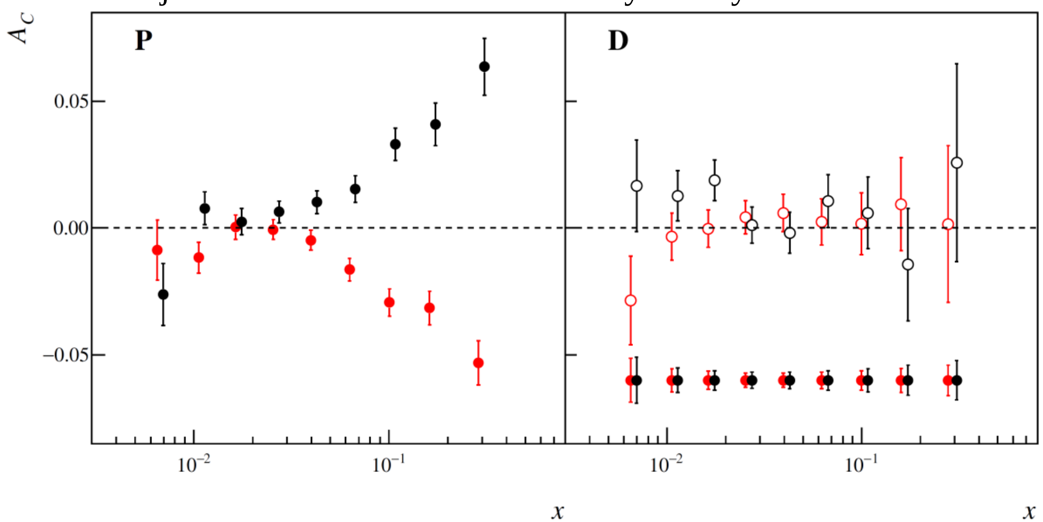

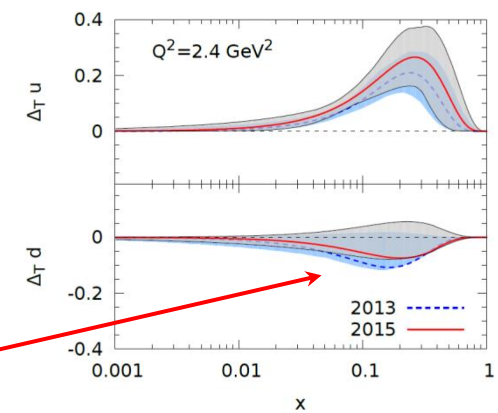

COMPASS-II (2021)

- Deuteron measurement to be repeated
- Will be crucial to constrain the transversity TMD PDF for the d-quark

SIDIS TSAs (Sivers)

$$\frac{d\sigma}{dxdydzdp_T^2 d\phi_h d\phi_S} \propto \left(F_{UU,T} + \varepsilon F_{UU,L}\right)\left\{1 + \ldots + S_T A_{UT}^{\sin(\phi_h - \phi_S)} \sin(\phi_h - \phi_S) + \ldots\right\}$$

$$F_{UT,T}^{\sin(\phi_h-\phi_S)} = C\left[-\frac{\hat{\boldsymbol{h}}\cdot\boldsymbol{k}_T}{M} f_{1T}^{\perp q} D_{1q}^h\right], F_{UT,L}^{\sin(\phi_h-\phi_S)} = 0$$

- Measured on proton and deuteron
- Gluon Sivers paper: submitted to PLB [CERN-EP/2017-003](), [hep-ex/1701.02453]()

COMPASS 2010 proton data

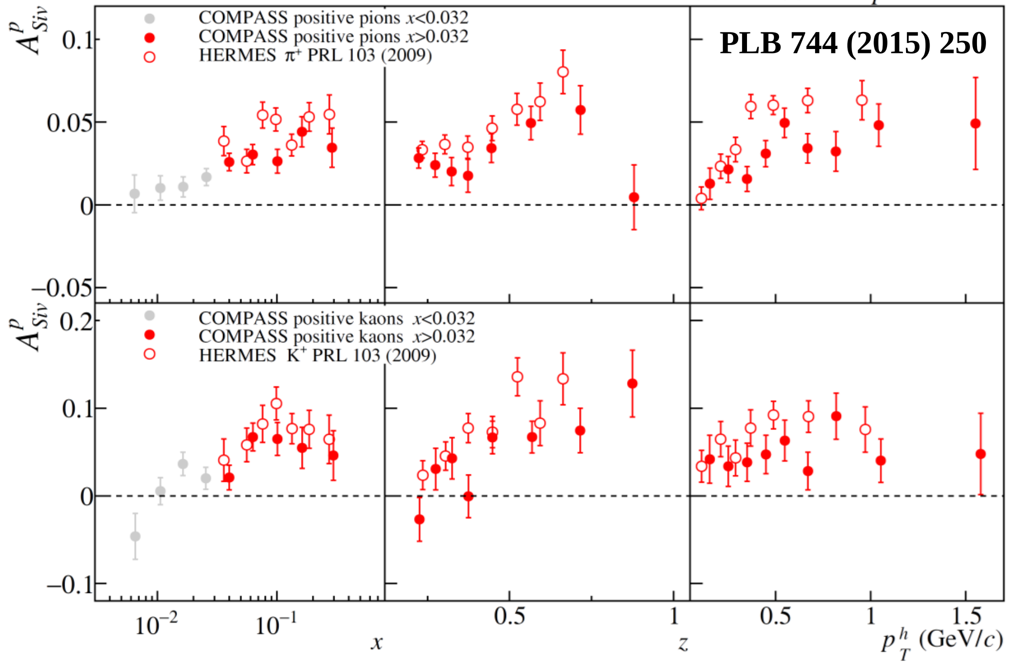

SIDIS TSAs (Sivers)

$$\frac{d\sigma}{dxdydzdp_T^2 d\phi_h d\phi_S} \propto \left(F_{UU,T} + \varepsilon F_{UU,L}\right)\left\{1 + \ldots + S_T A_{UT}^{\sin(\phi_h - \phi_S)} \sin(\phi_h - \phi_S) + \ldots\right\}$$

$$F_{UT,T}^{\sin(\phi_h-\phi_S)} = C\left[-\frac{\hat{\boldsymbol{h}}\cdot \boldsymbol{k}_T}{M} f_{1T}^{\perp q} D_{1q}^h\right], F_{UT,L}^{\sin(\phi_h-\phi_S)} = 0$$

- Measured on proton and deuteron
- Recently - gluon Sivers paper PLB 772 (2017) 854

- Sivers effect at COMPASS is slightly smaller w.r.t HERMES results (Q^2 is different by a factor of ~2-3)
- **Q^2-evolution? Intriguing result!**

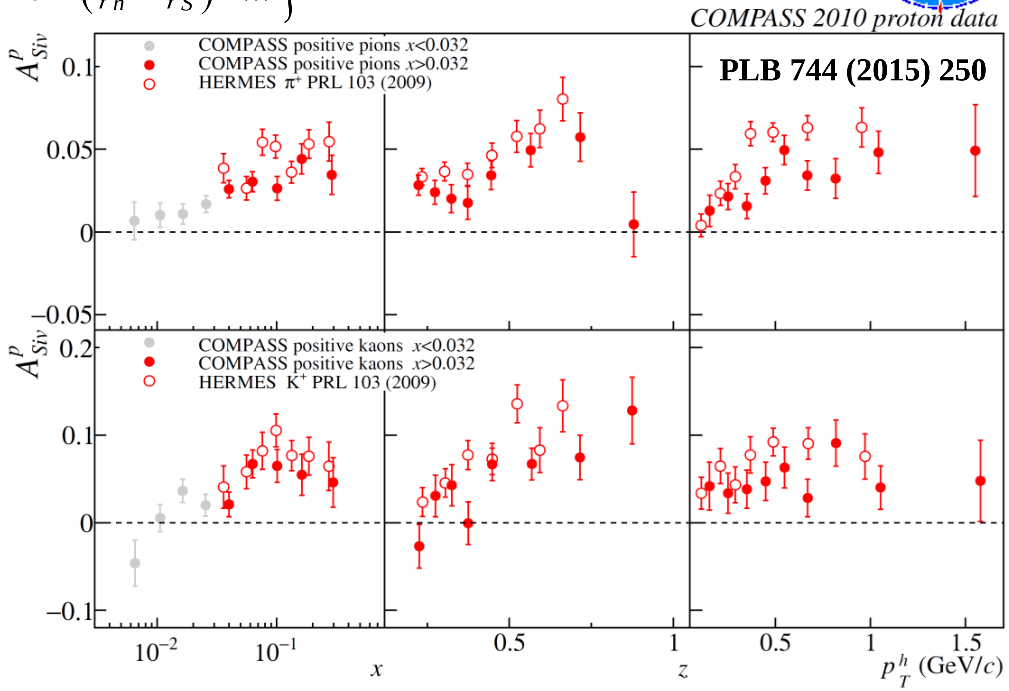

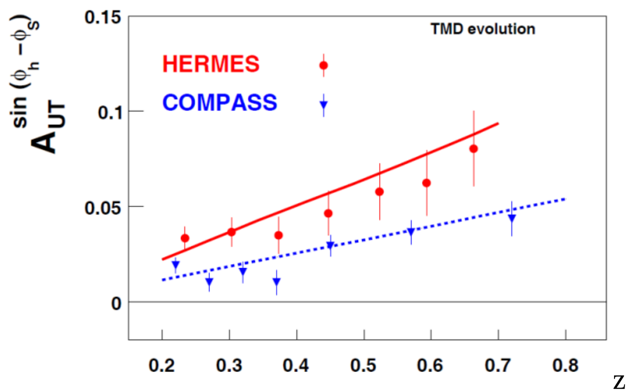

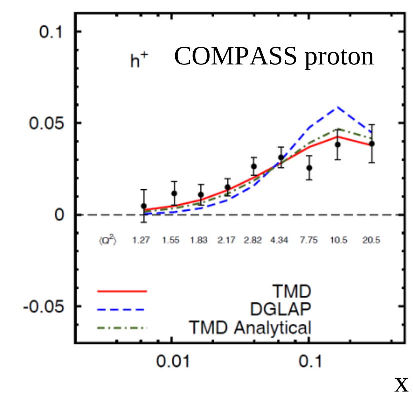

S. M. Aybat, A. Prokudin, T. C. Rogers **PRL 108 (2012) 242003**
M. Anselmino, M. Boglione, S. Melis **PRD 86 (2012) 014028**

SIDIS TSAs (Sivers)

$$\frac{d\sigma}{dx\,dy\,dz\,dp_T^2\,d\phi_h\,d\phi_S} \propto \left(F_{UU,T}+\varepsilon F_{UU,L}\right)\left\{1+\ldots+\ S_T\, A_{UT}^{\sin(\phi_h-\phi_S)}\sin(\phi_h-\phi_S)+\ldots\right\}$$

$$F_{UT,T}^{\sin(\phi_h-\phi_S)} = C\left[-\frac{\hat{\boldsymbol{h}}\cdot \boldsymbol{k}_T}{M}\, f_{1T}^{\perp q} D_{1q}^h\right],\ F_{UT,L}^{\sin(\phi_h-\phi_S)} = 0$$

- Measured on proton and deuteron
- Recently - gluon Sivers paper PLB 772 (2017) 854

- Sivers effect at COMPASS is slightly smaller w.r.t HERMES results (Q^2 is different by a factor of ~2-3)
- **Q^2-evolution? Intriguing result!**

- Global fits of available 1-D SIDIS data
- Different TMD-evolution schemes
- Different predictions for Drell-Yan

M.G. Echevarria, A.Idilbi, Z.B. Kang and I. Vitev, **PRD 89 074013 (2014)**

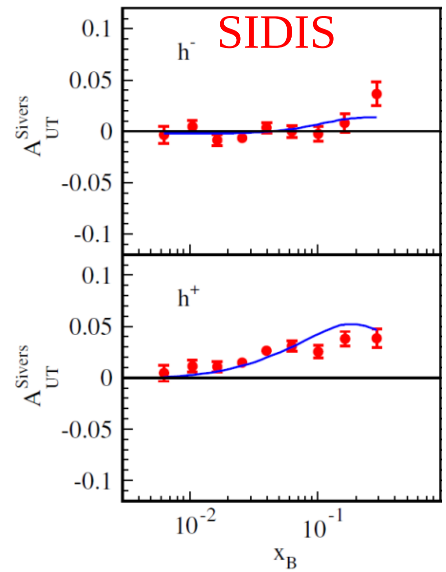

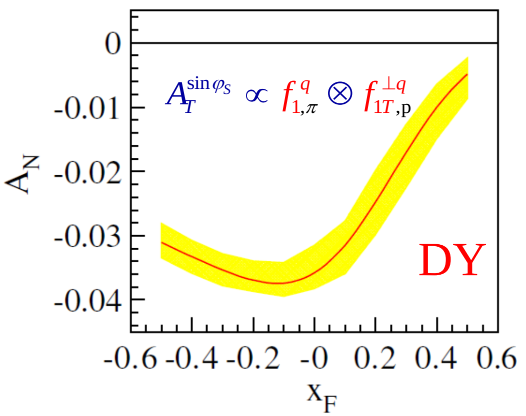

P. Sun and F. Yuan, **PRD 88 11, 114012 (2013)**

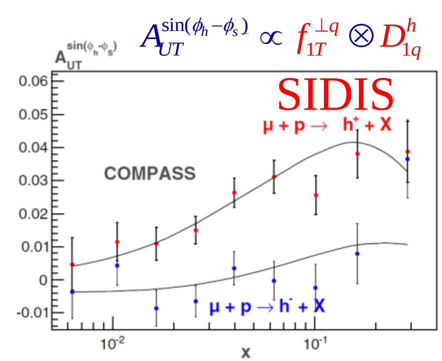

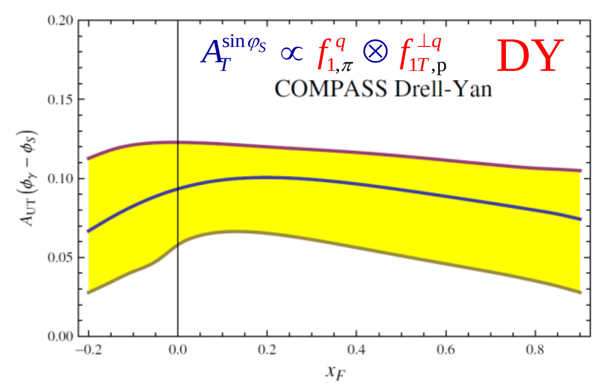

SIDIS TSAs (Sivers)

$$\frac{d\sigma}{dxdydzdp_T^2 d\phi_h d\phi_S} \propto \left(F_{UU,T} + \varepsilon F_{UU,L}\right)\left\{1 + \ldots + S_T A_{UT}^{\sin(\phi_h-\phi_S)} \sin(\phi_h-\phi_S) + \ldots\right\}$$

$$F_{UT,T}^{\sin(\phi_h-\phi_S)} = C\left[-\frac{\hat{h}\cdot k_T}{M} f_{1T}^{\perp q} D_{1q}^h\right], F_{UT,L}^{\sin(\phi_h-\phi_S)} = 0$$

- Measured on proton and deuteron
- Recently - gluon Sivers paper PLB 772 (2017) 854

- Sivers effect at COMPASS is slightly smaller w.r.t HERMES results (Q^2 is different by a factor of ~2-3)
- **Q^2-evolution? Intriguing result!**

- Global fits of available 1-D SIDIS data
- Different TMD-evolution schemes
- Different predictions for Drell-Yan

- First experimental investigation of Sivers-non-universality by STAR
- Different hard scale compared to FT
- Evolution effects may play a substantial role

STAR collaboration: **PRL 116, 132301 (2016)**

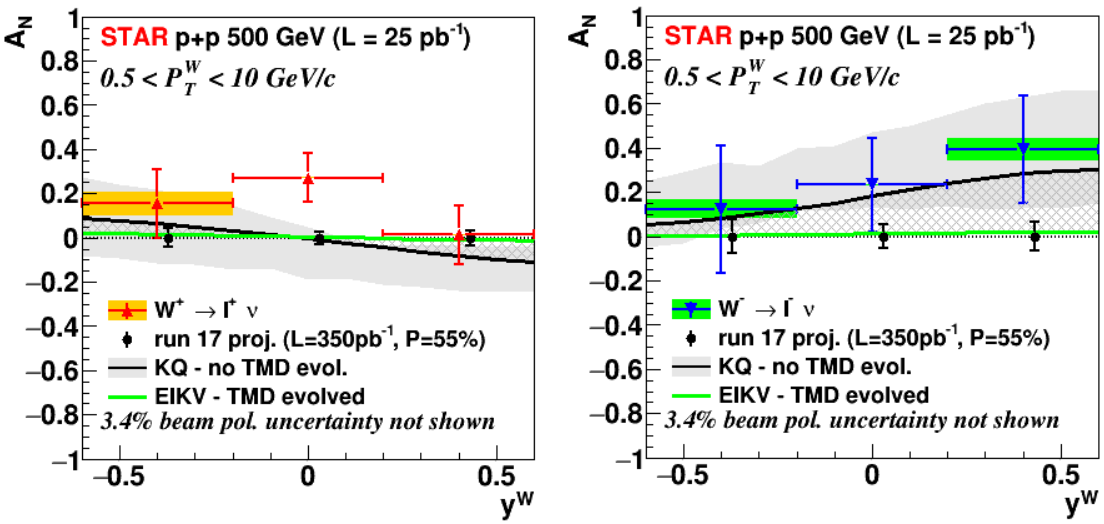

M. Anselmino et al., **JHEP 1704 (2017) 046**

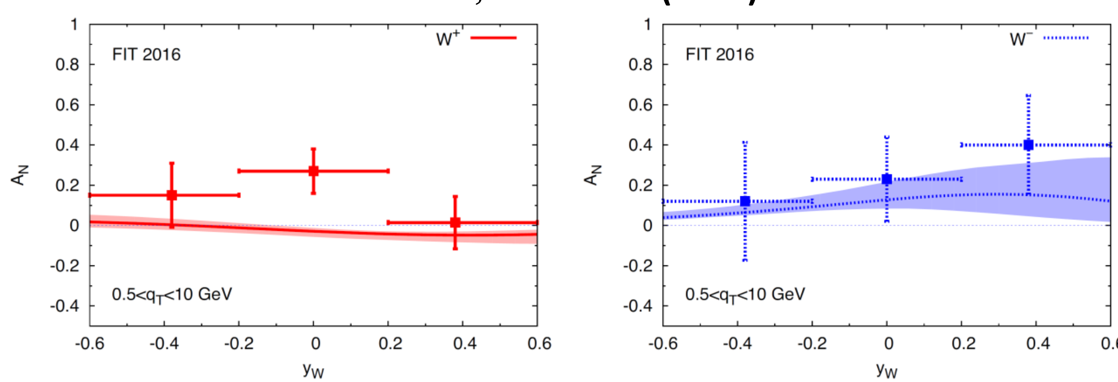

SIDIS Sivers TSA in COMPASS Drell-Yan Q^2-ranges

$$\frac{d\sigma}{dxdydzdp_T^2 d\phi_h d\phi_S} \propto \left(F_{UU,T} + \varepsilon F_{UU,L}\right)\left\{1 + \ldots + S_T A_{UT}^{\sin(\phi_h-\phi_S)} \sin(\phi_h-\phi_S) + \ldots\right\}$$

$$F_{UT,T}^{\sin(\phi_h-\phi_S)} = C\left[-\frac{\hat{\boldsymbol{h}}\cdot\boldsymbol{k}_T}{M} f_{1T}^{\perp q} D_{1q}^h\right], F_{UT,L}^{\sin(\phi_h-\phi_S)} = 0$$

COMPASS PLB 770 (2017) 138

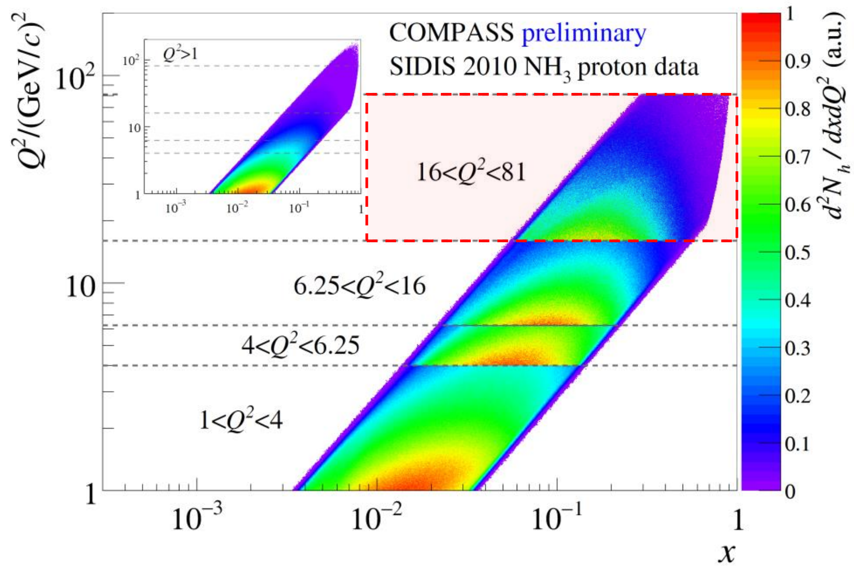

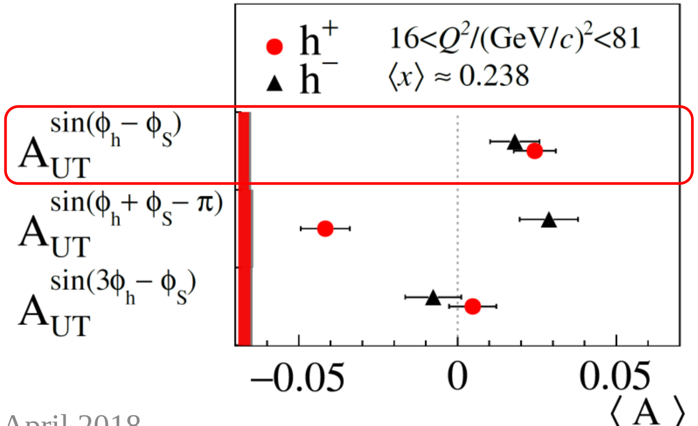

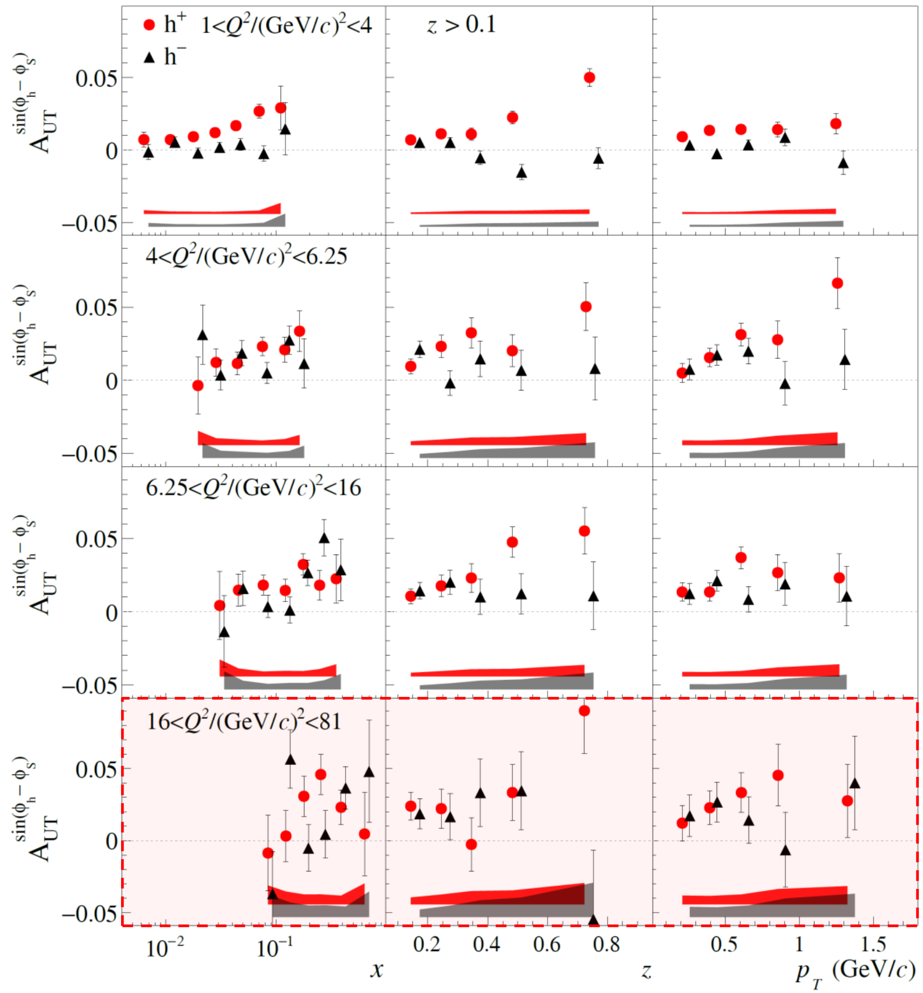

1st COMPASS multi-D fit done for all eight TSAs

Multi-D TSA analysis

$$\frac{d\sigma}{dxdydzdp_T^2 d\phi_h d\phi_S} \propto \left(F_{UU,T} + \varepsilon F_{UU,L}\right)\left\{1 + \ldots + S_T A_{UT}^{\sin(\phi_h - \phi_S)} \sin(\phi_h - \phi_S) + \ldots\right\}$$

$$F_{UT,T}^{\sin(\phi_h - \phi_S)} = C\left[-\frac{\hat{h}\cdot k_T}{M} f_{1T}^{\perp q} D_{1q}^h\right], F_{UT,L}^{\sin(\phi_h - \phi_S)} = 0$$

COMPASS 4-D fit (x-Q^2; z-p_T; x-Q^2-z-p_T)

All eight TSAs extracted simultaneously

First shown at the SPIN-2014, **arXiv:1504.01599 [hep-ex]**

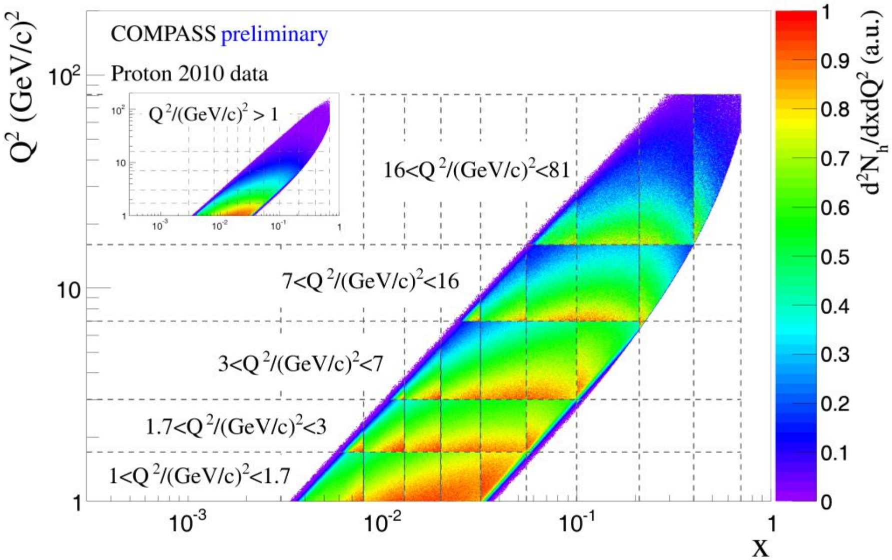

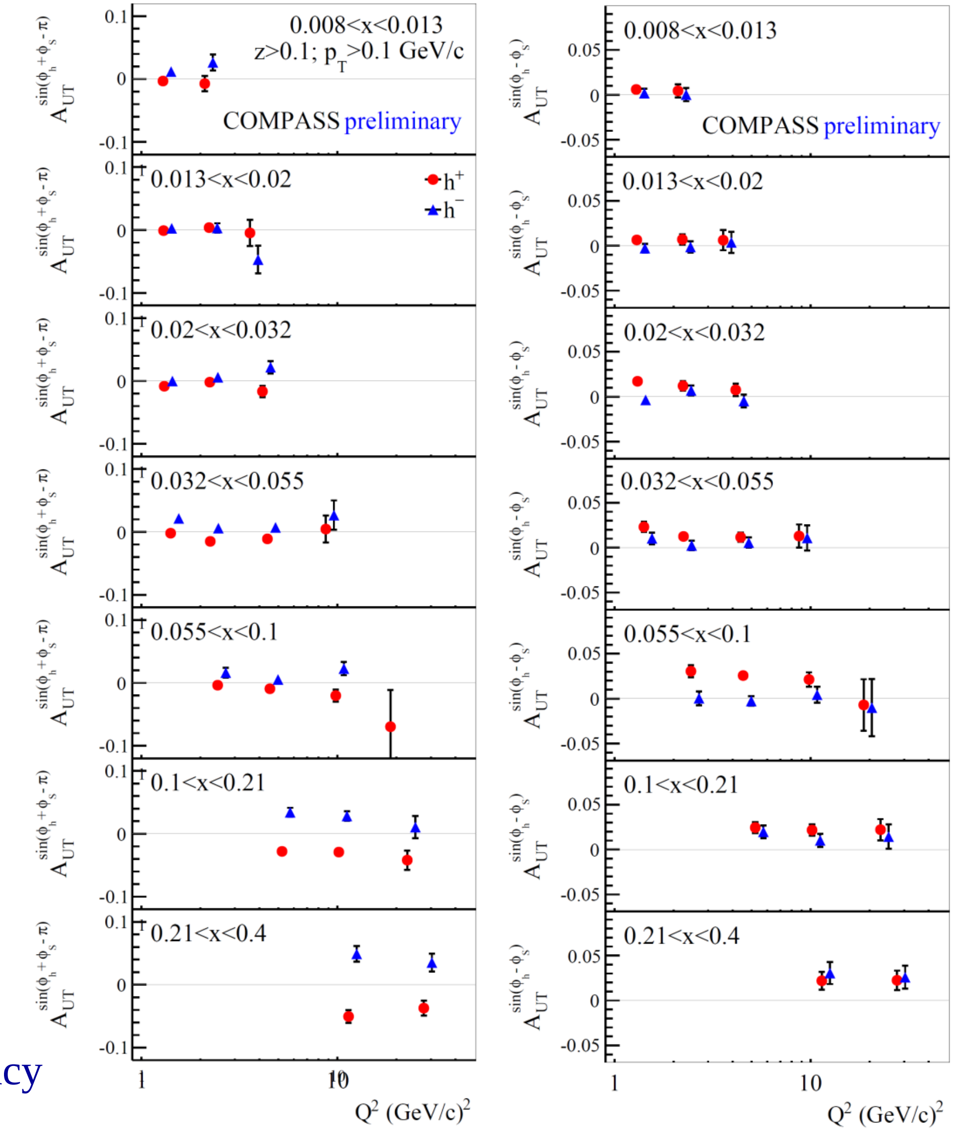

- No clear Q^2-dependence within statistical accuracy
- Possible decreasing trend for Sivers TSA?

Future Multi-D TSA analysis at JLab 12

Statistical precision

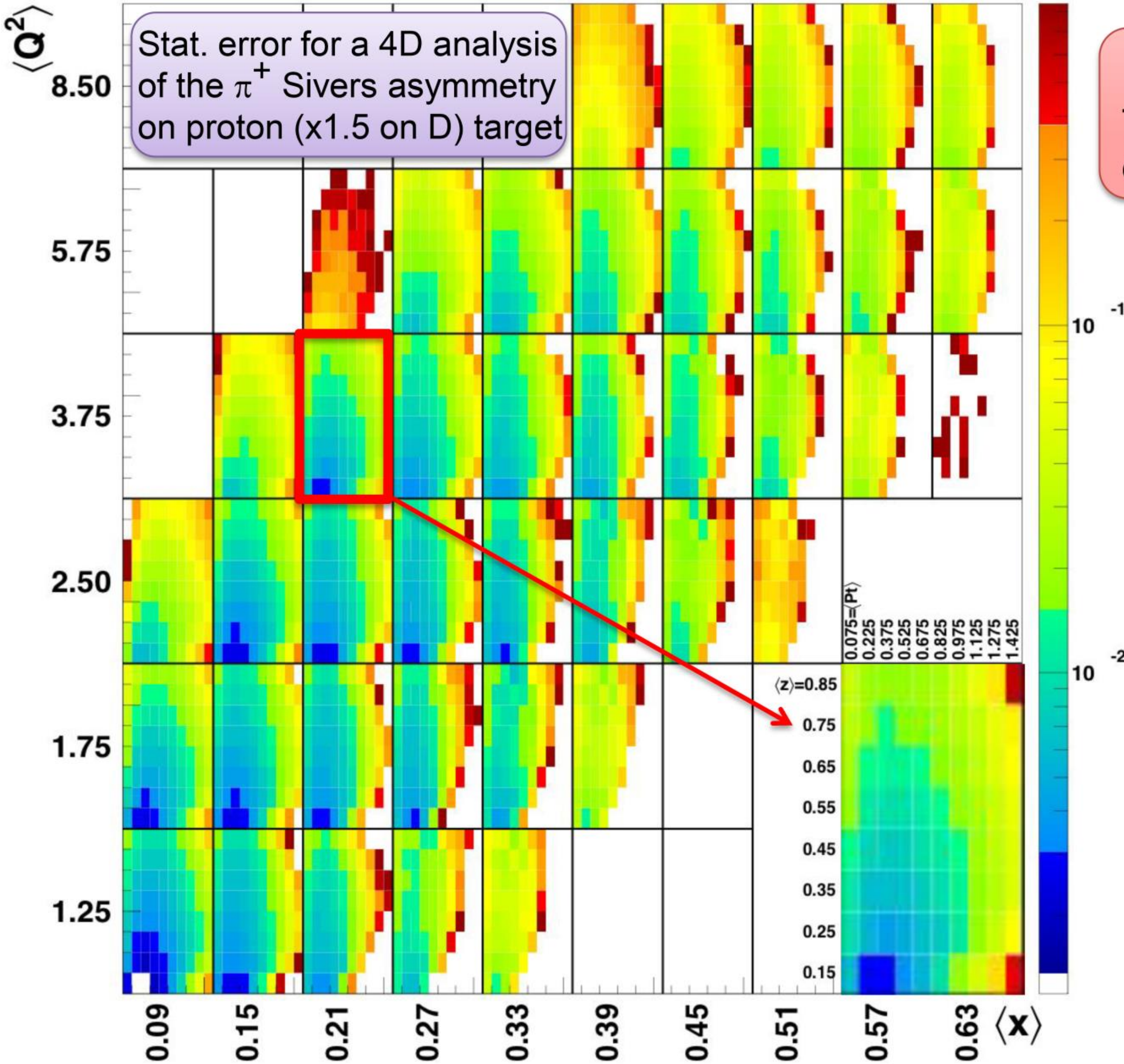

Stat. error for a 4D analysis of the π^+ Sivers asymmetry on proton (x1.5 on D) target

4D analysis is possible

The wanted high-Q^2 high-p_T defines the beam-time request

2D projection (x-p_T) of the π^+ Sivers asymmetry

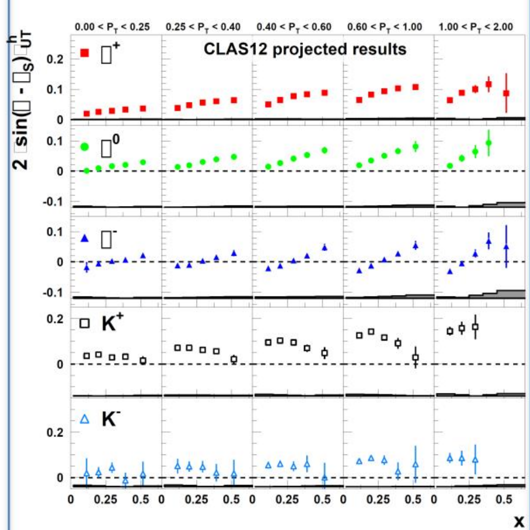

“Nature” *“1D”*

Raphael *“Madonna del Prato”*

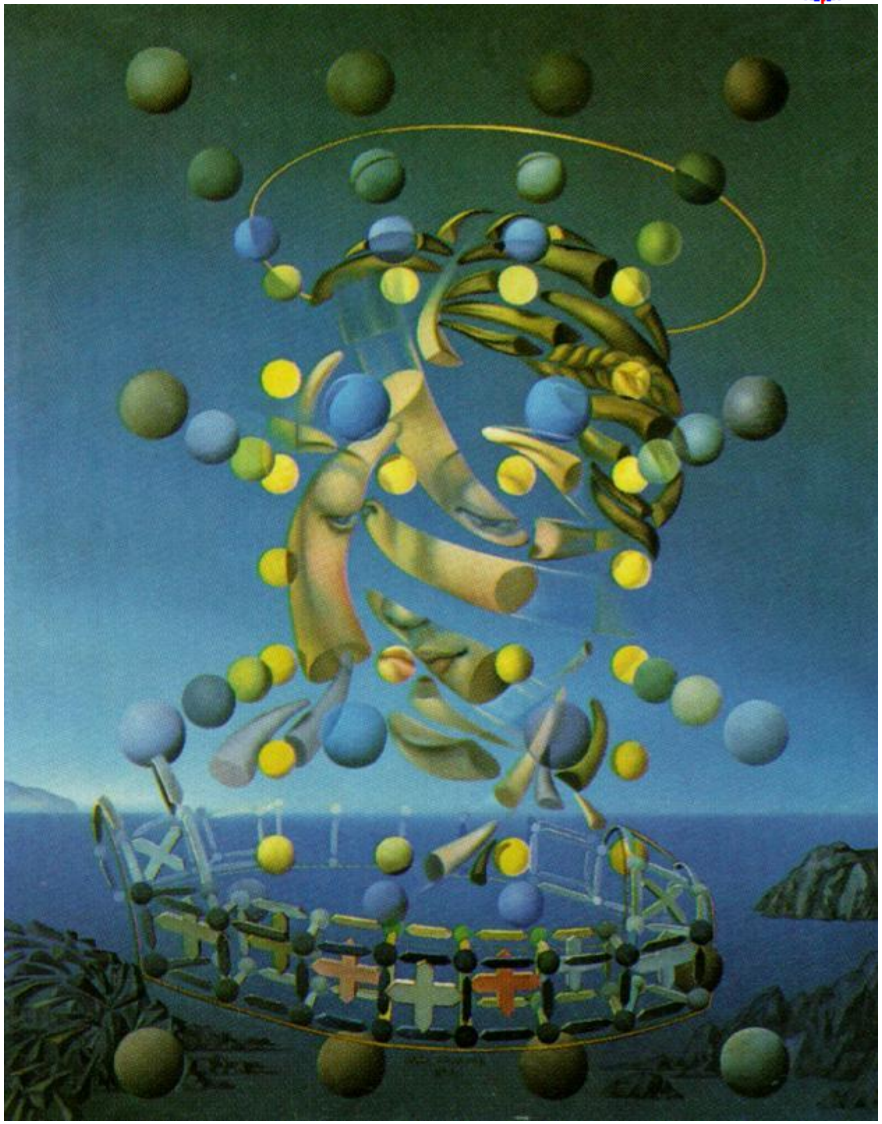

Salvador Dali *“Maximum Speed of Raphael's Madonna”*

“Nature” *“multi-D” with available statistics*

Raphael *“Madonna del Prato”*

Raphael *“Madonna del Prato” (poor resolution)*

- Results from first ever measurement of Drell-Yan TSAs

Single-polarized DY x-section: unpolarized part

ongoing analysis

$$\lambda = A_U^1 = \frac{F_U^1 - F_U^2}{F_U^1 + F_U^2}, \mu = A_U^{\cos\varphi_{CS}}, \nu = 2A_U^{\cos 2\varphi_{CS}}$$

- **“naive” Drell–Yan model**
  collinear (k_T=0) LO pQCD no rad. processes
  λ=1, (F_U^2=0), μ=ν=0
- **Intrinsic transverse motion + QCD effects**
  λ≠1, μ ≠ 0, ν ≠ 0 but 1–λ=2ν (Lam-Tung)
- **Experiment,**
  λ≠1, μ ≠ 0, ν ≠ 0

$$\frac{d\sigma}{d\Omega} \propto \left(F_U^1 + F_U^2\right) \times \left\{ \begin{array}{l} 1 + A_U^1 \cos^2\theta_{CS} + \\ \sin^2\theta_{CS} A_U^{\cos 2\varphi_{CS}} \cos 2\varphi_{CS} + \sin 2\theta_{CS} A_U^{\cos\varphi_{CS}} \cos\varphi_{CS} \end{array} \right\}$$

Single-polarized DY x-section: unpolarized part

ongoing analysis

$$\lambda = A_U^1 = \frac{F_U^1 - F_U^2}{F_U^1 + F_U^2}, \mu = A_U^{\cos\varphi_{CS}}, \nu = 2A_U^{\cos 2\varphi_{CS}}$$

- **"naive" Drell–Yan model**
  collinear (k_T=0) LO pQCD no rad. processes
  λ=1, (F_U^2=0), μ=ν=0
- **Intrinsic transverse motion + QCD effects**
  λ≠1, μ ≠ 0, ν ≠ 0 but 1–λ=2ν (Lam-Tung)
- **Experiment,**
  λ≠1, μ ≠ 0, ν ≠ 0
- ν ≠ 0 - Energy and quark flavour dependence, smaller effect for sea quarks, QCD radiative effects

$$\frac{d\sigma}{d\Omega} \propto \left(F_U^1 + F_U^2\right) \times \begin{Bmatrix} 1 + A_U^1 \cos^2\theta_{CS} + \\ \sin^2\theta_{CS} A_U^{\cos 2\varphi_{CS}} \cos 2\varphi_{CS} + \sin 2\theta_{CS} A_U^{\cos\varphi_{CS}} \cos\varphi_{CS} \end{Bmatrix}$$

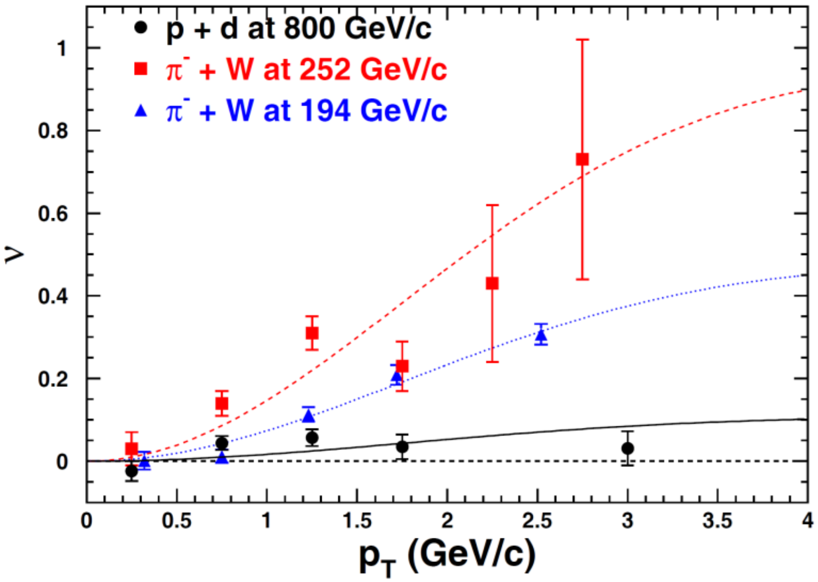

NA10 data **Z.Phys.C 37,545(1988)**

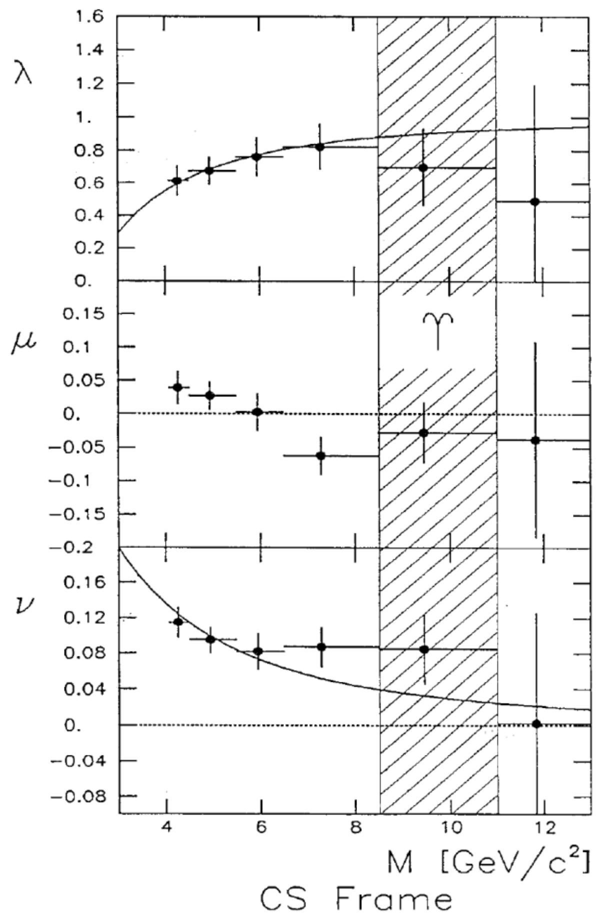

Single-polarized DY x-section: unpolarized part

ongoing analysis

$$\lambda = A_U^1 = \frac{F_U^1 - F_U^2}{F_U^1 + F_U^2}, \mu = A_U^{\cos\varphi_{CS}}, \nu = 2A_U^{\cos 2\varphi_{CS}}$$

$$\frac{d\sigma}{d\Omega} \propto \left(F_U^1 + F_U^2\right) \times \left\{ \begin{array}{l} 1 + A_U^1 \cos^2\theta_{CS} + \\ \sin^2\theta_{CS} A_U^{\cos 2\varphi_{CS}} \cos 2\varphi_{CS} + \sin 2\theta_{CS} A_U^{\cos\varphi_{CS}} \cos\varphi_{CS} \end{array} \right\}$$

- **"naive" Drell–Yan model**
  collinear (k_T=0) LO pQCD no rad. processes
  λ=1, (F_U^2=0), μ=ν=0
- **Intrinsic transverse motion + QCD effects**
  $\lambda \neq 1$, $\mu \neq 0$, $\nu \neq 0$ but $1-\lambda = 2\nu$ (Lam-Tung)
- **Experiment,**
  $\lambda \neq 1$, $\mu \neq 0$, $\nu \neq 0$
- $\nu \neq 0$ - Energy and quark flavour dependence, smaller effect for sea quarks, QCD radiative effects

See next talk by W. Vogelsang

M. Lambertsen, W. Vogelsang **PRD93, 114013 (2016)**

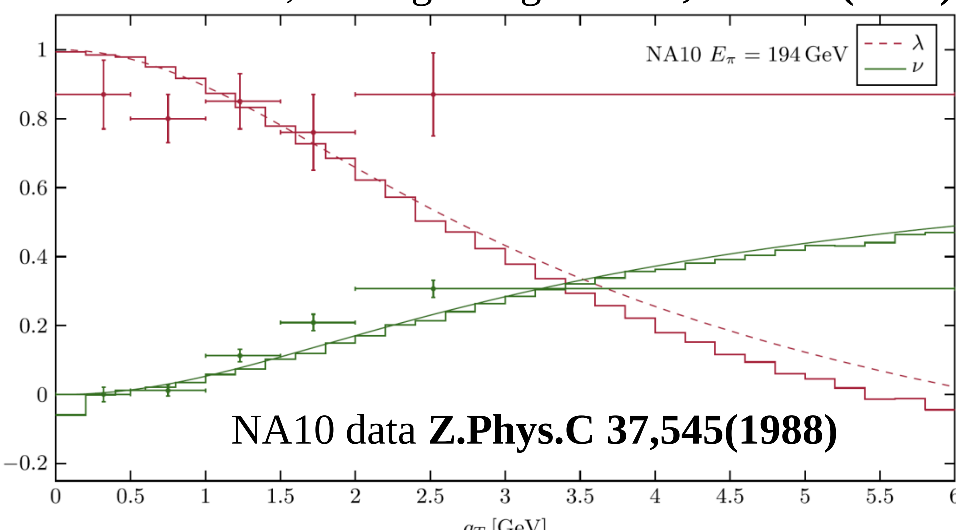

NA10 data **Z.Phys.C 37,545(1988)**

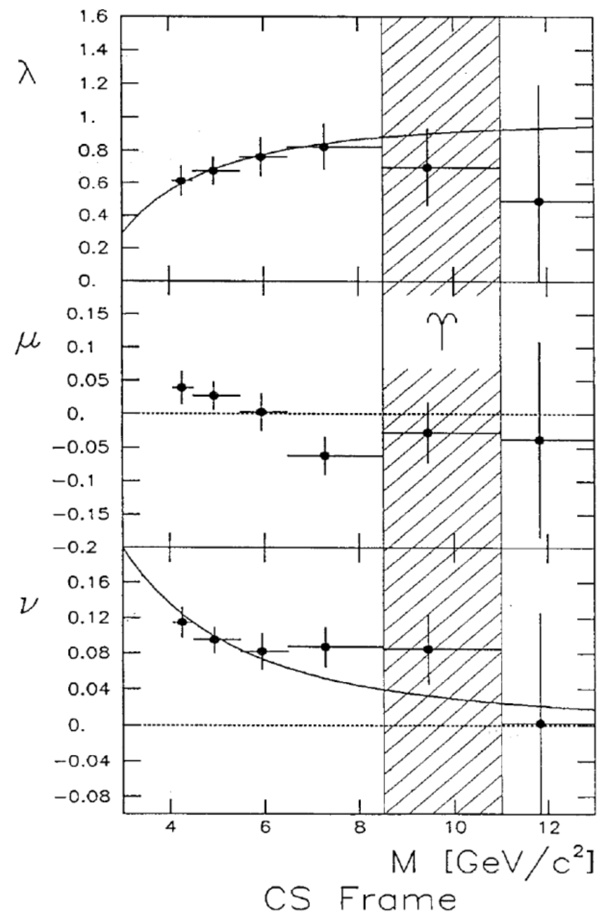

Single-polarized DY x-section: transverse part

$$\lambda = A_U^1 = \frac{F_U^1 - F_U^2}{F_U^1 + F_U^2}, \mu = A_U^{\cos\varphi_{CS}}, \nu = 2A_U^{\cos 2\varphi_{CS}}$$

- **"naive" Drell–Yan model**
  collinear (k_T=0) LO pQCD no rad. processes
  λ=1, (F_U^2=0), μ=ν=0
- **Intrinsic transverse motion + QCD effects**
  λ≠1, μ ≠ 0, ν ≠ 0 but 1–λ=2ν (Lam-Tung)
- **Experiment,**
  λ≠1, μ ≠ 0, ν ≠ 0

$$\frac{d\sigma}{d\Omega} \propto \left(F_U^1 + F_U^2\right)\left(1 + A_U^1 \cos^2\theta_{CS}\right) \times \left\{ \begin{array}{l} 1 + D_{[\sin^2\theta_{CS}]} A_U^{\cos 2\varphi_{CS}} \cos 2\varphi_{CS} + D_{[\sin 2\theta_{CS}]} A_U^{\cos\varphi_{CS}} \cos\varphi_{CS} \\ + S_T \left[\begin{array}{l} A_T^{\sin\varphi_S} \sin\varphi_S \\ + D_{[\sin 2\theta_{CS}]} \left(\begin{array}{l} A_T^{\sin(\varphi_{CS}-\varphi_S)} \sin(\varphi_{CS}-\varphi_S) \\ + A_T^{\sin(\varphi_{CS}+\varphi_S)} \sin(\varphi_{CS}+\varphi_S) \end{array} \right) \\ + D_{[\sin^2\theta_{CS}]} \left(\begin{array}{l} A_T^{\sin(2\varphi_{CS}-\varphi_S)} \sin(2\varphi_{CS}-\varphi_S) \\ + A_T^{\sin(2\varphi_{CS}+\varphi_S)} \sin(2\varphi_{CS}+\varphi_S) \end{array} \right) \end{array} \right] \end{array} \right\}$$

$$D_{[f(\theta_{CS})]} = f(\theta_{CS}) / \left(1 + A_U^1 \cos^2\theta_{CS}\right)$$

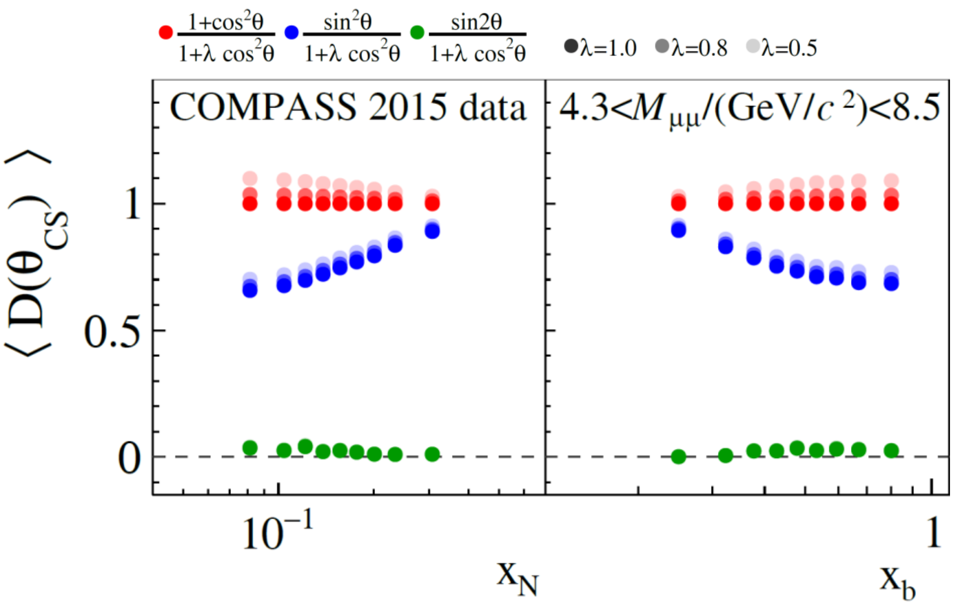

- All five Drell-Yan TSAs are extracted simultaneously using extended unbinned Maximum likelihood estimator.
- Depolarization factors are evaluated under assumption A_U^1=1
- Possible impact of A_U^1≠1 scenarios lead to a normalization uncertainty of at most −5%.

Drell-Yan TSAs – Transversity

$$\frac{d\sigma}{d\Omega} \propto 1 + \ldots + S_T \left[D_{[\sin^2\theta_{CS}]} A_T^{\sin(2\varphi_{CS}-\varphi_S)} \sin(2\varphi_{CS}-\varphi_S) + \ldots \right]$$

Transversity DY TSA

$$A_T^{\sin(2\varphi_{CS}-\varphi_S)} \propto h_{1,\pi}^{\perp q} \otimes h_{1,p}^{q}$$

COMPASS PRL 119, 112002 (2017)

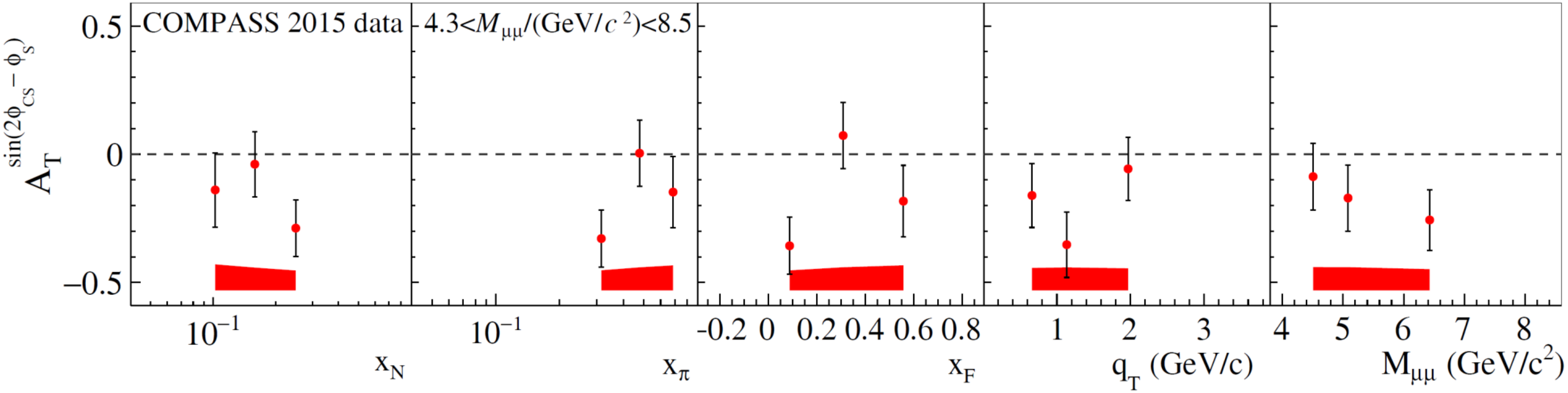

Drell-Yan TSAs – Transversity

$$\frac{d\sigma}{d\Omega} \propto 1+\ldots+\ S_T\left[D_{\left[\sin^2\theta_{CS}\right]} A_T^{\sin(2\varphi_{CS}-\varphi_S)} \sin\left(2\varphi_{CS}-\varphi_S\right)+\ldots\right]$$

Transversity DY TSA

$$A_T^{\sin(2\varphi_{CS}-\varphi_S)} \propto h_{1,\pi}^{\perp q} \otimes h_{1,p}^{q}$$

COMPASS PRL 119, 112002 (2017)

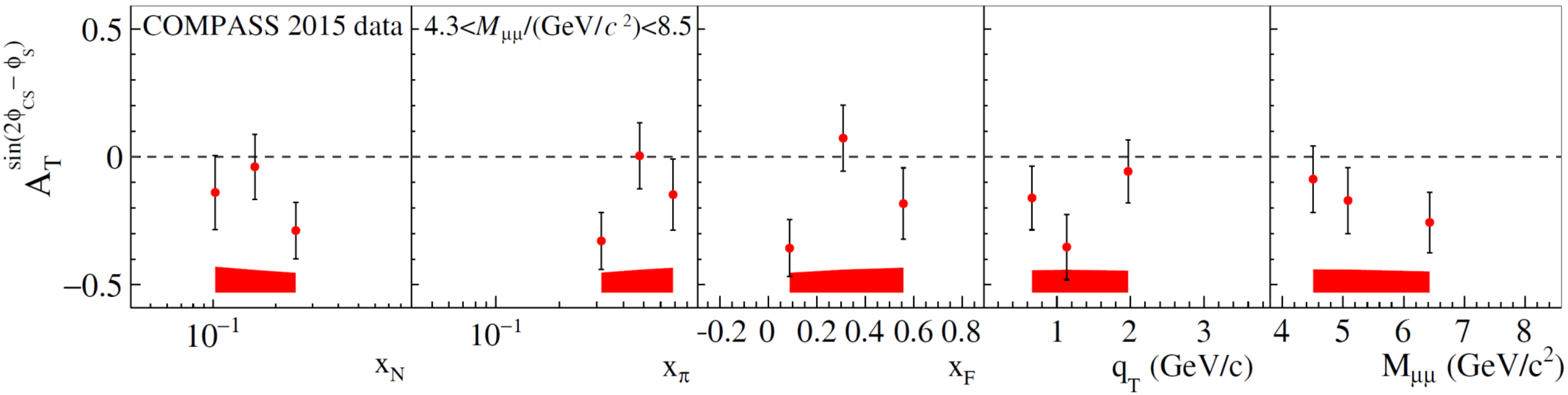

SIDIS in Drell-Yan *high-mass* range

Collins SIDIS TSA

$$A_{UT}^{\sin(\phi_h+\phi_s)} \propto h_1^q \otimes H_{1q}^{\perp h}$$

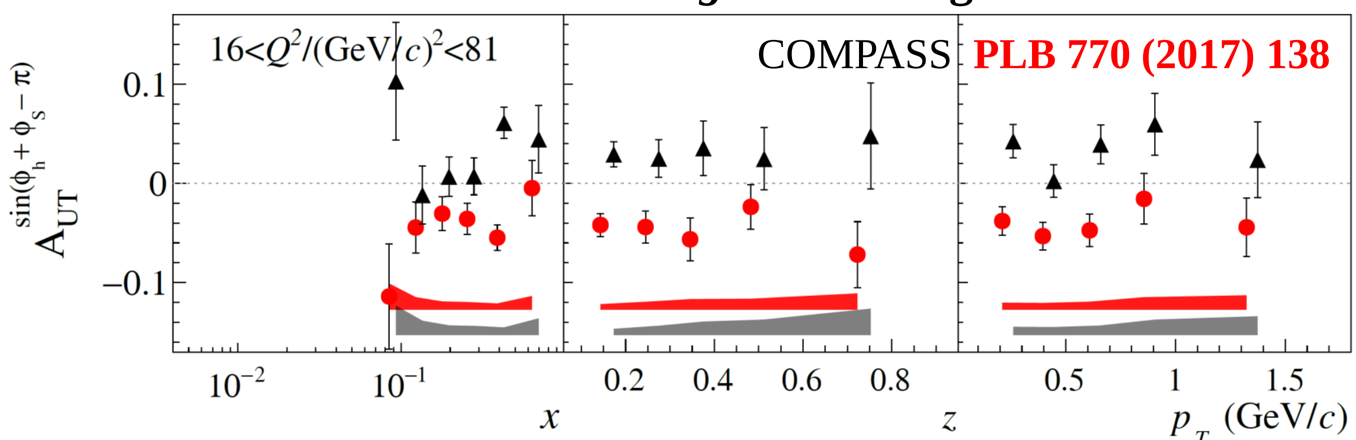

Drell-Yan TSAs – Transversity

$$\frac{d\sigma}{d\Omega} \propto 1 + \ldots + S_T \left[D_{[\sin^2\theta_{CS}]} A_T^{\sin(2\varphi_{CS}-\varphi_S)} \sin(2\varphi_{CS}-\varphi_S) + \ldots \right]$$

Transversity DY TSA

$$A_T^{\sin(2\varphi_{CS}-\varphi_S)} \propto h_{1,\pi}^{\perp q} \otimes h_{1,p}^{q}$$

COMPASS PRL 119, 112002 (2017)

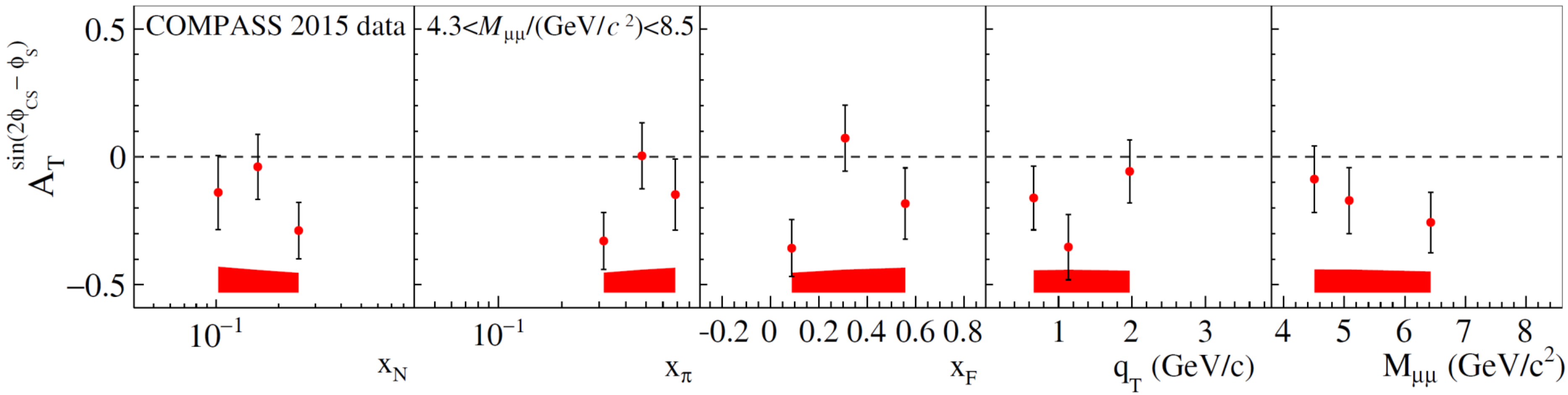

B. Pasquini, P. Schweitzer
Phys.Rev. D90 (2014) 014050

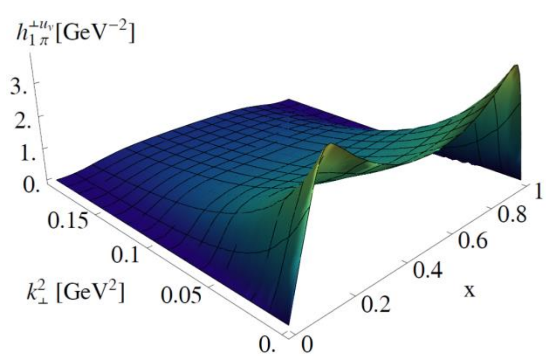

M. Anselmino et al.
Phys.Rev. D92 (2015) 114023

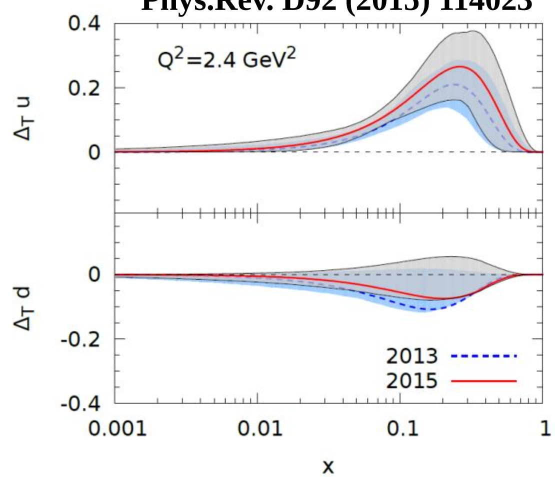

Drell-Yan TSAs – Transversity

$$\frac{d\sigma}{d\Omega} \propto 1 + \ldots + S_T \left[D_{[\sin^2\theta_{CS}]} A_T^{\sin(2\varphi_{CS}-\varphi_S)} \sin(2\varphi_{CS}-\varphi_S) + \ldots \right]$$

Transversity DY TSA

$$A_T^{\sin(2\varphi_{CS}-\varphi_S)} \propto h_{1,\pi}^{\perp q} \otimes h_{1,p}^{q}$$

COMPASS PRL 119, 112002 (2017)

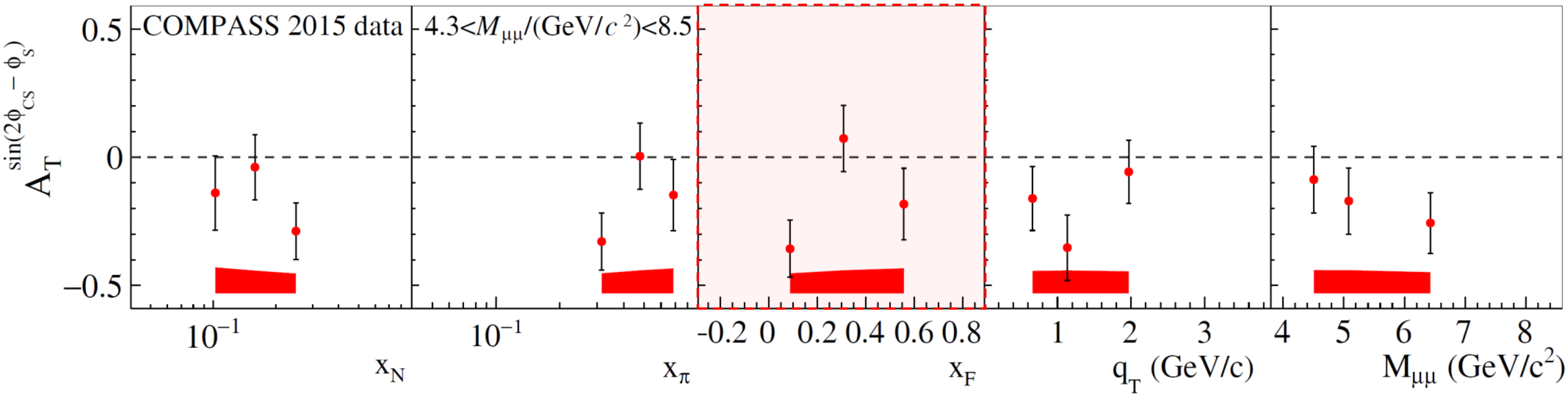

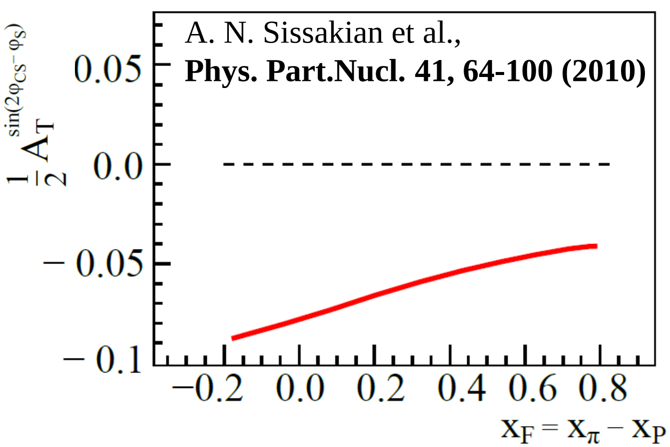

B. Pasquini, P. Schweitzer
Phys.Rev. D90 (2014) 014050

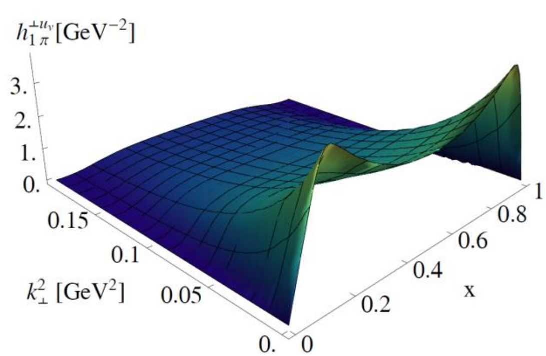

M. Anselmino et al.
Phys.Rev. D92 (2015) 114023

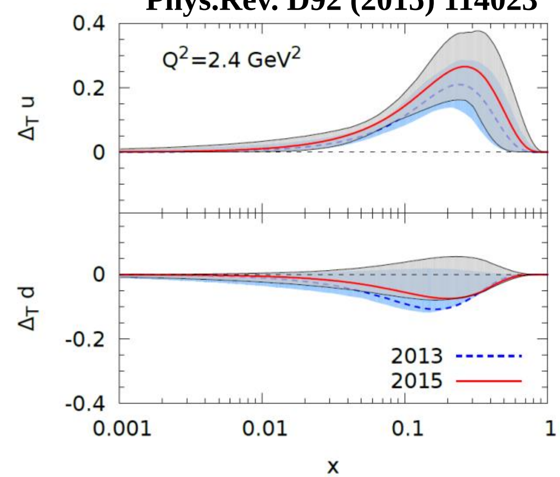

Drell-Yan TSAs – Pretzelosity

$$\frac{d\sigma}{d\Omega} \propto 1+\ldots+ S_T\left[D_{\left[\sin^2\theta_{CS}\right]} A_T^{\sin(2\varphi_{CS}+\varphi_S)} \sin(2\varphi_{CS}-\varphi_S)+\ldots\right]$$

Pretzelosity DY TSA

$$A_T^{\sin(2\varphi_{CS}+\varphi_S)} \propto h_{1,\pi}^{\perp q} \otimes h_{1T,p}^{\perp q}$$

COMPASS PRL 119, 112002 (2017)

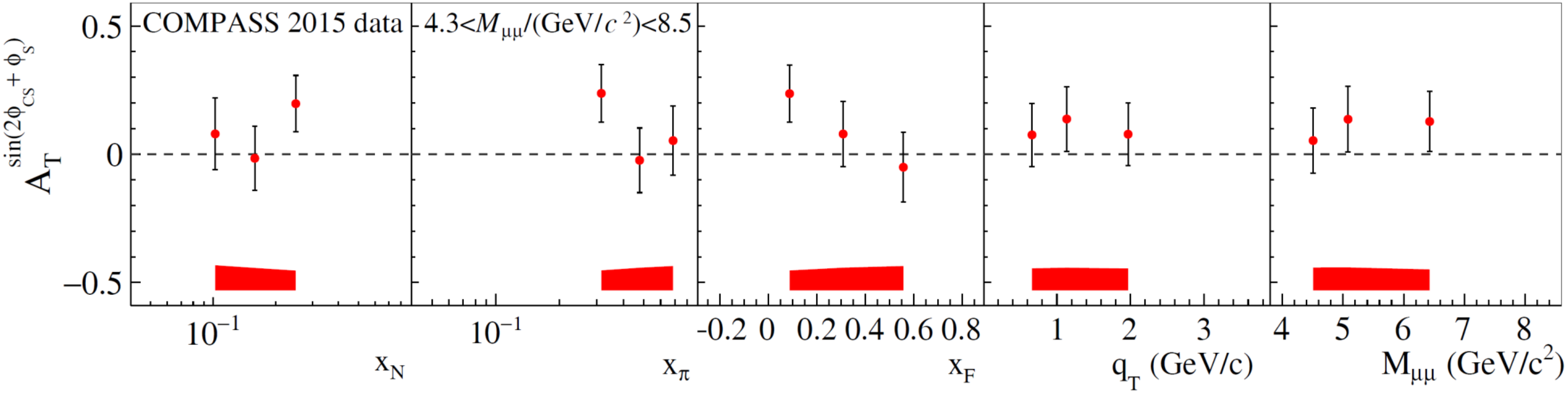

Drell-Yan TSAs – Pretzelosity

$$\frac{d\sigma}{d\Omega} \propto 1 + \ldots + S_T \left[D_{\left[\sin^2\theta_{CS}\right]} A_T^{\sin(2\varphi_{CS}+\varphi_S)} \sin(2\varphi_{CS} - \varphi_S) + \ldots \right]$$

Pretzelosity DY TSA

$$A_T^{\sin(2\varphi_{CS}+\varphi_S)} \propto h_{1,\pi}^{\perp q} \otimes h_{1T,\mathrm{p}}^{\perp q}$$

COMPASS PRL 119, 112002 (2017)

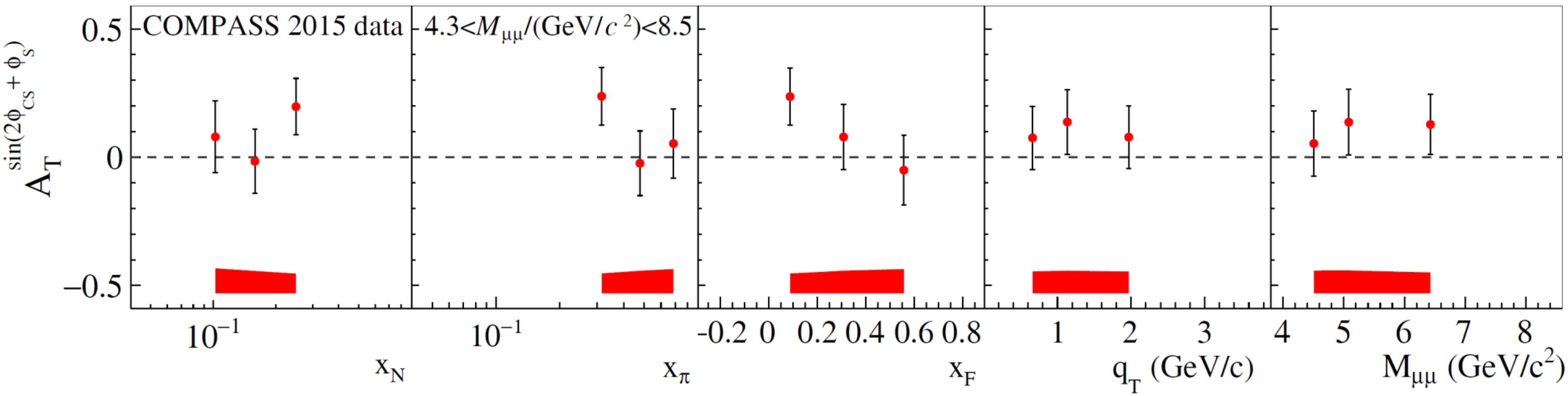

SIDIS in Drell-Yan *high-mass* range

Pretzelosity SIDIS TSA

$$A_{UT}^{\sin(3\phi_h-\phi_s)} \propto h_{1T}^{\perp q} \otimes H_{1q}^{\perp h}$$

COMPASS **PLB 770 (2017) 138**

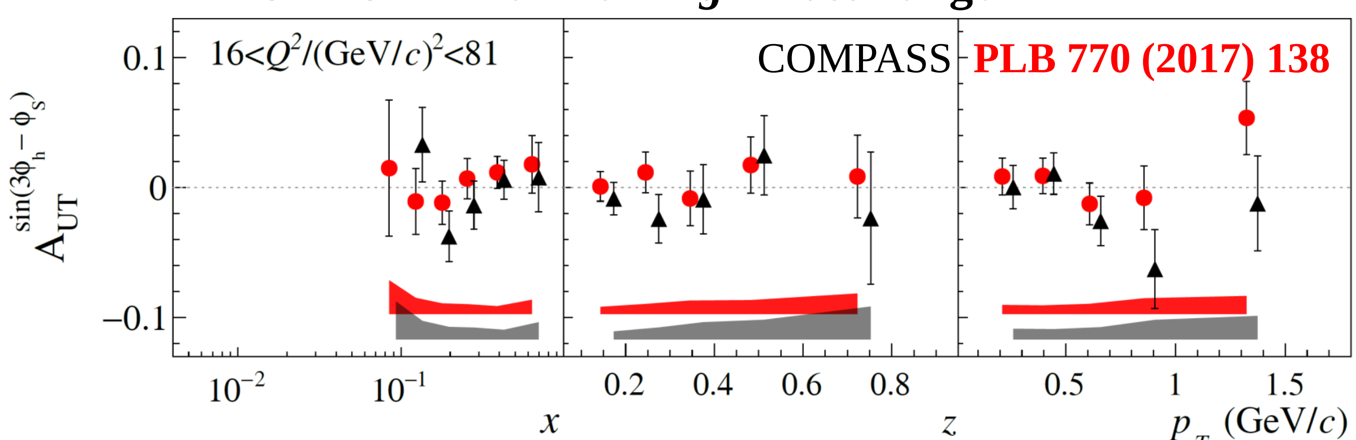

Drell-Yan TSAs – Pretzelosity

$$\frac{d\sigma}{d\Omega} \propto 1 + \ldots + S_T \left[D_{[\sin^2\theta_{CS}]} A_T^{\sin(2\varphi_{CS}+\varphi_S)} \sin(2\varphi_{CS}-\varphi_S) + \ldots \right]$$

Pretzelosity DY TSA

$$A_T^{\sin(2\varphi_{CS}+\varphi_S)} \propto h_{1,\pi}^{\perp q} \otimes h_{1T,p}^{\perp q}$$

COMPASS PRL 119, 112002 (2017)

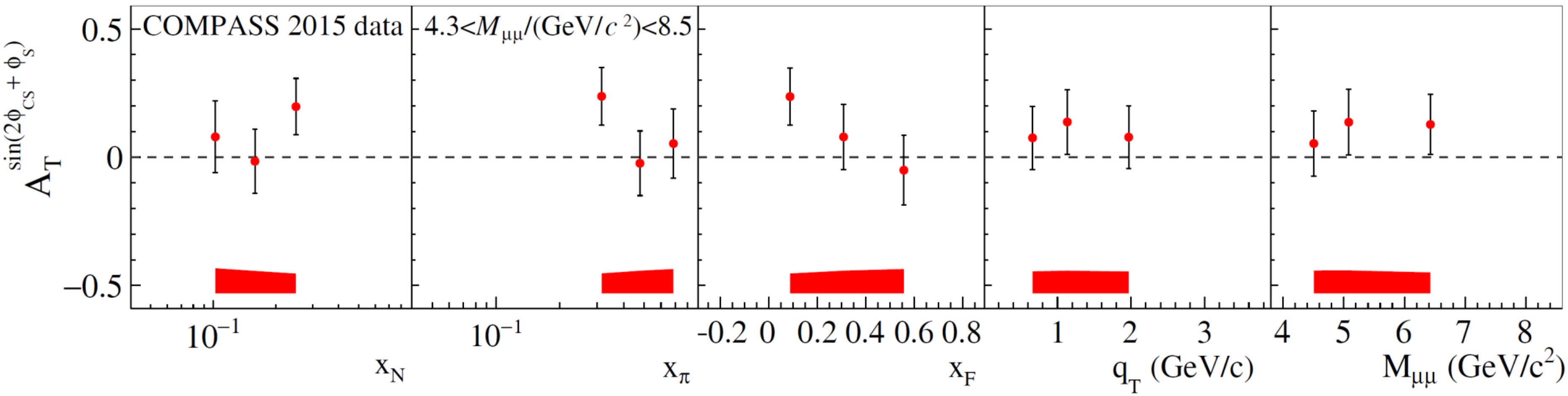

B. Pasquini, P. Schweitzer
Phys.Rev. D90 (2014) 014050

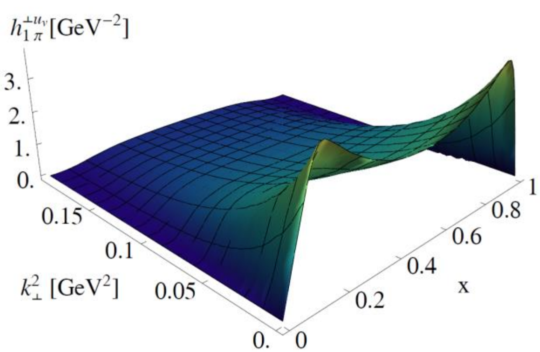

C. Lefky, A. Prokudin
PRD91 (2015) 034010

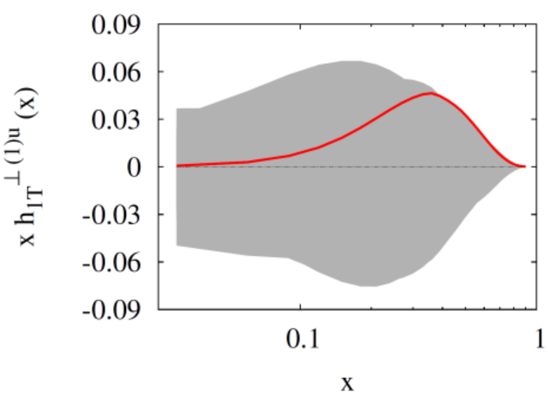

Drell-Yan TSAs – Sivers

$$\frac{d\sigma}{d\Omega} \propto 1 + \ldots + S_T \left[A_T^{\sin\varphi_S} \sin\varphi_S + \ldots \right]$$

Sivers DY TSA

$$A_T^{\sin\varphi_S} \propto f_{1,\pi}^{q} \otimes f_{1T,p}^{\perp q}$$

COMPASS PRL 119, 112002 (2017)

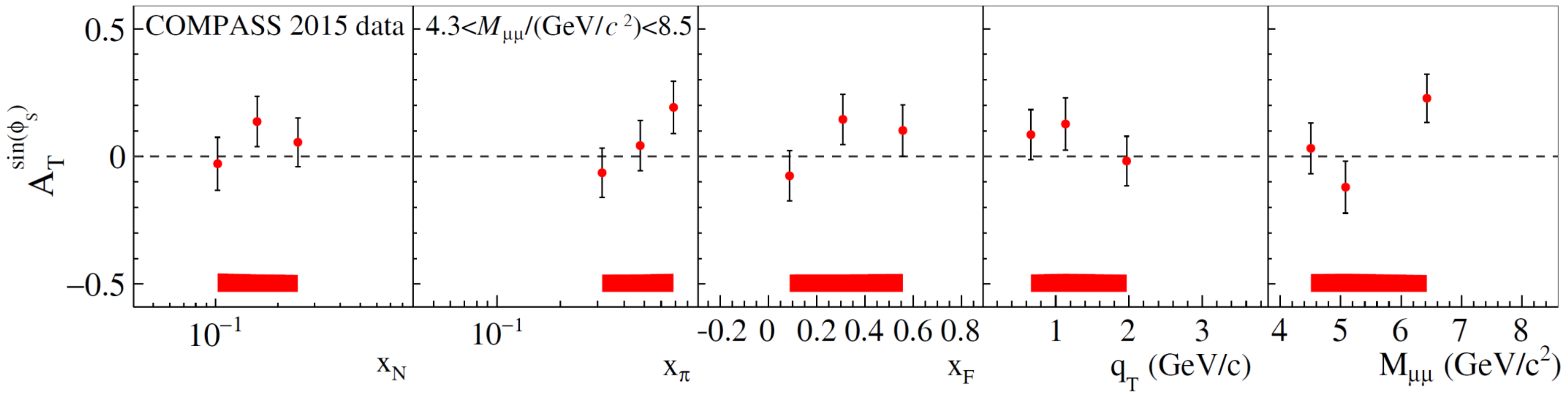

Drell-Yan TSAs – Sivers

$$\frac{d\sigma}{d\Omega} \propto 1+\ldots+ S_T\left[A_T^{\sin\varphi_S}\sin\varphi_S+\ldots\right]$$

Sivers DY TSA

$$A_T^{\sin\varphi_S} \propto f_{1,\pi}^{q} \otimes f_{1T,p}^{\perp q}$$

COMPASS **PRL 119, 112002 (2017)**

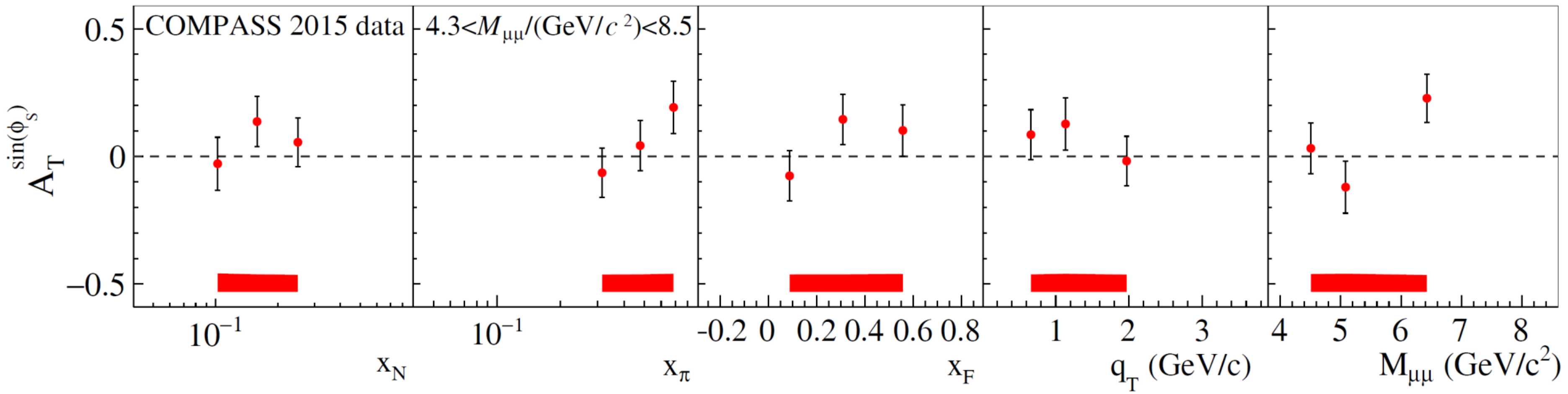

SIDIS in Drell-Yan *high-mass* range

COMPASS **PLB 770 (2017) 138**

Sivers SIDIS TSA

$$A_{UT}^{\sin(\phi_h-\phi_s)} \propto f_{1T}^{\perp q} \otimes D_{1q}^{h}$$

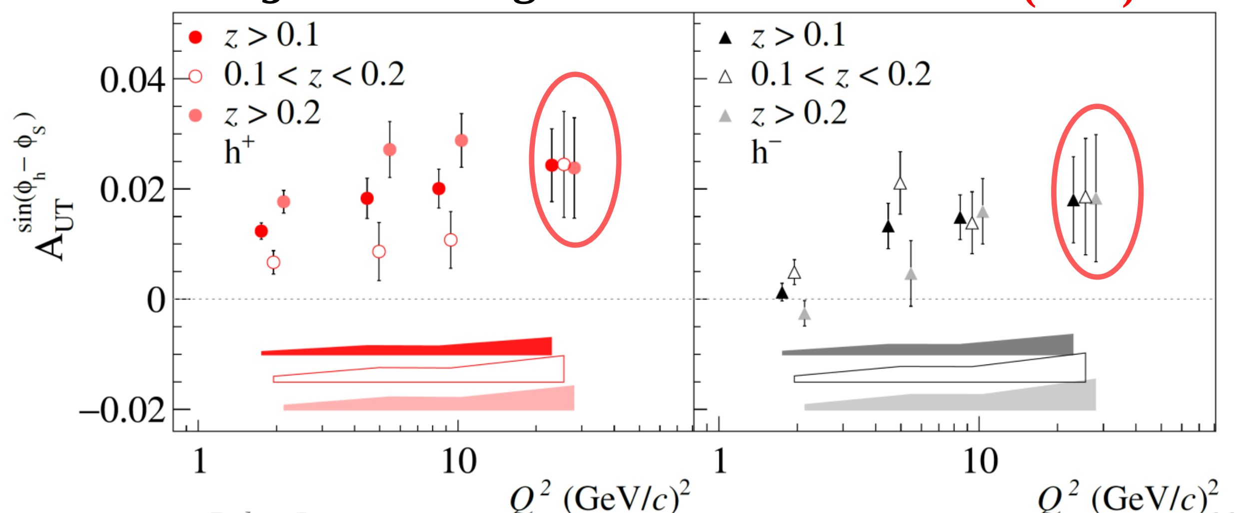

Drell-Yan TSAs – Sivers

$$\frac{d\sigma}{d\Omega} \propto 1 + \ldots + S_T \left[A_T^{\sin\varphi_S} \sin\varphi_S + \ldots \right]$$

Sivers DY TSA

$$A_T^{\sin\varphi_S} \propto f_{1,\pi}^{q} \otimes f_{1T,p}^{\perp q}$$

COMPASS PRL 119, 112002 (2017)

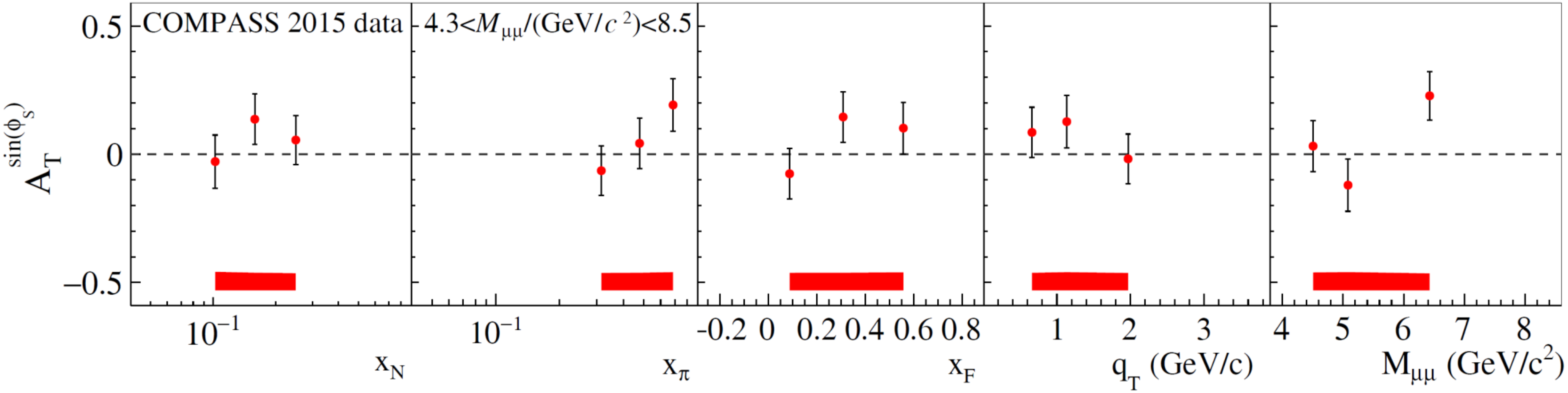

B. Pasquini, P. Schweitzer
Phys.Rev. D90 (2014) 014050

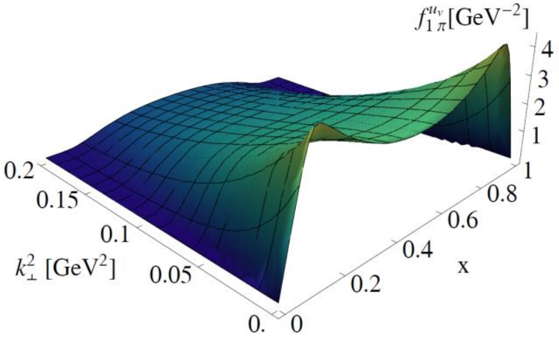

M. Anselmino et al.
arXiv:1612.06413[hep-ph]

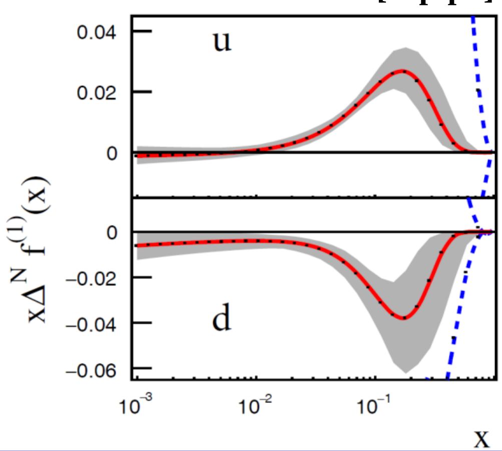

Sivers asymmetry in Drell-Yan: sign change

DGLAP (2016)
M. Anselmino et al., **arXiv:1612.06413**

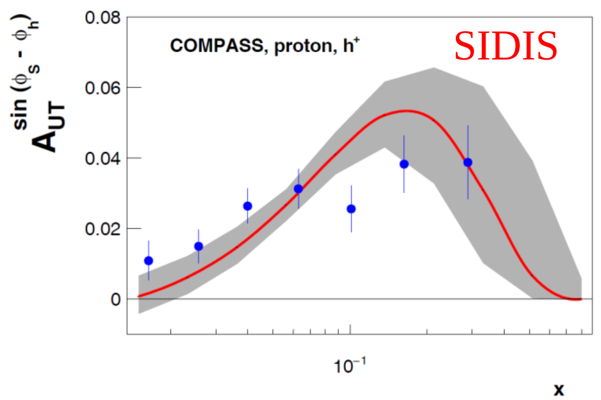

TMD-1 (2014**)**
M. G. Echevarria et al. **PRD89,074013**

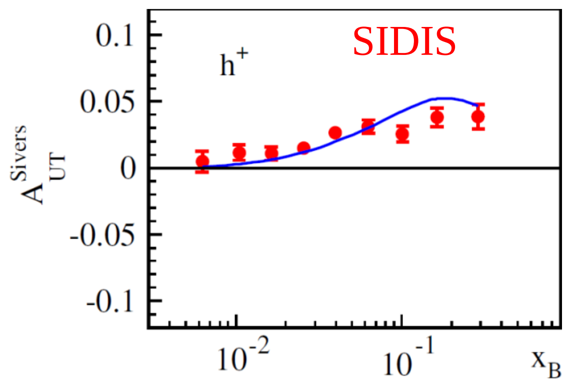

TMD-2 (2013)
P. Sun, F. Yuan, **PRD88, 114012**

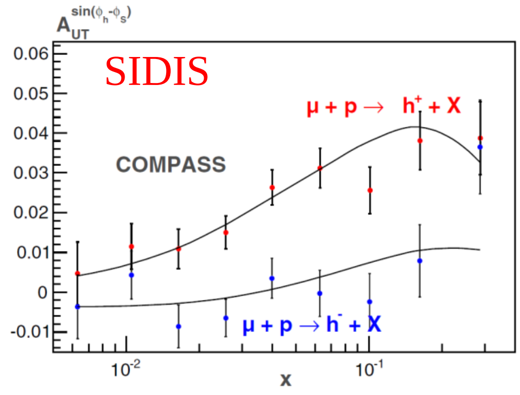

Sivers asymmetry in Drell-Yan: sign change

DGLAP (2016)
M. Anselmino et al., **arXiv:1612.06413**

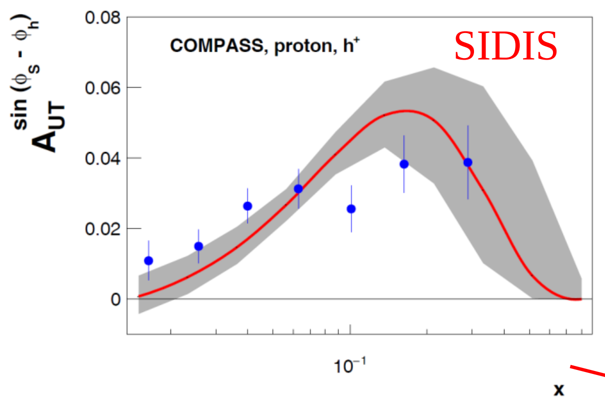

TMD-1 (2014)
M. G. Echevarria et al. **PRD89,074013**

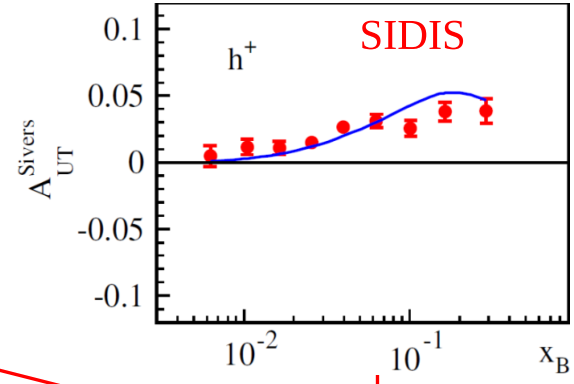

TMD-2 (2013)
P. Sun, F. Yuan, **PRD88, 114012**

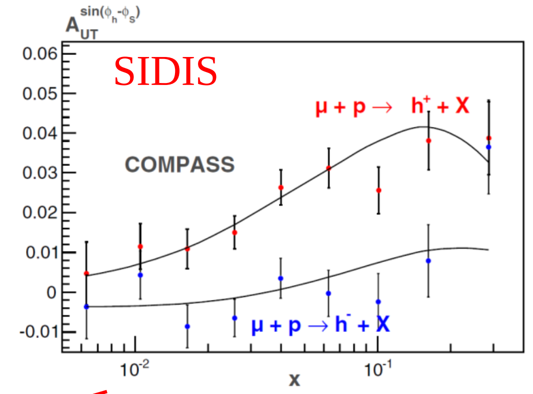

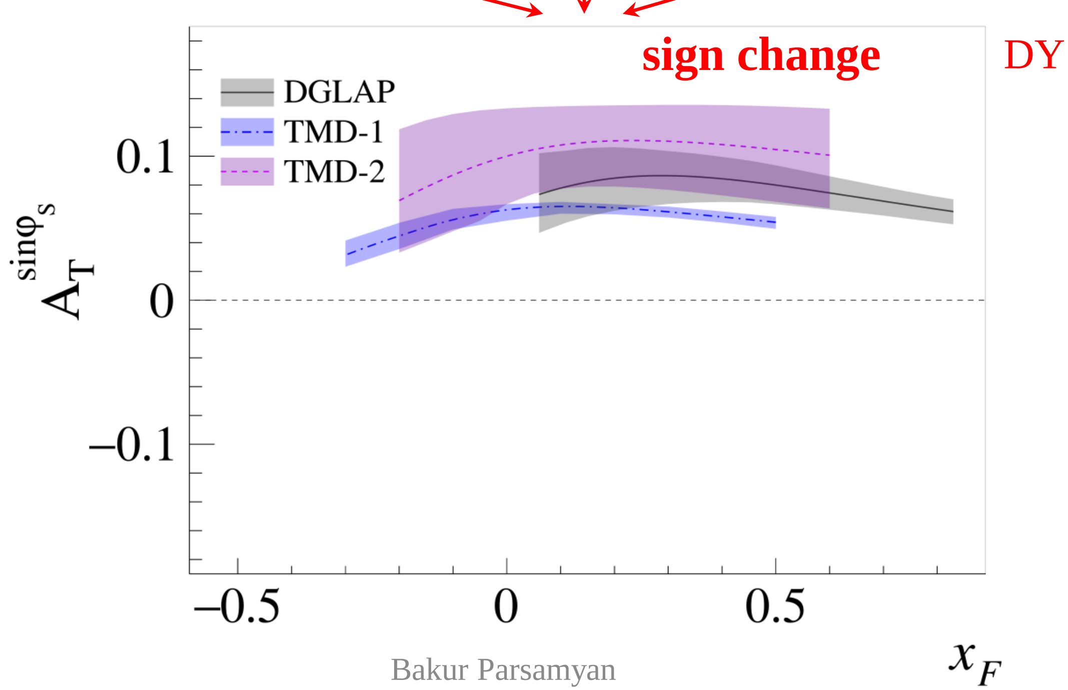

Sivers asymmetry in Drell-Yan: sign change

DGLAP (2016)
M. Anselmino et al., **arXiv:1612.06413**

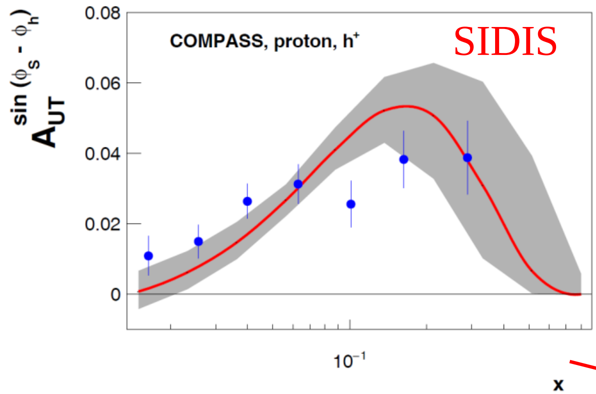

TMD-1 (2014)
M. G. Echevarria et al. **PRD89,074013**

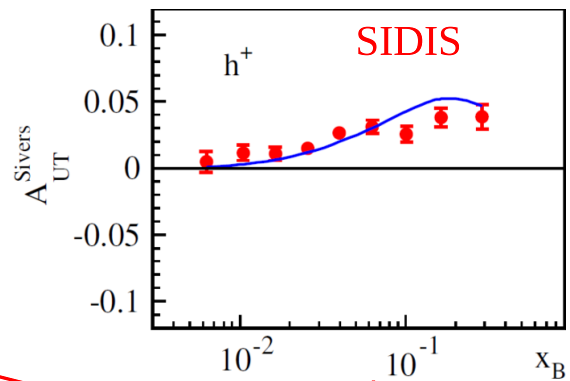

TMD-2 (2013)
P. Sun, F. Yuan, **PRD88, 114012**

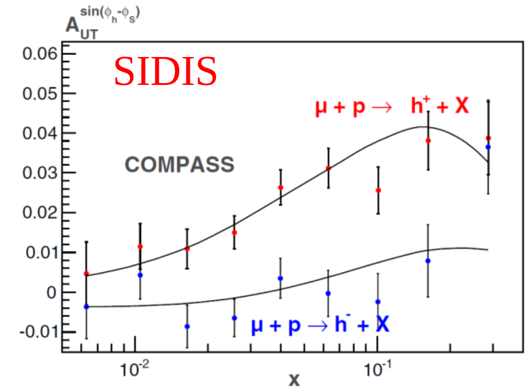

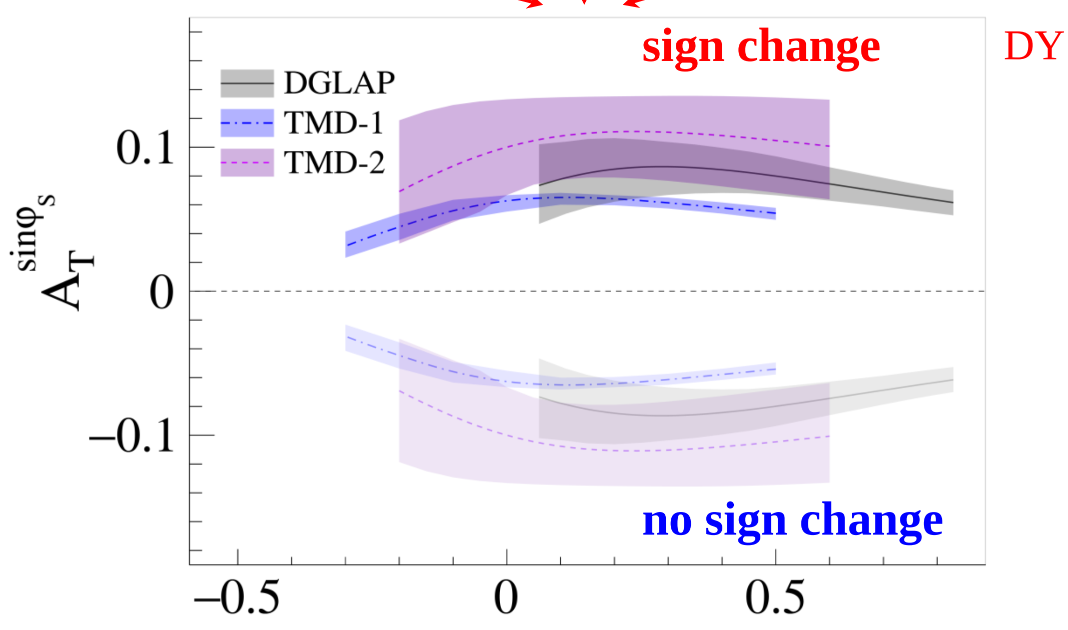

Sivers asymmetry in Drell-Yan: sign change

DGLAP (2016)
M. Anselmino et al., **arXiv:1612.06413**

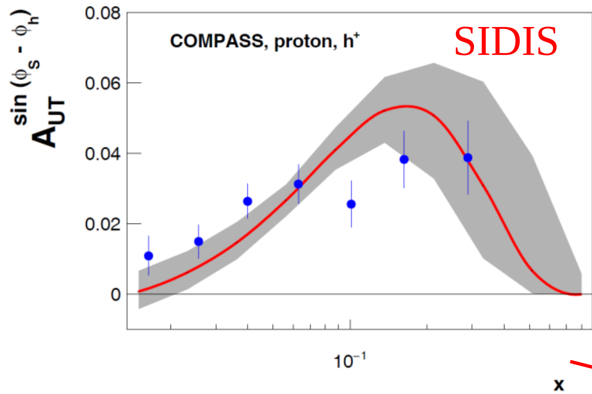

TMD-1 (2014)
M. G. Echevarria et al. **PRD89,074013**

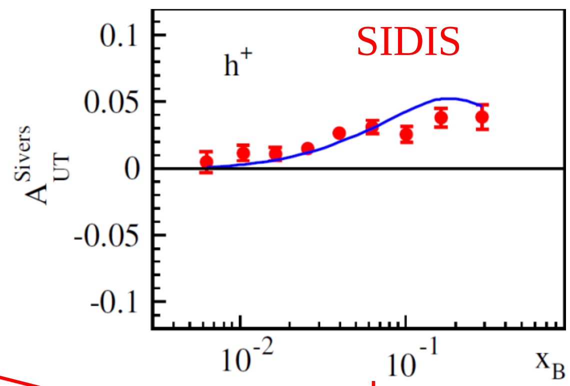

TMD-2 (2013)
P. Sun, F. Yuan, **PRD88, 114012**

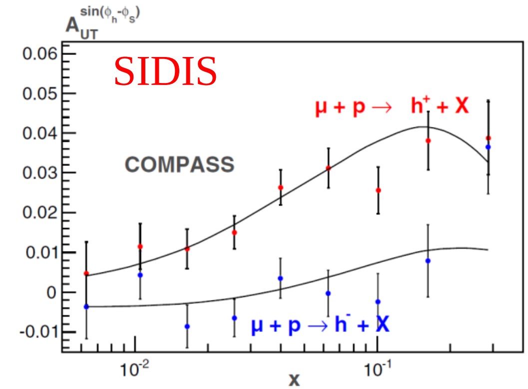

COMPASS
PRL 119, 112002 (2017)

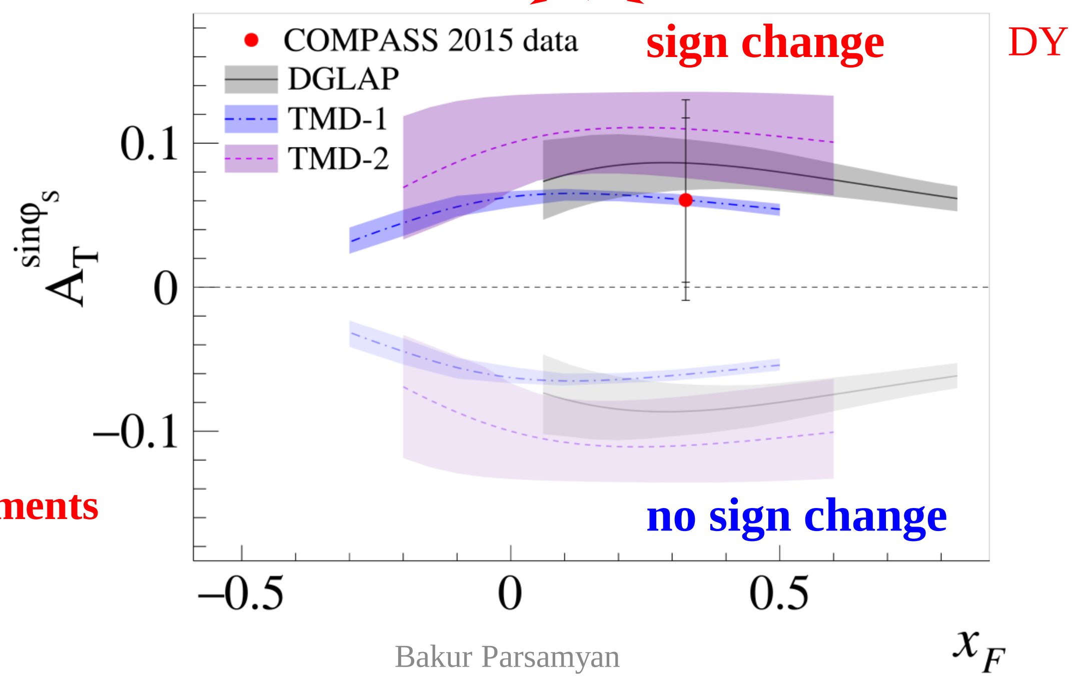

In 2018 – 2nd round of polarized DY measurements at COMPASS

SIDIS and DY TSAs at COMPASS (high-mass range)

$$\frac{d\sigma}{dxdydzdp_T^2 d\phi_h d\phi_S} \propto \left(F_{UU,T} + \varepsilon F_{UU,L}\right) \left\{ 1 + \ldots \right.$$

$$\left. + S_T \left[\begin{array}{l} A_{UT}^{\sin(\phi_h - \phi_S)} \sin(\phi_h - \phi_S) \\ + \varepsilon A_{UT}^{\sin(\phi_h + \phi_S)} \sin(\phi_h + \phi_S) \\ + \varepsilon A_{UT}^{\sin(3\phi_h - \phi_S)} \sin(3\phi_h - \phi_S) \\ + \sqrt{2\varepsilon(1+\varepsilon)} A_{UT}^{\sin\phi_S} \sin\phi_S \\ + \sqrt{2\varepsilon(1+\varepsilon)} A_{UT}^{\sin(2\phi_h - \phi_S)} \sin(2\phi_h - \phi_S) \end{array} \right] \right\}$$

$$\frac{d\sigma^{LO}}{d\Omega} \propto F_U^1 \left(1 + \cos^2\theta_{CS}\right) \left\{ 1 + \ldots \right.$$

$$\left. + S_T \left[\begin{array}{l} A_T^{\sin\varphi_S} \sin\varphi_S \\ + D_{[\sin^2\theta_{CS}]} \left(\begin{array}{l} A_T^{\sin(2\varphi_{CS} - \varphi_S)} \sin(2\varphi_{CS} - \varphi_S) \\ + A_T^{\sin(2\varphi_{CS} + \varphi_S)} \sin(2\varphi_{CS} + \varphi_S) \end{array} \right) \\ + D_{[\sin 2\theta_{CS}]} \left(\begin{array}{l} A_T^{\sin(\varphi_{CS} - \varphi_S)} \sin(\varphi_{CS} - \varphi_S) \\ + A_T^{\sin(\varphi_{CS} + \varphi_S)} \sin(\varphi_{CS} + \varphi_S) \end{array} \right) \end{array} \right] \right\}$$

COMPASS PLB 770 (2017) 138

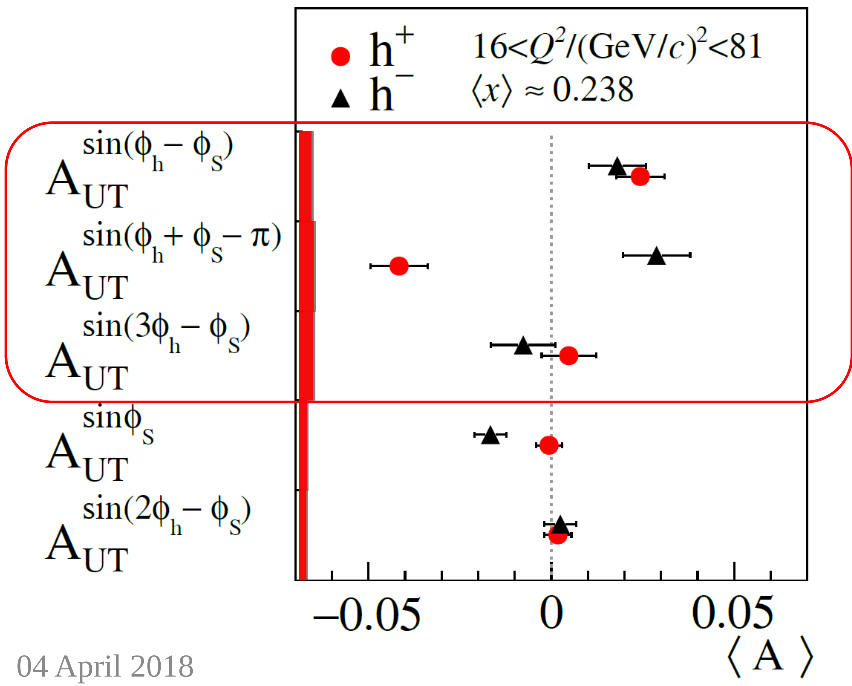

COMPASS PRL 119, 112002 (2017)

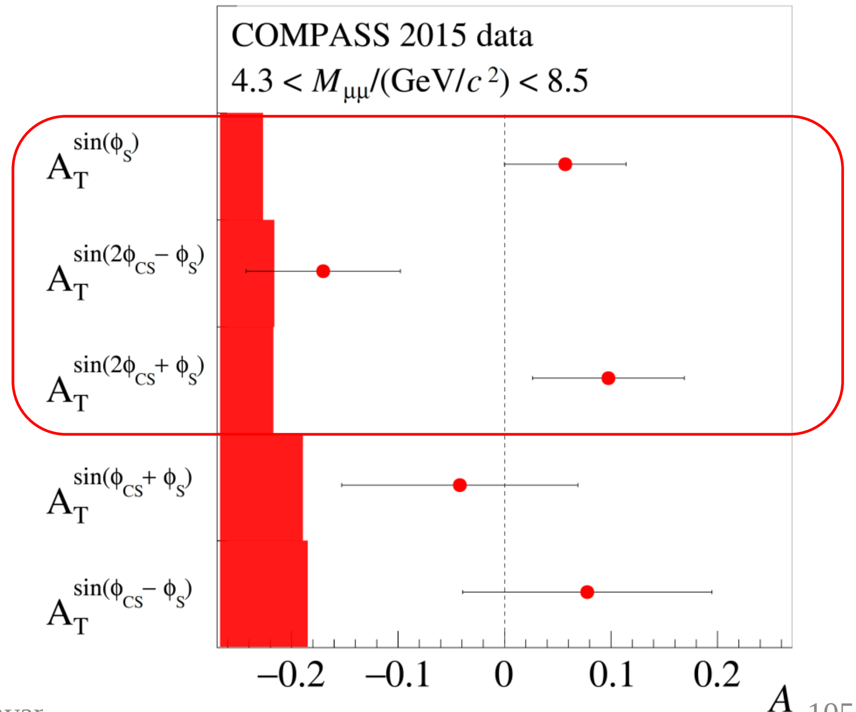

SIDIS in TFR or b2b SIDIS: TFR & CFR

A. Kotzinian, INT workshop Seattle, 24/09/2010

M. Anselmino, V. Barone, A. Kotzinian **PLB 699 (2011) 108–118**

A. Kotzinian et al. **Nuovo Cim. C036 (2013) no.05, 127-130**

$x_F < 0$

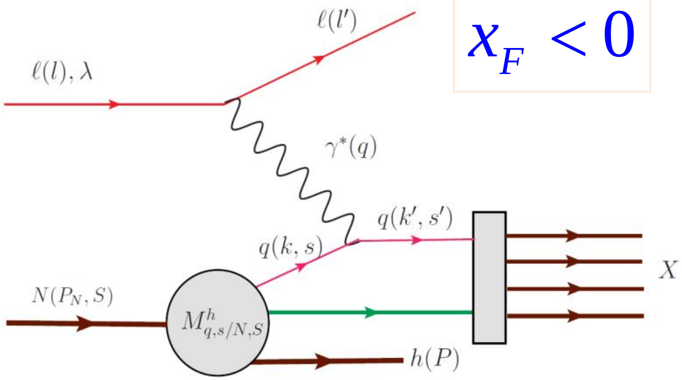

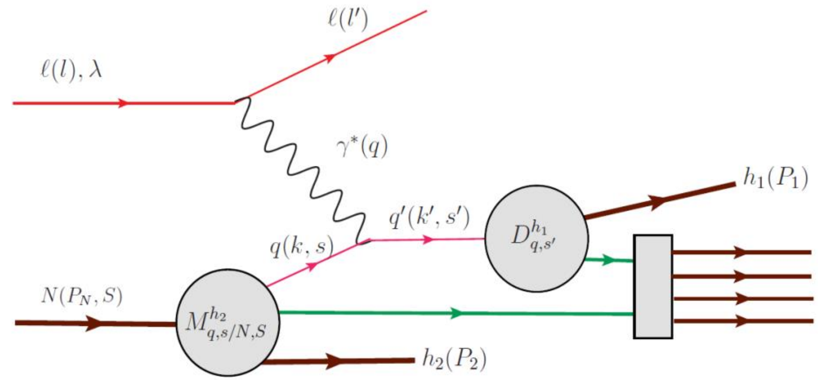

At LO 16 STMD fracture functions.

Probabilistic interpretation at LO: Conditional probability of finding a quark $q(x,k_\perp)$ in the fast moving proton fragmenting to $h(\zeta,P_{h\perp})$ moving in same direction ⇒ STMD CPDFs

Nucleon Polarization	Quark polarization: U	Quark polarization: L	Quark polarization: T
U	$\hat{u}_1$	$\frac{\mathbf{k}_T\times\mathbf{P}_T}{m_N m_h}\hat{l}_1^{\perp h}$	$\frac{\epsilon_T^{ij}P_T^j}{m_h}\hat{t}_1^h + \frac{\epsilon_T^{ij}k_T^j}{m_N}\hat{t}_1^\perp$
L	$\frac{S_L(\mathbf{k}_T\times\mathbf{P}_T)}{m_N m_h}\hat{u}_{1L}^{\perp h}$	$S_L\hat{l}_{1L}$	$\frac{S_L\mathbf{P}_T}{m_h}\hat{t}_{1L}^h + \frac{S_L\mathbf{k}_T}{m_N}\hat{t}_{1L}^\perp$
T	$\frac{\mathbf{P}_T\times\mathbf{S}_T}{m_h}\hat{u}_{1T}^h + \frac{\mathbf{k}_T\times\mathbf{S}_T}{m_N}\hat{u}_{1T}^\perp$	$\frac{\mathbf{P}_T\cdot\mathbf{S}_T}{m_h}\hat{l}_{1T}^h + \frac{\mathbf{k}_T\cdot\mathbf{S}_T}{m_N}\hat{l}_{1T}^\perp$	$\mathbf{S}_T\hat{t}_{1T} + \frac{\mathbf{P}_T(\mathbf{P}_T\cdot\mathbf{S}_T)}{m_h^2}\hat{t}_{1T}^{hh} + \frac{\mathbf{k}_T(\mathbf{k}_T\cdot\mathbf{S}_T)}{m_N^2}\hat{t}_{1T}^{\perp\perp} + \frac{\mathbf{P}_T(\mathbf{k}_T\cdot\mathbf{S}_T)-\mathbf{k}_T\cdot(\mathbf{P}_T\cdot\mathbf{S}_T)}{m_N m_h}\hat{t}_{1T}^{\perp h}$

CFR

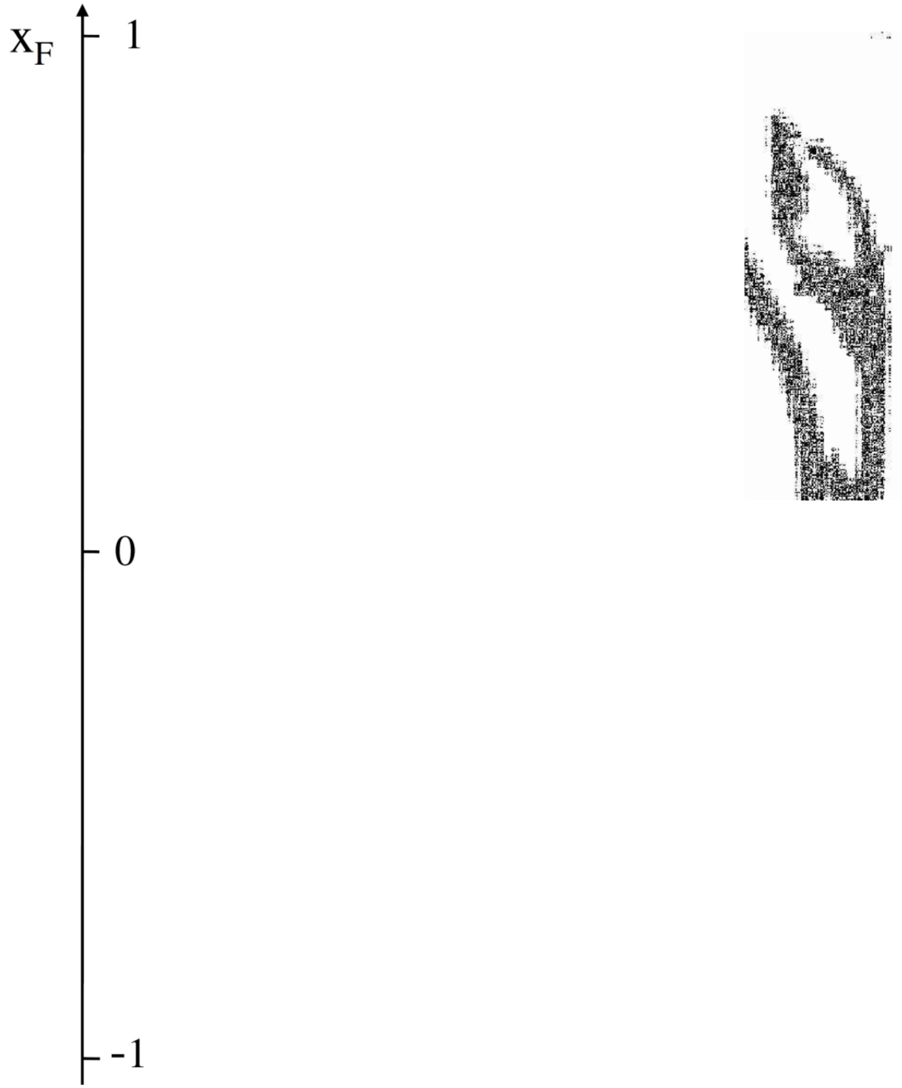

Larger phase space

higher W, z, x

different asymmetries

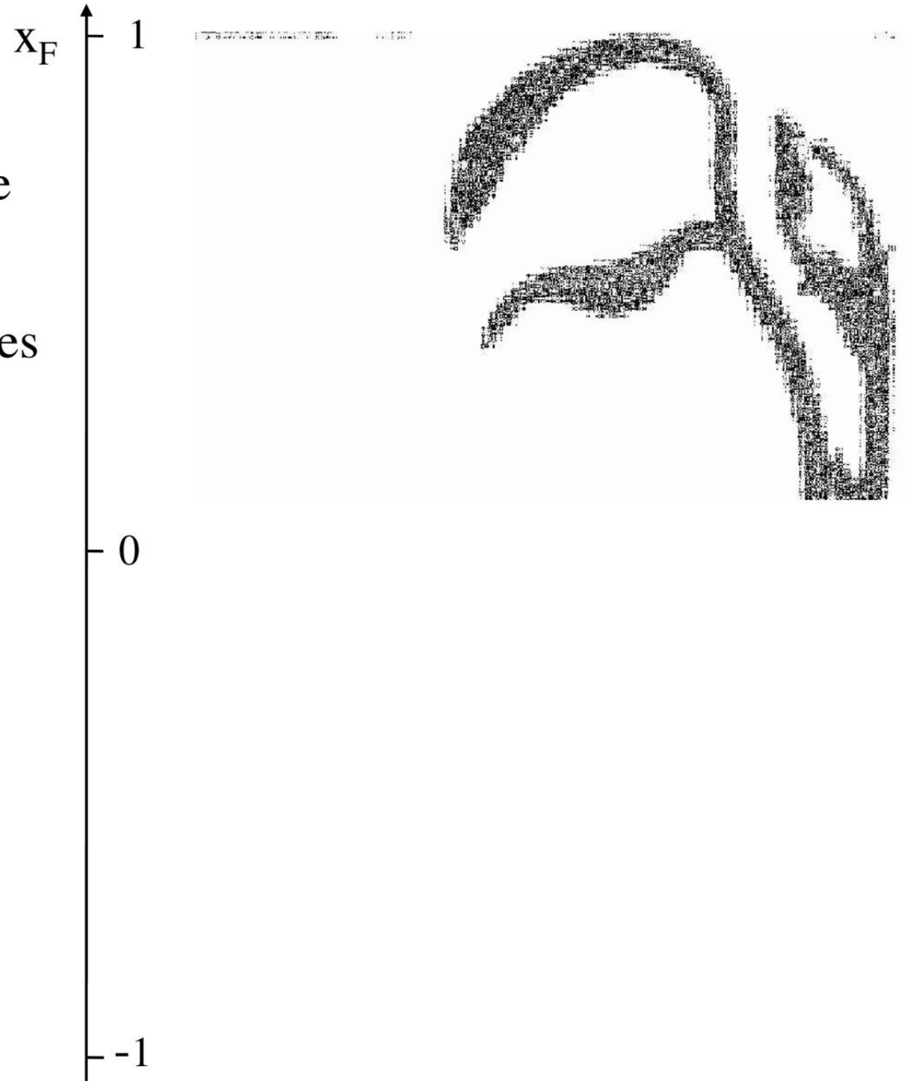

Better resolution,
higher statistics

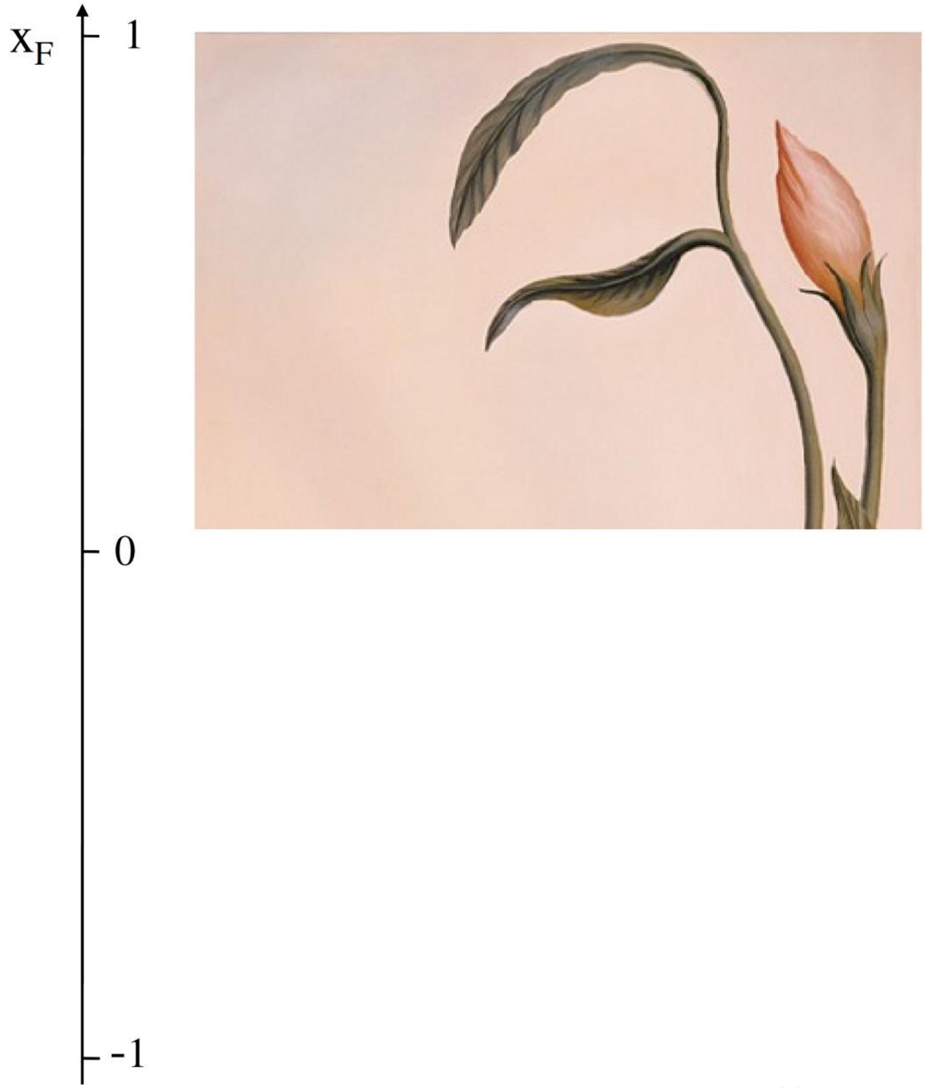

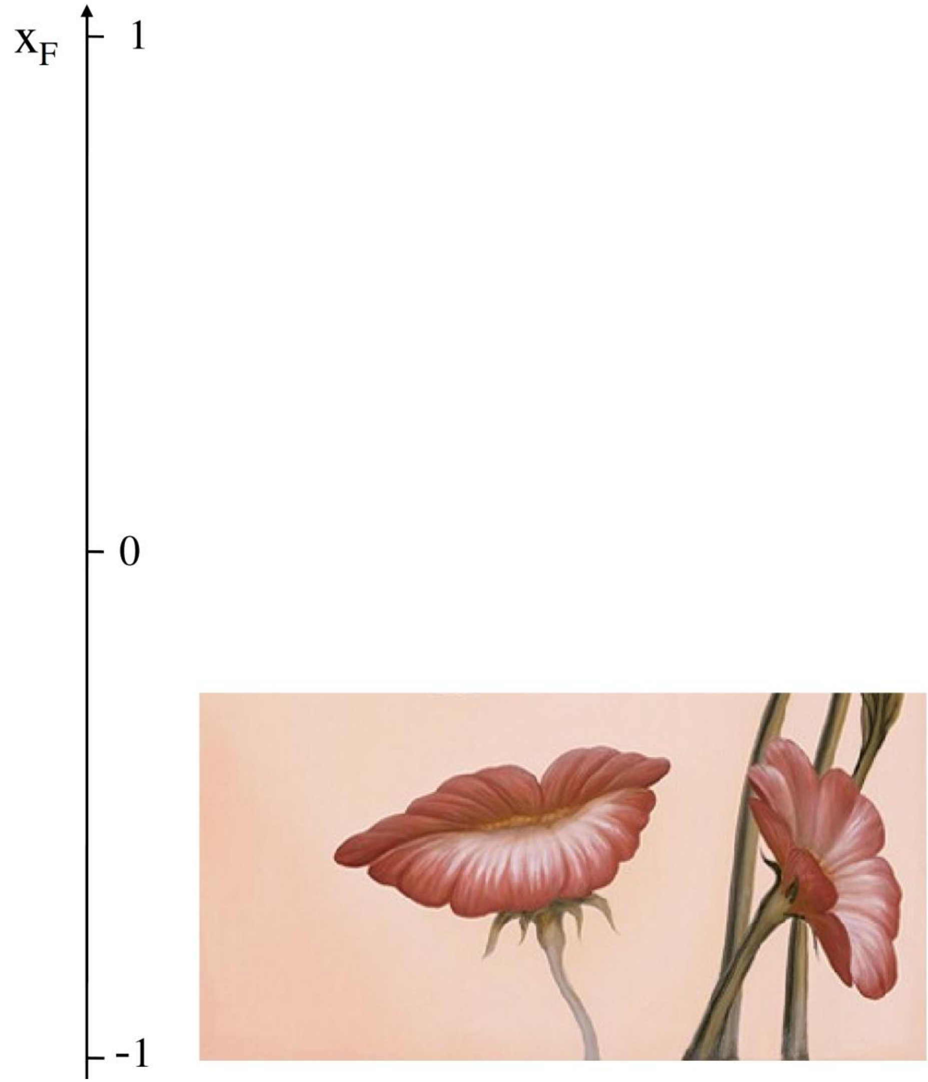

TFR with good resolution etc

Full picture can be surprising and beautiful

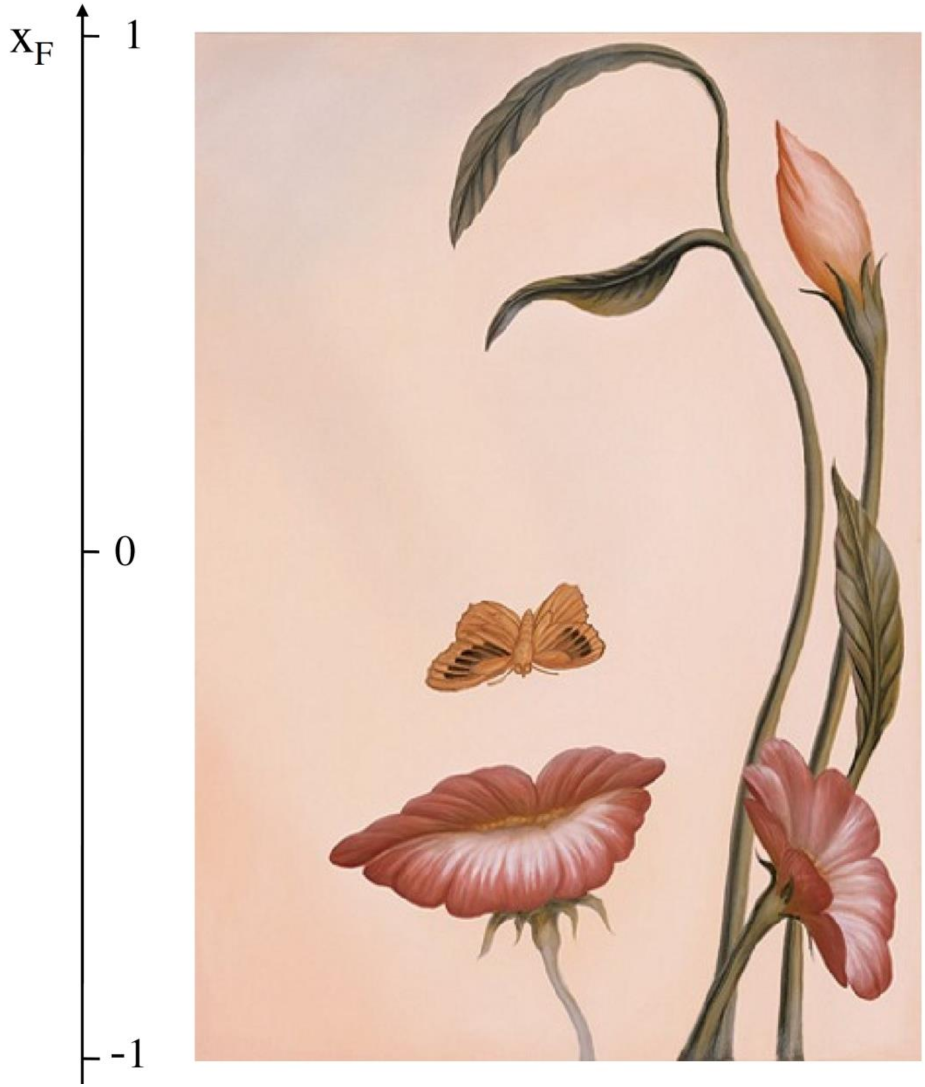

1. Exploration phase

First measurements

Parton model interpretation

Last decade

2. Consolidation phase

Measurements from several experiments

YOU ARE HERE

First global fits, validation of TMD factorisation and evolution

Next decade

3. Precision phase

Electron Ion Collider

Global fits, to a level comparable to standard PDFs

Spare slides

“COMPASS-like” future long-term experiment

COMPASS beyond 2020 workshop, CERN, March 21-22, 2016
Physics Beyond Colliders kick-off workshop CERN, September 6-7, 2016
IWHSS17 COMPASS workshop, Cortona, April 2-5, 2017
Dilepton Productions with Meson and Antiproton Beams workshop, ECT*, Trento, November 2017
Physics Beyond Colliders annual workshop, CERN, November 21-22, 2017

IWHSS18 – COMPASS workshop, Bonn, March 19-21, 2018

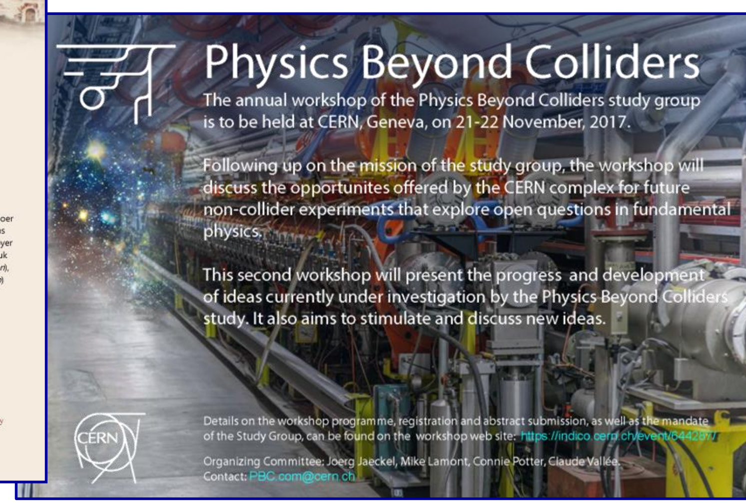

D. Kikoła et al. arXiv:1702.01546 [hep-ex]

Experiment	particles	beam energy (GeV)	$\sqrt{s}$ (GeV)	$x^{\uparrow}$	$\mathcal{L}$ (cm^{-2}s^{-1})	$\mathcal{P}_{\rm eff}$	$\mathcal{F}$ (cm^{-2}s^{-1})
AFTER@LHCb	$p + p^{\uparrow}$	7000	115	$0.05 \div 0.95$	$1 \cdot 10^{33}$	80%	$6.4 \cdot 10^{32}$
AFTER@LHCb	$p + {}^{3}\mathrm{He}^{\uparrow}$	7000	115	$0.05 \div 0.95$	$2.5 \cdot 10^{32}$	23%	$1.4 \cdot 10^{31}$
AFTER@ALICE$_{\mu}$	$p + p^{\uparrow}$	7000	115	$0.1 \div 0.3$	$2.5 \cdot 10^{31}$	80%	$1.6 \cdot 10^{31}$
COMPASS (CERN)	$\pi^{\pm} + p^{\uparrow}$	190	19	$0.1 \div 0.3$	$2 \cdot 10^{33}$	18%	$6.5 \cdot 10^{31}$
PHENIX/STAR (RHIC)	$p^{\uparrow} + p^{\uparrow}$	collider	510	$0.05 \div 0.1$	$2 \cdot 10^{32}$	50%	$5.0 \cdot 10^{31}$
E1039 (FNAL)	$p + p^{\uparrow}$	120	15	$0.1 \div 0.45$	$4 \cdot 10^{35}$	15%	$9.0 \cdot 10^{33}$
E1027 (FNAL)	$p^{\uparrow} + p$	120	15	$0.35 \div 0.9$	$2 \cdot 10^{35}$	60%	$7.2 \cdot 10^{34}$
NICA (JINR)	$p^{\uparrow} + p$	collider	26	$0.1 \div 0.8$	$1 \cdot 10^{32}$	70%	$4.9 \cdot 10^{31}$
fsPHENIX (RHIC)	$p^{\uparrow} + p^{\uparrow}$	collider	200	$0.1 \div 0.5$	$8 \cdot 10^{31}$	60%	$2.9 \cdot 10^{31}$
fsPHENIX (RHIC)	$p^{\uparrow} + p^{\uparrow}$	collider	510	$0.05 \div 0.6$	$6 \cdot 10^{32}$	50%	$1.5 \cdot 10^{32}$
PANDA (GSI)	$\bar{p} + p^{\uparrow}$	15	5.5	$0.2 \div 0.4$	$2 \cdot 10^{32}$	20%	$8.0 \cdot 10^{30}$

Drell-Yan TSAs – "higher twists"

$$\frac{d\sigma}{d\Omega} \propto 1+\ldots+ S_T\left[D_{[\sin 2\theta_{CS}]} A_T^{\sin(\varphi_{CS}+\varphi_S)} \sin(\varphi_{CS}+\varphi_S) + D_{[\sin 2\theta_{CS}]} A_T^{\sin(\varphi_{CS}-\varphi_S)} \sin(\varphi_{CS}-\varphi_S)\ldots \right]$$

New! COMPASS arXiv:1704.00488[hep-ex]

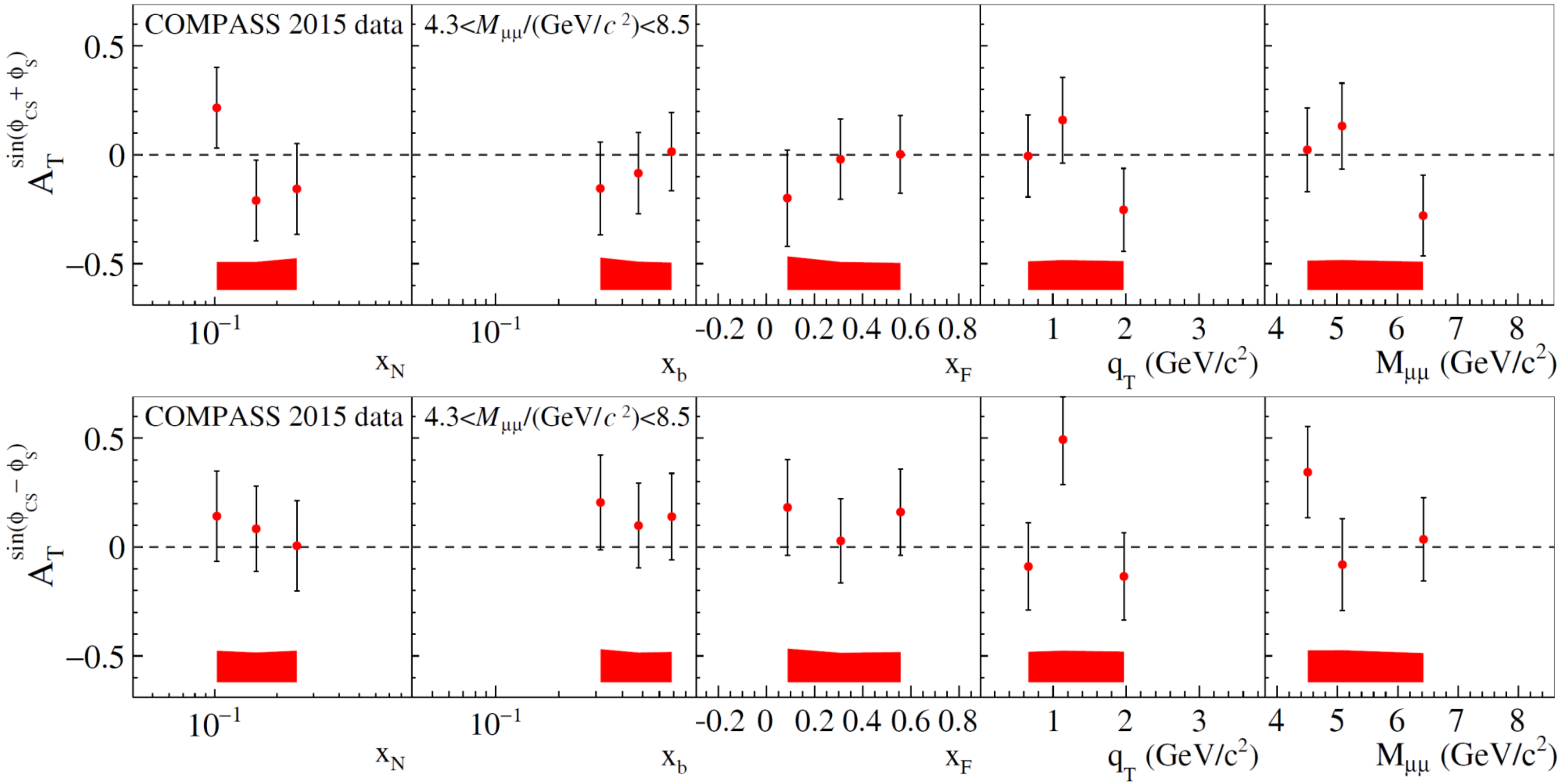

SIDIS Sivers TSA in COMPASS Drell-Yan Q^2-ranges

$$\frac{d\sigma}{dxdydzdp_T^2 d\phi_h d\phi_S} \propto \left(F_{UU,T} + \varepsilon F_{UU,L}\right)\left\{1 + \ldots + S_T A_{UT}^{\sin(\phi_h-\phi_S)} \sin(\phi_h - \phi_S) + \ldots\right\}$$

$$F_{UT,T}^{\sin(\phi_h-\phi_S)} = C\left[-\frac{\hat{\boldsymbol{h}}\cdot\boldsymbol{k}_T}{M} f_{1T}^{\perp q} D_{1q}^h\right], F_{UT,L}^{\sin(\phi_h-\phi_S)} = 0$$

PLB 770 (2017) 138

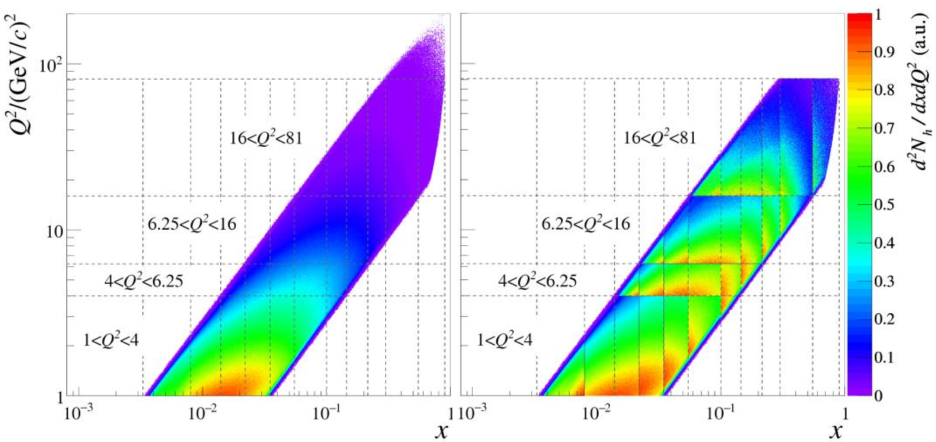

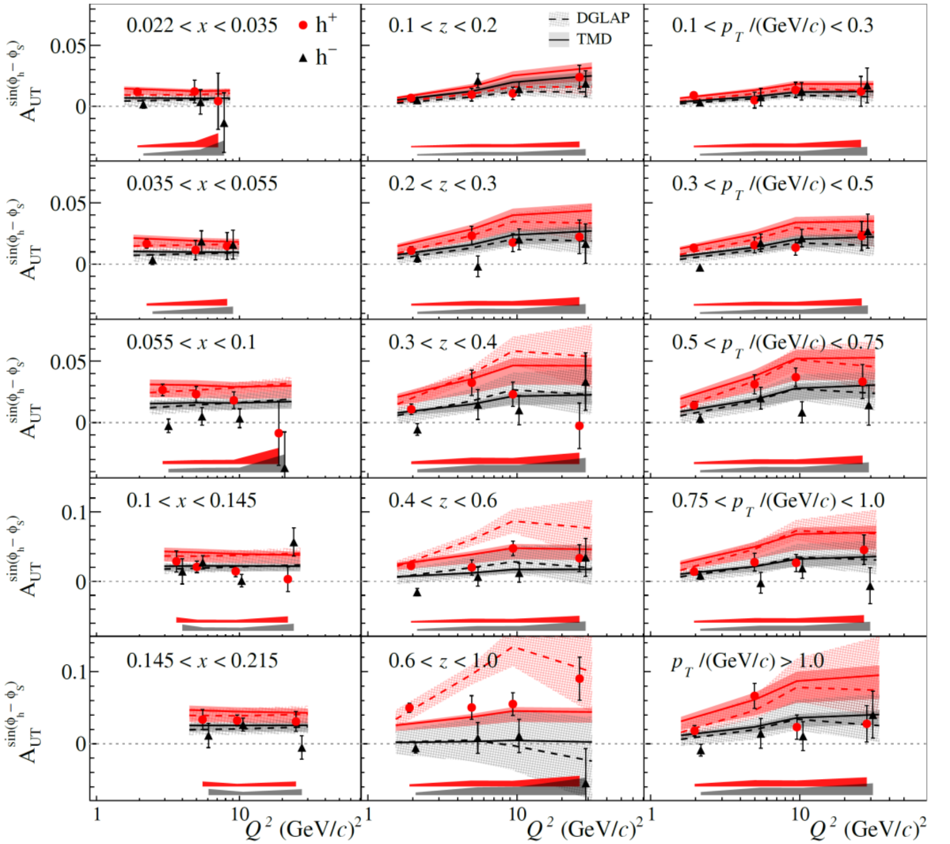

Multi-dimensional input for TMD evolution studies

- No clear Q^2-dependence within statistical accuracy
- Possible decreasing trend for Sivers TSA?

The solid (dashed) curves represent the calculations for TMD (DGLAP) evolution for the Sivers TSAs based on the best fit of 1D COMPASS and HERMES data from **Phys. Rev. D86 (2012) 014028** by M. Anselmino et al.

Kinematic map: high mass range

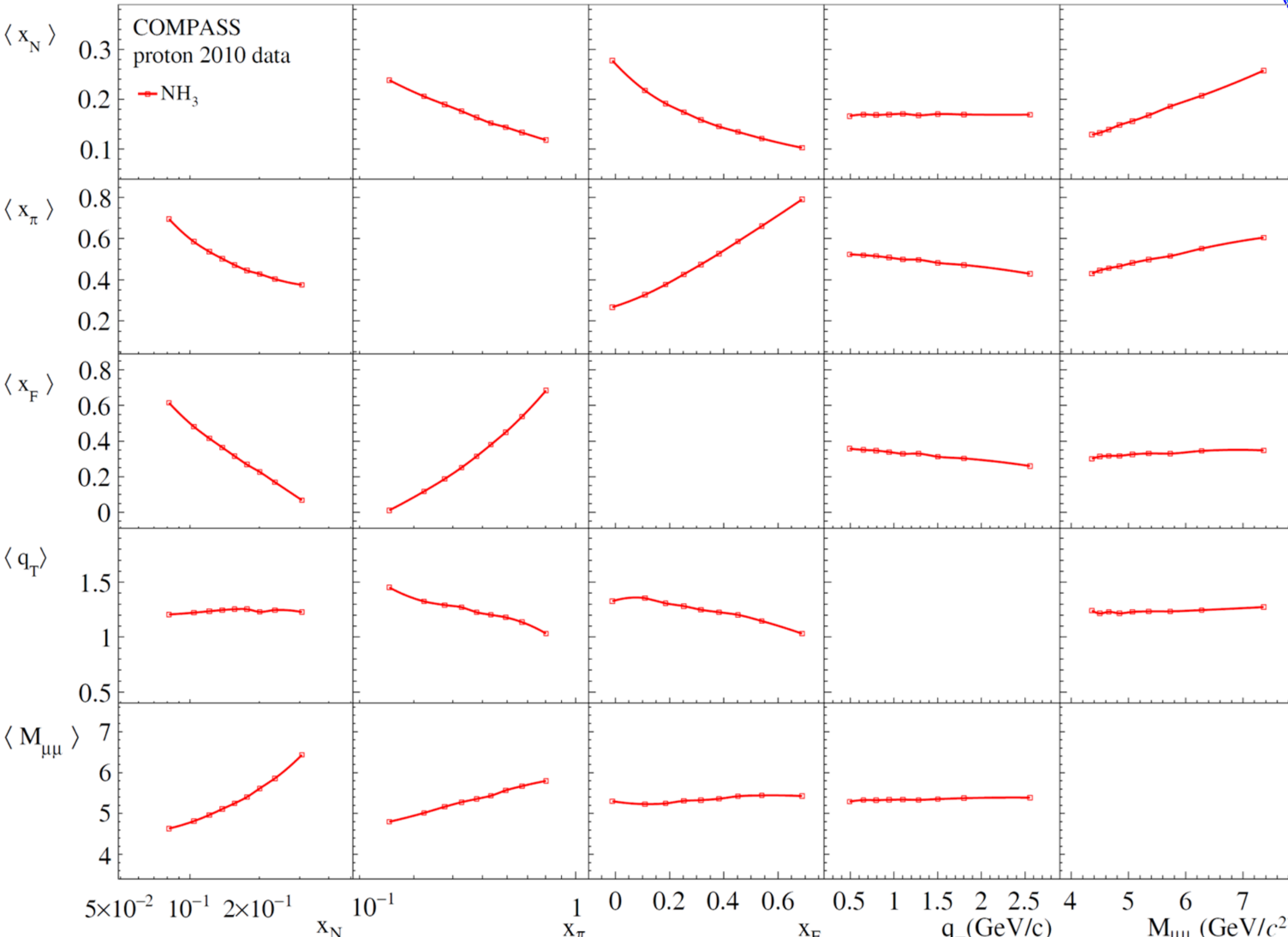

Correlation coefficients

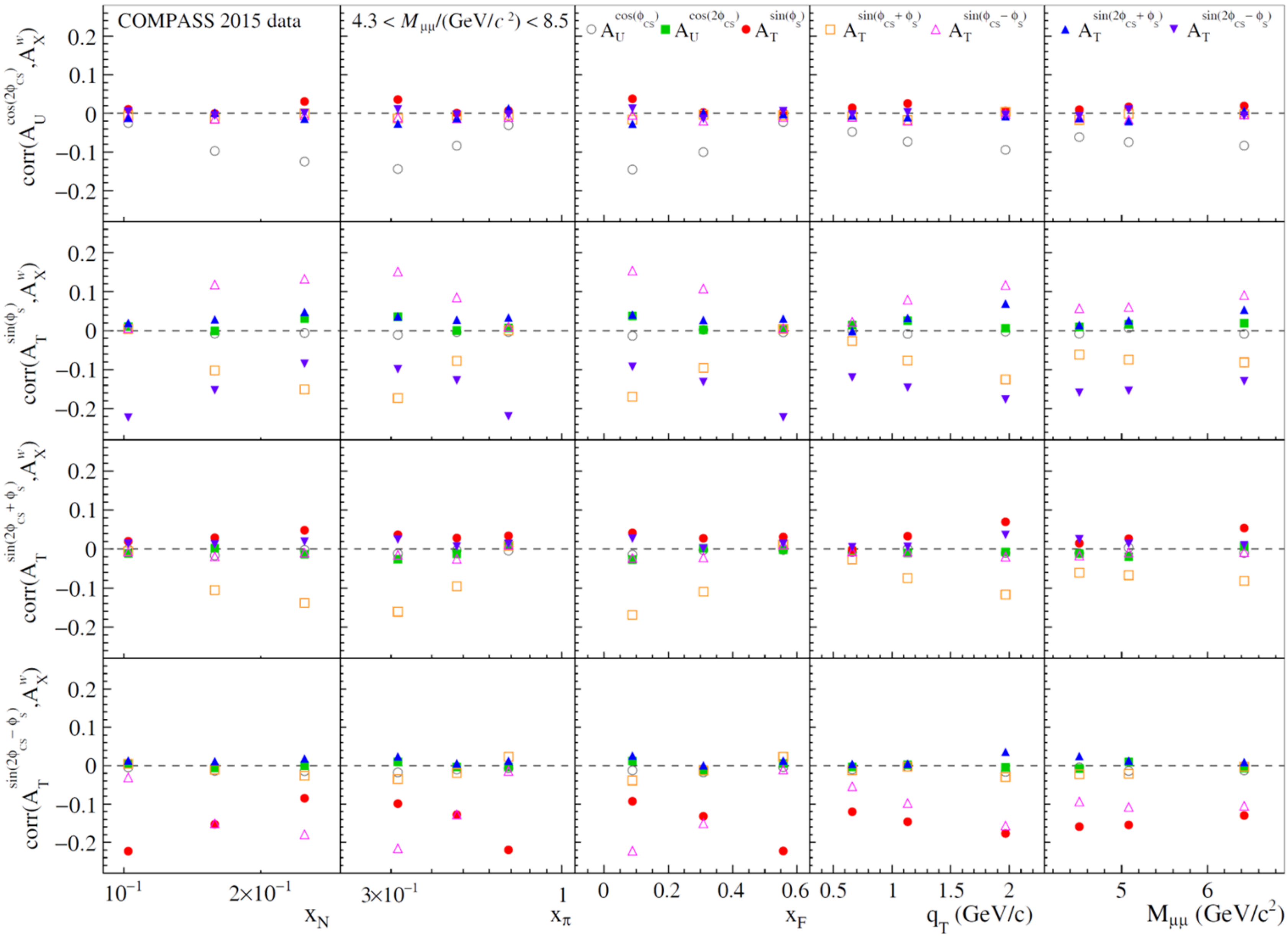

Maximum correlations are about ~0.2

The p_T (q_T) – weighted SIDIS(DY) Sivers asymmetry

General formalism was first introduced in 1997 (A. Kotzinian and P. Mulders, **PLB 406 (1997) 373**)

$$\int d^2 \boldsymbol{q_T} \frac{q_T}{M_p} F_T^{\sin\phi_S} = -\int d^2 \boldsymbol{q_T} \frac{q_T}{M_p} \mathcal{C}\left[\frac{\boldsymbol{q_T}\cdot\boldsymbol{k_{pT}}}{q_T M_p} f_{1,\pi} f_{1T,p}^{\perp}\right]$$

$$= -\frac{2}{N_c}\sum_q e_q^2 \left[f_{1,\pi}^{\bar{q}}(x_\pi)\, f_{1T,p}^{\perp(1)q}(x_p) + (q \leftrightarrow \bar{q})\right]$$

$$\approx \frac{2e_u^2}{N_c} f_{1,\pi}^{\bar{u}}(x_\pi) f_{1T}^{\perp(1)u}(x_N)$$

Sivers TSA in SIDIS:	$A_{UT}^{\sin(\phi_h-\phi_s)} \propto f_{1T}^{\perp q} \otimes D_{1q}^h$
Sivers *w*TSA in SIDIS:	$A_{UT}^{\sin(\phi_h-\phi_s)} \propto f_{1T}^{\perp q\,(1)} \times D_{1q}^h$
Sivers TSA in DY:	$A_T^{\sin\varphi_S} \propto f_{1,\pi}^q \otimes f_{1T,p}^{\perp q}$
Sivers *w*TSA in DY:	$A_T^{\sin\varphi_S} \propto f_{1,\pi}^q \times f_{1T,p}^{\perp q\,(1)}$

$$f_{1T}^{\perp(1)q}(x) = \int d^2\boldsymbol{k_T}\, \frac{k_T^2}{2M^2}\, f_{1T}^{\perp q}(x, k_T^2)$$

$$A_{UT,T,h^\pm}^{\sin(\phi_h-\phi_S)\frac{P_T}{zM}}(x,Q^2) = 2\,\frac{\frac{4}{9}\, f_{1T}^{\perp(1)u}(x,Q^2)\,\tilde{D}_{1,u}^{h^\pm}(Q^2) + \frac{1}{9}\, f_{1T}^{\perp(1)d}(x,Q^2)\,\tilde{D}_{1,u}^{h^\pm}(Q^2)}{\sum_q e_q^2\, f_1^q(x,Q^2)\,\tilde{D}_{1,u}^{h^\pm}(Q^2)}$$

$$\tilde{D}_{1,q}^{h^\pm}(Q^2) = \int_{0.2}^{1} dz\, D_{1,q}^{h^\pm}(z,Q^2) \qquad x f_{1T}^{\perp(1)q}(x) = a_q\, x^{b_q}\,(1-x)^{c_q}$$

$$A_T^{\sin\phi_S\frac{q_T}{M_p}}(x_N,Q^2) \approx 2\,\frac{f_{1T,p}^{\perp(1)u}(x_N,Q^2)}{f_{1,p}^{u}(x_N,Q^2)}$$

COMPASS collaboration and ОИЯИ-ЛИТ

Artem Petrosyan
Danila Oleynik

The PanDA
Production ANd Distributed Analysis system

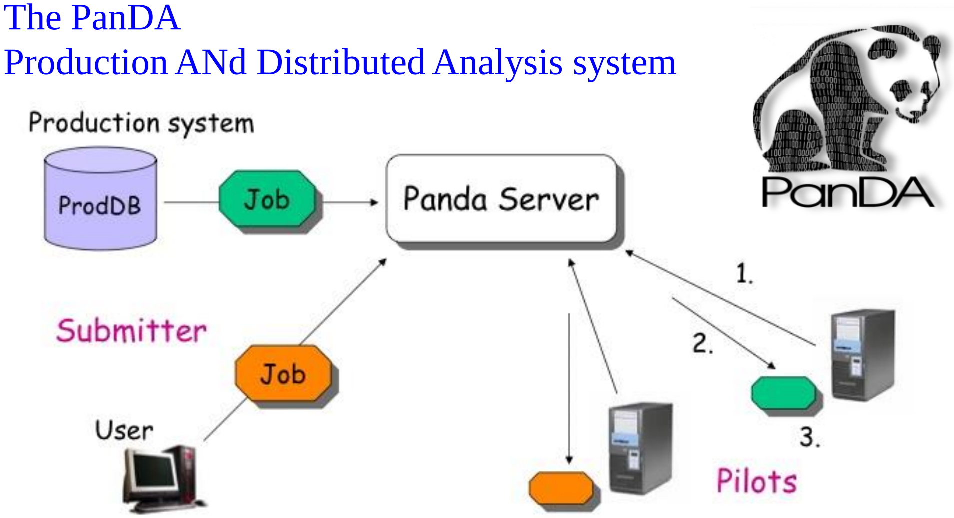

New COMPASS production system

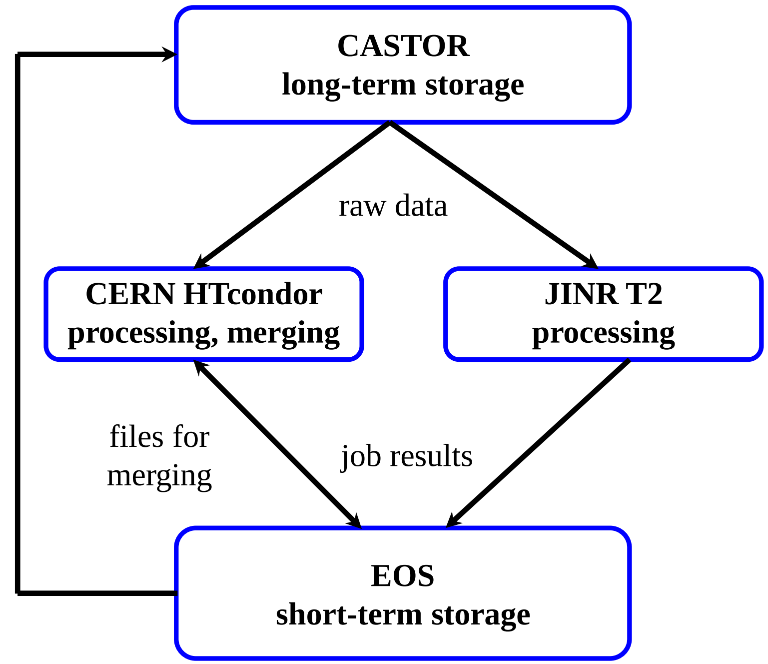

What is Rucio ?

- Rucio is the Data Management system of the ATLAS experiment
- It was built using more than 10 years of experience in Data Management:
  - Designed from experience from the previous data management system DQ2
  - Integrate new features and technologies
- Modular, highly scalable, well supported
- Who is using Rucio ?
  - Used by ATLAS, AMS and Xenon1T
  - Being evaluated by other small and big HEP/Astro experiments (CMS, LIGO, IceCube, LSST...)
  - Rucio community workshop on March 1st-2nd 2018 to present Rucio to more collaboration/scientific communities

Workflow management and monitoring

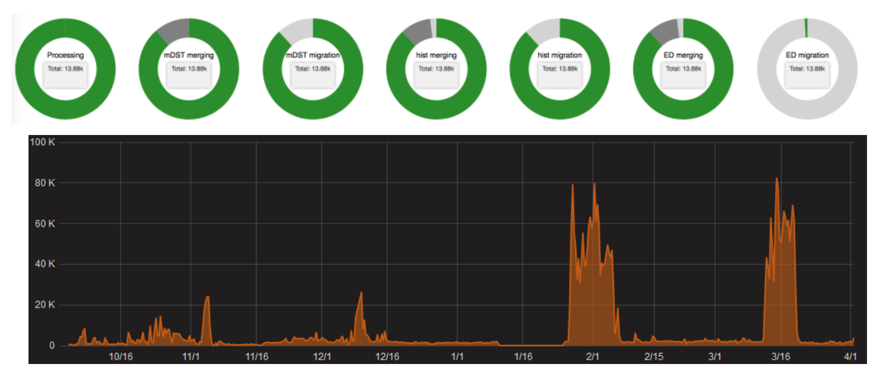

COMPASS collaboration and ОИЯИ-ЛЯП

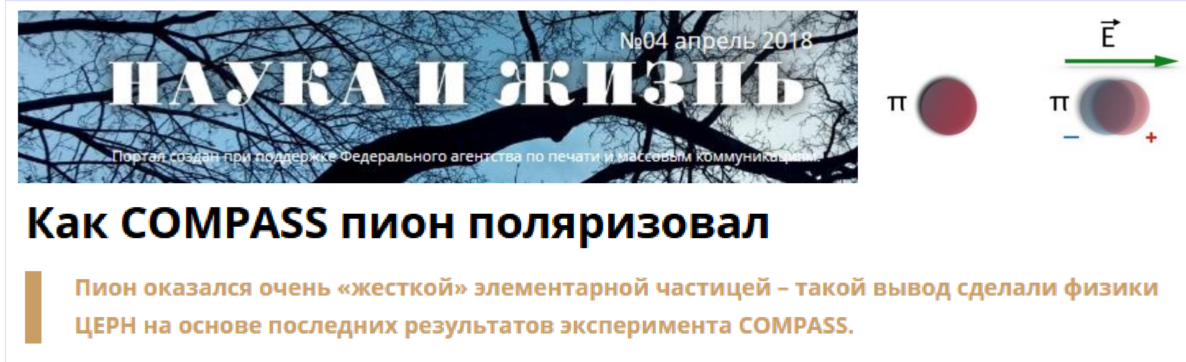
№04 апрель 2018
НАУКА И ЖИЗНЬ
Портал создан при поддержке Федерального агентства по печати и массовым коммуникациям.

Как COMPASS пион поляризовал

Пион оказался очень «жесткой» элементарной частицей – такой вывод сделали физики ЦЕРН на основе последних результатов эксперимента COMPASS.

Alexey Guskov

- “Measurement of the charged-pion polarisability” – PRL 114 (2015) 062002
- “Search for exclusive photoproduction of $Z_c^{\pm}$ (3900) at COMPASS” – PLB 742 (2015) 330
- “Search for muoproduction of the X(3872) at COMPASS” – Submitted to PLB

Letter of Intent: Fixed-Target Experiment at M2 Beamline beyond 2020

- Study of gluon distribution in kaon via prompt photon production
  - Prompt photon production rate estimation
- Primakoff Reactions
  - Kaon polarizability

Andrei Gridin – Double J/ψ and intrinsic charm

Evgeniy Mitrofanov – EMC effect at COMPASS

Igor Denisenko – Pion gluon structure functions in J/ψ production

Andrey Maltsev – COMPASS 2012 Primakoff data analysis

Bakur Parsamyan

- COMPASS analysis coordinator
- Azimuthal asymmetries in SIDIS and Drell-Yan


CERN Courier March 2015

News

QCD PHYSICS

COMPASS measures the pion polarizability

The COMPASS experiment at CERN has made the first precise measurement of the polarizability of the pion – the lightest composite particle built from quarks. The result confirms the expectation from the low-energy expansion of QCD – the quantum field theory of the strong interaction between quarks – but is at variance with the previously published values, which overestimated the pion polarizability by more than a factor of two.

Every composite system made from charged particles can be polarized by an external electromagnetic field, which acts to separate positive and negative charges. The size of this charge separation – the induced dipole moment – is related to the external field by the polarizability. As a measure of the response of a complex system to an external force, polarizability is directly related to the system's stiffness against deformability, and hence the binding force between the constituents.

The pion, made up of a quark and an antiquark, is the lightest object bound by the strong force and has a size of about 0.6×10^{-15} m (0.6 fm). So to observe a measurable effect, the particle must be subjected to electric fields in the order of 100 kV across its diameter – that is, about 10^{18} V/cm. To achieve this, the COMPASS experiment made use of the electric field around nuclei. To high-energy pions, this field appears as a source of (almost) real photons, on which the incident pions scatter.

Such pion–photon Compton scattering, also known as the Primakoff mechanism, was explored in the early 1980s in an experiment at Serpukhov, but the small data sample led to only an imprecise value for the polarizability of 6.8 ± 1.4 (stat.) ±1.2 (syst.) $\times10^{-4}$ fm^3, where the systematic uncertainty was underestimated, presumably.

COMPASS has now achieved a modern Primakoff experiment, using a 190 GeV pion beam from the Super Proton Synchrotron at CERN directed at a nickel target. Importantly, COMPASS was also able to use muons, which are point-like and hence non-deformable, to calibrate the experiment. The Compton $\pi\gamma\rightarrow\pi\gamma$ scattering is extracted from the reaction $\pi^-\mathrm{Ni}\rightarrow\pi^-\gamma\mathrm{Ni}$ by selecting events from the Coulomb peak at small momentum transfer. From the analysis of a sample of 63,000 events, the collaboration obtained a value of the pion electric polarizability of 2.0 ± 0.6 (stat.) ±0.7 (syst.) $\times10^{-4}$ fm^3 – that is, about 2×10^{-4} of the pion's volume. This value is in good agreement with theoretical calculations in low-energy QCD, therefore solving a long-standing discrepancy between these calculations and previous experimental efforts to determine the polarizability.

Although this measurement is the first to allow a self-calibration, the accuracy is still below the quoted uncertainty of the calculations. With more data already recorded, the COMPASS collaboration expects to improve on this result by a significant factor in the near future, and thereby probe further a benchmark calculation of non-perturbative QCD.

The COMPASS experiment in the North Area on the Prévessin site at CERN studies hadron structure both with pion beams and with muon beams – a powerful combination. (Image credit: CERN-EX-1105182-01.)

Further reading
COMPASS Collaboration 2015 arXiv:1405.6377 [hep-ex], to be published in *Phys. Rev. Lett.*

The International Year of Light

INTERNATIONAL YEAR OF LIGHT 2015

On 20 December 2013, the UN General Assembly proclaimed 2015 as the International Year of Light and Light-based Technologies (IYL 2015). The aim is to raise awareness about how these technologies provide solutions to global challenges in energy, education, agriculture and health.

In its quest to "see" the fundamental structure of matter, high-energy particle physics goes beyond the wavelengths of light to the wavelengths of particle beams. Over the years, developments in the accelerators that create those beams have led to new ways of producing light that have a big impact on other disciplines.

To celebrate the IYL 2015, this issue of *CERN Courier* looks at how brilliant, accelerator-based X-ray free-electron lasers are enabling exciting new studies in biology (p19). Meanwhile, as Lucio Rossi points out in Viewpoint, accelerators provide the finest form of "light", and experiments can now "see" down to distances as small as 10^{-20} m (p54). The High-Luminosity LHC project (p28) will allow CERN's collider to cast still more of this fine light on matter. Finally, Inside Story (p53) looks at how light and particle physics came together in the life of one physicist.

Sommaire en français